The potential and role of breast tumour kinase (Brk) isoforms in breast cancer therapeutics

A thesis submitted for the degree of Doctor of Philosophy by

Haroon Ali Hussain

0702030

Department of Life Sciences

College of Health and Life Sciences

Brunel University

Declaration

I hereby declare that the research presented in this thesis is my own work except where otherwise stated and has not been submitted for any other degree.

Haroon Ali Hussain

Dedication

For my parents

“My Lord be merciful to them as they brought me up in my childhood” (Quran 17:24)

Abstract

Breast tumour kinase (Brk)/PTK6 is over-expressed in 80% of all breast cancers and has shown to be involved in tumour development and progression of breast cancer. There is a lack of development of breast tumour kinase (Brk) inhibitors and, therefore the clinical benefits associated with Brk inhibition are unknown. Due to Brk's known role in proliferation and cell death, it was hypothesised that it may modulate responses to common breast cancer therapies. ALT-PTK6 is an alternatively spliced isoform of Brk and may act as a competitive inhibitor of the full-length form. Little is known regarding ALT-PTK6's role in breast cancer therapeutics. I hypothesised ALT-PTK6 may negatively regulate cell proliferation within breast cancer cell lines and thus reduce the oncogenic functions of the full-length form. Initially, *in vitro* studies using multiple breast cancer cell showed survival at 2Gy radiation dose (SF2) correlated with Brk expression levels for some cell lines, with high SF2 survival there was also higher Brk expression. DNA repair kinetics and Brk interaction with ataxia telangiectasia mutated protein (ATM) showed no significant differences in relation to Brk expression. Brk modulates response to: Paclitaxel (Taxol), Doxorubicin, Lapatinib, Tamoxifen and showed significant reduction in cell proliferation in combination with a novel Brk inhibitor (Compound 4f) suggesting potential for a Brk targeted therapy. It was hypothesised that due to the proposed role of ALT-PTK6 as a negative regulator of Brk, *ALT-PTK6/PTK6* transcript ratios will be lower in breast cancer cells and tissues. There were increased *ALT-PTK6* to *PTK6* transcript ratios in non-cancerous cell lines, hormone (ER/PR) positive and HER2 positive breast cancer cell lines compared to hormone negative cell lines. *ALT-PTK6/PTK6* ratios were increased in patients with improved overall survival. Thus, there is potential for *ALT-PTK6/PTK6* ratios as a prognostic factor for long term overall survival in breast cancer patients.

Acknowledgments

I would like to extend my eternal gratitude towards my principal supervisor, Amanda Harvey, without whom this would not be possible. I am forever grateful to her for this opportunity, for her patience and guidance and all the knowledge she has imparted throughout the years. My thanks also extend towards the rest of my supervisory team; Professor Christopher Parris and Dr Rhona Anderson as well as towards my review panel members: Dr Kishore Uday and Dr Ansar Pathan, for their valuable input. Many thanks to my examination panel, Dr Isabel Pires and Dr Predrag Slijepcevic as well as the chair Dr Sabrina Tosi.

Thank you to Dr Emma Bourton (Brunel University) for her assistance with my radiation studies. Thank you also to Professor Wen Jiang (Cardiff University), Professor Kefah Mokbel (The Princess Grace Hospital) and group for the work on *PTK6* and *ALT-PTK6* transcript expression in breast tumour tissues. Thank you to Dr Julie Davies and Dr Karly Rai Rodgers-Broadway for welcoming me to the life of a PhD student all those years ago. Thank you to the rest of my lab group and academics for their support and feedback in my studies. Thank you to my friends and colleagues who went through this process with me and who somehow managed to make it a little easier, Ezgi, Sheila, Chrissi, Sarah, Stephen and Dimple - thanks for your care, laughs and understanding throughout the years. Thanks also to Gerry and Matt for all their help. Thanks to Zee and Naf, you know what you guys have done for me and I am grateful to have you as friends. Thanks to Farah and Adam for everything you guys have done too. Thanks to my colleagues in the corporate apps team for your support throughout my PhD. Thanks to my aunts, uncles and cousins for their prayers and good wishes. Thanks to my brothers and sisters, my nieces and nephews for their support. Last but not the least thanks to my parents for their patience and continued support.

Table of Contents

List of Tables

List of Figures

1.0 Chapter 1

2.0 Chapter 2

3.0 Chapter 3

4.0 Chapter 4

5.0 Chapter 5

Abbreviations

18S	18S RNA
ACTB	Beta actin
ADAM	Disintegrin and metalloprotease domain protein
AF	Alexafluor 488
Akt	RAC-alpha serine/threonine-protein kinase
ALT-PTK6	Alternative Protein Tyrosine Kinase 6
ANOVA	Analysis of variance
APS	Ammonium persulfate
ARAP1	Arf-GAP, Rho-GAP, ankyrin repeat and pleckstrin homology (PH) domain containing protein 1
ATCC	American type culture collection
ATF-4	Activating transcription factor 4
ATM	Ataxia telangiectasia mutated
ATP5BATP	synthase subunit
ATR	Ataxia telangiectasia and Rad3-related protein
B2M	Beta-2-microglobulin
Bcl	B-cell lymphoma
BRCA	Breast cancer susceptibility gene
Brk	Breast Tumour Kinase
BSA	Bovine serum albumin
c-cbl	Proto-oncogene encoding a E3 ubiquitin ligase
CDK	Cyclin dependent kinases
cDNA	Complementary deoxyribonucleic acid
cDNA	Complementary deoxyribonucleic acid
CSC	Cancer stem cell
CT	Cycle Threshold
CYC1	Cytochrome C1
D5	Draq 5
DCIS	Ductal carcinoma in situ
DMEM	Dulbecco’s Modified Eagle Medium

DMSO	Dimethyl sulfoxide
Dox	Doxorubicin
ECL	Enhanced Chemiluminescence
ECM	Extracellular Matrix
EGF	Epidermal growth factor
EGFR	Epidermal growth factor receptor
EIF4A2	Eukaryotic translation initiation factor 4A isoform 2
ELISA	Enzyme-linked immunosorbent assay
ER	Oestrogen receptor
ERK	Extracellular signal regulated kinase
ESCC	Oesophageal squamous cell carcinoma
FAK	Focal adhesion kinase
FBS	Foetal bovine serum
FISH	Fluorescent in situ hybridisation
Fox03a	Forkhead box O3 a
FoxO	Forkhead box transcription factors of the class O
GAPDH	Glyceraldehyde-3-phosphate dehydrogenase
GFP	Green fluorescent protein
GOI	Gene of interest
GSK3β	Glycogen Synthase kinase 3 Beta
Gy	Gray
H2AX	Histone-2AX
HER2	Human epidermal growth factor 2/erb-b2 receptor tyrosine kinase 2
HR	Homologous recombination
HRP	Horseradish peroxidase
IDC	Invasive ductal carcinoma
IGF	Insulin like growth factor
IGRT	Image guided radiotherapy
ILC	Invasive lobular carcinoma
IMRT	Intensity modulated radiotherapy
IMS	Industrial methylated spirit
IRS	Insulin like receptor substrate

KAP3A	Keratin associated protein 3-4
KIF3A/3B	Kinase like protein family member 3A/3B
KM	Kinase mutant
Lap	Lapatinib
LAR	Luminal androgen receptor
LCIS	Lobular carcinoma in situ
MAPK	Mitogen activated protein kinase
MD	Mammographic Density
MIK16	Marker of proliferation Ki-67
mTOR	Mechanistic target of Rapamycin
MTT	(3-(4,5-Dimethylthiazol-2-yl)-2,5-Diphenyltetrazolium Bromide)
NF-kB	Nuclear kappa factor B
NLS	Nuclear localisation sequence
NSCLC	Non-small cell lung cancer
NST	No specific type
P13K	Phosphoinositide 3-kinase
PEI	Polyethylenimine
PIK3CA	Phosphatidylinositol 4,5-bisphosphate 3-kinase catalytic subunit alpha isoform
PP	Pyrazolopyrimidines
PPARγ	Peroxisome proliferator-activated receptors gamma
PR	Progesterone receptor
PSF	Splicing factor proline and glutamine rich
PTB	Polypyrimidine tract-binding protein
PTEN	Phosphatase and tensin homolog
PTK	Protein Tyrosine Kinase
PTK6	Protein Tyrosine Kinase 6
PUFA	Polyunsaturated fatty acids
Rac1	Ras-related C3 botulinum toxin substrate-1
Raf	Rapidly accelerated fibrosarcoma
RNA	Ribonucleic acid
ROS	Reactive oxygen species

RPL13A	Ribosomal protein L13A
RPMI	Roswell Park Memorial Institute
RQ	Relative quantification
RS	Recurrence score
RT	Radiotherapy
Sam68	SRC associated in mitosis of 68 kDa
SDHA	Succinate dehydrogenase complex
SDS-PAGE	Sodium dodecyl sulphate - polyacrylamide gel electrophoresis
SEER	Surveillance, Epidemiology and End Results databases
SERM	Selective oestrogen receptor modulator
SF2	Survival at 2Gy radiation dose
SFA	Saturated fatty acids
SH	Src homology
SLM	Sam68 like mammalian protein
SRC	Proto-oncogene tyrosine kinase Src
STAT	Signal transducer and activator of transcription
TAE	Tris-acetate-EDTA
Tam	Tamoxifen
Tax	Taxol
TBS	Tris buffered saline
TBST	Tris buffered saline -Tween20
TCF	T-Cell factor transcription factor
TDLU	Terminal duct lobular unit
TEMED	Tetramethylethylenediamine
TIC	Tumour initiating cells
TK	Tyrosine Kinase
TNBC	Triple negative breast cancer
TNM	Tumour (T), Lymph node (N), Metastasis (M)
TOP1	Topoisomerase DNA 1
TP53/p53	Tumour protein 53
UBC	Ubiquitin C

VEC	Vector
VEGF	Vascular endothelial factor
VUS	Variants of unknown significance
WNT	Wingless relating integrated site
WT	Wild type
YWHAZ	Phospholipase A2

Publications

1. **Hussain, H. A**., & Harvey, A. J. (2014*).* Evolution of breast cancer therapeutics: Breast tumour kinase's role in breast cancer and hope for breast tumour kinase targeted therapy. World journal of clinical oncology, 5(3), 299-310.
2. Bourton, EC., **Hussain, H**., Plowman, PN., Harvey, AJ. and Parris, C. (2015) 'Radiosensitivity of Human Breast Cancer Cell Lines Expressing the Breast Tumor Kinase (Brk)'. Journal of Cancer Science and Therapy, 7 (3). pp. 95 - 101.
3. Rajpal S Burmi, Gary A Box, **Haroon A Hussain**, Caroline J Pennington, Julie A Davies, William J Court, Suzanne A Eccles, Dylan R Edwards, Amanda J Harvey. Breast tumour kinase (Brk/PTK6) contributes to breast tumour xenograft growth and modulates chemotherapeutic responses *in vitro*. *Pending submission for publication*.

Conferences and Presentations

External Conferences:

1. Hussain, H. and Harvey, A. (2018) 'Abstract P3-07-05: Potential of breast tumour kinase (Brk) as a therapeutic target: Brk modulates drug responses in breast cancer cell lines', Cancer Research. American Association for Cancer Research, 78(4 Supplement), pp. P3-7-5-P3-7–5. doi: 10.1158/1538-7445.SABCS17-P3-07-05. San Antonio Breast Cancer Symposium, San Antonio, December 2017.
2. Haroon Hussain, Emma C. Bourton , Piers N. Plowman, Christopher N. Parris, Amanda Harvey. Radio-sensitivity of human breast cancer cell lines expressing the breast tumour kinase. (Brk). BACR: Bridging gaps in breast cancer research, Newcastle, October 2015.

3MT (3 minute) Thesis Presentations:

1. Haroon Hussain. Title: Is there potential for a novel Breast Cancer Therapy? January 2016, ***Semi-Finalist***, Brunel University.
2. Haroon Hussain. Potential for a novel Breast Cancer Therapy. January 2017, ***Finalist***, Brunel University.

1.0 Chapter 1: General Introduction

1.1 Introduction

Although there has been a decline in breast cancer mortality rates since the 1970s, the rate of breast cancer incidence has increased by 19% since the 1990s (Cancer Research UK, 2014). It has been previously shown that breast cancer is the most common malignancy in the UK with over 356,000 cases of cancer diagnosis reported in the UK in 2014 with 55,222 for breast cancer (Cancer research UK, 2014). Breast cancer has been shown to be the second most common cause of cancer death for women in the UK, accounting for 11,400 deaths in 2014 (Cancer Research UK, 2014). The introduction of early diagnostic techniques as well as the development of improved and novel breast cancer therapies have attributed to the overall reduced mortality rates. For example, the introduction of the NHS breast screening programme which screens women aged between 50-70 years old (and is currently trialling screening for women aged 47 onwards) for early detection of breast cancer and may explain the increase in incidence in the UK. These diagnostic techniques may detect cancers that would have gone unnoticed until much later, thus allowing for early diagnosis of breast cancer at a more treatable or curable stage. Nonetheless, there is still room for improvement. Furthermore, breast cancer therapies need to be effective, patient specific, relatively non-toxic and increase patient overall survival. There is also progress needed towards understanding recurrence, resistance and spread (Eccles *et al.*, 2013).

A closer look at breast cancer pathology, molecular biology, and progression may lead to a better understanding of the underlying factors involved in breast cancer tumorigenesis and metastasis. A particular interest has risen in breast tumour kinase (Brk) also known as PTK6 (protein tyrosine kinase 6). Over a number of years, the Brk research field has grown and Brk has shown as being a desirable therapeutic target in relation to tyrosine kinase inhibition as well as disruption of its kinase independent activity (reviewed in Harvey and Burmi, 2011).

1.1.1 Breast cancer pathological types

Breast cancer malignancies constitute adenocarcinomas, accounting for over 95% of all breast cancers (Kumar et al. 2014). Invasive or infiltrating breast cancer involves invasion of neoplastic cells through the duct wall and into the stoma, of which there are two types including infiltrating ductal carcinoma (IDC) and infiltrating lobular carcinoma (ILC). The variation between these two types is based on the site they originate from (the ducts or the lobes). Ductal carcinoma *in situ* (DCIS) describes a non-invasive proliferation of epithelial cells confined to the ducts, and its features consist of nuclear atypia, potential malignancy capacity and it is usually considered as a precursor for subsequent invasive breast carcinoma (Makki 2015). Lobular carcinoma in situ (LCIS) describes growth of uniform cells originating from the terminal duct lobular unit (TDLU) that, under the microscope, show intact underlying architecture and lobules; however, in comparison to DCIS, there is rarely any pleomorphism, mitosis or necrosis (Hanby, Hughes 2008). IDC constitutes a group of carcinomas which lack specific features to be histologically categorised and thus are known as IDC no specific type (NST) which make up 40-75% of all invasive ductal carcinomas (Moinfar 2007). There is usually a range of morphological variations including pleomorphisms, variation in shape and size, and obvious nucleoli which show numerous mitosis (Hanby, Hughes 2008). Tubular carcinoma is rare and defines a well differentiated IDC characterised by proliferation of elongated tubules with disorganised structure and a single layer of epithelium lining an open lumen with some invasion of the stroma and fat at the periphery of the tumour (Juan 2011). This subtype is more common amongst elderly females and is most likely associated with lymph node metastasis (Makki 2015). Medullary carcinoma is common in patients with breast

cancer susceptibility gene 1 (*BRCA1*) mutations and is characterised by well circumscribed carcinoma, composed of poorly differentiated cells with scanty stroma and lymph infiltration, mucin secretion and no glandular differentiation (Armes, Venter 2002). Invasive papillary carcinoma comprises 1-2% of all invasive breast carcinomas and is predominately an intraductal lesion (Juan 2011).

1.1.2 Breast cancer molecular subtypes

Before the advent of molecular profiling, breast cancers were mainly categorised according to histology, tumour grade, lymph node involvement and presence of predictive markers (Holliday and Speirs, 2011). However due to the advent of high throughput assays, gene expression profiling is now possible. This scientific advance has provided further insight into the molecular characteristics of breast cancer whereby tumour cell response has been shown to be dependent not on only pathological features, but also age and gender as prognostic factors (Weigelt, Baehner and Reis-Filho, 2010). This allows for more specific categorisation of breast cancer, leading to improved diagnosis, more accurate prognosis as well as a better informed therapeutic decisions to provide the greatest clinical response for individual patients (Pusztai *et al.*, 2008).

It has become increasingly more evident which patients will respond better to treatments at the same time allowing clinicians to predict patient prognosis. Due to these differences and the fact breast cancer is not a single disease, it has become difficult to find a treatment that is effective for all subtypes. Since Brk is expressed in over 86% of breast cancers (J H Ostrander *et al.*, 2007) and it's expression is detectable in a range of breast cancer subtypes (Luminal A, B, HER2 positive and triple negative breast cancers), a potential Brk therapy could be beneficial for all types of breast cancers. The characteristics of breast cancer subtypes are further discussed below.

1.1.2.1 Luminal A breast cancer cell lines

Luminal A breast cancer is characterised by the presence of oestrogen (ER) and progesterone receptors (PR) but lacks human epidermal growth factor receptor 2 (HER2) expression. Luminal A breast cancers are associated with more favourable outcomes (Juan, 2011). The Luminal A subtype consists of tubular carcinoma, cribriform carcinoma and low grade infiltrating ductal carcinoma of no specific type (IDC NST) (Makki, 2015). Luminal A subtypes exhibit a lower number of mutations and chromosomal changes in comparison to Luminal B cancers and have reduced number of mutations in their *p53* gene and higher number of mutations in P1K3CA (Koboldt *et al.*, 2012). Oestrogen receptor (ER) is the most prevalent biomarker for categorising breast cancers and has a key role in carcinogenesis of breast cancer (reviewed in Dai *et al.*, 2016). ER positive tumours comprise over 75% of all breast cancer cases and are usually well differentiated histologically as well as being less aggressive in comparison to ER negative breast cancers (Dunnwald, Rossing and Li, 2007). An exact role for progesterone on its own is difficult to elucidate as breast cancers with PR isoforms, PR-A and PR-B can also express ER and require oestrogen for PR-A expression (Lange and Yee, 2008). Furthermore, expression of these isoforms are not induced unless other factors are present, including epidermal growth factor (EGF) (Ankrapp, Bennett and Haslam, 1998).

T47D cells carry receptors for a variety of steroids and calcitonin. They express mutant tumour suppressor protein p53 protein. Under normal culturing conditions, they express progesterone receptor constitutively and are responsive to oestrogen. They can lose the ER during long-term oestrogen deprivation *in vitro* (Yu *et al.*, 2017).

1.1.2.2 Luminal B breast cancer cell lines

Lumina B breast cancer cell lines express low levels of oestrogen receptor, may be progesterone receptor positive or negative as well as HER2 positive (reviewed in Eroles *et al.*, 2012). Although Luminal A and Luminal B are distinct subtypes, there are some molecular similarities. Tumour cells from the Luminal B subtype have higher proliferation rates and more DNA amplifications than those from Luminal A. Luminal B cancers are also characterised by higher levels of chromosomal aberrations than any other subtype and the 'wingless relating integrated site' (WNT) and NOTCH signalling pathways are stimulated, which are involved in regulation of breast tumour initiating cells (TICs) (Sircoulomb *et al.*, 2011). This is of importance, as these TICs, also known as cancer stem cells (CSCs), have been proposed to be involved in *de novo* resistance of breast cancer treatments due to their ability to self-renew and develop new tumour cells which are clonogenically derived from the parental tumour (Wei and Lewis, 2015). The new tumour cells will be resistant to the type of therapy the parental tumour was exposed to therefore rendering the treatment ineffective. Clinically, Luminal B cancers are more aggressive with poorer prognostic outcomes than Luminal A cancers and show increased 5-year relapse rates after diagnosis as well as a metastatic dissemination time pattern similar to basal-like and HER2 subtypes of breast cancer (Ignatiadis *et al.*, 2009). In comparison to Luminal A tumours, Luminal B breast cancers have the tendency to metastasise to the bone more than other metastatic sites (Smid *et al.*, 2008). Neoadjuvant chemotherapy showed greater effect in reducing overall tumour volume in Luminal B cancers than Luminal A (Ades et al., 2014). An example of a Luminal B cell line is BT474 (Kao *et al.*, 2009). Both Luminal A T47D and Luminal B BT474 cell lines form tight cohesive structures exhibiting robust cell-cell adhesions whereas HER2 positive cell line SKBR3 and triple negative cell lines MDA-MB 231 show loose cohesive grape-like

or stellate structures (Kato *et al.*, 2009). Morphologically, both Luminal A and Luminal B types of cells display a similar epithelial structure when viewed under a light microscope (Holliday and Speirs, 2011).

1.1.2.3 Metastatic model cell line

Xenotransplantation success rates of breast cancer into experimental animal models were previously relatively low (7-20%) and there was reportedly little evidence of metastatic growth (Hurst et al., 1993). However, advancements in xenotransplantation over the years have contributed significantly to our understanding of breast tumorigenesis and progression as well as novel therapeutic strategies (Cariati, Marlow and Dontu, 2011). The GI101 cell line is an oestrogen receptor-negative metastatic breast tumour cell line derived from an infiltrating ductal breast carcinoma xenograft. When cells from a tumour derived from an infiltrating ductal adenocarcinoma were injected subcutaneously, the tumour grew slowly and metastasized to the lungs, lymph nodes and bone marrow of athymic murine (Hurst *et al.*, 1993). The GI101 cell line is negative for c-erbB-2 oncogene, but positive for p53 protein and both the tumour implant and lung metastases were negative for ER and PR (Hurst *et al.*, 1993; Allen *et al.*, 2011).

1.1.2.4 HER2 positive breast cancer cell line

Human epidermal growth factor receptor 2 (HER2) positive cancers are usually ER and PR negative and have elevated expression of a proliferation related gene called marker of proliferation of Ki-67 (MKI67) (Smith *et al.*, 2017). The HER2 protein is membrane spanning

and 185 kDa in size, and encoded by the *HER/neu* oncogene on chromosome 17q21 (Schechter *et al.*, 1984). HER2 as a heterodimer with EGFR, is involved in various cancer promoting processes including cell proliferation (Lenferink *et al.*, 2001), inhibition of cell death mechanisms, for example apoptosis (Yarden and Sliwkowski, 2001) as well as promotion of angiogenesis (Wen *et al.*, 2006). A representative of HER2 positive cell line, SKBR3, is a mammalian breast cancer epithelial cell line that overexpresses the *Her2* (Neu/ErbB-2) gene (Fogh, Fogh and Orfeo, 1977). This cell line can form poorly differentiated tumours in immune-compromised mice (van Slooten *et al.*, 1995) and thus is used as a model to study therapeutic effects of drugs, for example, Herceptin that targets HER2 as well as to study therapeutic drug resistance mechanisms.

1.1.2.5 Triple negative breast cancer cell lines

Triple negative breast cancer (TNBC) or basal like breast cancers are characterised by reduced expression of luminal-related genes along with little or no HER2 expression and elevated levels of KMKI67 (Prat *et al.*, 2015). These types of cancers are more difficult to treat in comparison to other subtypes of breast cancer due to the lack of receptor expression which means targeted therapy is not appropriate. Thus most of these cancers are treated with chemotherapy, although treatments are being evaluated as many basal-like cancers are inherently refractory to chemotherapy (Lachapelle and Foulkes, 2011). Nonetheless, a small subset of these cancers show sensitivity to chemotherapy and have a good prognosis (Foulkes, Smith and Reis-Filho, 2010). TNBC cancers account for approximately 10-15% of all breast tumours; they are more clinically aggressive than the other subtypes, and most are diagnosed at a higher tumour grade (Foulkes, Smith and Reis-Filho, 2010). Furthermore,

these tumours have a high number of mutations across the genome, hypomethylation and a high percentage of them are *TP53* and *BRCA1* mutated (Prat *et al.*, 2014). The characterisation of TNBC indicates distinct features including expression of genes linked with both basal epithelium and myoepithelium of the normal mammary gland (Reis-Filho and Tutt, 2007). Claudin low tumours were identified in 2007 as a distinct subtype of TNBC (Herschkowitz *et al.*, 2007). These were characterised by low gene expression of tight junction proteins claudin 3, 4 and 7 as well as E-cadherin, a calcium dependent cell to cell adhesion protein (Prat *et al.*, 2014). Claudin low tumour subtypes lack common epithelial cell features and are enriched with tumour initiating cell (TIC) features (Herschkowitz *et al.*, 2007).

Studies have further identified up to 6 molecular subtypes within the triple negative breast cancer including, basal like, immunomodulatory, mesenchymal, a mesenchymal stem like and a luminal androgen receptor subtype (LAR) which is HER2 enriched (Lehmann *et al.*, 2011). Due to the presence of sub-categories of triple negative breast cancers, there is a lack in a unifying definition and there may still be a need to define and separate basal like and triple negative breast cancers, since they identify different risk factors. Basal like and TNBCs tend to be mainly associated with high grade invasive ductal carcinomas (Lachapelle and Foulkes, 2011). Although this indicates the heterogeneity of TNBC subtype, there is a suggestion that subtyping within triple negative breast cancer may not have a clinical impact based on prognosis (Prat *et al.*, 2015). Treatment with chemotherapy has shown patients with TNBC tend to show greater response despite an overall poorer prognosis compared to other subtypes of breast cancer (Cortazar *et al.*, 2014). Anthracyclines and Taxanes indicate the most effective types of chemotherapy drugs (Henderson *et al.*, 2003; Mazouni *et al.*, 2007). Nonetheless, less than 30% of patients with metastatic breast cancer survive 5 years after diagnosis with cause of death most likely due to metastatic disease (Bonotto *et al.*, 2014).

1.1.3 Breast cancer Risk Factors

Risk factors that have been intensively examined and which actively contribute towards neoplastic transformation of breast cells include gender, age (where women over 40 are at increased risk of developing breast cancer), history of mammary gland diseases including family history of breast cancer, early menarche and late childbearing, menopause as well as race (reviewed in Bucholc et al. 2001). A summary of breast cancer risk factors is shown in Table 1.1. Interestingly most risk factors are only associated with 20-30% of newly diagnosed breast cancer whereas the 70-80% majority indicate no risk factors (reviewed in Kaminska *et al.*, 2015).

Table 1.1 Summary of breast cancer risk factors.

Breast Cancer Risk Factor	**Description**
Gender	Women are at an increased risk of developing breast cancer. Approximately only 390 cases of male breast cancer were diagnosed in the UK in 2014 (Cancer Research UK). Generally, male breast cancer rates are less than 1 in 100,000 (Ly *et al.*, 2013).
Age	Women over the age of 40 are at a higher risk of developing breast cancer. In the UK, 48% of breast cancer cases each year are diagnosed in women over the age of 65 (Cancer Research UK, 2014)
Genetic	Breast cancer relative risk increases with increasing numbers of affected first degree relatives (Dossus and Benusiglio, 2015). A number of breast cancer susceptibility genes have been identified including *BRCA1* (Miki *et al.*, 1994), *BRCA2* (Wooster *et al.*, 1994), *TP53* (Børresen *et al.*, 1992), *ATM* (Athma, Rappaport and Swift, 1996) and *PTEN* (Liaw *et al.*, 1997).
Ethnic background	Frequency of breast cancer occurrence in Caucasian women is higher than in African American women. In addition, African American women are twice as likely to develop triple negative breast cancer (TNBC) than Caucasian women with Hispanic women in-between the two groups (Ban and Godellas, 2014).
Early menarche and late menopause	Breast cancer risk increases in early menarche (relative risk increased by a factor of 1.050 for every year younger at menarche) and late menopause (relative risk increased by a factor of 1.029 for every year older at menopause) (Collaborative Group on Hormonal Factors in Breast Cancer, 2012).
Diet	Certain dietary factors contribute towards the risk of breast cancer development, including high dietary fat intake (Wynder *et al.*, 1997), although data are conflicting due to study bias, data discrepancy and other inherent difficulties involved in obtaining dietary information (reviewed in

	Martin and Weber, 2000). Alcohol also increases relative risk of developing breast cancer (Hamajima *et al.*, 2002).

Intrinsic factors like race are linked with elevated breast cancer risk in studies which used data from Surveillance, Epidemiology and End Results (SEER) databases (Ban and Godellas, 2014). These showed a frequency of occurrence of breast cancer in Caucasian women as approximately 127.4 in 100,000 people whereas the frequency of occurrence of breast cancer in African American women was approximately 121.4 in 100,000 people. Amongst African American women, breast cancer presents at a more advanced stage with more aggressive characteristics as well as a less favourable survival rate in comparison to Caucasian women (Danforth Jr, 2013). Individuals with familial history of breast cancer are at an increased risk of developing the cancer themselves and this is one of the strongest risk factors. Approximately 5-10% of all breast cancers are hereditary (Claus, Risch and Thompson, 1991). Studies comparing cancer incidence in relatives of breast cancer patients shows increasing relative risk (RR) with increasing number of first-degree relatives that are affected with breast cancer (reviewed in Dossus and Benusiglio, 2015). These include inheriting mutations in breast cancer susceptibility genes; *BRCA1* and *BRCA2*. *BRCA1* acts as a tumour suppressor gene which encodes a nuclear phosphoprotein that functions mainly in maintaining genomic stability (Claus, Risch and Thompson, 1991). *BRAC2* functions more specifically in the homologous recombination (HR) pathway which is involved in the repair of double strand DNA breaks and is encoded by a large gene with 27 exons with potential mutations throughout the gene (Apostolou and Fostira, 2013). Germline mutations in these genes, although rare, account for a high proportion of familial breast cancer. Other genes, contributing to risk, include tumour protein 53 *(TP53*), which is a tumour suppressor gene that

encodes the protein p53 and is mutated in approximately half of all cancers including in 20-30% breast cancers with more than 15,000 known mutations (Hainaut, 2013).

Phosphatase and tensin homolog (*PTEN*) is located at the chromosome 10q23 region and encodes a phosphatidylinositol-3,4,5-trisphosphate 3-phosphatase and is another tumour suppressor protein as it negatively regulates the AKT/P13K signalling pathway (Li *et al.*, 1997). Germline mutations in the *PTEN* gene renders individuals with Cowden Syndrome, an autosomal dominant disease that is characterised by hamartomas, at an increased risk of tumours of the thyroid, endometrium as well as breast (reviewed in Apostolou and Fostira, 2013). Most individuals with Cowden Syndrome have a 50% increased risk of developing breast cancer (reviewed in Apostolou and Fostira, 2013).

Other extrinsic factors include dietary habits, although epidemiological data is conflicting for specific food groups. Excess fat intake can contribute to the increase in occurrence of mammary tumours in animal models (Holmes and Willett, 2004). However, large meta-analysis studies also show weak association between polyunsaturated fat and the link to breast cancer (Kotepui, 2016).

Alcohol consumption increases the relative risk of breast cancer by 7.1% for each additional 10g per day intake of alcohol (Hamajima *et al.*, 2002). Alcohol consumption over the recommended amount, which is 14 units a week in the UK, is associated with a linear increase in incidence of breast cancer (Smith-Warner *et al.*, 1998). Alcohol metabolises to reactive oxygen species (ROS), including acetaldehyde, which are known to generate DNA modifications via various mechanisms including protein adducts and chromosomal aberrations (Dorgan *et al.*, 2001).

1.2 Breast Tumour Kinase (Brk)/PTK6

PTKs (protein tyrosine kinases) are products of a large multigene family and mainly function in signalling pathways to regulate cell differentiation, tumour growth, migration and survival (Easty *et al.*, 1997). Many function as oncogenes and are implicated in a large number of cancers. Brk, also known as protein tyrosine kinase 6 (PTK6), was originally identified in a study involving human melanocytes (Mitchell *et al.*, 1994) and was subsequently isolated from breast cancer cell lines in a study identifying novel kinases with therapeutic potential (Mitchell *et al.*, 1994). Brk expression in normal tissue has been indicated in differentiating cells in gastrointestinal tract, oral cavity, skin and prostate (Llor *et al.*, 1999; Derry *et al.*, 2003; Petro *et al.*, 2004). Originally it had been thought there were low or undetectable levels of Brk in normal mammary tissue, however more recently Brk expression has also been detected in the immortalised non-tumorigenic MCF10A human mammary gland epithelial cell line as well as in normal mammary gland tissues (Peng *et al.*, 2014). Since expression has only been more recently detected, this suggests there are relatively very low levels of Brk in normal mammary tissue. Total activity of Brk is significantly higher in malignancy than in normal mammary tissue, and over-expression has been noted in 60-85% of invasive ductal breast tumours (Barker, Jackson and Crompton, 1997; J H Ostrander *et al.*, 2007; Aubele *et al.*, 2009; Harvey *et al.*, 2009).

Differing Brk protein expression levels have been detected in majority of breast cancer cell lines (Barker, Jackson and Crompton, 1997). Gene sequencing indicated similarities with the SRC-family of protein tyrosine kinases, however there are distinct differences such as the lack of N-terminal extension and consensus sequences for fatty acylation and membrane association (Mitchell *et al.*, 1997). Furthermore, its genomic structure is quite distinct from the

SRC-family PTKs, which demonstrates an evolutionary divergence (Mitchell, Sara and Crompton, 2000). Brk gene *ptk6* has also been shown to have a significant degree of similarity with the Drosophila src related gene known as *Dsrc41*, with six out of seven of Brk's exon boundaries conserved with the *Dsrc41* gene which has 9 exons. This could indicate Brk is likely to share a common ancestor with *Dsrc41*. The *ptk6* gene comprises 8 exons, encoding a 451 amino acid protein with FISH studies indicating localization to chromosome 20q13.3 (Mitchell *et al.*, 1997). The protein product has a predicted molecular weight of 50kDa, which generally resolves to around 48kDa on an SDS-PAGE gel (reviewed in Harvey and Burmi, 2011).

1.3 Short isoform - ALT-PTK6

An alternatively spliced Brk transcript which was named originally as λm5 and much later coined as *ALT-PTK6* was also identified (Mitchell *et al.*, 1997; Brauer *et al.*, 2011). This short isoform is 15Kda and 134 amino acids long with a 122 base pair deletion at the 3' end of the SH3 coding region thus it lacks a functional SH2 domain and tyrosine kinase domain but has a C-terminal proline rich sequence (Figure 1.1). Thus far *ALT-PTK6* expression has been shown in breast, colon and prostate cancer cells (Mitchell *et al.*, 1997; Brauer *et al.*, 2011; Peng *et al.*, 2014). Unlike the full-length form, its expression has not yet been reported in normal mammary tissue. The protein expression of ALT-PTK6 has been shown in the T47D cell line along with the full length form (Mitchell *et al.*, 1997). There is still speculation on the role that this isoform plays in breast cancer, however, it is suggested that it could be a competitive inhibitor for the SH3 binding partners of the full length Brk as both possess functional SH3 domains (Mitchell *et al.*, 1997; Brauer *et al.*, 2011)

The localisation of Brk may play an important role in development of cancer since Brk's arrangement in the cellular environment may affect its role due to the variety of substrates available in nucleus and cytoplasm (Ie Kim and Lee, 2009). As it was shown adding a myristoylation sequence to Brk's N-terminal resulted in enhanced oncogenic functions of Brk in cell proliferation, survival and migration whereas adding a synthetic nuclear localisation sequence (NLS) to trap Brk in the nucleus annulled these effects (Ie Kim and Lee, 2009). Also, the role of Brk in various tissue types has shown to be dramatically different. For example, in normal tissues it is involved in regulation of differentiation process (Wang *et al.*, 2005) whereas in tumour cells it promotes cell proliferation and survival (Kamalati *et al.*, 1996; Harvey and Crompton, 2003; Julie Hanson Ostrander *et al.*, 2007). Therefore, Brk's function will depend on the tissue it is expressed in, its intracellular location, and the substrate it interacts with along with its interactions with the shorter isoform. The range of Brk functions dependent on its localisation and substrate/protein interactions are further explored in sections 1.5 and 1.6 below.

The role of ALT-PTK6 has been more fully described within prostate cancer cells, where the full length Brk is expressed in normal and benign tissues as well as in cancerous cells (Brauer *et al.*, 2011). Initially, it was shown that β-catenin was a substrate of Brk (Palka-Hamblin *et al.*, 2010) and now there is indication that the ALT-PTK6 isoform may also be involved in regulation of β-catenin/TCF transcription (Brauer *et al.*, 2011). ALT-PTK6 has been proposed to act as an inhibitor against the full-length form of Brk since there was reduced phosphorylation of tyrosine-phosphorylated proteins as well as phosphorylation of Brk in the presence of ALT-PTK6 which was further decreased with increasing levels of ALT-PTK6 (Brauer *et al.*, 2011). In co-transfection experiments with full length of Brk and ALT-PTK6, increased ALT-PK6 expression resulted in an increase of constitutively active form of Brk in the nucleus with a decreased proportion at the membrane (Brauer *et al.*, 2011). There was

also reduced proliferation in ALT-PTK6 expressing prostate tumour cells compared to those without this short isoform. These data therefore suggest that ALT-PTK6 may contribute towards limiting Brk localisation to the nucleus and acting as a competitive inhibitor thus reducing the ability of Brk to interact with its substrates that promote tumour cell growth in the cytoplasm and plasma membrane. Further clarification and confirmation is needed for specificity in breast cancer cell lines. Also, PTK6 down regulation was shown to promote tumorigenicity and metastasis via an altered Akt/GSK3β/β-catenin signalling pathway; thus, a closer look at the interaction between ALT-PTK6, PTK6 and β-catenin in different tissue types and cell lines may give a more accurate overview of its role. Furthermore, it should be noted Brk's substrates include RNA binding proteins sam68, SLM1 and SLM2 (Derry *et al.*, 2003; Haegebarth *et al.*, 2004) which have reported roles in RNA splicing (Paronetto *et al.*, 2007) thus it is possible that Brk may regulate alternative splicing. In addition, sam68 contains at least five proline rich splicing motifs which interact with SH3 domain of *Src* (Taylor and Shalloway, 1994), which shares homology with Brk. More specifically, via a Glutathione S-transferase (GST) pull down approach, it was determined the GST-P3 proline motif of sam68 was the main polypeptide that mediated interaction with Brk SH3 domain (Derry *et al.*, 2000). This suggests sam68 may also interact with ALT-PTK6 via the SH3 domain and thus have a role in the splicing process and regulation of itself as well as the full-length form.

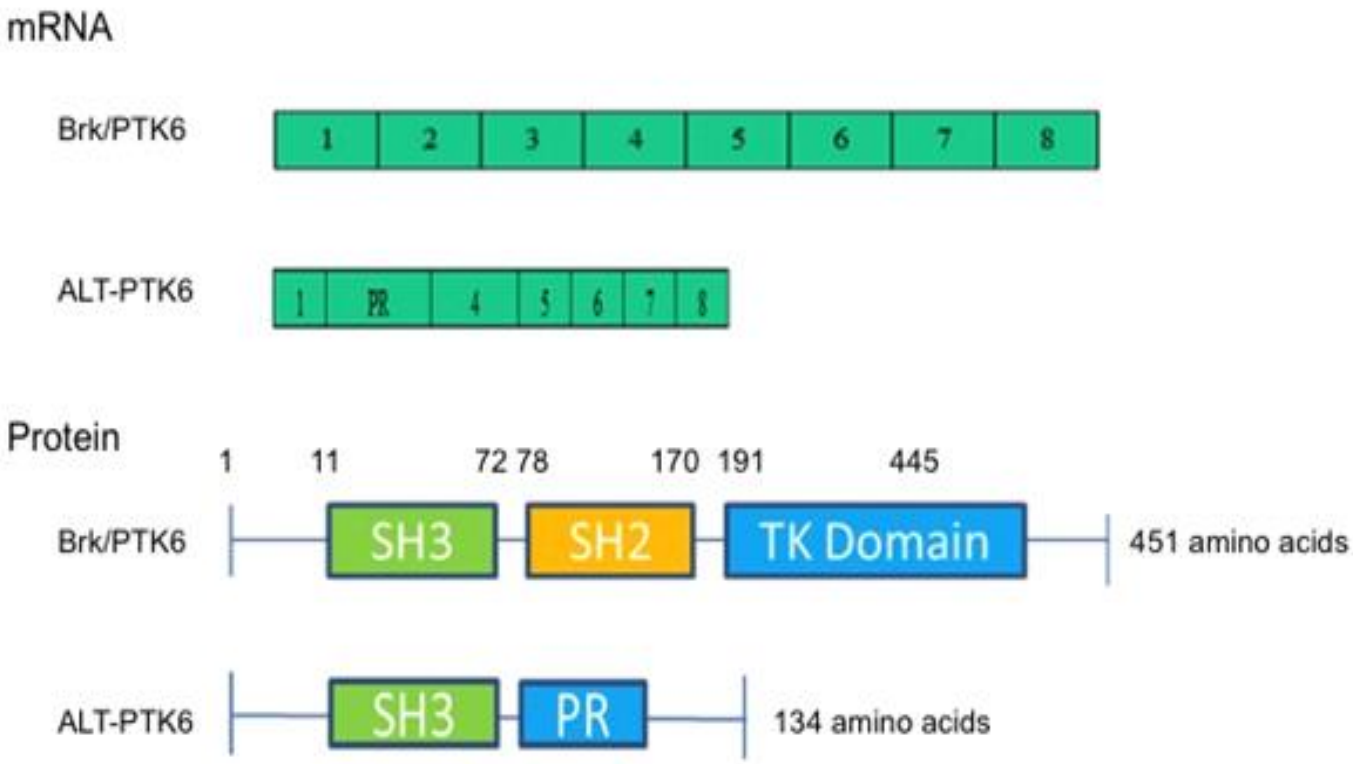

Figure 1.1 Full length BRK/PTK6 and short isoform ALT-PTK6 structure Indicating: the cDNA structure of both isoforms, with each box indicating each exon (total of 8 exons). ALT-PTK6 has deletion at exon 2 and lacks SH2 domain due to shift in open reading frame, which gives a proline rich sequence at exon 3 instead of a SH3 domain. Underneath, the protein structure shows SH3 domain in green, SH2 domain in orange and a tyrosine kinase domain for Brk/PTK6 or proline rich sequence for ALT-PTK6 in blue (Hussain and Harvey, 2014).

1.3.1 Brk and ALT-PTK6 structure

As discussed above in Section 1.3, Brk consists of SH2, SH3 a linker region and catalytic domains (Figure 1.1). SH3 domains are small protein domains made up of β-sheets that allow the assembly of specific protein complexes via proline-rich peptide binding, (reviewed in Mayer, 2001). Brk's SH2 and SH3 domains are used for substrate recognition (Hong *et al.*, 2001; Qiu and Miller, 2004). The Brk SH3 domain has been known to undergo conformational changes due to pH fluctuations indicating that its structure could determine substrate and protein interaction. The SH3 domain may also have a role in enzyme regulation, as a proline rich peptide that binds to the SH3 domain of the Src family of kinases was able to activate wild type Brk (Qiu and Miller, 2002). The importance of the SH3 domain in enzyme regulation of Src kinases has been well documented previously (reviewed in Engen *et al.*, 2008) suggesting similarly the SH3 domain of Brk may also play a role in enzyme regulation (Qiu and Miller, 2002). In addition, The SH2 domain contains α/β folds and a phosphotyrosine binding surface with two α-helices opposite a central β-sheet made up of four anti-parallel strands (Hong E et al 2004). This domain plays a role in protein-protein interactions and is important for regulation of catalytic activity (Hong *et al.*, 2001). Due to the lack of myristoylation and a nuclear localization sequence (NLS), Brk's regulation is difficult to determine which allows for more flexibility with its subcellular localization, (reviewed in Harvey and Burmi, 2011). It has been proposed that Brk can 'piggy back' onto other protein complexes and thus is able to travel to and from the nucleus or it may simply diffuse from one cellular localisation to another (reviewed in Harvey and Burmi, 2011).

1.4 Brk Expression in different tissues

Brk activity is increased in malignant melanomas which may be due to upregulation of normal melanocytic kinases or due to expression of additional PTKs (McArdle *et al.*, 2001). *ptk6* expression has been shown in metastatic melanomas but not in primary melanomas or normal melanocytes (Easty *et al.*, 1997). Brk protein expression was also reported in the normal gastrointestinal tract, oesophagus, stomach, and duodenum (Llor *et al.*, 1999). More specifically, within the small intestine, Brk is present in the non-dividing villus epithelium and has shown to be involved in negatively regulating Akt, resulting in growth inhibition and increased villus heights as seen in *ptk6* null mice (Haegebarth *et al.*, 2006) . Brk expression has also shown to be downregulated in over 93% of oesophageal squamous cell carcinoma (ESCC) compared to non-tumorous oesophageal tissue (Ma *et al.*, 2012).

Brk expression has been detected in normal luminal prostate epithelial cells as well as in secretory epithelial cells of prostate adenocarcinomas (Brauer *et al.*, 2011). Brk expression has also been detected in normal oral epithelial cells and oral squamous cell carcinoma. In normal ovarian surface epithelium Brk expression is undetectable but overexpressed in high grade serous ovarian tumours (Schmandt *et al.*, 2006).

Brk expression was detected in normal T cells and malignant T cells, where it was expressed in a constitutively active form suggesting a role for Brk in pathogenesis of lymphomas (Kasprzycka *et al.*, 2006) . Most malignant T cell lines expressed Brk at higher levels and there was also Brk expression in normal B lymphocytes and malignant B cell lymphomas. Brk expression in head and neck cancers was first described in 2004 (Lin *et al.*, 2004), where over 37% of head and neck squamous cell carcinomas overexpressed Brk. Furthermore, up-regulation of Brk in thyroid tumours relative to normal thyroid tissue was noted (Cho *et al.*, 2012).

In non-small cell lung cancer (NSCLC), Brk was first identified in a study investigating oncogenic kinases in lung cancer and was shown to be over phosphorylated (Rikova *et al.*, 2007). Brk levels were higher in the cytoplasm of NSCLC compared to nuclear localisation. High expression levels did not associate with differentiation of NSCLC but rather with increased tumour size in NSCLC suggesting a role for Brk in tumour growth.

Unlike melanocytes, Brk expression was shown in normal colon and adenocarcinomas of the colon. There was a moderate increase in Brk expression levels in adenocarcinomas of the colon (Llor *et al.*, 1999). Chromosome 20q13, to which the *ptk6* gene is localised, is over amplified in not only breast tumours but also in gastro-oesophageal tumours (El-Rifai *et al.*, 1998) and colon tumours (Schlegel *et al.*, 1995). Within the context of colon tumours, the increase in expression was not enough to indicate gene amplification as the cause for overexpression. Brk is found in both the nucleus and cytoplasm (Llor *et al.*, 1999).

In terms of localisation, Brk in oesophageal squamous cell carcinoma (ESCC) is detected in the nucleus and the cytoplasm (Ma *et al.*, 2012). In normal luminal prostate epithelial it is highly localised to the nucleus and in secretory epithelial cells in prostate adenocarcinomas its localisation is altered (Derry *et al.*, 2003). It was noticed there was lower nuclear expression in high grade regions and higher nuclear expression in low grade regions of prostate tumours. Brk localised to the nucleus in normal prostate cells and the cytoplasm in prostate tumours. Knock down of Brk, which was mostly confined to the cytoplasm in prostate cancer cell lines, resulted in decreased cell proliferation (Brauer *et al.*, 2011). It is localised to both the nucleus and cytoplasm in normal oral epithelium and oral squamous cell carcinoma (Petro *et al.*, 2004). However; as with prostate tumours, in oral squamous cell carcinomas Brk nuclear levels are decreased with tumours that are poorly differentiated compared to those that are well differentiated (Petro *et al.*, 2004). In ovarian cancer cells, Brk is localised to the cytoplasm however in some ovarian tumour cells Brk was also detected

in the nucleus (Schmandt *et al.*, 2006). Brk was localised in the nucleus of lymphocytes within both T and B cell malignant lymphoma cell lines (Kasprzycka *et al.*, 2006). Furthermore, Brk expression in normal and in non-small cell lung cancer (NSCLC) has been indicated in both the nucleus and cytoplasm (Fan *et al.*, 2011).

Overall, this shows the range of tissues Brk expression is detected, suggesting a potential Brk targeted therapy may be beneficial in a range of cancers. This also shows the impact of localisation considering cytoplasmic Brk mainly shows oncogenic functions for Brk as higher Brk levels are detected in cytoplasm compared to nuclear Brk in tumour cells. This is further supported by Kim and Lee studies which showed adding a myristoylation sequence to Brk's N-terminal resulted in enhanced oncogenic functions of Brk in proliferation, survival and migration of tumour cells whereas adding a synthetic nuclear localisation sequence (NLS) to trap Brk in the nucleus negated these effects (Ie Kim and Lee, 2009).

1.5 Brk substrates and protein interactions

It has been previously reported there were over 30 Brk interacting proteins that have been identified (reviewed in Harvey and Burmi, 2011), however, a number of additional interactions have since been identified including; hypoxia inducible factor 1-alpha (Regan Anderson *et al.*, 2013) as a regulator of Brk, identification of Brk as a novel substrate of phosphatase and tensin homolog (PTEN) (Wozniak *et al.*, 2017), induction of Brk expression by glucocorticoid receptor (GR) in triple negative breast cancers (Regan Anderson *et al.*, 2016), downregulation of tumour suppressor Dok1 by Brk (Miah *et al.*, 2014) and inhibition of calpain 1 activity via HER2 increasing Brk stability and upregulating calpastatin (Ai *et al.*, 2013) Table 1.2 shows a summary of Brk substrates and interacting proteins. This is an indication of the wide variety of pathways Brk is involved in. Although Brk is capable of phosphorylating

some of these and others may bind directly with Brk, there is still speculation on how the other interactions are mediated.

Table 1.2 Summary of known Brk substrates and interacting proteins, adapted from (Harvey and Burmi, 2011). Proteins marked with (*) show Brk substrates.

Brk substrate/interacting Protein	**Localisation**
EGFR	Membrane
HER2	Membrane
HER3	Membrane
HER4	Membrane
IGF-1R	Membrane
*ARAP1	Membrane-associated
*AKT	Cytoplasmic/Membrane-associated
ADAM-15A	Membrane
ADAM-15B	Membrane
*β-Catenin	Membrane/Cytoplasmic/Nuclear
*KAP3A	Cytoplasmic/Nuclear
*STAT3	Cytoplasmic/Nuclear
*STAT5a/b	Cytoplasmic/Nuclear
Insulin Receptor Substrate-1	Cytoplasmic/Membrane-associated
*Insulin receptor Substrate-4	Cytoplasmic/Membrane-associated
ERK5	Cytoplasmic
ERK	Cytoplasmic
MAPK	Cytoplasmic
*PTEN	Cytoplasmic
*Paxillin	Cytoplasmic

*BKS-STAP-2	Cytoplasmic
*GNAS	Cytoplasmic
*FL139441	Cytoplasmic
GAPA-p65	Cytoplasmic/Membrane-associated
*Sam68	Nuclear
*SLM-1/*SLM-2	Nuclear
PSF	Nuclear
*β-Tubulin	Cytoplasmic
*p190 Rho GAP	Cytoplasmic
23KDa	Cytoplasmic
100kDa	Cytoplasmic
HIF-1α	Nuclear
Glucocorticoid receptor (GR)	Nuclear
Dok1	Cytoplasmic/Nuclear
Calpain 1	Membrane
*Esp8	Membrane

Of the many interacting proteins, ARAP1 is a membrane associated protein. ARAP1 (also known as Arf-GAP, Rho-GAP, ankyrin repeat and pleckstrin homology (PH) domain containing protein 1) protein displays RHO-GAP and phosphatidylinositol (3,4,5) trisphosphate (PIP3)-dependent ARF-GAP activity. The encoded protein is thought to be involved in cell specific trafficking of a receptor protein involved in apoptosis. Co-immunoprecipitation assays of proteins interacting with Brk revealed ARAP1 as an interacting protein (Kang *et al.*, 2010). Upon further investigation, it was shown binding of ARAP1 with Brk decreased in serum-depleted conditions showing there was some growth factor involvement. EGFR has shown to interact with Brk suggesting it may be involved in stimulating ARAP1 binding to Brk (Kamalati *et al.*, 1996). When using a EGFR inhibitor, the association between Brk and ARAP1 was blocked (Kang *et al.*, 2010). Furthermore, Brk's catalytic activity was needed for full interaction with ARAP1, in some cases Brk's catalytic activity is required for binding whereas at other times it is not required as with the sam68 protein (Derry *et al.*, 2000). This is important due to Brk having kinase independent functions suggesting that inhibiting the catalytic domain may not always be enough to inhibit Brk's oncogenic role.

Sam68, SLM1 and SLM2 are members of the signal transducers and activators family which are involved in regulation of RNA metabolism. Sam68 (Src-associated protein in mitosis of 68 kDa) functions in regulation of transcription as well as post-transcriptional alterations including alternative splicing resulting in mRNA variability (reviewed in Sánchez-Jiménez and Sánchez-Margalet, 2013). SLM1 and SLM2 are sam68 mammalian like proteins with approximately 70% sequence homology, with SLM1 interacting with many of the same proteins as sam68 (Chen *et al.*, 1999) and SLM2 interacting with RNA binding motifs (UA rich sequences) (Feracci *et al.*, 2016) thus both proteins are involved in post transcriptional regulation of gene expression, similar to sam68. Furthermore, both proteins are involved in

regulation of alternative splicing sites transcripts encoded by CD44 minigene (Stoss *et al.*, 2001, 2004). SLM1 and SLM2 proteins have been shown to be substrates of Brk (Haegebarth et al., 2004). With increasing expression of Brk, there is increased phosphorylation of SLM1 and SLM2 and nuclear retention of Brk which indicates Brk localisation plays a role in the varying functions of Brk. SLM1 shows much similarity with sam68 including interacting with the same proteins and SLM2 showed the ability to interact with RNA-binding motif (UAAA), since sam68 was identified as a substrate, these two were predicted to also interact with Brk (Haegebarth *et al.*, 2004). Brk showed significant degree of specificity when binding to sam68, SLM1 and SLM2 along with selectively phosphorylating these proteins as opposed to other KH -domain containing proteins (Haegebarth *et al.*, 2004). Upon closer investigation with RNA -binding studies involving activated Brk and vector, there was a clear indication of Brk negatively regulating the RNA binding abilities of sam69 and the sam68 -like mammalian proteins.

Brk has shown binding with the ADAM family of proteins. These are transmembrane proteins containing disintegrin and metalloprotease domains thus allowing for cell adhesion and protease functions. There are over 25 variants within the human family, some still without a clear function, but most are involved in cell adhesion, cell fusion, proteolysis as well as intracellular signalling (reviewed in Giebeler and Zigrino, 2016). Brk associates specifically with ADAM-15 which is mainly involved in cell adhesion and cell to cell interactions. These functions of ADAM-15 may have significance in cancer progression due to its association with tumour cell invasion, migration and metastasis (Zhong *et al.*, 2008). In relation to breast cancer, it has been shown that ADAM-15 may be an indicator of disease free survival for patients with breast cancer, there was a clear link between poor survival in node negative patients and ADAM-15 expression (Zhong *et al.*, 2008). Brk showed strong binding to the ADAM-15A and ADAM-15B variants and no association with ADAM-15C, and patients

associated with poor relapse-free survival showed high expression of ADAM-15A and ADAM-15B whereas patients with favourable outcomes had high expression of ADAM-15C.

Another interesting substrate of Brk is Akt, which Brk has shown to influence indirectly via regulation of ErbB3 which results in potentiated activation of Akt (Kamalati *et al.*, 2000). Akt is involved in cell proliferation, and phosphorylation of various substrates and alterations within the P13K and Akt proteins or components in the pathway are involved in cancer progression and development (Osaki, Oshimura and Ito, 2004). Further investigations revealed that Brk directly interacts with Akt as immunoprecipitation studies showed Akt and Brk associations (Zhang *et al.*, 2005). More interestingly for breast cancer cell lines, Brk-Akt complexes did not dissociate upon EGF stimulation whereas the alternative is true in keratinocytes and fibroblast-like cell lines derived from monkey kidney tissue known as COS-1 cells (Zhang *et al.*, 2005).

STAT3 and STAT5 are also recognised as substrates of Brk and are involved in cellular processes leading to cell proliferation, migration and survival (Liu *et al.*, 2006; Weaver and Silva, 2007; Gierut *et al.*, 2011). STAT3 is regarded as an oncogene, with tyrosine phosphorylation of STAT3 connected to breast cancer development as discussed in (Gierut *et al.*, 2011). Activation of STAT3 by Brk may contribute towards cell transformation and uncontrolled growth in initial stages of breast cancer. Brk also mediates STAT3 regulation in established tumours (Liu *et al.*, 2006), and constitutive activation of Brk accelerated cell migration and tumour growth *in vivo* (Miah, Martin and Lukong, 2012). More specifically in breast cancer, Brk suppression in HER2 positive and negative breast cancer cell lines resulted in reduced cell migration indicating a role for Brk in cell migration in a EGFR-family independent manner (Miah, Martin and Lukong, 2012). This study suggests that Brk's promotion of cell migration may require the full activation of Brk.

1.5.1 Brk and Her2 interactions

In cancer cells, alterations in HER receptors or in their downstream signalling components are known to occur; HER2 is a negative prognostic factor, the presence of which indicates aggressive phenotype and reduced overall survival rate reviewed in (Montemurro and Scaltriti, 2013), although it should be noted that survival rates for HER2 positive cancers are improving due to the introduction of targeted therapies (Rugo *et al.*, 2012).

HER2 is overexpressed in approximately 20-30% of breast cancers (Hayes and Thor, 2002) and it has been suggested that Brk may be involved in regulation of signal transduction from HER tyrosine kinases. Several studies have shown a link between *HER2/neu* expression and *PTK6* (Zhao *et al.*, 2003; Born *et al.*, 2005; Aubele *et al.*, 2007; Xiang *et al.*, 2008).

This is of interest because HER2 targeted therapy, although clinically proven to be effective, does pose some restrictions such as lack of effect in some HER2/neu positive cancers as well as resistance. Therefore, a Brk targeted therapy maybe of clinical benefit especially when used in combination with existing HER2/neu targeted therapy. Due to the strong correlation between Brk and HER2, there is evidence suggesting that it may also be linked with prognosis thus indicating a role for Brk as a prognostic factor in breast cancer. Brk expression studied in 426 breast cancer cases further supports its potential as an independent prognostic factor regardless of morphological and molecular markers such as lymph node involvement, tumour size and HER2 status (Aubele *et al.*, 2008). Co-expression of Brk and HER2 has been linked to co-amplification of both the *ErbB2* and *ptk6* genes (Xiang *et al.*, 2008), although this is not a consistent finding in other patient studies (Irie *et al.*, 2010). It is worth noting that although HER2 is over expressed in 20-30% of breast cancers (Hayes and Thor, 2002), Brk is over

expressed in up to 86% of breast cancers (Harvey *et al.*, 2009), which indicates that in the majority of breast cancers Brk is over expressed independently of HER2 status.

At a protein level, Aubele and colleagues showed that Brk forms protein complexes with HER2 using paraffin-embedded tissues from invasive breast carcinomas (Aubele *et al.*, 2010). The effect of simultaneous knockdown of Brk and HER2 was analysed in the Herceptin-resistant cell line JIMT-1 (Ludyga *et al.*, 2013). The results indicated significant reduction in phosphorylation of important signalling intermediates, namely, ERK and p38MAPK and PTEN, which are involved in regulating tumorigenesis. More specifically for PTEN, which is a tumour suppressor, phosphorylation at Ser380/Thr382/383 reduces its activity as a tumour suppressor (Vazquez *et al.*, 2000). Furthermore, there was reduced migration and invasion of JIMT-1 cells when expression of both proteins was suppressed. HER2 may also be involved in elevating Brk levels via upregulating calpastatin and inhibiting calpain-1 activity in breast cancer cells (Ai *et al.*, 2013).

These combined data further support the study of dual inhibition of Brk and HER2, firstly for a greater clinical effect and secondly to overcome anti-HER2 therapeutic resistance.

1.5.2 Brk and EGFR interactions

ErbB signalling in breast tumour progression has been extensively documented. EGFR tyrosine kinases have been involved in regulation of normal and abnormal cellular proliferation and survival reviewed in (Kim and Muller, 1999). Both EGFR and HER2 are intrinsically linked; HER2 potentiates EGFR signalling by enhancing binding ability of EGF

and reducing its degradation and studies have indicated that HER2 signalling is reduced via EGFR-specific inhibitors (Moasser *et al.*, 2001).

The EGF receptor family are linked to the tumorigenic transformation of breast epithelial cells. When Brk-transfected mammary epithelial cell lines, MCF10A and Hb4a, were treated with human growth factors (EGF), mitogenic activity of Brk was observed. This reveals Brk's role in sensitizing human mammary epithelial cells to growth factors such as EGF (Kamalati *et al.*, 1996). Furthermore, Brk association with the EGF receptor has also been detected, even in the absence of EGF, leading to proliferation of epithelial cells. EGFR expression also plays a role in keratinocyte differentiation (Tran *et al.*, 2012), a process in which Brk is involved (Tupper, Crompton and Harvey, 2011). Inhibition of EGFR signalling during differentiation induces growth arrest; however, Brk's promotion of EGFR signalling suggests that one of its roles may involve promoting cell survival during early differentiation.

EGF stimulation results in rapid phosphorylation of Brk indicating the involvement of Brk in the EGF signalling complex (Kamalati *et al.*, 2000). EGF binding to its receptor, EGFR, not only induces its phosphorylation but also the phosphorylation of other EGFR family members (HER2, 3 and 4). The expression of Brk therefore not only increases phosphorylation of EGFR and HER2 but also of HER3 (erbB3) in breast cell lines (Kamalati *et al.*, 2000). It may do this via direct interaction with an erbB3-containing complex in response to EGF stimulation. Brk's ability to enhance EGFR signalling could be mediated by inhibition of EGFR downregulation (Li *et al.*, 2012), which is achieved by phosphorylation of either ARAP-1 (Kang *et al.*, 2010) or c-Cbl (Kang and Lee, 2013), thereby prolonging EGFR signalling.

Expression of Brk enhances EGF-induced ErbB3 phosphorylation and recruitment of P13K to ErbB3 thus inducing P13K activity (Kamalati *et al.*, 2000). Since the P13K pathway is implicated in breast cancer and is linked with resistance to HER2 targeted therapies, its

interaction with Brk may give a wider overview of the mechanisms involved in developing resistance. P13K has been a desirable therapeutic target of its own and current therapies focus on anti-mTOR agents, tyrosine kinase inhibitors and P13K inhibitors reviewed in (Baselga, 2011). However, to create a greater clinical effect, combinations of these treatments including a potential Brk tyrosine kinase inhibitor maybe more useful and reduce the activation of compensatory feedback loops which could decrease efficacy of single agents. Since Akt is a known substrate of Brk, and Brk negatively regulates its phosphorylation in epithelial cells, the potential consequences of this therapy may need to be fully assessed (Haegebarth *et al.*, 2006). Nonetheless, due to most of the normal cells that express Brk being outside the proliferative areas of the tissues, Brk targeted therapy may still be highly specific reviewed in (Harvey and Crompton, 2004).

Overall Brk prolongs EGFR signalling, sensitises tumour cells to EGF stimulation, inhibits the degradation of EGFR and reduces the sensitivity of EGFR inhibitors in Brk overexpressing cells. This suggests Brk inhibition could reduce tumour proliferation and growth via reduced EGFR signalling and increase EGFR inhibitor sensitivity.

1.5.3 Brk and IGF interactions

Insulin receptor substrate 4 (IRS-4) is part of the insulin receptor substrate family, which also contains IRS-1, IRS-2 and IRS-3. Their function includes a variety of biological effects such as cell proliferation, growth, survival and differentiation downstream of insulin and insulin-like growth factor 1 (IGF-1) receptors (reviewed in Sachdev, 2008). IRS-4, upon IGF-1

stimulation, is phosphorylated which leads it to binding to P13K activating the MAPK pathway. The link between insulin-like growth factor (IGF) and breast cancer has been well documented; the IGF-1 receptor is significantly overexpressed in tumour cell lines compared to normal breast cancer epithelial tissue and benign tumours reviewed in (Zeng and Yee, 2007) and there is also a clear correlation between poor breast cancer prognosis and overexpression of IGF-1R (Klinakis *et al.*, 2009). In the MCF-7 breast carcinoma cell line, IGF stimulation results in Akt activation leading to cell proliferation through phosphorylation of Raf kinase. Along with this, IGF stimulation leads to resistance to anoikis (Irie *et al.*, 2010), a process whereby epithelial cells undergo apoptosis due to loss of interaction with neighbouring cells and the basement membrane (Frisch and Francis, 1994). Overexpression of IGF-1R is also implicated in resistance against breast cancer therapy, especially against Herceptin (reviewed in Fink and Chipuk, 2013).

Immunoprecipitation and mass spectrometry have shown IRS-4 substrate interaction with Brk in co-transfected HEK 293 cells (Qiu *et al.*, 2005). In addition to this interaction with IRS-4, Brk also co-precipitates with IRS-1 and IGF-IR (Irie *et al.*, 2010). The interaction of Brk with IGF-IR as well as EGFR and HER2 gives an indication of the range of Brk activity in regulating signalling. EGFR, HER2 and IGF-1R are overexpressed in different subsets of breast cancers whereas Brk is overexpressed in majority of breast cancers and has a role in each of these signalling pathways, thus making it an attractive therapeutic target for disrupting signalling cross-talk. Since Brk interacts with IGF-1R, disrupting this association may also reduce the chance of developing resistance against current breast cancer therapies such as Herceptin, through HER2-IGF-R1 heterodimer formation resulting in phosphorylation and activation of HER2 (reviewed in Bender and Nahta, 2008). Figure 1.2 shows the summary of Brk interactions with HER2, EGFR and IGF as well as some other substrates or interacting proteins involved in the complex signalling pathways that lead to the activation of signalling

intermediates resulting in increased cell proliferation, migration and reduced cancer cell death in breast cancer.

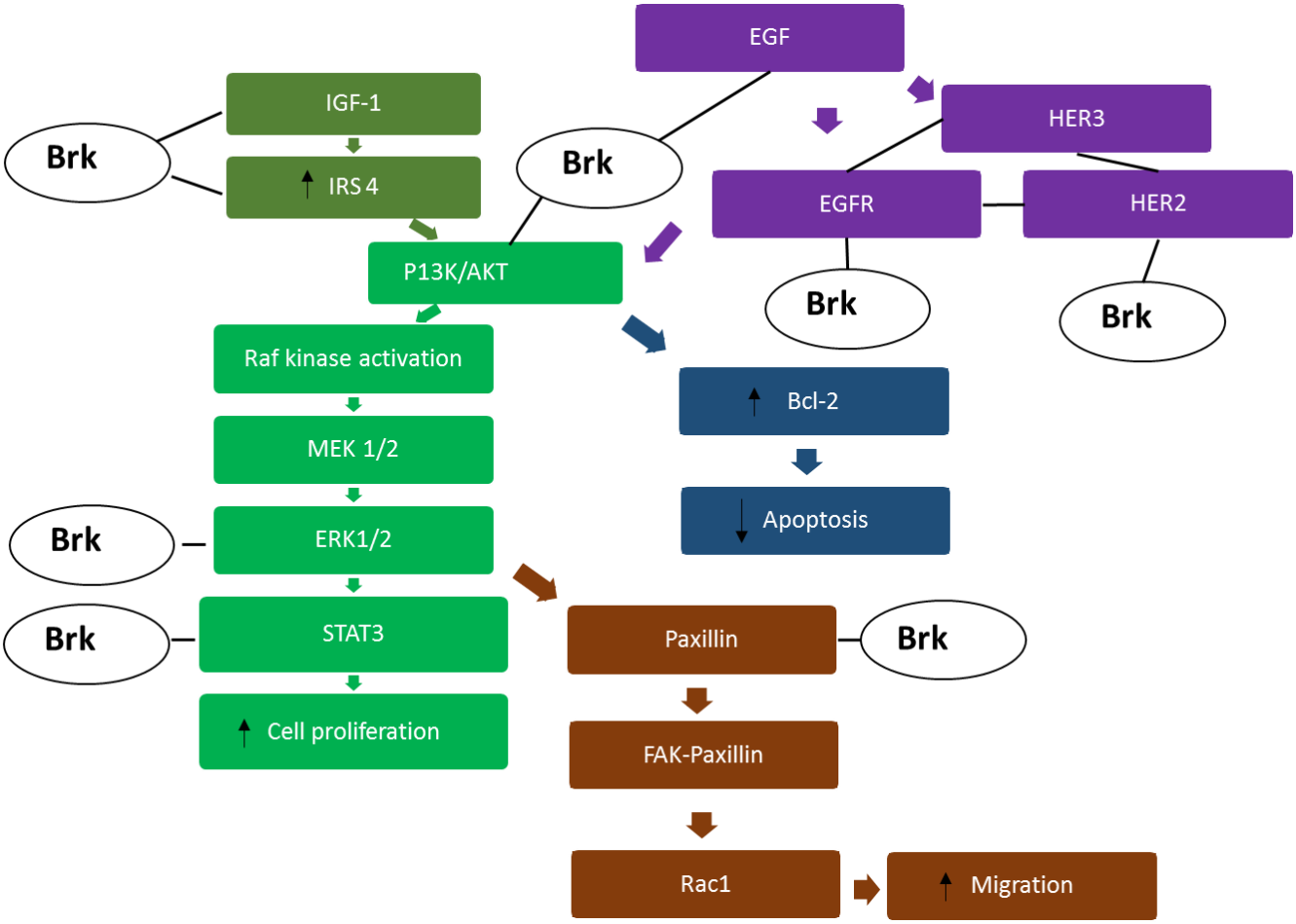

Figure 1.2 Summary of Brk interactions in the signalling pathways leading to increased breast cancer cell proliferation, migration and reduced cell death. Brk interacts with IRS-4 (Qiu *et al.*, 2005) and co-precipitates with IGF-1R (Irie et al., 2010). IRS-4, upon IGF-1 stimulation, is phosphorylated which leads it to binding to P13K activating the MAPK pathway and resulting in increased cell proliferation. EGF stimulation results in rapid phosphorylation of Brk (Kamalati *et al.*, 2000) and leads to HER3 phosphorylation and recruitment of P13K to HER3 thus inducing P13K activity. EGF stimulation also results in Brk phosphorylation of paxillin leading to increased cell migration and invasion (Chen et al., 2004). Brk forms protein complexes with HER2 (Aubele et al., 2010). Simultaneous knockdown of Brk and HER2 results in reduced phosphorylation of important signalling intermediates such as ERK and p38MAPK as well as reduced cancer cell migration and invasion (Ludyga et al., 2013). Brk overexpression increases ERK1/2 activity (Ono, Basson and Ito, 2014). Activation of STAT3 by Brk contributes toward cell transformation and uncontrolled growth (Liu et al., 2006). P13/AKT activation leads to Akt phosphorylation and inhibition of pro-apoptotic Bcl-2 family members thus reducing apoptosis of cancer cells. Furthermore, Brk oncogenic functions include protecting breast cancer cells from autophagic induced death under anchorage independent conditions (Harvey et al., 2009).

1.6 Brk and Differentiation

One of the major roles of Brk within normal tissues is inducing cellular differentiation as indicated in tissues of skin and intestine (Llor *et al.*, 1999; Wang *et al.*, 2005). Keratins are fundamental components of cytoskeleton and have roles in integrity as well as mechanical stability (reviewed in Moll, Divo and Langbein, 2008) and changes in keratin expression in the epidermis are particularly important. For example, during wound healing or other hyperproliferative conditions such as cancer, epidermal expression of some keratins including keratin 10 is significantly reduced (Santos et al., 2002). Keratin 10, a type I keratin, is expressed in post-mitotic suprabasal keratinocytes of the skin and is involved in suppressing cell proliferation and tumour formation in skin cells (Chen et al., 2006). Brk has been detected within the epidermis of the skin mainly in differentiating layers in the suprabasal keratinocytes (Wang *et al.*, 2005). This was shown in immortalized non-tumorigenic HaCaT cell lines which closely resemblance differentiation pattern of primary keratinocytes. It was hardly detected in basal layer and was more abundant in the differentiating layer. It has been indicated Brk expression is more intense in well differentiated squamous cell carcinoma (Wang *et al.*, 2005). Indirect immunofluorescence indicated an increased up-regulation of Brk during keratinocytes differentiation; calcium addition was shown within this study to enhance Brk kinase activity. After transfection of Brk, there was increased expression of Keratin10, indicating Brk is involved in regulation of keratinocyte differentiation in some way. Brk also been shown to be involved in enterocyte differentiation within colon cells (Haegebarth *et al.*, 2006). Earlier studies indicated enhanced expression of the epidermal differentiation marker, filaggrin, within differentiating cells (Vasioukhin and

Tyner, 1997). This further suggests a role for Brk in epithelial cell differentiation. There is some speculation that inhibition of Akt may be involved in the differentiation process as inhibiting Akt may allow for efficient cell cycle exit and differentiation (Haegebarth *et al.*, 2006). Further to this, Brk protein levels in normal adult human keratinocytes decreased as cells became more terminally differentiated in *vitro* (Tupper, Crompton and Harvey, 2011). Brk suppression resulted in increased number of cells incorporating trypan blue which is an indication of early keratinocyte differentiation. It was proposed Brk may promote survival in early keratinocyte differentiation and the subsequent decrease may be a result of the requirement of the differentiation process of primary cells.

1.7 Brk in cell proliferation and cell cycle progression

It has been shown that Brk can increase breast cancer cell proliferation as well as anchorage independent growth (Harvey and Crompton, 2003; Harvey *et al.*, 2009; Chan and Nimnual, 2010) as well as sensitize mammary epithelial cells to growth factors such as epidermal growth factor (EGF) (Kamalati *et al.*, 1996). Since Brk has shown to phosphorylate Akt on the tyrosine, which results in inhibition of Akt within COS-1 cells, there is some evidence that it may be involved in negative regulation of growth (Haegebarth *et al.*, 2006). However, this role may be dependent on the tissue type and substrate or protein interactions as Brk has largely cell proliferating and cell growth roles in various tumour cell lines including breast tumour cells (Kamalati *et al.*, 1996). Furthermore, Brk's localisation within the cellular compartments may also contribute towards its function in cell proliferation as it has been reported that Brk's interaction with Akt resulted in promotion of cell growth and cell proliferation (Zheng and Tyner, 2013). Studies have indicated knockdown or suppression of

Brk in Brk-expressing cell lines such as SKBR3 (a HER2 positive cell line), T47D (ER positive cell line) and MDA-MB-231 (triple negative cell line) resulted in decreased cell proliferation of up to a 60% decrease in cell population (Chan and Nimnual, 2010).

To some extent, Brk's role in cell proliferation and its ability to promote cell cycle progression may contribute towards breast cancer development. Cell cycle deregulation has been known to contribute towards neoplasia, progression to mitosis is tightly controlled by cyclins and cyclin dependent kinases (Chan and Nimnual, 2010). The kinase activity of these CDKs is inhibited by CDK inhibitors such as CDK1 (p27) which is deregulated in cancers. Brk has shown to down regulate p27, which leads to a disruption in the cell cycle progression and cells enter S phase in a growth factor independent manner (Chan and Nimnual, 2010). Previously, Brk suppression has shown a significant reduction in DNA synthesis which indicated that cells were progressing through S-phase at a slower rate (Harvey and Crompton, 2003). It has been shown that Brk may downregulate p27 expression as suppression of endogenous Brk showed an increase in p27 levels in MDA-MB 231 breast cancer cells and this is mediated by nuclear exclusion of the transcriptional factor proteins called FoxO which are involved in regulation of p27. Brk-transfected cells showed FoxO3a was localised mainly in the cytoplasm compared to control cells which have nuclear FoxO3a (Chan and Nimnual, 2010). Along with the substrates and interacting proteins, as well as the type of tissue Brk is expressed in, Brk's cellular localisation also determines its function. As previously described, Brk's localisation varies widely within different tissue types. In addition, in the presence of Brk, polypyrimidine tract-binding protein- (PTB) associated splicing factor (PSF), which is involved in mammalian spliceosomes (Chanas-Sacré *et al.*, 1999) compromised cell cycle progression by arresting cells in the S-phase (Lukong, Huot and Richard, 2009). PTB associated splicing factor (PSF) has been identified as a novel peroxisome proliferator activated receptor gamma (PPARγ) interacting protein (Tsukahara,

Haniu and Matsuda, 2013). PPARγ is a nuclear receptor involved in regulation of cell proliferation and apoptosis and its expression is increased in a number of cancers including colon, lung and breast (Tsukahara, Haniu and Matsuda, 2013). Suppression of PSF by siRNA significantly suppressed the proliferation of colon cancer cells and induced apoptosis in DLD-1 human adenocarcinoma cells (Tsukahara, Haniu and Matsuda, 2013).

1.8 Brk in cell migration and metastasis

To a large extent Brk is involved in breast cancer cell proliferation, however it is also involved in cell migration (Shin *et al.*, 2017). A reduced ability for T47D and JIMT-1 breast cancer cell migration was observed in response to Brk suppression (Ludyga *et al.*, 2013). Paxillin is a multidomain protein that is recruited to edges of the cell once migration is initiated, (as reviewed in (Deakin and Turner, 2008), and Brk has been recognised as a novel paxillin tyrosine kinase that binds to, as well as phosphorylates, paxillin (Chen *et al.*, 2004). Brk also acts a mediator of EGF-induced paxillin phosphorylation, thus promoting activation of Rac1 and stimulating cell migration and invasion. KAP3A is a subunit of the kinesin-2 heterotrimeric complex and binds microtubule-based subunits KIF3A/3B to various cargo proteins, which enable membrane morphogenesis (Yamazaki *et al.*, 1996). KAP3A has also been identified as a substrate of Brk and is phosphorylated at its C-terminus, a process required for Brk-induced cell migration (Lukong and Richard, 2008). Another study revealed that, upon Met receptor activation, Brk acts upstream of ERK5 activation which mediates cell migration (Castro and Lange, 2010). It appears that Brk's kinase activity was not required for Brk/ERK5 interaction or induction of migration within breast cancer cell lines. ERK5 has recently been indicated to be elevated in invasive breast cancers (Liu, Zhang and Song, 2017) indicating

disrupting Brk/ERK5 interaction may reduce cell migration and cell proliferation. Met signalling pathways increase tumour cell migration and disease progression by promoting tumour vasculature and increasing volume, thus a Brk-targeted therapy potentially could prevent spread and progression of tumours (Castro and Lange, 2010). Along with this, p190, another substrate of Brk, once phosphorylated is associated with p120 leading to Rho inactivation and Ras activation (Shen *et al.*, 2008). p190 also known as p190RhoGAP-A, is an inhibitor of RhoA signalling and associated with p120RasGAP (p120), and both these GTPase-activating proteins (GAP) mediate cross-talks between Rho and Ras (Bernards and Settleman, 2005). Migratory effects of Brk are greatly impaired in cells lacking p190. These interactions indicate an important function of Brk in regulating tumour cell migration via various systems, thus a Brk-targeted therapy could potentially cause disruption in these processes.

Angiogenesis has been recognised as an essential process in survival of cancerous cells *in vivo*; it is involved in tumour growth, progression and metastasis (Otrock *et al.*, 2007). One of the main pro-angiogenic factors involved in promoting tumour angiogenesis is vascular endothelial factor (VEGF) reviewed in (Niu and Chen, 2010). Osteopontin is a secreted non-collagenous chemokine-like protein that regulates VEGF expression via a Brk/nuclear factor-kappa B (NF-κB)/ ATF-4 signalling cascades (Chakraborty, Jain and Kundu, 2008). Briefly, osteopontin induced VEGF regulation of tumour angiogenesis is mediated through autocrine, paracrine and juxtracrine mechanism as highlighted in Figure 1.3 (Chakraborty, Jain and Kundu, 2008). Osteopontin was shown to enhance VEGF and Neuropilin 1 (NRP-1), a transmembrane glycoprotein and VEGF-specific receptor (Herzog *et al.*, 2011), interactions in breast cancer cells and there was enhanced osteopontin induced wound migration in cells transfected with wild type Brk compared to kinase mutant Brk suggesting osteopontin regulation of VEGF dependent wound migration through NRP-1 mediated autocrine

mechanism (Chakraborty, Jain and Kundu, 2008). Furthermore, VEGF interaction with endothelial cell surface VEGF receptor -2 (KDR) induces phosphorylation of KDR which has shown to lead to tumour angiogenesis (Cross *et al.*, 2003), thus osteopontin induced VEGF regulation of KDR phosphorylation via paracrine loop was assessed in MDA-MB 231 breast cancer. In addition, osteopontin induced VEGF showed to act as a link between NRP-1 which is expressed in tumour cells and KDR which is expressed in endothelial cells through the juxtracrine mechanism (Chakraborty, Jain and Kundu, 2008). In all these signalling pathways, osteopontin was shown to stimulate Brk phosphorylation and Brk mediated NF-κB-dependent/independent ATF-4 activation which leads to VEGF expression and enhanced angiogenesis (Chakraborty, Jain and Kundu, 2008). Furthermore, higher levels of expression of Brk, NF-κB and ATF-4 correlated with higher tumour grades. As osteopontin is secreted from the bone and expressed in brain (Oldberg, Franzen and Heinegard, 1986; Saitoh *et al.*, 1995), which are frequent sites for breast cancer metastasis (reviewed in Irvin Jr, Muss and Mayer, 2011), this study provides a mechanism whereby Brk could be involved in the formation of metastases.

Overall Brk's ability to promote cell migration and metastasis via various mechanisms may indicate that targeting Brk via tyrosine kinase inhibitors and disrupting its protein-protein interactions may provide a way to block the pathways leading to cell migration and tumour metastasis.

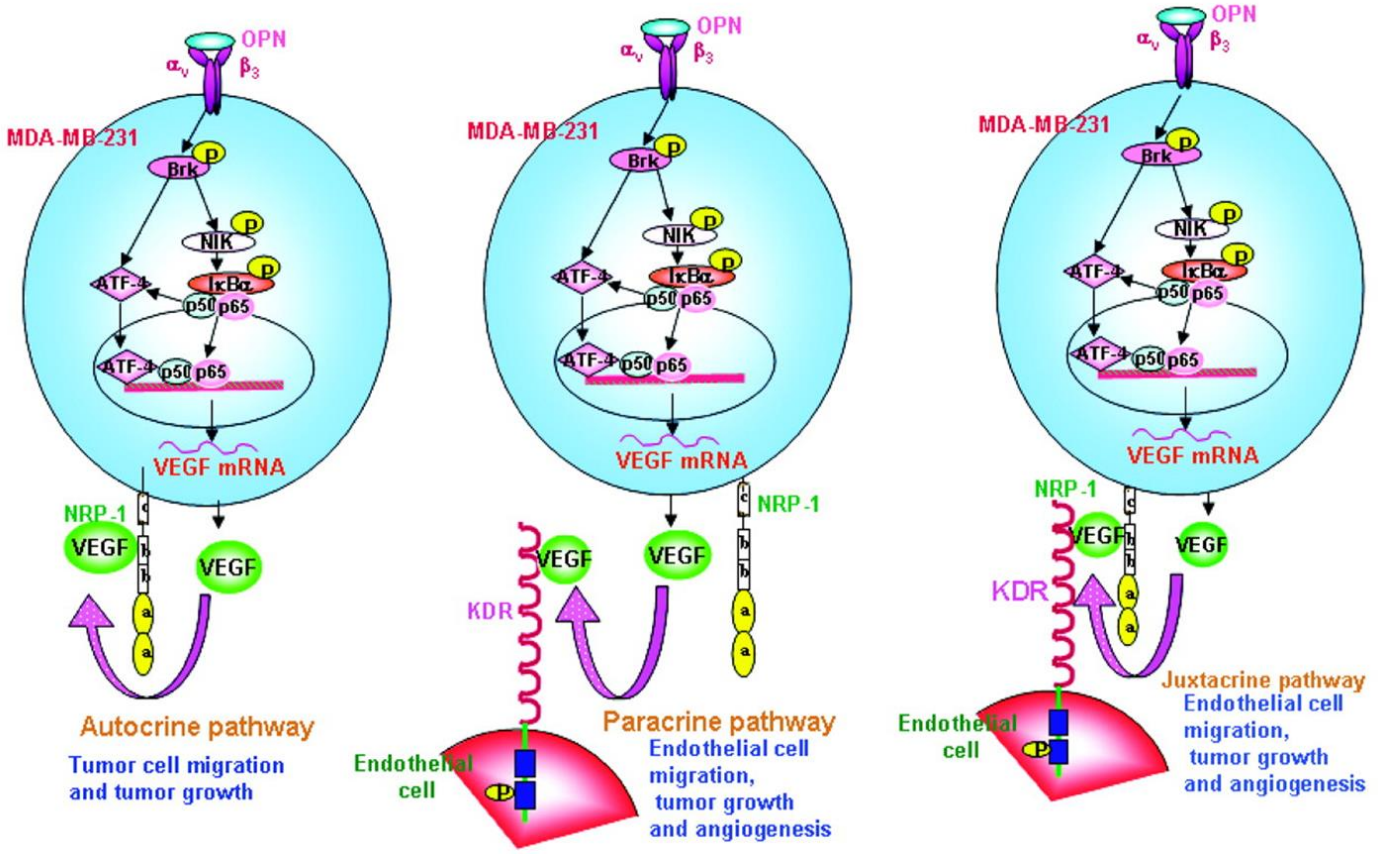

Figure 1.3 Brk/nuclear factor-kappa B (NF-κB)/ ATF-4 signalling cascades involved in osteopontin induced VEGF expression. Osteopontin induced Brk/ nuclear factor-kappa B (NF-κB)/ATF-4 mediated signalling results in VEGF expression leading to tumour migration, growth and angiogenesis via autocrine, paracrine and juxtacrine pathways (Chakraborty, Jain and Kundu, 2008).

1.9 Brk and cell death

Brk's role in cell death has thus far shown to be contradictory, in certain cellular environments Brk tends to promote apoptosis and cell death whereas in other cases it protects cells from cell death.

Brk's proliferative ability when coupled with its ability to protect cancerous cells from cell death promotes tumour cell survival. Brk has shown association with the P13-K/Akt pathway which is not only involved in cell proliferation but in apoptosis; thus activation of this pathway may reduce the ability of cells to undergo apoptosis (Kamalati *et al.*, 2000). Furthermore, Brk can protect breast cancer cells from autophagy; reduced expression of Brk coupled with suspension of culture increased the number of dead cells compared to controls (Harvey *et al.*, 2009). Brk also increases phosphorylation of p38 MAPK which is associated with pro-survival cell phenotypes in breast cancer (Lofgren *et al.*, 2011). Brk's ability to protect cancer cells from cell death is further enhanced due to its ability to protect cells from DNA damage-induced apoptosis in colon cancer cells. Knockdown of Brk in HCT116 cells led to increased apoptosis following γ-irradiation (Gierut *et al.*, 2012). In addition, p53 was recognised as a possible positive regulator of Brk activity in response to DNA damage (Gierut *et al.*, 2012). Reduced expression of p21 and STAT3 were also noticed in Brk-suppressed cells, leading to increased apoptosis and decreased survival (Gierut *et al.*, 2012). This gives indication for Brk inhibitors reducing tumour cell growth and survival.

Brk suppression in breast cancer cells suspended in culture resulted in increased the rate of cell death via autophagy compared to controls whereas Brk expression in Brk negative cancer cells resulted in increased cell survival, showing a role for Brk in protecting cancer cells from cell death (Harvey *et al.*, 2009). Brk also protected cells from anoikis via IGF-I signalling (Irie

et al., 2010). Further to this, Brk was shown to protect cells from anoikis via direct phosphorylation of focal adhesion kinase (FAK) and activating Akt (Zheng *et al.*, 2013). Knockdown of Brk in PC3 prostate cancer cell line disrupted FAK and Akt activation which in consequence promoted anoikis thus indicating an important protective role for Brk in anchorage independent survival (Harvey *et al.*, 2009).

Within a different cellular context such as the non-transformed rat fibroblasts, Brk has shown a role contradictory to that seen in breast cancer since it sensitises cells to apoptosis (Haegebarth, Nunez and Tyner, 2005). Furthermore, it also promotes apoptosis in crypt epithelial cells in response to DNA damage (Haegebarth *et al.*, 2009). This may show a role for Brk as a damage sensor that promotes apoptosis in response to cellular stress in normal tissue. These differences in Brk's role may again depend on its cellular localisation, substrates and protein interactions.

1.10 Brk and Hypoxia

Hypoxia refers to low oxygen levels (below the normal physiological tissue level). Hypoxia has shown to be a characteristic of malignancy and an important survival feature of the tumour microenvironment (reviewed in Challapalli, Carroll and Aboagye, 2017). Hypoxia arises due to high metabolic demand for oxygen as a consequence of rapid tumour growth and ineffectiveness of the tumour vasculature (Brown and Giaccia, 1998). Hypoxia inducible factors are mediators of transcriptional responses to hypoxia and are involved in many cellular functions within cancer cells leading to progression and metastasis (Semenza, 2010). HIFα subunits are overexpressed in breast cancers especially in triple negative breast cancers and indicate higher risk of metastasis (Dales *et al.*, 2005; Yamamoto *et al.*, 2008). Brk/PTK6 has shown to be induced in hypoxic conditions in a HIF-dependent manner (Regan

Anderson *et al.*, 2013). In contrast, Hammond and colleagues showed Brk is rapidly stabilised in hypoxic conditions in a HIF-1α independent manner (Pires *et al.*, 2014). Brk was induced rapidly in response to hypoxia and Brk induction occurred prior to HIF-1α stabilization in breast and colorectal cancer cell lines. In addition, it was shown that in response to hypoxia, Brk ubiquitylation was reduced and proteasomal-mediated degradation was decreased compared to normoxia (Pires *et al.*, 2014). This may be regulated via E3 ligases such as c-Cbl independently of HIF, however Brk has shown to promote the degradation of c-Cbl itself and thus may be involved in a reciprocal feedback loop with Brk (Kang and Lee, 2013; Pires *et al.*, 2014). Furthermore, the study showed Brk regulates cellular invasion and migration through relocalisation to the cellular membrane, a process which is important for Brk's oncogenic functions (Pires *et al.*, 2014). This suggests a Brk targeted therapy may have potential to reduce tumour metastasis which may be particularly important for triple negative breast cancers.

1.11 Issues with current breast cancer treatments

Chemotherapy and radiotherapy have been recognized to target normal rapidly dividing cells such as bone marrow, gastrointestinal tract or hair follicles; the range and intensity of adverse effects reduces the specificity and increases toxicity of these therapies. Both these types of treatments therefore have a limited therapeutic index and can often be palliative in use as reviewed by Arora (Arora and Scholar, 2005). Hormonal therapies have also been in use; for example Tamoxifen, which has been used for early stage and metastatic breast cancer since its license in 1972 (Smith, 2012). Although proven to be effective against pre-menopausal breast cancer, especially those that are oestrogen receptor positive, there are still many

issues that need to be overcome for maximum effect of the drug to be achieved, whether by itself or as combination therapy. These include the diverse adverse toxicities such as thrombosis, strokes and development of secondary cancers. Other issues include resistance against Tamoxifen and subsequent disease recurrence in some patients (Chang, 2012; Mayor, 2017). Furthermore, this drug is only effective against oestrogen or progesterone receptor positive breast cancers thus making it unsuitable for other types of breast cancer such as HER2 positive/ER/PR negative and triple negative breast cancers (den Hollander, Savage and Brown, 2013). However, there are treatments available for HER2 positive cancers such as Herceptin, a monoclonal antibody that binds to HER2 thus negatively affecting receptor function, as well as a number of kinase inhibitors. Unfortunately the more advanced stages of breast cancer do not always respond to Herceptin therapy and those that do, often progress in 12 months from the start of the treatment (Fink and Chipuk, 2013). In addition resistance may occur due to the involvement of a number of signalling pathway molecules such as activation of the PI3K/AKT pathway, loss of PTEN and activation of PIK3CA (reviewed in Brauer and Tyner, 2010). Brk is expressed in a wide range of cancer types including in hormone positive (ER/PR/HER2) and negative breast cancers, thus making it an ideal candidate for therapeutic intervention (Barker, Jackson and Crompton, 1997;, reviewed in Brauer and Tyner, 2010).

1.12 Tyrosine kinase inhibition

The potential for a Brk tyrosine kinase targeted therapy was investigated in this thesis, therefore a brief introduction to targeted therapy is needed. Targeted therapy is largely directed specifically towards tumour cells thus reducing many side effects and providing a

wider therapeutic window. They can also be used in combination with traditional chemotherapy or radiotherapy to enhance anticancer effects. Further patient benefit includes convenience with oral consumption rather than intravenous administration as is the case for many chemotherapy drugs.

Tyrosine kinases have been implicated in a range of cancers; they are involved in cellular signalling and play a significant role in growth factor signalling. In their active form tyrosine kinases can promote tumour cell proliferation, growth and induce anti-apoptotic effects, as well as promote angiogenesis and tumour cell metastasis. Since most of these cellular events contribute to tumour progression and decreased patient prognosis, tyrosine kinases are considered ideal candidates for targeted therapy.

There are two main types of kinases; these can be categorized as receptor protein kinases that are generally membrane spanning, or non-receptor protein kinases that relay intracellular signals from the receptors, of which, Brk is one example. Briefly, when ligands bind to their cognate receptors, they stimulate receptor dimerization followed by autophosphorylation and activation of tyrosine kinase activity. As a result, multiple signalling pathways are activated and intracellular mediators in these pathways transduce signals from membrane receptors through the cytosol and into the nucleus which ultimately alters DNA synthesis and cell division as well as a wide range of biological processes (Arora and Scholar, 2005). Protein tyrosine kinase activity within breast tumour tissues has been reported to be significantly higher in comparison to benign or normal breast tissues (Romain *et al.*, 1994). For example, the tyrosine kinase activity of the product of *c-src* proto-oncogene has been found to be elevated in human breast tumours (Ottenhoff-Kalff *et al.*, 1992), and several tyrosine kinase receptors with links to Brk have also been implicated in breast cancer development and progression for example , epidermal growth factor receptor (EGFR) and HER2/neu transmembrane tyrosine kinase receptor, as well as receptors for insulin like growth factors

(IGF) such as IGF-1R (Meric et al., 2002; Nielsen et al., 2004). Others include fibroblast growth factor receptor (Fearon, Gould and Grose, 2013) and met receptor tyrosine kinase reviewed in (Ponzo and Park, 2010).

41.13 Breast cancer radiation sensitivity

Radiation therapy after breast conserving surgery has been indicated to be more beneficial to patients than initially thought. A wide variety of breast cancer patients show increased survival rate and reduced chance of recurrence as well as reduced metastasis in a 10 and 15-year study (Early Breast Cancer Trialists' Collaborative Group (EBCTCG) *et al.*, 2011). *BRCA1* and *BRCA2* are genes that, once mutated, cause a higher chance of cancer forming and indicate a reduced ability for DNA repair. Approximately 19% of all triple negative breast cancers have *BRCA* gene mutations and thus are known to have defective DNA repair mechanisms (Wong-Brown *et al.*, 2015). The *BRCA* genes are tumour suppressors and the proteins encoded by them are involved in homologous recombination, a double strand DNA break repair mechanism (Welcsh and King, 2001). This would suggest this subtype of breast cancers with defective DNA repair mechanisms would be more susceptible to radiotherapy and chemotherapy. However, the opposite is true, triple negative breast cancers with *BRCA* mutations, are more radio-resistant and patients with these tumours have a higher overall mortality rate when treated with radiotherapy compared to hormone receptor and HER2 positive breast cancers (Kyndi *et al.*, 2008). This contradiction may be due to enhanced DNA repair mechanisms compensating for the defects in the BRCA genes meaning cells are forced to repair damage via other repair mechanisms such as non-homologous end joining (NHEJ) (Langlands *et al.*, 2013). The cell cycle phase is an important factor in determining the radio-

sensitivity/resistance as cells in the G2 phase are most sensitive to radiation, less sensitive in the G1 phase and least sensitive in the late S phase (Pawlik and Keyomarsi, 2004). The NHEJ repair pathway has shown to be predominantly active in the G1 phase whereas HR in comparison, is active in the G2 phase of the cell cycle (Mao *et al.*, 2008) thus suggesting the alternative NHEJ repair pathway may reduce the sensitivity of radiotherapy.

1.14 Brk and breast cancer chemotherapy

Despite improvements in treatment of breast cancer with adjuvant chemotherapy; there is still a need for novel breast cancer therapies. Treatment of the majority of invasive and higher grade/stage cancers is heavily chemotherapy based (Lee and Newman, 2007; Roche and Vahdat, 2011) thus the significance of how Brk may influence breast cancer cell sensitivity to chemotherapy agents as well as other drug-based treatments needs to be understood. Previous studies have shown that Brk may contribute towards influencing chemotherapeutic sensitivity in breast cancer (Burmi *et al.*, 2009; Harvey *et al.*, 2009). The mechanism proposed involves Brk altering the ratios of anti and pro-apoptotic proteins; Bcl-$_{XL}$ and Bcl-$_{XS}$ respectively, in respect of Bcl-$_{XL}$. Suppression of Brk in T47D breast cancer cells, which are representative of Luminal A breast cancer subtype, significantly increased sensitivity to chemotherapeutic drugs paclitaxel and doxorubicin, however this was not studied in triple negative breast cancers (Burmi *et al.*, 2009). The anti-apoptotic protein Bcl-$_{XL}$ is associated with chemotherapeutic resistance (Gul, Basaga and Kutuk, 2008) and reduced levels of Brk protein resulted in reduced levels of Bcl-$_{XL}$ protein and thus increased sensitivity to chemotherapy (Harvey *et al.*, 2009). Furthermore, breast cancer cells treated with methotrexate and 5-flurouracil showed decreased apoptosis due the inhibition by Bcl-$_{XL}$ *in*

vitro and *in vivo*. Based on these studies, it is expected a Brk targeted therapy would modulate chemotherapeutic drug response.

1.15 Aims and Objectives

Considering the extensive research on breast tumour kinase (Brk)'s oncogenic role in breast cancer including cancer cell proliferation and protection against cell death to migration and metastasis (reviewed in Hussain and Harvey, 2014); little is known of the role Brk plays in breast cancer therapeutics. The main aims of this thesis were; to investigate if Brk influences radio-sensitivity of breast cancer cell lines as well as to determine the potential mechanism that mediates the radio-sensitivity, to determine the potential of a novel Brk targeted therapy as a monotherapy and in combination with other breast cancer therapies, and to determine the ratios of mRNA levels of *PTK6* and *ALT-PTK6* transcripts in response to Brk inhibition and other breast cancer therapies as well as the potential of *ALT-PTK6/PTK6* expression ratios as prognostic factors for overall and disease free survival in breast cancer.

The objectives were to:

- To determine the radio-sensitivity of different breast cancer cell lines to γ-radiation through clonogenic survival in relation to Brk protein expression.
- Investigate the role of Brk in the DDR response pathway through γ-H2AX DNA repair assays.
- Examine whether there is a functional link between Brk and ATM signalling through analysis of total and phosphorylated protein levels of ATM in breast cancer cell lines.
- To investigate the effect on cell viability of breast cancer cells using the novel Brk inhibitor known as Compound 4f (Mahmoud *et al.*, 2014) through MTT assays as a

monotherapy as well as in combination with breast cancer therapies; Taxol, Doxorubicin, Lapatinib and Tamoxifen.

- To investigate the effect on Brk activity including the activity of its downstream signalling molecule STAT3, as well as determine levels of ALT-PTK6 protein in response to Compound 4f treatment over a 48-hour time period in breast cancer cell lines.
- To determine expression of both full length *PTK6* transcript and the short splice variant; *ALT-PTK6* in breast cancer cell lines using Real Time-PCR.
- To quantify the relative mRNA expression and ratios of both *PTK6* transcripts in breast cancer cell lines at basal levels and before and after treatment with compound 4f as well as in response to standard breast cancer treatments: Taxol, Doxorubicin, Lapatinib as well as Tamoxifen.
- To determine *ALT-PTK6* to *PTK6* mRNA expression ratios in normal and tumour breast tissue samples in relation to overall and disease-free survival.

2.0 Chapter 2: Materials and Methods

2. 1 Materials

2.1.1 Equipment

Table 2.1 List of Equipment

Equipment	Supplier	Address
^{60}Cobalt source	Puridec Technologies Ltd	REVISS Services (UK) Ltd, 179 Brook Drive, Milton Park, Abingdon, Oxon, England OX14 4SD
Fisher Scientific Power pack 300	Fisher Scientific	Fisher Scientific, Bishop Meadow Road, Loughborough, Leicestershire, LE11 5RG
Gel Doc™ XR+ Gel and blot imaging System	Bio Rad	Bio-Rad Laboratories Ltd. The Junction, Station Road, Watford, Hertfordshire, WD17 1ET
Imagestream Amnis® Imaging Flow Cytometer	Amnis® - part of Millipore	Millipore UK Limited, Suite 21, Building 6, Croxley Green Business Park Watford Hertfordshire WD18 8YHUnited Kingdom
Incubator Hera Cell 240	Heraeus	Heraeus Noblelight Ltd. Cambridge Science Park, Milton Road, Cambridge, CB4 0GQ
Laminar Flow Cell Culture Hood Hera Safe	Heraeus	Heraeus Noblelight Ltd. Cambridge Science Park, Milton Road, Cambridge, CB4 0GQ
Microplate reader	BioTek	Papermakers House, Rivenhall Road, Swindon SN5 7BD, United Kingdom
Pipettes, P10, P20, P200, P1000	Gilson	Gilson Scientific UK, 3B Humphrys Road, Woodside Estate, Dunstable Bedfordshire, LU5 4TP
QuantStudio 7 Flex Real-Time PCR System	Applied Biosystems	Stafford House, 1 Boundary Park, Hemel Hempstead HP2 7GE

Sorvall Legend T Benchtop Centrifuge	Fisher Scientific	Fisher Scientific, Bishop Meadow Road, Loughborough, Leicestershire, LE11 5RG
Spectrophotometer Nanodrop 2000c	Thermo Fisher Scientific	Stafford House, 1 Boundary Park, Hemel Hempstead HP2 7GE
Thermo cycler DNA engine Tetrad 2	Bio Rad	Bio-Rad Laboratories Ltd. The Junction, Station Road, Watford, Hertfordshire, WD17 1ET
Olympus CK400 Light Microscope	Olympus	KeyMed House Stock Road Southend-on-Sea, Essex SS2 5QH United Kingdom

2.1.2 Consumables

Table 2.2 List of main consumables.

Consumables	**Supplier**	**Address**
BioLite Multidishes and Microwell plate (6 wells, 12 wells, 24 wells, 96 wells)	Fisher Scientific	Fisher Scientific, Bishop Meadow Road, Loughborough, Leicestershire, LE11 5RG
Falcon™ 50mL/15mL Conical Centrifuge Tubes	Fisher Scientific	Fisher Scientific, Bishop Meadow Road, Loughborough, Leicestershire, LE11 5RG
Fisherbrand™ Eppendorf Microcentrifuge Tubes (1.5ml, 0.5ml, 200µl)	Fisher Scientific	Fisher Scientific, Bishop Meadow Road, Loughborough, Leicestershire, LE11 5RG

Fisherbrand™ Polypropylene Pipet Tips and Filter Tips (0.5-10µl, 1-200µl, 200-1000µl)	Fisher Scientific	Fisher Scientific, Bishop Meadow Road, Loughborough, Leicestershire, LE11 5RG
Fisherbrand™ Sterile Polystyrene Disposable Serological Pipets (10ml, 5ml, 25ml)	Fisher Scientific	Fisher Scientific, Bishop Meadow Road, Loughborough, Leicestershire, LE11 5RG
GE Healthcare Amersham™ Hyperfilm™ MP	Fisher Scientific	Fisher Scientific, Bishop Meadow Road, Loughborough, Leicestershire, LE11 5RG
MicroAmp® Fast Optical 96-Well Reaction Plate, 0.1 mL	Applied Biosystems by Life Technologies	3 Fountain Drive Inchinnan Business Park Paisley PA4 9RF, UK
MicroAmp® Optical Adhesive Film (100 covers)	Applied Biosystems by Life Technologies	3 Fountain Drive Inchinnan Business Park Paisley PA4 9RF, UK
MicroAmp® Splash-Free 96-Well Base	Applied Biosystems by Life Technologies	3 Fountain Drive, Inchinnan Business Park, Paisley PA4 9RF, UK
Nalgene™ Cryogenic Vials (1.5ml)	Fisher Scientific	Fisher Scientific, Bishop Meadow Road, Loughborough, Leicestershire, LE11 5RG
Nunc™ EasYFlask™ Cell Culture Flasks (T25/T75)	Fisher Scientific	Fisher Scientific, Bishop Meadow Road, Loughborough, Leicestershire, LE11 5RG
Sterilin™ Standard 90mm Petri Dishes	Fisher Scientific	Fisher Scientific, Bishop Meadow Road, Loughborough, Leicestershire, LE11 5RG

Thermo Scientific™ Sterile White Top 5ml Vials	Fisher Scientific	Fisher Scientific, Bishop Meadow Road, Loughborough, Leicestershire, LE11 5RG

2.1.3 Reagents

Table 2.3 List of main reagents and chemicals.

Reagents /Chemicals	**Supplier**	**Address**
10% SDS Solution	Fisher Scientific	Fisher Scientific, Bishop Meadow Road, Loughborough, Leicestershire, LE11 5RG
100ML Ethanol, Absolute (200 Proof), Mol Biology Grade, DNase, RNase & Protease-Free	Fisher Scientific	Fisher Scientific, Bishop Meadow Road, Loughborough, Leicestershire, LE11 5RG
1Kb Plus DNA Ladder (Invitrogen)	Fisher Scientific	Fisher Scientific, Bishop Meadow Road, Loughborough, Leicestershire, LE11 5RG
250ng Random Primers	Fisher Scientific	Fisher Scientific, Bishop Meadow Road, Loughborough, Leicestershire, LE11 5RG
Accumax Solution	Sigma-Aldrich	Sigma-Aldrich Company Ltd. The Old Brickyard, New Road, Gillingham, Dorset, SP8 4XT
Tetramethylethylenediamine (TEMED) 25ml	Fisher Scientific	Fisher Scientific, Bishop Meadow Road, Loughborough, Leicestershire, LE11 5RG
Acetic acid glacial	Fisher Scientific	Fisher Scientific, Bishop Meadow Road, Loughborough, Leicestershire, LE11 5RG

Acetone	Fisher Scientific	Fisher Scientific, Bishop Meadow Road, Loughborough, Leicestershire, LE11 5RG
Agarose 50g	Fisher Scientific	Fisher Scientific, Bishop Meadow Road, Loughborough, Leicestershire, LE11 5RG
Ammonium Persulfate powder 25g	Fisher Scientific	Fisher Scientific, Bishop Meadow Road, Loughborough, Leicestershire, LE11 5RG
Bovine Serum Albumin (BSA) powder 100g	Fisher Scientific	Fisher Scientific, Bishop Meadow Road, Loughborough, Leicestershire, LE11 5RG
Brilliant Blue (Coomassie) 25g	Fisher Scientific	Fisher Scientific, Bishop Meadow Road, Loughborough, Leicestershire, LE11 5RG
Compound 4f powder (5.506mg/ml DMSO)	Hilgeroth and group (Mahmoud *et al.*, 2014)	Institute of Pharmacy, Martin-Luther University Halle-Wittenberg, Wolfgang-Langenbeck-Str. 4, 06120 Halle, Germany
Coumaric Acid powder 5g	Sigma-Aldrich	Sigma-Aldrich Company Ltd. The Old Brickyard, New Road, Gillingham, Dorset, SP8 4XT
Dimethyl sulfoxide (DMSO)	Fisher Scientific	Fisher Scientific, Bishop Meadow Road, Loughborough, Leicestershire, LE11 5RG
dNTP set: dATP, dTTP, dCTP, and dGTP (100mM each) (Invitrogen)	Fisher Scientific	Fisher Scientific, Bishop Meadow Road, Loughborough, Leicestershire, LE11 5RG
Doxorubicin powder (100mg/ml DMSO)	Sigma- Aldrich	Sigma-Aldrich Company Ltd. The Old Brickyard, New Road, Gillingham, Dorset, SP8 4XT

Kodak Developer and Fixer (1 gal each)	Sigma- Aldrich	Sigma-Aldrich Company Ltd. The Old Brickyard, New Road, Gillingham, Dorset, SP8 4XT
DRAQ 5 Staining solution 5.0mM	Biostatus	56A Charnwood Road, Shepshed, Leicestershire, LE12 9NP, United Kingdom
G418 (Invitrogen)	Fisher Scientific	Fisher Scientific, Bishop Meadow Road, Loughborough, Leicestershire, LE11 5RG
Gibco™ DMEM/F-12, HEPES, No Phenol Red	Fisher Scientific	Fisher Scientific, Bishop Meadow Road, Loughborough, Leicestershire, LE11 5RG
Gibco™ Foetal Bovine Serum	Fisher Scientific	Fisher Scientific, Bishop Meadow Road, Loughborough, Leicestershire, LE11 5RG
Gibco™ Foetal Bovine Serum, charcoal stripped	Fisher Scientific	Fisher Scientific, Bishop Meadow Road, Loughborough, Leicestershire, LE11 5RG
Gibco™ L-Glutamine 200mM	Fisher Scientific	Fisher Scientific, Bishop Meadow Road, Loughborough, Leicestershire, LE11 5RG
Gibco™ Penicillin-Streptomycin (5,000 U/mL)	Fisher Scientific	Fisher Scientific, Bishop Meadow Road, Loughborough, Leicestershire, LE11 5RG
Gibco™ Rabbit Serum 500ml	Fisher Scientific	Fisher Scientific, Bishop Meadow Road, Loughborough, Leicestershire, LE11 5RG
Gibco™ RPMI 1640 Medium, no glutamine	Fisher Scientific	Fisher Scientific, Bishop Meadow Road, Loughborough, Leicestershire, LE11 5RG
Gibco™ RPMI 1640 Medium, No Phenol Red	Fisher Scientific	Fisher Scientific, Bishop Meadow Road, Loughborough, Leicestershire, LE11 5RG
Gibco™ TrypleExpress	Fisher Scientific	Fisher Scientific, Bishop Meadow Road, Loughborough, Leicestershire, LE11 5RG

Glycine powder 5kg	Fisher Scientific	Fisher Scientific, Bishop Meadow Road, Loughborough, Leicestershire, LE11 5RG
Hydrogen Peroxide 30% in water (w/w)	Fisher Scientific	Fisher Scientific, Bishop Meadow Road, Loughborough, Leicestershire, LE11 5RG
Isopropanol, Molecular Biology Grade 500ml	Fisher Scientific	Fisher Scientific, Bishop Meadow Road, Loughborough, Leicestershire, LE11 5RG
Lapatinib powder (20mg/ml DMSO)	Sigma- Aldrich	Sigma-Aldrich Company Ltd. The Old Brickyard, New Road, Gillingham, Dorset, SP8 4XT
Luminol powder 2g	Sigma-Aldrich	Sigma-Aldrich Company Ltd. The Old Brickyard, New Road, Gillingham, Dorset, SP8 4XT
Methanol	Fisher Scientific	Fisher Scientific, Bishop Meadow Road, Loughborough, Leicestershire, LE11 5RG
Methylene Blue 100g	Fisher Scientific	Fisher Scientific, Bishop Meadow Road, Loughborough, Leicestershire, LE11 5RG
MTT reagent A 50mg/vial (5 vials)	Millipore	Suite 21, Building 6, Croxley Green Business Park Watford Hertfordshire WD18 8YHUnited Kingdom
Non-fat skimmed milk powder	Marvel	Premier House, Centrium House, Centrium Business Park, Griffiths Way, St Albans AL1 2RE
Paclitaxel powder (50mg/ml DMSO)	Sigma- Aldrich	Sigma-Aldrich Company Ltd. The Old Brickyard, New Road, Gillingham, Dorset, SP8 4XT

Phosphate Buffered Saline (PBS) no magnesium and calcium 1x	Lonza	Lonza, Unit 5, Brunel Drive, Stretton Business Park, Stretton, Burton on Trent Staffordshire DE13OBY
Phosphate Buffered Saline (PBS) 1 x pH 7.4	Severn Biotech	Severn Biotech Limited, Unit 2, Park Lane, Kidderminster, Worcestershire, DY11 6TJ
PrecisionPLUS™ 2X qPCR Mastermix with SYBR Green, low ROX	Primerdesign	Primerdesign, The Mill Yard, Nursing Street Southampton SO16 0AJ
Prestained Protein Ladder 10-250kDa	Fisher Scientific	Fisher Scientific, Bishop Meadow Road, Loughborough, Leicestershire, LE11 5RG
REDTaq® ReadyMix™ PCR Reaction Mix (20mM Tris-HCl, pH 8.3, with 100 mM KCl, 3 mM MgCl2, 0.002 % gelatin, 0.4 mM dNTP mix (dATP, dCTP, dGTP, TTP), stabilizers, and 0.06 unit/mL of Taq DNA Polymerase)	Sigma-Aldrich	Sigma-Aldrich Company Ltd. The Old Brickyard, New Road, Gillingham, Dorset, SP8 4XT
RNase, DNase Free Water	Fisher Scientific	Fisher Scientific, Bishop Meadow Road, Loughborough, Leicestershire, LE11 5RG
RNaseOUT™ Recombinant Ribonuclease Inhibitor -40 units/µL (Invitrogen)	Fisher Scientific	Fisher Scientific, Bishop Meadow Road, Loughborough, Leicestershire, LE11 5RG
RNeasy Plus Mini Spin Kit (50 columns)	Qiagen	Skelton House, Lloyd St N, Manchester M15 6SH

Sodium Chloride powder 1kg	Fisher Scientific	Fisher Scientific, Bishop Meadow Road, Loughborough, Leicestershire, LE11 5RG
Sodium Dodecyl Sulphate (SDS) White Powder 500g	Fisher Scientific	Fisher Scientific, Bishop Meadow Road, Loughborough, Leicestershire, LE11 5RG
SuperScript II Reverse Transcriptase Kit (10,000 units 200U/µL). Also contains:5X First Strand buffer (250mM Tris-HCl (pH 8.3), 375mM KCl, 15mM MgCl2) and 100mM DTT (Invitrogen)	Fisher Scientific	Fisher Scientific, Bishop Meadow Road, Loughborough, Leicestershire, LE11 5RG
Sybr Safe DNA gel stain-10,000x concentrate in DMSO(Invitrogen)	Fisher Scientific	Fisher Scientific, Bishop Meadow Road, Loughborough, Leicestershire, LE11 5RG
Tamoxifen powder (2mg/ml DMSO)	Sigma- Aldrich	Sigma-Aldrich Company Ltd. The Old Brickyard, New Road, Gillingham, Dorset, SP8 4XT
Tris Base powder 5kg	Fisher Scientific	Fisher Scientific, Bishop Meadow Road, Loughborough, Leicestershire, LE11 5RG
Triton X-100 (density 1.067g/cm^3) 100ml	Fisher Scientific	Fisher Scientific, Bishop Meadow Road, Loughborough, Leicestershire, LE11 5RG
Tween 20	Fisher Scientific	Fisher Scientific, Bishop Meadow Road, Loughborough, Leicestershire, LE11 5RG
Tri-Reagent	Sigma-Aldrich	Sigma-Aldrich Company Ltd. The Old Brickyard, New Road, Gillingham, Dorset, SP8 4XT

LB Broth	Sigma-Aldrich	Sigma-Aldrich Company Ltd. The Old Brickyard, New Road, Gillingham, Dorset, SP8 4XT
Oxoid™ Agar Bacteriological	Fisher Scientific	Fisher Scientific, Bishop Meadow Road, Loughborough, Leicestershire, LE11 5RG
QIAprep Spin Miniprep Kit (50)	Qiagen	Skelton House, Lloyd St N, Manchester M15 6SH
Ampicillin (5g)	Sigma-Aldrich	Sigma-Aldrich Company Ltd. The Old Brickyard, New Road, Gillingham, Dorset, SP8 4XT
Polyethylenimine (PEI) 250ml	Sigma-Aldrich	Sigma-Aldrich Company Ltd. The Old Brickyard, New Road, Gillingham, Dorset, SP8 4XT
Gibco™ Opti-MEM medium (100ml)	Fisher Scientific	Fisher Scientific, Bishop Meadow Road, Loughborough, Leicestershire, LE11 5RG

2.1.4 Antibodies

Table 2.4 Primary and corresponding secondary antibodies used for western blot and immunocytochemistry. *Antibody diluted in 5% BSA/TBST, ** Antibody diluted in 5% milk/TBST, *** Antibody diluted in blocking buffer (100µl TritonX-100, 95ml PBS and 5ml rabbit serum). All secondary antibodies were diluted in the corresponding diluent used for primary antibodies.

Primary Antibody	Protein Size(kDa)	Final Concentration	Secondary Antibody	Dilution
*Brk (ICR100-Kamalati et al 1996)	52	1 µg/ml	Anti-Rat (Dako)	1:100
**Anti-GAPDH (Abcam)	40	0.001 µg/ml	Ant-Mouse (Dako)	1:1000
**Anti-β Actin (Abcam)	42	0.0005 µg/ml	Anti-Mouse (Dako)	1:1000
*Anti-STAT3 (Cell Signaling Technologies)	88	0.001 µg/ml	Anti-Rabbit (Dako)	1:1000
*Anti-phospho-STAT3 (Cell Signaling Technologies)	88	0.001 µg/ml	Anti-Mouse (Dako)	1:1000
*Anti-phospho-Brk (Tyr342) (Millipore)	50	4 µg/ml	Anti-Rabbit (Dako)	1:1000
*Anti-Brk polyclonal antibody N-Terminal (Abcam) for ALT-PTK6.	15	2 µg/ml	Anti-Rabbit (Dako)	1:1000
***Anti-phospho-histone H2A·X (Serine 139) monoclonal antibody. (Millipore)	17	0.2 µg/ml	Alexa Fluor 488 rabbit anti-mouse (Invitrogen)	1:1000
*Anti-EGFR (Abcam) monoclonal antibody	134	0.112 µg/ml	Anti-Rabbit (Dako)	1:1000
*Anti-HER2/ErB2 antibody (Cell Signaling Technology)	185	0.001 µg/ml	Anti-Rabbit (Dako)	1:1000
**Anti-oestrogen Receptor alpha antibody (Abcam)	68	2 µg/ml	Anti-Goat (Dako)	1:1000
*Anti-Progesterone receptor A/B (Cell Signaling Technology)	90	0.001 µg/ml	Anti-Rabbit (Dako)	1:1000

***ATM (C-terminal region) Mouse Monoclonal (ECM Biosciences)	370	2 µg/ml	Alexa Fluor 488 rabbit anti-mouse (Invitrogen)	1:1000
***ATM (Ser-794), phospho-specific (ECM Biosciences) Rabbit Polyclonal	370	2 µg/ml	Alexa Fluor 488 goat anti-rabbit (Invitrogen)	1:1000
Company Addresses				
Abcam	330 Cambridge Science Park Rd, Milton, Cambridge CB4 0FL			
Cell Signaling Technologies	New England Biolabs (UK) Ltd. 75-77 Knowl Piece Wilbury Way Hitchin, Hertfordshire SG4 0TY			
ECM Biosciences	EMELCA Bioscience – Belgium, Kapucinessenstraat 30 B-2000 Antwerpen, Belgium			
Millipore	Suite 21, Building 6, Croxley Green Business Park Watford Hertfordshire WD18 8YHUnited Kingdom			

2.1.5 Primers

Table 2.5 PCR primer sequences. Primer sequences were verified using the primer BLAST -NCBI tool.

Gene Name (Final Concentration)	**Strand**	**Primer Sequence (5'-3')**
PTK6 (1µM)	Forward	ATGAAGAAGCTGCGGCACAA
	Reverse	CCGAAACGGGCAGGACTT
β actin (1µM)	Forward	AAGAGAGGCATCCTCACCCT
	Reverse	TACATGGCTGGGGTGTTGAA

Table 2.6 qPCR primer sequences for reference genes (*RPL13A* and *SDHA*) and genes of interest (*PTK6* and *ALT-PTK6*). Primer sequences were verified using the primer BLAST -NCBI tool.

Gene Name (Final Concentration)	**Strand**	**Primer Sequence (5'-3')**
RPL13A (400nM)	Forward	CCTGGTCTGAGCCCAATAAA
	Reverse	CTTGCTCCCAGCTTCCTATG
SDHA (400nM)	Forward	TGGGAACAAGAGGGCATCTG
	Reverse	CCACCACTGCATCAAATTCATG
PTK6 (300nM)	Forward	GGTGGAGTCGGAACCGTGG
	Reverse	GTAGTCGGCACTCGGCTTC
ALT-PTK6 (300nM)	Forward	GAAGCACGAGCCTGAGC
	Reverse	CGAAGACCTCCCCAAAGTAG

2.1.6 Recipes

2.1.6.1 Immunocytochemistry Recipes

Table 2.7 Recipe for buffers used in immunocytochemistry (final concentrations).

Buffer	**Triton X-100 volume (µl)**	**PBS volume (ml)**	**Rabbit Serum volume (ml)**
Permeabilization Buffer	500	99.5	0
Blocking Buffer	100	95.0	5
Wash Buffer	100	99.9	0

2.1.6.2 SDS-polyacrylamide gel electrophoresis (SDS-PAGE), Western blotting and Coomassie staining recipes

- 10x SDS PAGE Running Buffer: 30.2g Tris base, 188g Glycine and 100ml 10% SDS dissolved in 1L H_2O
- 1x SDS PAGE Running Buffer: 100ml 10x SDS PAGE running buffer and 900ml H_2O
- 10x Towbin (Transfer) Buffer: 30g Tris base, 144g Glycine and 1L H_2O
- 1x Transfer Buffer: 100ml of 10x Transfer buffer, 800ml H_2O and 100ml of methanol
- 10x Tris buffered saline (TBS): 60.5g Tris base and 87.6g sodium chloride, pH 7.6 and 1L H_2O
- 1 x TBS Tween 20 (TBST): 100ml 10x TBS, 900ml H_2O and 1ml Tween 20 (Fisher Scientific).

- 5 % Blocking Buffer: 2.5g non-fat skimmed milk powder (Marvel) and 50ml 1x TBST
- Antibody diluent:
    - 0.5g Bovine Serum Albumin (BSA) (Fisher Scientific) and 10ml 1x TBST.
    - 0.5g non-fat skimmed milk powder (Marvel) and 10ml 1x TBST.
- Enhanced Chemiluminescence (ECL) solution:
    - 100Mm Tris: 1.214g Tris base in 100ml H_2O.
    - Coumaric Acid (Sigma Aldrich): 0.0148g in 1ml Dimethyl Sulfoxide (DMSO).
    - Luminol (Sigma Aldrich): 0.0443g in 1ml DMSO.
    - Solution A: 22µl coumaric acid and 55µl luminol in 3ml 100mM Tris pH8.
    - Solution B: 3µl hydrogen peroxide (Fisher Scientific) in 3ml 100mM Tris pH8.
- 10 % SDS: 10g SDS and 100ml H_2O.
- 10% Ammonium Persulfate (APS): 0.5g APS in 5ml H_2O.
- Coomassie Blue: 300ml H_2O, 150ml methanol (Fisher Scientific), 50ml Acetic acid (Fisher Scientific) and small drops of Brilliant Blue for colourisation.
- Destain: 450ml H_2O, 450ml methanol and 100ml Acetic acid.
- 1M Tris: 30.29g Tris base and 250ml H_2O, pH 6.8.
- 1.5M Tris: 18.15g Tris base in 100ml H_2O, pH 8.8.

Table 2.8 2x SDSPAGE Loading buffer recipe.

Reagent	**Volume (ml)**
Glycerol	2
1M Tris-HCL Ph 6.7	1
B-mercaptoethanol (Fisher Scientific)	0.5
10% SDS	4
HPLC pure water	2.5
Bromophenol Blue (Sigma Aldrich)	Small drops to achieve desired colourization

Table 2.9 SDS-PAGE resolving gel recipe with total volume 10ml.

Reagent	**Volume for 10% gel**	**Volume for 12% gel**	**Volume for 15% gel**
dH_2O	4ml	3.3ml	2.3ml
30% acrylamide	3.3ml	4ml	5.0ml
1.5M Tris pH 8.8	2.5ml	2.5ml	2.5ml
10% SDS	100µl	100µl	100µl
10% Ammonium Persulfate (APS)	100µl	100µl	100µl
Tetramethylethylenediamine (TEMED)	4µl	4µl	4µl

2.2 Methods

2.2.1 Breast cancer cell lines

The immortalized non-transformed (non-tumorigenic) cell line MCF10A was used as a close representative of normal mammary epithelial cells. The MCF10A cell line was derived from human fibrocystic mammary tissue and lacks expression of typical breast cancer receptors, for example, oestrogen receptor (ER) (Soule *et al.*, 1990).

T47D cell line was derived from pleural effusion obtained from a 54-year-old female patient with infiltrating ductal carcinoma and is representative of Luminal A subtype of breast cancer (Keydar *et al.*, 1979). GI101 is ER negative and derived from an infiltrating ductal breast carcinoma xenograft and representative of a metastatic model for breast cancer (Daoud,

Leathers and Hurst, 2002). SKBR3 cell line is ER negative and progesterone receptor (PR) negative but overexpresses human epidermal growth factor receptor 2 (HER2) and was established from the pleural effusion of a 43-year-old Caucasian female with malignant adenocarcinoma (Fogh and Trempe, 1975; Fogh, Fogh and Orfeo, 1977). BT474 cell line is derived from a 60-year-old female patient with invasive ductal carcinoma and is representative of Lumina B type as well as HER2 positive breast cancer (Lasfargues, Coutinho and Redfield, 1978). MDA-MB 231 was derived from a pleural effusion of a 51-year-old patient with adenocarcinoma (Cailleau *et al.*, 1974). MDA-MB 436 cell line was derived from the pleural effusion of a 43-year-old female patient with infiltrating ductal carcinoma (Cailleau, Olivé and Cruciger, 1978). MDA-MB 157 cell line was derived from pleural effusion of a 44-year-old female patient with metaplastic carcinoma (Langbois *et al.*, 1979) whereas the MDA-MB 468 cell line was derived from pleural effusion of a 51-year-old female patient with adenocarcinoma (Cailleau, Olivé and Cruciger, 1978). All the MDA-MB cell lines used in my studies are representative of triple negative or basal like breast cancer subtype. All cell lines were originally purchased from American Type Culture Collection (ATCC). Table 2.10 shows summary of breast cancer cell lines corresponding to their breast cancer subtype and their characteristics. Fresh stocks of each cell line were used. Cell lines were verified after culturing through morphology check by microscope and cell growth curves compared to literature. Cell lines were routinely checked for mycoplasma contaminations by light microscopy.

Table 2.10 Breast cancer subtypes and corresponding cell lines. ER= oestrogen receptor, PR= progesterone receptor, HER2= human epidermal growth factor receptor 2.

Breast Cancer Subtype	**Characteristics**	**Cell line**	**Supplier**
Luminal A	ER+, PR+/- and HER2-	T47D,	American type culture collection (ATCC) LGC Standards Queens Road Teddington Middlesex TW11 0LY UK
Luminal B	ER+, PR+/- and HER2+	BT474	
Basal Like	ER-, PR- and HER-	MDA-MB 157, MDA-MB 468, MDA-MB 231 and MDA-MB 436	
HER2 positive	ER-, PR- and HER+	SKBR3, BT474	

2.2.2 Transfected Cell lines

The triple negative, Brk negative cell lines; MDA-MB 468 and MDA-MB 157 were originally purchased from ATCC and had previously been transfected with the pRc/CMV empty vector (Vector) or vector containing the cDNA for wild type Brk (Brk-WT) or kinase inactive Brk (Brk-KM) as previously described (Harvey et al, 2009). Briefly cells had been transfected at 3:1 ratio with Fugene (Roche) and DNA. Cells were incubated for 48 hours before sub-culturing into fresh medium containing 400µg/ml G418 (Invitrogen).

2.2.3 Cell culturing protocol

Tissue culture was performed in a designated tissue culture laboratory within a sterilized and

filtered LaminAir Class II tissue culture hood. The hood was maintained weekly by thorough cleaning with Trigene (Distel) and 70% industrial methylated spirit (IMS). All materials and reagents were sterile before being used and all equipment was cleaned with 70% IMS before use within the laminar flow hood. MCF10A cells were grown in 1:1 HamsF12: Dulbecco's Modified Eagle's medium (DMEM) (Fisher Scientific) and supplemented with the following: 100 Uml-1 Penicillin-Streptomycin (Fisher Scientific), 10% foetal bovine serum (FBS) containing high content of embryonic growth promoting factors (Fisher Scientific), 2.0 mM L-Glutamine, 5ng/ml epidermal growth factor (EGF), 1 µl/ml hydrocortisone and 5 µg/ml insulin (Fisher Scientific). The MCF10A cell line was sub-cultured once a week, once confluent. The GI101 cell line was cultured with Roswell Park Memorial Institute (RPMI) 1640 medium (Fisher Scientific) supplemented with 10% FBS, 2.0 mM L-Glutamine, 100 Uml-1Penicillin-Streptomycin and 5µg/ml insulin. The remainder of the cell lines (T47D, SKBR3, BT474, MDA-MB 231, MDA-MB 436, MDA-MB 157 and MDA-MB 468) were cultured in RPMI 1640 medium supplemented with 10% FBS, 100 Uml-1 Penicillin-Streptomycin and 2.0 mM L-Glutamine. The MDA-MB 468 and MDA-MB 157 transfected cell lines were additionally supplemented with 400 µg/ml G418 (Invitrogen), an aminoglycoside antibiotic. All these breast cancer cell lines were sub-cultured at least twice a week depending on them reaching 70-80% confluency. Cell lines were grown in either a T25 or T75 tissue culture flask (Fisher Scientific) and cultured at 37˚C and 5% carbon dioxide (CO_2) in a humidified incubator. To subculture, cells were washed with 1x phosphate buffered saline (PBS) (Severn Biotech) twice before detaching cells from the flask with TrypleExpress (Fisher Scientific) and incubated at 37˚C, 5% CO_2 for 2-5 minutes. Cells were resuspended in the appropriate medium at ratio of 1:5 TrypleExpress/medium. The cell mixture was then mixed thoroughly before pipetting appropriate volume into new flasks as required.

2.2.4 Cell cryopreservation and thawing

In order to maintain cells and for long-term storage of cells, cryopreservation was performed. To preserve cells, cells were grown to 80% confluency in two or more T75 flasks. The medium was removed, and cells were washed with 1x PBS; trypsinisation with TrypleExpress was carried out as before and incubation at 37˚C and 5% CO_2 for 2-5 minutes. Once cells were detached, they were resuspended in fresh 8ml of the appropriate medium. The suspension from each flask was then pipetted into a sterile 50ml Falcon tube (Fisher Scientific) before being centrifuged at 1500 revolutions per minute (rpm) for 5 minutes. The supernatant was removed, and cell pellet resuspended with 10% dimethyl sulfoxide (DMSO) (Fisher Scientific) in the appropriate medium and mixed thoroughly. Approximately 1ml of the mixture was added to a 1.5ml cryovial (Fisher Scientific- Nalgene Cryogenic Vials) and placed in a cryovial rack within a liquid nitrogen dewar to begin slow freezing of the cells for 2 hours before placing the rack deeper in the dewar overnight and finally submerging the cryovials into the liquid nitrogen completely within a cryovial box.

To thaw cells from cryopreservation, the appropriate culturing medium was left to warm in a water bath set to 37˚C before pipetting into a T25 flask. A vial of cells from cryopreservation were taken out of liquid nitrogen and thawed within the water bath before being sprayed with 70% IMS and placed inside the tissue culture hood. The cells were diluted in the appropriate medium (1:10) and centrifuged (1000rpm for 4 mins) to remove DMSO before decanting the supernatant and adding l fresh medium and placed in an incubator at 37˚C and 5% CO_2 for 24 hours before removing the medium and adding fresh medium in order to remove any remaining DMSO.

2.2.5 Cell counting and cell growth curves

Cells were trypsinised as described in above and the cell suspension pipetted into a 50ml Falcon tube. The tube was centrifuged at 1500 rpm for 5 minutes. Meanwhile, the haemocytometer was prepared with the coverslip placed tightly onto the surface. The medium was removed from the tube carefully so as not to disturb the cell pellet and cells suspended in fresh medium. A 10µl aliquot was pipetted into the haemocytometer chamber for cell counting. The middle 5x5 square was counted. The number of cells counted was used to obtain the appropriate volume of cell suspension needed and the rest of the volume was made up by adding the appropriate amount of medium. For cell proliferation curves, 0.04x106 cells/cm2 were seeded in a 24 well plate. The 24 well plate was incubated, and cell numbers determined by haemocytometer counting daily for 6 consecutive days in order to determine cell numbers. Medium was aspirated out of 4 wells, cells were washed with PBS and detached with 200µl of TrypleExpress from each well before adding 200µl of fresh medium. Cells were counted using a haemocytometer. To determine total number of cells, the number of cells counted in the middle square of the haemocytometer was multiplied by 10^4 and the dilution factor (0.4). Growth curves were generated to show growth rate of each cell line.

2.2.6 Radiation Treatments

2.2.6.1 Clonogenic Assays

Cells were harvested, counted as before and diluted to 1000 cells per ml (for 0Gy and 2Gy γ-radiation doses), 1500 cells per ml (for 4Gy dose) and 2000 cells per ml (for 6Gy and 8Gy

doses) in medium and pipetted into sterile 10cm petri dishes (Fisher Scientific). Cells were subjected to γ-irradiation using the high energy ^{60}Cobalt source (Puridec Technologies Ltd) at 2,4,6 and 8Gy. The exposure time for the 2Gy dose was determined by the distance from the radiation source (25cm) and the known current emission rate. Once the 2Gy exposure time was complete the petri dishes with 2Gy dose were removed and the rest of the petri dishes exposed to a further 2Gy dose for the 4Gy dose. This continued until the desired accumulative doses were reached. After irradiation, 1ml of each cell suspension was pipetted into each of three petri dishes per dose. The petri dishes were kept in the incubator at 37ºC and 5% CO_2 for up to two weeks to allow for formation of colonies.

2.2.6.2 Fixing and staining cells for clonogenic assays

To fix and stain cells, IMS and methylene blue solution (0.01% w/v in distilled water) were used. Medium was decanted, and cells were washed with 1x PBS and then fixed in 100% IMS for 20 minutes inside the sterile tissue culture hood. Once fixed, the IMS was removed and petri dish briefly rinsed under running tap water. Methylene blue solution was then added to the petri dish at sufficient volume to cover the surface of the petri dish and left overnight to stain the cells. The methylene blue solution was then removed, and the petri dishes washed with H_2O to remove the excess stain before being left to air dry. Once the dishes were dry, the number of blue dots representing colonies were counted. Approximately 50 cells constituted one colony formation. Survival curves were plotted as percentage of control in semi-log form as follows:

Control - 0Gy (100%).

Radiation dose 2Gy - (number of colonies at 2Gy / (number of colonies at 0Gy)) x 100

Radiation dose 4Gy - (number of colonies at 4Gy/ (number of colonies at 0Gy x1.5)) x 100

Radiation dose 6 and 8Gy - (no colonies at 6 or 8Gy/ (no of colonies at 0Gy x 2)) x 100

2.2.6.3 γ-H2AX DNA Repair Assay

γ-H2AX DNA repair assays were carried out to investigate levels of DNA repair occurring using γ-H2AX as a DNA repair marker. $2x10^6$ cells were seeded into petri dishes for each time point (30 minutes, 3 hours, 5 hours and 24 hours) along with control and compensation samples. Compensation samples were needed to compensate for the overlap between two channels of the Imagestream machine due to fluorescence leakage from nearby channels. Cells were then irradiated with 2Gy gamma radiation as previously described (section 2.2.6). Cells were processed and fixed at 30 mins, 3 hours, 5 hours and 24 hours post radiation. The Alexaflour 488 (AF) and Draq5 (D5) compensation plates were exposed to radiation and fixed at the 30 minutes time point. The fixing procedure for 30 minutes, AF and D5 compensation samples was started immediately on return to the laboratory. Control un-irradiated samples were fixed prior to radiation. To fix, the medium was decanted, the cells were washed with 1x PBS, trypsinised with TrypleExpress as previously described and resuspended in fresh media. The cell suspension was transferred to a sterile 50ml Flacon tube and centrifuged at 1500rpm for 5 minutes before being washed with ice cold 1x PBS (Severn Biotech). The cells were then fixed by resuspension in methanol/acetone solution (50:50 v/v) and transferred to a 1.5ml microcentrifuge tube. Fixed cells were then stored at -20°C until ready to process for the next step.

2.2.6.4 Immunocytochemistry

The fixed cells were centrifuged at 3000 rpm for 3 minutes and the methanol/acetone solution removed by aspiration. Cell pellets were rehydrated by resuspending in 1x PBS and placed on the rotary mixer for 5 minutes at 25rpm (at room temperature). Tubes were centrifuged as before, and PBS removed. Permeabilizing buffer (0.5% Triton X-100 solution (Sigma-Aldrich) in 1x PBS) was added to each of the tubes and mixed thoroughly (but gently), placed on the rotary mixer for 5 minutes before centrifuged at 3000 rpm for 3 minutes. The permeabilizing buffer was then removed by centrifugation and aspiration and the cells resuspended in blocking buffer (5% rabbit serum (Biosera) and 0.1% Triton X-100 in 1x PBS) and then placed on the rotary mixer for 1 hour at 25rpm. The samples were then removed from the rotary mixer and centrifuged at 3000 rpm for 3 minutes before the blocking buffer was removed by aspiration. Primary antibody; anti-phospho-histone H2AX (Serine 139) monoclonal antibody (Millipore) was diluted in blocking buffer (1:10000 dilution), and 500µl added to each tube. The cells were then incubated overnight at 4°C with rotation at 25rpm using the rotary mixer.

The following day, the cells were centrifuged at 3000rpm for 3 minutes and the primary antibody removed. The cell pellet was then resuspended in wash buffer (0.1% Triton X-100 in PBS) and incubated for 5 minutes with 25rpm rotation. The cells were resuspended in fresh wash buffer and incubated with rotation as before. Once the wash buffer was removed, the secondary antibody, Alexa Fluor 488 rabbit anti-mouse IgG antibody (Invitrogen) was prepared as a 2 mg/ml dilution and 500µl was added to each sample except for the D5 compensation samples which were resuspended in blocking buffer without antibody. The samples were covered in foil and left to incubate at room temperature on the rotary mixer (25rpm) for 1 hour. Table 2.7 (Section 2.1.6) lists all the buffers and their composition. Samples were removed from the rotary mixer and centrifuged at 3000rpm for 3 minutes

before aspirating the secondary antibody. Then wash buffer was added to each tube and rotated on a tube rotator for 5 minutes at 25rpm. The samples were centrifuged as before, and the wash buffer removed by aspiration. The cells were washed with the wash buffer a second time before they were resuspended with 100µl of Accumax solution. All samples were stored at 4°C overnight covered in foil if not processed immediately.

2.2.6.5 Imagestream Analysis

Samples were removed from the rotary mixer and centrifuged at 3000rpm for 3 minutes before aspirating the secondary antibody. . The cells were washed with the wash buffer twice before they were resuspended with 100µl of Accumax solution. All samples were stored at 4°C overnight covered in foil if not processed immediately. The samples were then stained with Draq 5 (D5) staining solution (1:100 D5/Accumax ratio) except for the Alexa Fluor (AF) compensation samples and ready for analysis with the Imagestream IDEAS software (Amins). Table 2.11 indicates the parameters used for my experiments for all Imagestream analysis. For each time point a minimum of 10,000 events or cells were captured for analysis. Cell classifiers identified the size of object to be collected by the Imagestream for analysis, Channel 1 showed Brightfield images of cells which showed a live image of the cell as it was collected and processed by the Imagestream (Figure 2.1). Channel 2 was used to show staining of the primary antibody (anti-phospho-histone H2AX (Serine 139) monoclonal antibody) with Alex Fluor 488 as secondary antibody. This was shown as a green colour representative of induction of γ-H2AX foci. Channel 5 indicated nuclear staining of the cell using D5 which is represented as a blue colour. After acquisition of cells, the IDEAS software was used to analyse the cells. The cell population was first narrowed to include only single cell population thus eliminating any clusters of cells. This was done by manual examination of objects collected and 'gating' of the cell population to only include single cells. Only cells

in focus were used for analysis and these were selected by determining gradient of cells based on image focus and the normalized frequency. Cell population was further selected by determining best stained cells and the cells that were negative for γ-H2AX staining in order to additionally 'gate' cells based on staining intensity of the primary antibody. The spot counting analysis wizard prompted the selection of low and high number of foci which were user determined. The images were selected based on range of features including, size, shape, fluorescence intensity and number of foci for each selection of the low and high truth populations . These truth populations were used to create masks in order to determine γ-H2AX foci enumeration in each cell. The nuclear morphology mask was created first using the DRAQ 5 channel and then the spot mask for channel 2 (Figure 2.2). Using both masks, a combined mask was created in order to determine the number of foci within the nuclear region of the cell. The number of foci in cells were counted using the 'Features' option in the IDEAS analysis software and a histogram was plotted of normalised frequency of foci against the foci number. This template was saved and applied to all time points for each cell line. The average number of foci per cell were plotted against each time point.

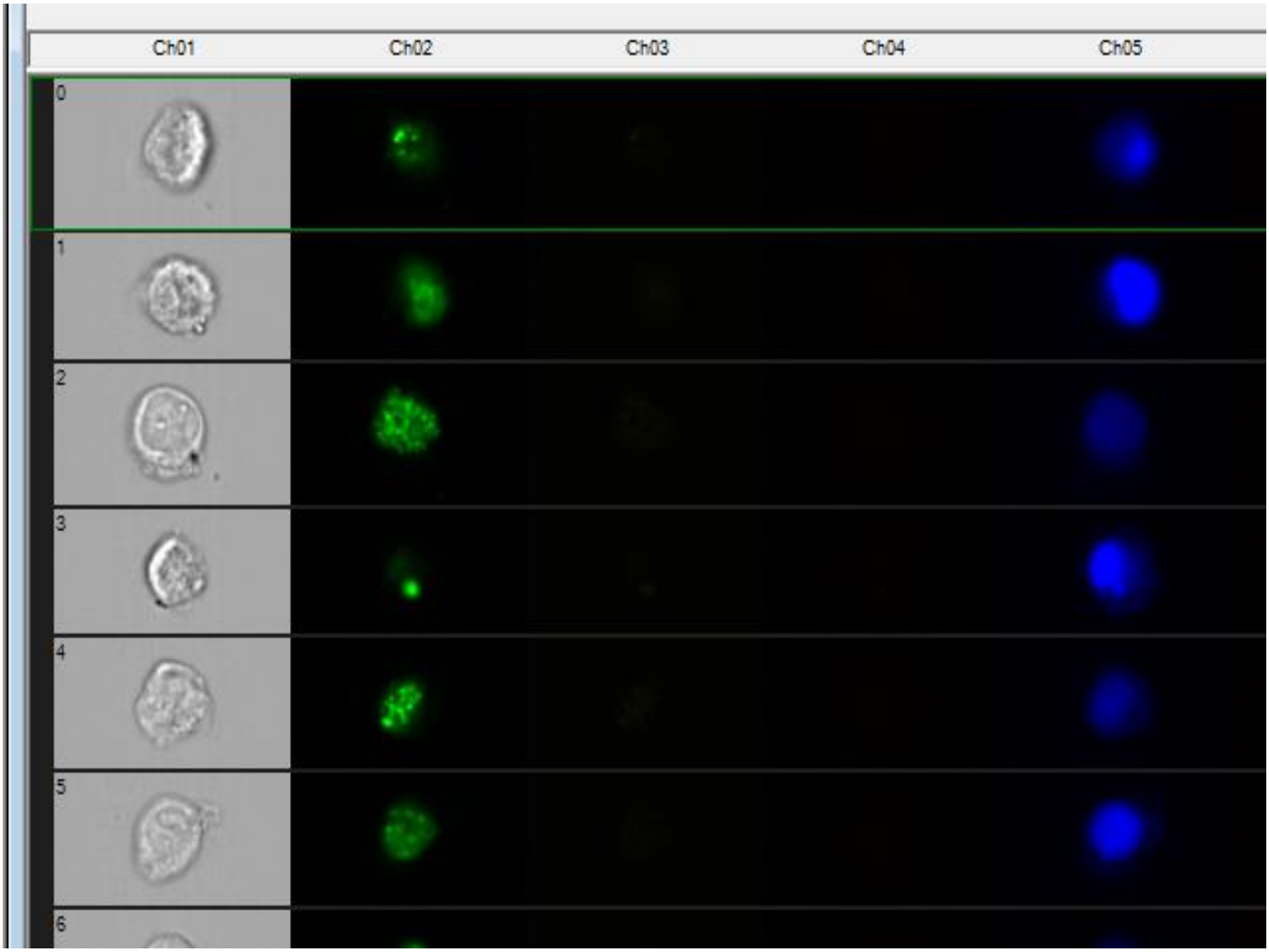

Figure 2.1 Images captured by the Imagestream. Channel 1 shows the live image of the cell (Brightfield). Channel 2 shows the primary antibody staining of the cells in green and channel 5 shows the nuclear staining with DRAQ5 staining in blue.

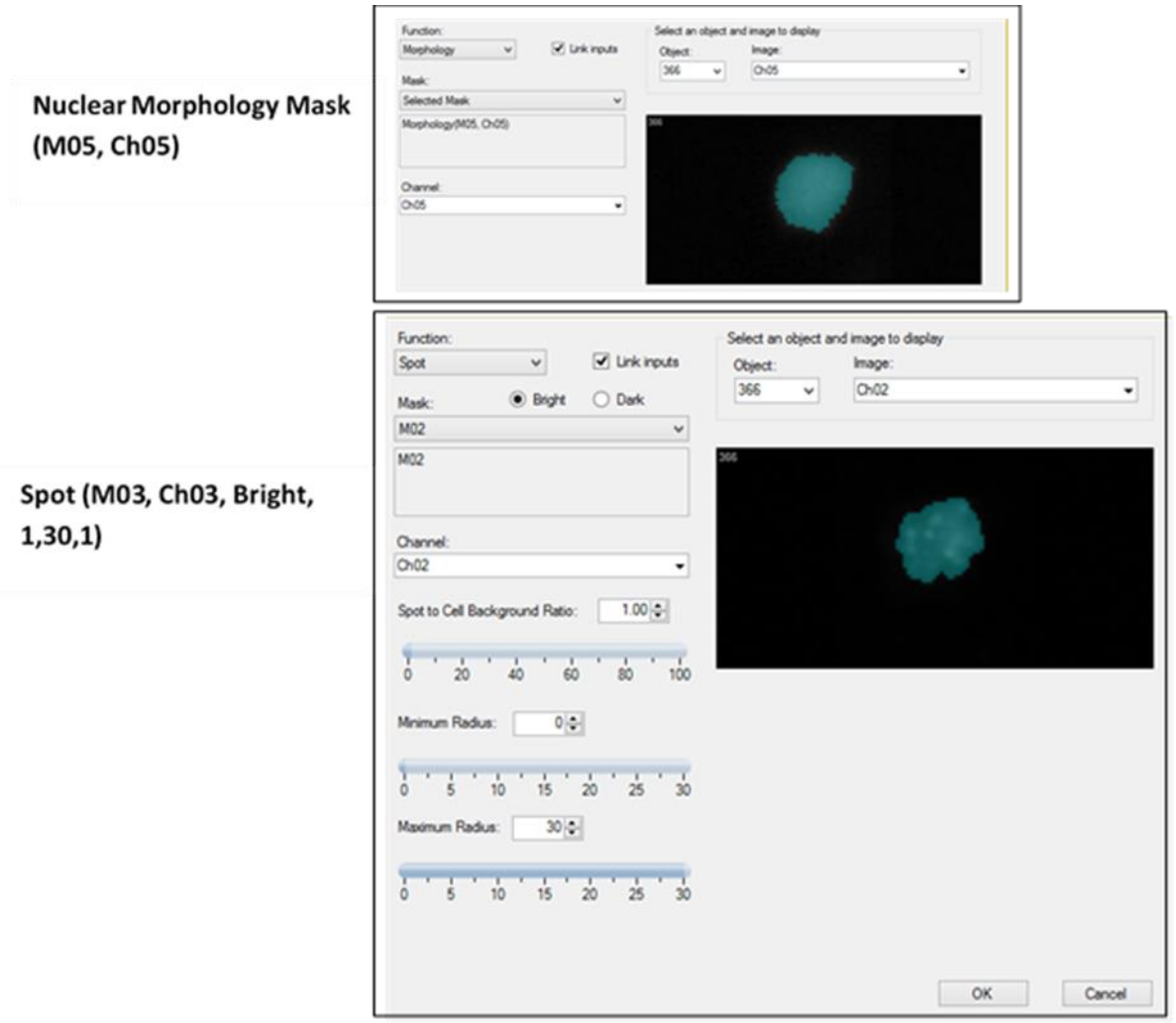

Figure 2.2 Masking of γ-H2AX foci for enumeration. Masking identified region of interest and Nuclear morphology using channel 5 was created. The spot mask was generated based on the selection of 'truth population' whereby a range of images were selected with foci ranging from zero to 30 or more. The spot mask was generated for ch02 with the γ-H2AX staining. The two masks were combined to create a new mask which identified number of foci within a specific nuclear region of each cell.

Table 2.11 Imagestream parameters for analysis.

Imagestream Parameters	
Channels	• Channel 1: Brightfield • Channel 2: Alex Fluor 488 stain • Channel 5: Draq 5 stain • Channel 6: Side Scatter
Target Total Number of Events (cells) to be acquired	• Dose samples: 10,000 events • Compensation samples: 1000 events
Lasers	• Brightfield laser intensity approximately at 800 • Excitation laser 488nm = 60.0Mw • Excitation laser 785nm =1.00mW
Fluidics	• Diameter = 10 microns • Core Velocity approximately 60mm/sec • Percent beads =7
Cell Classifier	Used for channels 1,2 and 5. • Lower limit = 50 • Upper limit = 250
Channel Colours and Gain values	• Channel 1: White, Gain Value=3 • Channel 2: Green, Gain Value = 6 • Channel 5: Blue, Gain Value =8

2.2.6.7 Image Compensation

Image compensation involves compensating for the overlap between two channels of the Imagestream machine due to fluorescence leakage from nearby channels. Along with the samples prepared to be fixed at 0. 0.5, 3, 5 and 24 hours, two extra samples were fixed at 30 minutes for image compensation. Images were captured of cells at 488nm wavelength only and no Brightfield illumination. Cells with AF and D5 only staining were used for the compensation matrix. The Imagestream software compensation wizard (IDEAS software from Amins) provides a table of coefficients and the produced light placed into the correct channel, with channel 2 for the antibody and channel 5 for Draq 5 only. After normalization, any calculated compensation was automatically applied to rest of the samples.

2.2.6.6 Determination of total and phosphorylated ATM protein levels

Breast cancer cell lines; MDA-MB 468 Brk WT, Brk KM, vector a well as cell lines; MDA-MB 157 Brk WT, Brk KM were exposed to 2Gy gamma radiation as described in section 2.2.6.1. The method for γ-H2AX DNA repair assay (section 2.2.6.3) was followed but with total ATM and phospho-ATM antibodies (section 2.1.4, Table 2.4). . For detection of total and phosphorylated ATM protein levels, cells were labelled with primary antibody (1.500) diluted in blocking buffer and incubated foe 24 hours at 4˚C with gentle agitation. Mouse monoclonal antibody ATM for C-terminal region (ECM Biosciences) was used for total ATM detection and rabbit polyclonal for phosphorylated serine794 of the ATM protein (ECM Biosciences) to detect phosphorylated ATM. Following washes as described in section 2.2.6.4, cells (except D5 compensation cells) were stained with rabbit anti-mouse or goat anti-rabbit secondary antibody solutions containing Alexa Fluor488 IgG (diluted to 1:1000 in blocking buffer) to detect total and phosphorylated ATM levels respectively. Cells were incubated for 1 hour at room temperature, washed with wash buffer and left overnight at 4˚C in Accumax solution. D5 solution was added to each sample except Alexa Fluor488 compensation cells and cells were analysed as described previously (section 2.2.6.5). Analysis of total and phospho-ATM protein in control un-irradiated and irradiated cells involved identification of the nuclear region of the cells using masking feature of the Ideas Software and the fluorescent intensity of the cells calculated by determining the intensity of channel 2 (Alex Fluor488) within the nucleus and the mean levels of antibody staining were recorded to represent ATM protein levels in

the cells.

2.2.7 Drug Treatments

At the time of the studies there were no commercially available Brk inhibitors. However after the discovery of 4-anilino α-carbolines as novel Brk inhibitors, compound 4f was identified as the most potent and selective Brk inhibitor (Mahmoud *et al.*, 2014). Thus, compound 4f was obtained from Hilgeroth and group for the experiments. Compound 4f was weighed and dissolved in DMSO (5.506mg/ml) and filter sterilized to give a stock concentrations of 20mM, and stored in -80˚C. Paclitaxel/Taxol (50mg/ml in DMSO), Doxorubicin (100mg/ml in DMSO), Lapatinib (20mg/ml in DMSO) and Tamoxifen (2mg/ml in DMSO) were purchased from Sigma-Aldrich, dissolved in DMSO at stock concentrations of 10 or 20mM, filter sterilized and stored at -20˚C.

For each drug, serial dilutions were performed in vehicle (DMSO) to produce 1000-fold stock solutions; the drugs were diluted 1:1000 in appropriate culture medium and added to the 96 well plate. The final concentrations used for compound 4f treatment were: 0.625µM, 1.25µM, 2.5µM, 5µM, 10µM, 20µM with DMSO as a control. The final concentrations used for Taxol or Doxorubicin single agent treatments and in combination with compound 4f (5µM) were: 0.15µM, 0.3125µM, 0.625µM, 1.25, 2.5µM and 5µM along with DMSO control. Final concentrations for lapatinib as single or combination treatment with compound 4f (5µM) were: 0.3125µM, 0.625µM, 1.25µM, 2.5µM, 5µM, 10µM and DMSO as control. Final concentrations for Tamoxifen as single or combination treatment with compound 4f (5µM) were: 0.3125µM, 0.625µM, 1.25µM, 2.5µM, 5µM, 10µM and DMSO as control. For Tamoxifen treatments, due to the presence of oestrogen in growth serum and phenol red being a weak oestrogen

(Berthois, Katzenellenbogen and Katzenellenbogen, 1986); cells were cultured and seeded as normal but medium was changed to RPMI 1640 Medium, No Phenol Red (Fisher Scientific) and supplemented with 10% charcoal stripped foetal bovine serum (Fisher Scientific), 2.0 mM L-Glutamine and 100 Uml-1Penicillin-Streptomycin before addition of the drug. 1:1000 dilution of DMSO was used as control for all treatments. For each drug 6 wells were used per concentration for single treatments. For combination treatments, half the 96 well plate was used for the anticancer agent as a single treatment and the other half for combination with compound 4f. . The 96 well plate layout is shown in Figure 2.2.6

For analysis of *PTK6* and *ALT-PTK6* transcripts in response to compound 4f treatment or the anticancer drugs mentioned above, cells were seeded in 6 well plate at density of $2x10^5$. Cells were incubated (37˚C, 5% CO_2) over night before the appropriate drug concentration was added in each well. 5μM was used for compound 4f, Taxol, Doxorubicin or Tamoxifen treatment whereas 2.5μM (this was the IC50 dose in combination treatment with compound 4f) was used for Lapatinib treatments. . Along with a treated 6 well plate, an untreated control plate was prepared. RNA lysates using RNeasy Mini Spin Column extraction kit (Qiagen) as shown in section 2.2.15.3, were collected at the following time points for each cell line or treatment: 0, 2 hours, 4 hours, 8 hours, 24 hours and 48 hours. cDNA and qPCR were performed as previously described (Chapter 2, sections 2.2.17 and 2.2.20).

For analysis of protein expression and activity of Brk isoforms, Brk substrate STAT3 and breast molecular markers (HER2/ER) in response to Brk inhibition (5μM of compound 4f), cells were seeded in a 6 well plate or T25 flask at density of $3\text{-}7x10^5$ (depending on confluency and proliferation rate of cell line). Protein lysates were taken at the following time points after treatment along with control lysate: 4 hours, 6 hours, 24 hours and 48 hours. Western blots were performed as shown below in section 2.2.11.

2.2.8 MTT assay protocol

.

Cells were harvested by trypsinisation and $5x10^3$ cells were counted as described in section 2.2.5 and seeded per well in a 96 well plate. The 96 well plate was incubated overnight at 37°C and 5% CO_2 before addition of the appropriate drug/s.

The 96 well plates were then incubated at 37˚C, 5% CO2 for 7 days with fresh medium and drug added every 2/3 days. MTT reagent (50mg per vial) was purchased from Millipore and diluted to stock concentrations of 5mg/ml with 1x PBS and stored at -20˚C. After incubation, the medium and drug mixture was removed. The MTT reagent was further diluted in 1:10 with the appropriate medium. The 96 well plate was incubated at 37˚C, 5% CO_2 for 2 hours. After which the mixture was poured out and the formazan was dissolved by addition of 100µl 0.04M HCI isopropanol (Fisher Scientific) per well before absorbance was read using a multiplate reader at wavelengths 570nm for MTT and 630nm for background. Background absorbance was subtracted from absorbance for MTT (570nm-630nm) and the average of each concentration from 6 wells calculated. Cell viability was determined as percentage of control for all MTT assays. Graphs were plotted as average of n=3 repeats per treatment with standard deviation as error bars.

2.2.9 Cell lysis

To obtain protein lysates, cells were washed with 1x PBS twice, detached from the flask with TrypleExpress and resuspended in fresh medium. Cells were centrifuged at 1500 rpm for 5

minutes before being resuspended in PBS. Cells were counted using a haemocytometer, centrifuged and the resulting cell pellet lysed with 100µl of hot 2x SDS-PAGE loading buffer per 1 million cells. The 2x SDS-PAGE loading buffer recipe is shown in Table 2.8 (section 2.1.6) and was preheated to 90˚C on a heat block within a fume cupboard. The loading buffer and cell pellet were mixed together, and samples heated at 90˚C for denaturation of protein before snap cooling on ice. Protein lysates were then briefly centrifuged using a table top microcentrifuge to collect contents and stored at -20˚C.

2.2.10 Coomassie Staining

For the Coomassie blue staining, the appropriate percentage of SDS PAGE resolving gel was prepared as shown in Table 2.9 (section 2.1.6). Resolving gels were overlaid with ethanol which was removed once the gel had polymerised. A stacking gel was prepared using: 2.1mls of dH2O, 500µl of 30% acrylamide, 380µl of 1M Tris pH 6.8 for a total volume of 3ml per gel. Gel electrophoresis was performed with 1X SDS-PAGE buffer and BioRad power pack was used to run the gel at 300 volts and 40mAps for 45 minutes. Once the proteins had separated, the gel was stained with Coomassie blue (recipe: 300ml H2O, 150ml methanol (Fisher Scientific), 50ml Acetic acid (Fisher Scientific) and small drops of Brilliant Blue for colourisation) and left to incubate at room temperature on a shaker for 30 minutes. The Coomassie blue was drained off and the gel destained (450ml H2O, 450ml methanol and 100ml Acetic acid) with two 10-minute washes using destain before a final wash for 30 minutes on an orbital shaker

.

2.2.11 Western blotting

Protein lysates were prepared as described above (section 2.2.13) and gel electrophoresis performed as described in section 2.2.14. The proteins were then electro-blotted onto nitrocellulose membrane in 1x transfer buffer (100ml of 10x Transfer buffer, 800ml H2O and 100ml of methanol) for 1 hour at 300 volts and 400mAps. The membranes were then blocked in 5% non-fat skimmed milk/TBS-T (2.5g non-fat skimmed milk powder (Marvel) and 50ml 1x TBST) for another hour and incubated overnight at 4°C in primary antibodies. Primary antibodies were either diluted in 5% BSA/TBST (0.5g Bovine Serum Albumin (BSA) (Fisher Scientific) and 10ml 1x TBST) or 5% Milk/TBST (Table 2.4, section 2.1.4). The membranes were washed in 1X TBST (100ml 10x TBS, 900ml H_2O and 1ml Tween 20 (Fisher Scientific)) for three 15-minute washes before incubating for 1 hour with appropriate secondary antibodies (HRP-Conjugated Dako), diluted in 5% BSA/TBST or 5% milk/TBST (Table 2.4, section 2.1.4). Membranes were washed as before with 1x TBST. For detection and visualisation of protein bands, membranes were transferred to the dark room with red filter light and chemiluminescent substrate containing 0.0148g/ml of Coumaric acid and 0.0443g/ml of luminol (solution A) and 1:1000 dilution of H_2O_2 (solution B) in 100mM Tris pH 7.0, were added directly onto each membrane and incubated for 1 minute. Substrates were drained off the membrane before placing between two pieces of clingfilm/saran wrap or plastic bag and gently smoothed to remove air bubbles. The appropriate size of autoradiography film (Amersham Hyperfilm GE Healthcare) was added on top of the membrane and the cassette closed. Exposure time was initially for 1 minute for each experiment before adjusting for optimum exposure time. Kodak Developer mixed with H_2O (1:4 dilution) was used to develop the film for 1 minute before rinsing in water and fixed using Kodak Fixer mixed with approximately of H_2O (1:4 dilution). Membranes were then rinsed with water and dried.

2.2.12 RNA extraction

Cells for RNA extraction were prepared first by aspiration of the culture medium from the flask, washing with 1x phosphate buffered saline (PBS, Severn Biotech Ltd) then adding TrypleExpress (Fisher Scientific)and incubating at 37°C 5% CO_2 for 2-5 minutes. Cells were resuspended in fresh medium before centrifugation at 5,000rpm for 5 minutes. Cells were washed with 1x PBS (Severn Biotech Ltd) and cell pellets collected after centrifugation at 5,000rpm for 5 minutes. All RNA samples not processed immediately after extraction were stored at -80°C. RNase Away or 70% IMS were utilized throughout RNA extraction, cDNA synthesis, RT-PCR and qPCR processing for prevention of RNase contamination and filtered tips were also used. RNA extraction was carried out using the following two methods.

2.2.12.1 Tri Reagent RNA extraction

For Tri-reagent (Sigma-Aldrich) RNA extraction, lysates were prepared by resuspending cell pellet in Tri-reagent (1ml per 5 x 10^6 cells) and stored at -80˚C until ready for processing. The RNA extraction involved thawing the RNA lysate in ice at room temperature. Once completely thawed, the homogenate was transferred to a smaller tube (1.5ml) and 200µl of chloroform (Fisher Scientific) was added per ml of lysate. Chloroform causes the denaturing of the proteins within the cells thus making them soluble in the organic phase whilst the nucleic acids remain in the aqueous phase. The tube was then shaken vigorously for 15 seconds and allowed to stand for 5 minutes at room temperature. The mixture was then centrifuged at 12000 rpm for 15 minutes after which, the aqueous phase was carefully isolated and

pipetted into another pre-labelled tube. 1:2 ratio of 2-propanol to TRI reagent) (Fisher Scientific) was subsequently added to the tube with the aqueous phase and mixed. The mixture was allowed to stand at room temperature for 5 minutes then centrifuged at 12000 rpm for 10 minutes. The RNA precipitate formed a pellet at the side and bottom of the tube. The supernatant was then pipetted out carefully to avoid disturbing the pellet. The RNA pellet was then washed with 1ml of 70% Ethanol. The sample was vortexed and centrifuged at 7500 rpm for 5 minutes. Once the supernatant was removed, the RNA pellet was air dried at room temperature for 5-10 minutes avoiding drying it completely as it would decrease the solubility. The final preparation of RNA was diluted in 50µL of sterile DNase/RNase free water.

2.2.12.2 RNeasy Mini Spin Column Extraction (Qiagen)

For quantitative-PCR, RNA was prepared using RNeasy mini Kit from Qiagen. This is a commercially available kit that uses silica-membrane RNeasy spin columns to extract high quality purified RNA. The kit contains: RLT, RPE and RW1 buffers with RNase free water, RNeasy spin columns, 2ml and 1.5ml collection tubes. Cell pellets were prepared as above for RNA extraction. Lysates were prepared by adding 350µl of RLT buffer provided with the kit. This is a denaturing buffer containing guanidine-thiocyanate which inactivates RNases to ensure purity of sample. 70% Ethanol was added at an equal volume to ensure appropriate binding conditions to the silica membrane. Up to 700µl of the mixture was added to the RNeasy Mini spin column placed in a 2ml collection tube before centrifugation at ≥ 10,000rpm for 15 seconds. The flow–through was discarded before washing the RNeasy Mini spin column with 700µl of buffer RW1. The column was centrifuged for 15 seconds at ≥ 10,000rpm

and flow-through discarded. The spin column membrane was further washed with 500µl buffer RPE. Buffer RPE was supplied as concentrate and a working solution was prepared by adding 4 volumes of 100% ethanol. The mini spin column was then centrifuged for 15 seconds at ≥ 10,000rpm before a second wash with 500µl of RPE buffer and centrifugation for 2 minutes at ≥ 10,000rpm. This allowed the column membrane to dry ensuring no ethanol remains in the RNA elution process. The RNeasy spin column was then placed in a new 2ml collection tube and centrifuged at full speed for 1 minute to ensure total elimination of the Buffer RPE. The RNeasy spin column was then placed in a pre-labelled 1.5ml collection tube before adding 50µl of RNase-free water directly onto the spin column membrane. The tube was then centrifuged for 1 minute at ≥ 10,000rpm to elute the RNA.

2.2.12.3 RNA quantification and purity

The RNA was diluted 1:4 in sterile DNase/RNase free water and 1µl of sample was placed onto the nanodrop machine (Spectrophotometer Nanodrop 2000c) and read for concentration of RNA at 260nm. The results were presented in ng/µl. Purity was determined by calculating absorbance ratio at 260nm and 280nm. A ratio between 1.8-2.0 is generally determined to show pure RNA and free of DNA and protein contamination.

2.2.13 Complementary DNA (cDNA) Synthesis

Complementary DNA was synthesised using SuperScript II Reverse Transcriptase (Invitrogen) kit. To begin with, RNA samples were defrosted on ice. Once defrosted, 1µl of random primers (100ng) and 1µl of dNTP Mix (10mM each) were added to the appropriate

volume of RNA used for each sample. The volume of RNA to use was calculated by: desired RNA concentration for cDNA synthesis (250ng/ul) /RNA concentration as determined by nanodrop reading (ng/µl). Sterile distilled water was added for a total volume of 12µl. The mixture was then centrifuged and placed on the heat block at 65˚C for 5 minutes. Once incubated, the samples were placed on ice immediately and centrifuged to collect the contents. 5X First-Strand Buffer (250mM Tris-HCl) was then added (4µl) along with 1µl of RNaseOUT (40 units/uL) and 2µl of 0.1 M DTT to the RNA mixture. The contents were mixed gently, and tubes incubated for 25˚C for 2 minutes. SuperScript II RT was added (1µl) to the tube and pipetted up and down to mix together. The mixture was then incubated on a heat block with the following parameters: 10 minutes at 25˚C, then 50 minutes at 42 ˚C and finally at 70˚C for 15 minutes to inactivate the reaction. The cDNA was stored at -20˚C until further processing.

2.2.14 Polymerase Chain Reaction (PCR)

Primers for *PTK6* were designed as described in (Harvey *et al.*, 2009). The primer sequences of *PTK6* and β actin (Sigma) are shown in Table 2.5 (section 2.1.5). Primers were provided at concentration of 100µM and diluted to 1µM using sterilised water. The cDNA was defrosted on ice along with the reagents required for this procedure. The master mix was prepared

with (per sample) for total of 25µl:

- 1x of REDTaq Readymix PCR Reaction Mix with MgCI2 (Sigma-Aldrich)
- Sterile distilled water
- Forward Primer (1µM)
- Reverse Primer (1µM)
- cDNA (250ng/µl).

Master mix was pipetted into each tube and the cDNA was carefully pipetted into the lid of each tube and the lid closed tightly. The contents were mixed together by centrifuging briefly to collect them at the bottom of the tube. The tubes were then incubated in the thermal cycle with the following parameters.

For the reaction with β actin primers:

- 35 cycles of denaturing at 95˚C for 30 seconds
- Primer annealing at 58˚C for 30 seconds and extensions at 72˚C for 45 seconds.
- The final step was at 72˚C for 10 minutes.

For the reaction with *PTK6* primers:

- 35 cycles of denaturing at 95˚C for 30 seconds
- Primer annealing at 63˚C 30 seconds and extensions at 72˚C for 45 seconds
- The final step was at 72˚C for 10 minutes.

2.2.15 Gel Electrophoresis

Once the PCR reaction was completed, the PCR product validity was determined by gel electrophoresis. A 50x stock solution of TAE (Tris-acetate-EDTA) was prepared with 242g

Tris base, 57.1ml acetic acid and 500ml of 500Mm EDTA pH 8.0 with final volume of 1L made up with water. 1g of agarose (Fisher Scientific) was dissolved in 100ml of 1x TAE buffer. The mixture was carefully heated in a microwave until all the agarose had completely dissolved. The mixture was cooled before adding 5µl of SYBR Safe, a DNA gel stain (Invitrogen) and poured onto a sealed tray with a comb and left to set for approximately 20 minutes. The gel was then placed onto a tank containing 1x TAE buffer. 15µl of the PCR product was loaded into the wells along with 5µl of a 1Kb DNA Hyperladder (Fisher Scientific). The gel was run at 100V and 400mAps for approximately 45 minutes. Once the PCR product had migrated through the gel, it was visualised using Gel Doc Imaging System (BioRad).

2.2.16 Quantitative PCR (qPCR)

2.2.16.1 geNORM Analysis

Before quantitative PCR experiments, geNORM analysis was performed to determine the appropriate reference genes to use as control for stably expressed genes in the cell lines as well as determining the number of reference genes to use. The Primer Design geNORM analysis kit for 12 genes was used for this and protocol carried out according to the manufacturer's guidelines. The genes used for geNORM analysis are shown in Table 2.12. Upon receipt of the primers, they were briefly centrifuged and resuspended in RNase/DNase free water (220µl). The master mix for each reference gene was made as shown in Table 2.13. 15µl of the master mix for each gene was pipetted in duplicate into a 96 well plate along with 5µl of cDNA (5ng/µl) or water as negative control. The plates were then sealed using MicroAmp Clear Adhesive Film (Applied Biosystems) to prevent evaporation and well-to-well contamination. The amplification conditions are outlined in Table 2.14. The experiments

were carried out using the QuantStudio 7 Flex Real Time PCR system. The geNORM analysis was carried out using duplicate wells for each gene and repeated twice using QuantStudio 7 Flexi Real-Time PCR system (Applied Biosystems) for all experimental conditions and average values taken to determine the reference genes to use. geNORM analysis was carried out with the Primer Design recommended qBase+ software (Biogazelle).

Table 2.12 The 12 reference genes in geNORM analysis (Primer Design).

Gene	**Full Name**
ACTB	Beta actin
GAPDH	Glyceraldehyde-3-phosphate dehydrogenase
UBC	Ubiquitin C
B2M	Beta-2-microglobulin
YWHAZ	Phospholipase A2
RPL13A	Ribosomal protein L13A
18S	18S RNA
CYC1	Cytochrome C1
EIF4A2	Eukaryotic translation initiation factor 4A isoform 2
SDHA	Succinate dehydrogenase complex
TOP1	Topoisomerase DNA 1
ATP5B	ATP synthase subunit

2.2.16.2 Quantitative PCR (qPCR) protocol for detection of *PTK6* transcripts

qPCR was carried out to detect and quantify relative gene expression. Primers for *RPL13A*, *SDHA*, *PTK6* and *ALT-PTK6* transcripts are shown in Table 2.6 (section 2.1.5). Primers for *PTK6* and *ALT-PTK6* were custom made by Primer Design and the primer sequences provided by them. For *RPL13A* and *SDHA*, which were used as endogenous controls, Primer Design do not provide the sequences, so to comply with MIQE guidelines (Bustin *et al.*, 2009) new primers were designed and produced by Sigma Aldrich. These primers were shipped lyophilised and resuspended in RNase/DNase free water (100µM) and further diluted to 1µM to use as stock. Final concentration used was same as template primers. For custom made primers by Primer Design, the manufacturers protocol was used. The primers were provided lyophilised and were centrifuged to collect the contents before mixing with RNase/DNase free water to 300nM concentration. The master mix was prepared with Primer Design primers as indicated in Table 2.13 and the experimental parameters used are shown in Table 2.14. For negative control, water was substituted for cDNA instead. The appropriate volume was first pipetted into each of the wells in a MicroAmp Optical 96 well reaction plate (Applied Biosystems) and then 5µl of cDNA/water added. Each experiment was carried in triplicate using duplicate wells. The plates were then covered with MicroAmp® optical adhesive film (Applied Biosystems) and briefly centrifuged, and qPCRs were carried out using QuantStudio 7 Flex Real-Time PCR system (Applied Biosystems) and results analysed using the accompanying QuantStudio™ Software V1.3—for QuantStudio™ 6 and 7 Flex and ViiA™ 7 Real-Time PCR software system (Applied Biosystems).

Table 2.13 Mastermix volumes used for qPCR experiments with PrecisionPLUS Mastermix with ROX at lower level premised with SYBRgreen.

Components	**Volume for 1 Reaction (µl)**
PrecisionPLUS MasterMix with ROX at a lower level premixed with SYBRgreen	10
Primer Mix	1
RNase/DNase Free water	4
cDNA	5
Total	20

Table 2.14 The thermal parameters for qPCR.

	Step	**Time**	**Temperature (°C)**
40x Cycle	Enzyme Activation	2 minutes	95
	Denaturation	10 seconds	95
	Data Collection	60 seconds	60

qPCR analysis was carried out using the average CT (Cycle Threshold) values obtained after each run. This value is determined as the number of cycles required for the fluorescent signal to exceed the background (threshold) levels and is proportional to amount of target gene expressed in the sample. Using this CT value, the relative quantification (RQ) value was obtained. This indicates the amplification of the target gene relative to the untreated control samples which are used as endogenous control for all experimental conditions. The most common way to analyse relative quantification qPCR data is by using delta (Δ)C_q or Δ ΔC_q method (Livak and Schmittgen, 2001). To obtain the RQ value, the following steps were

carried out.

1. Normalization of Gene of Interest (GOI) to reference gene:
    a. Average CT value of GOI – Average CT value of Reference gene 1(*RPL13A)*
    b. Average CT value of GOI – Average CT value of Reference gene 2 (*SDHA*)
2. The average was obtained for both reference genes which gives the delta C_q value (ΔC_q) and normalised to untreated control samples.
3. The RQ value was obtained using the following equation: $RQ=2^{-\Delta\Delta Cq}$

2.2.17 *PTK6* and *ALT-PTK6* expression in breast cancer tissue

The experimental procedures for determining the expression of *PTK6* and *ALT-PTK6* mRNA transcripts in breast cancer tissue samples was performed by the clinical collaborators; Professor Wen Jiang (Cardiff University) and Professor Kefah Mokbel (The Princess Grace Hospital). Tissue samples with informed consent and ethical approval for the experiments were obtained as stated in (Wazir *et al.*, 2013). Breast cancer tissues (n=127) and normal background tissue (n=33) were collected and stored in -80˚C until commencement of study. The patient cohort has been part of a number of completed and on-going studies and the clinicopathological data describing the patient cohort is further described in (Wazir *et al.*, 2013). The Kaplan Meier survival graphs and statistical analysis were performed by the collaborators. Statistical analysis was determined at multiple levels using a number of statistical tests including Logrank (Mantel Cox) for significant difference between high and low *PTK6* expression in relation to overall survival at later time points with Breslow (generalized Wilcoxon) test showing significant difference at the earlier time points. The

Tarone-Ware test was used to further assess distribution of overall survival with assumptions that there is identical distribution as well as equal variance.

2.2.18 Statistical Analysis

Statistical analysis was performed to assess any changes that were observed for my experiments. Students unpaired t-test using Excel was used to assess differences in means between two independent samples. The IC50 (IC50 indicates dose at which 50% of cell death occurs) values were determined using Excel. Correlation analysis was performed using Graphpad Prism Software, Spearman rho correlation coefficient and *P* values were determined. To determine whether there are any statistically significant differences between the means of three or more independent groups, one-way Analysis of Variance (ANOVA) test was used. This test was performed using GraphPad Prism Software (GraphPad Software). The results of the ANOVA test are reported as, for example, ANOVA ($F(2,27) = 4.467$, $P = .021$).

The first F value (2 as shown in the example) shows the degree of freedom (variation) between samples. The second F value (27 as shown in the example) shows the degree of freedom (variation) within the samples. The F value is the ratio of variance (e.g. the value 4.467 is the F statistic ratio as shown in the example above). It is calculated as: variation between samples/variation within samples. The *P* value is shown as *P* = (e.g. the value *P*=.021 in the example above). Statistical difference ($P<0.05$) is denoted by an asterisk (*) on graphs.

3.0 Chapter 3: Investigating the role of Brk in radio-sensitivity and the DNA DSB damage response pathway in breast cancer cell lines

3.1 Introduction

Since the discovery of X-rays in 1895 by German physicist W.C. Roentgen, radiotherapy (RT) has evolved to become a major therapy for cancer patients. With the advancement of technology and our understanding of cancer, radiotherapy has proven to be an effective mode of treatment whether as a stand-alone therapy or in combination with surgery, chemotherapy and other targeted treatments. Approximately, over 27% of patients diagnosed with cancer received radiotherapy during 2013-2014 in England and 63% of breast cancer patients received palliative or curative radiotherapy (NCRAS, 2017). The studies in this chapter utilised the ^{60}Cobalt radiation source (Puridec Technologies Ltd) which was first applied for patient treatment in 1948 and allowed for radiation doses of up to 60 Gy to be delivered to deep-rooted tumours without exceeding their tolerance dose (reviewed in Thariat *et al.*, 2013). The exact method of cell death induced by radiation is not entirely clear although it is mostly due to mitotic cell death. Radiation is known to effectively induce DNA double strand breaks which, if not repaired efficiently or correctly may lead to loss of reproductive and replicative ability. Eventual cell death can be via programmed cell death or through mitotic catastrophe; a process whereby cells improperly enter mitosis resulting in aberrant chromosome segregation and cell division with formation of abnormally sizes cells displaying improper nuclear morphology (Eriksson and Stigbrand, 2010). The clinical significance of RT was seen early on especially in breast cancer patients, where randomised studies showed RT combined with 'quadrantectomy' and axillary dissection was just as effective as radical mastectomy (Veronesi *et al.*, 1981). This proved to be a clinical breakthrough, allowing for treatment of breast cancer patients with an alternative method that did not involve such radical mastectomies. The benefits of radiotherapy extended to increase patient overall survival and local control, and the combination of radiotherapy and adjuvant chemotherapy

led to better survival outcomes compared to chemotherapy alone (Ragaz *et al.*, 2005). Advances in radiotherapy treatment modalities have led to better delivery of dose to the cancerous sites aided by computational models and 3D imaging. With the advent of computerised tomography (CT), planning of radiation doses and shaping of the radiation field around the tumour volume has made it possible to deliver the radiation dose more accurately thus avoiding any non-cancerous organs at risk of being exposed. Intensity modulated radiotherapy (IMRT) enables further modulation of multiple beams, again ensuring better conformity around the cancer and surrounding organs (reviewed in (Thariat *et al.*, 2013)). Further improvements are involving 4-D radiotherapy using image guided radiotherapy (IGRT), a technique that considers the movement and position of the patient, tumour or organ (Bucci, Bevan and Roach, 2005). This technique is useful to account for changes in breathing patterns during treatment in patients with lung cancer or changes to the position of the prostate due to bladder filling or air within the rectum (Ling, Yorke and Fuks, 2006). Accordingly, new technologies are paving the way for high dose radiotherapy treatments targeting cancerous tissues while minimizing surrounding organs and reducing any adverse toxicities.

3.1.1 Radiotherapy and signalling pathways

Exposure of carcinoma cells to radiation causes DNA damage by direct ionisation of the macromolecules as well as by generation of reactive oxygen species (ROS) (Wang *et al.*, 2016). The damage results in activation of the DNA damage response (DDR) pathway, subsequently leading to activation of p53, ataxia telangiectasia mutated (ATM) and ATM - Rad3-related (ATR) protein as well as the activation of growth factor receptors in the plasma

membrane, for example the ERBB family of receptors (Dittmann *et al.*, 2017). In effect, cells recognising DNA damage induced by irradiation, utilise complex signalling pathways that control cellular responses involved in apoptosis, cell cycle arrest and/or repair (reviewed in Lewanski and Gullick, 2001). More specifically, double strand breaks induced by ionising radiation, which are the most deleterious lesions, are repaired by either non-homologous end joining (NHEJ) or homologous recombination (HR). The HR pathway uses a sister chromatid or homologous chromosome as a template to repair the broken DNA (Hartlerode and Scully, 2009). Due to the reliance of a sister chromatid, HR repair is usually less error prone compared to NHEJ and more active during the S and G2 phase of the cell cycle, whereas NHEJ is active throughout the cell cycle (Cannan and Pederson, 2017). The mechanism of HR repair requires generation of 3'-single stranded DNA (tail ends) which are rapidly coated by replication protein A (RPA) and protects against degradation (Barker and Powell, 2010). The RPA is replaced by the BRCA2 protein on single stranded DNA and promotes formation of Rad51 filaments (Barker and Powell, 2010). Rad51 assists in the repair of DSBs by catalysing the homology and strand exchange between homologous DNA. Strand invasion leads to formation of a 'D-loop' which can directly act as the template for repairing DSB (Barker and Powell, 2010). Once the Rad51 is removed, leaving the 3'OH end free, DNA is synthesised by the DNA polymerase δ and DNA ends joined by DNA ligase (Borrego-Soto *et al.*, 2015). Once the regions of strand exchange extend and two double stranded molecules are separated into 4 strands behind the invading 3' strand, a structure known as a Holliday Junction forms which is a cross shaped structure involved in the exchange of genetic information during recombination (Barker and Powell, 2010). There are many proteins involved in HR and their recruitment and functions are promoted by upstream proteins such as MRE-11-Rad5—NBS1 (MRN) complex as well as other effectors downstream of DNA damage sensor such as ataxia telangiectasia (ATM) (Barker and Powell, 2010). Defects in

any of the steps during HR repair can lead to impairment of damaged DNA including DSB induced by ionising radiation, for example, mutations in BRAC1 or BRCA2 increases radio-sensitivity (Barker and Powell, 2010).

Majority of the DSBs are repaired by the NHEJ pathway and involves the recognition and binding of the Ku70/80 heterodimer and MRN complex to the exposed end of the DSB leading to the recruitment of the catalytic subunit of the DNA dependent protein kinase (DNA-PK), which translocates the Ku complex along the DNA and allows tethering of the two DNA molecules (Borrego-Soto *et al.*, 2015). DNA ligase IV interacts with the Ku heterodimer to ligate the DNA ends, which exists in complex with X-ray cross complementing gene 4 (XRCC4) and XRCC4-like factor (XLF) (Wang and Lees-Miller, 2013). Nucleases exonuclease 1 (Exo1), Mre11 and Artemis are involved in processing any damaged DNA termini before DNA ligation (Weterings *et al.*, 2009; Xie, Kwok and Scully, 2009; Bahmed *et al.*, 2011).

Furthermore, upon DNA damage, the DNA damage sensors (ATM, ATR and DNA-PK) are also involved in activation of Akt (Liu *et al.*, 2014). The Akt and DNA-PK complex stimulates binding of DNA-PK with Ku heterodimer as well as the release of DNA-PKcs from the damage needed for ligation and termination of double strand break repair (Liu *et al.*, 2014). The mechanistic target of rapamycin (mTOR) is a prominent downstream effector of Akt signalling which upon activation cell survival, growth and proliferation is induced by phosphorylation of effector molecules such as ribosomal S6 kinases (reviewed in Karimian *et al.*, 2019). There is evidence of signalling cross talk between the DNA damage response and P13K/Akt pathways, as Nbs1 which is a component of the MRN sensor complex for detecting double strand break repair, also interacts with the catalytic subunit of P13K and stimulates its activity (Chen *et al.*, 2008).

Improving our understanding of the signalling pathways involved in radiotherapy-induced DNA damage in the target cancer cells may provide a potential method by which radio-sensitisation of cancer cells can be assessed clinically as well as to prevent resistance. Many of these signalling molecules, for example p53, ATM/ATR, ERK1/2, AKT and mTOR, are activated to increase cancer cell survival and ultimately lead to development of radio-resistant tumour cells (reviewed in Hein, Ouellette and Yan, 2014). Interestingly, Brk appears to interact with most of these signalling molecules and thus, may have a role in sensitising cells to radiotherapy. Following exposure of colon cancer cells to γ-radiation, Brk is induced at significantly higher levels in cells with wild type p53 than it is in p53-null cell lines, suggesting a potential role for p53 in Brk induction (Gierut *et al.*, 2012). Furthermore, knockdown of Brk was shown to increase apoptosis in p53 +/+ colon cancer cells following DNA damage induced by chemotherapeutic agents or γ-radiation (Gierut *et al.*, 2012). Brk and Akt association has also been previously shown (Zhang *et al.*, 2005), with Akt activation leading to increased tumour cell proliferation (Zheng *et al.*, 2010). However, a contradictory function for Brk is shown in oesophageal squamous cell carcinoma (ESCC), where it is involved in down-regulating Akt activation and thus may have a role as a tumour suppressor (Miah, Martin and Lukong, 2012). In addition, in a non-tumorigenic context, Brk promotes cell death in intestinal crypt epithelial cells via inhibition of Akt and Erk1/2 after DNA damage induced by γ-radiation (Haegebarth *et al.*, 2009).

3.1.2 Brk and ATM

Many cancers have deregulated mechanistic target of rapamycin (mTOR) activity and it is involved in the development and progression of malignancies (Pópulo, Lopes and Soares,

2012). The mTOR pathway is considered a potential therapeutic target in breast cancer and early stage clinical studies in HER2 positive breast cancer patients show promising results with a combination of mTOR inhibitors and HER2 targeted therapies (Vinayak and Carlson, 2013). Since Brk induces ErbB3 phosphorylation and recruitment of P13Kp85 to ErbB3 thus enhancing P13K activity (Kamalati et al., 2000), it may have an indirect effect on the mechanistic target of rapamycin (mTOR), as ErbB is an upstream activator of mTOR. Furthermore, elevated mTOR signalling suppresses ataxia telangiectasia mutated (ATM) protein expression by inducing microRNAs targeting ATM for destruction (Shen and Houghton, 2013). One of the major hallmarks of cancer is genomic instability (reviewed in Hanahan and Weinberg, 2011) and ATM is a key regulator of the cell cycle (Helt *et al.*, 2005). It is an essential component for mediating checkpoint control after cells are exposed to ionising radiation leading to double strand breaks (Lavin and Shiloh, 1997). Thus, mutations in the ATM gene, which lead to its inactivation or suppression of ATM, may increase cancer cell sensitivity to radiotherapy.

3.2 Aims and Objectives

Aims:

Previous studies have not shown a direct link between Brk and radio-sensitivity in breast cancer cell lines. The aims of this chapter were to investigate if Brk expression influences radio-sensitivity of breast cancer cell lines as well as to determine the potential mechanism that mediated the radio-sensitivity. It was hypothesised that cell lines with high Brk expression may sensitise breast cancer cell lines to radiotherapy and this may be through deregulating the DNA DSB response pathway and through direct interaction with the ataxia telangiectasia mutated (ATM) protein.

The objectives were to:

- To determine the radio-sensitivity of different breast cancer cell lines to γ-radiation through clonogenic survival in relation to Brk protein expression
- Investigate the role of Brk in the DDR response pathway through γ-H2AX DNA repair assays
- Examine whether there is a functional link between Brk and ATM signalling through analysis of total and phosphorylated protein levels of ATM in breast cancer cell lines.

3.3 Results

3.3.1 Clonogenic assays show a decrease in colony formation after exposure to increasing doses of gamma radiation

The first aim was to determine the radio-sensitivity of the cell lines highlighted for study. These cell lines included MCF10A an immortalised non-transformed cell line, T47D representing Luminal A subtype of breast cancer, SKBR3 and BT474 which are HER2 positive cell lines, GI101 a metastatic model and triple negative cell lines MDA-MB 231and MDA-MB 436. To do this, radiation experiments were carried out for each cell line in triplicate petri dishes from three independent repeats. Cells were exposed to increasing doses of γ-radiation then plated and incubated to allow colonies of approximately 50 cells to develop. After two weeks, colonies were counted for each cell line and dose.

With increasing dose of radiation, there was a decrease of methylene blue stained colonies as expected for all cell lines. A representative image of the colony formation is shown in Figure 3.1 and it can be seen that colony sizes varied between different breast cancer lines. The size of colonies was larger in the HER2 positive BT474 cell line as well as the triple negative cell lines MDA-MB 231 and MDA-MB 436 in comparison to some of the other cell lines (data not shown). The difference in size of colonies was initially thought to relate with levels of Brk expressed in each cell line. For example, when the triple (and Brk) negative cell line MDA-MB 468 was transfected to express Brk, cells with wild-type Brk formed larger colonies than those expressing kinase inactive Brk. However, comparable results were not observed in the MDA-MB-157 cell line and this was not consistent with the rest of the breast cancer cell lines. For example, the T47D colony morphology showed smaller colony sizes compared to BT474 but had high levels of Brk expression. These data suggest that the size of colonies formed in the clonogenic assays are not dependent on Brk expression levels.

Each survival curve represents the average from three independent experiments. The number of colonies for each time point and cell line in irradiated cells were expressed as percentage of control and survival curves were plotted on a semi-logarithmic scale (Figures 4.2 and 4.3). There is a proportionate decrease in the overall survival in all cell lines as the dose of γ-radiation increased. My experiments involved many different types of breast cancer cell lines that were representative of different subtypes of breast cancer in order to investigate radio-sensitivity in relation to Brk expression. The MCF10A cell line is classified as a non-tumorigenic immortalised breast cell line (Physical Sciences - Oncology Centers Network *et al.*, 2013). This cell line was one of the most sensitive cell lines to gamma radiation (Figure 3.2), with an average survival of only 2.85% at the highest dose (8Gy).

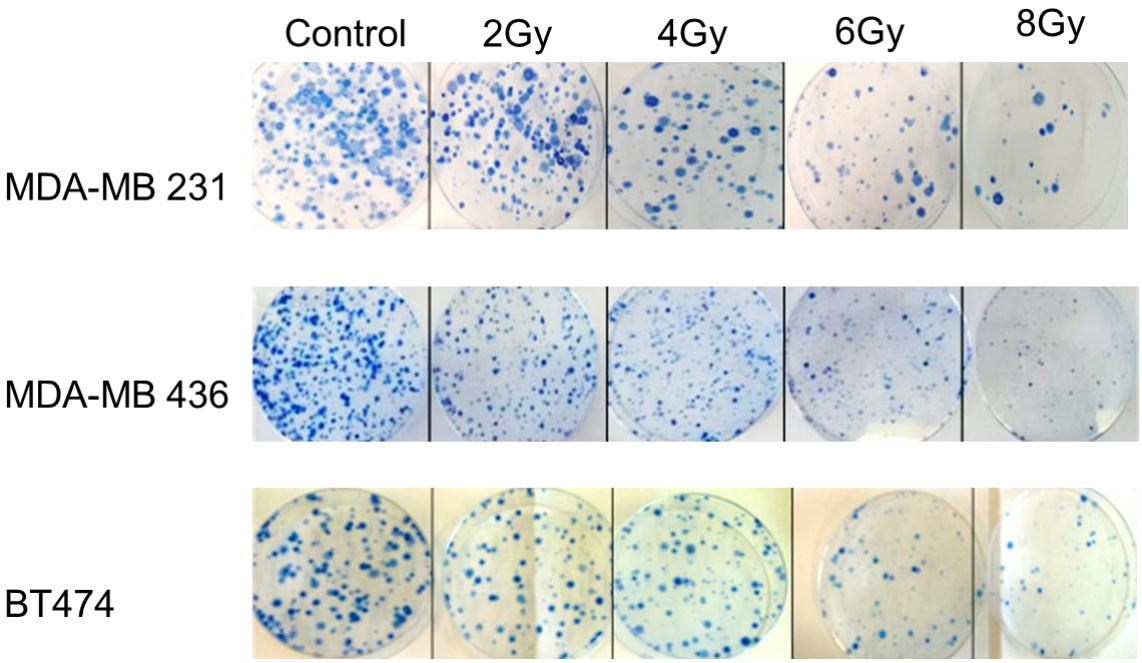

Figure 3.1. Colony formation decreases with increasing dose of gamma radiation. Cell lines were harvested and diluted to 1000 cells per ml (for 0Gy and 2Gy), 1500 cells per ml (for 4Gy) and 2000 cells per ml (for 6Gy and 8Gy) in 10ml medium and exposed to gamma radiation in 2Gy fractions. Cells were plated, incubated at 37˚C, 5% CO_2 for two weeks, fixed with 100% IMS and stained with methylene blue solution. Each blue dot represents one colony of at least 50 cells. . All images are representative of n=3 plates, from 3 independent experiments.

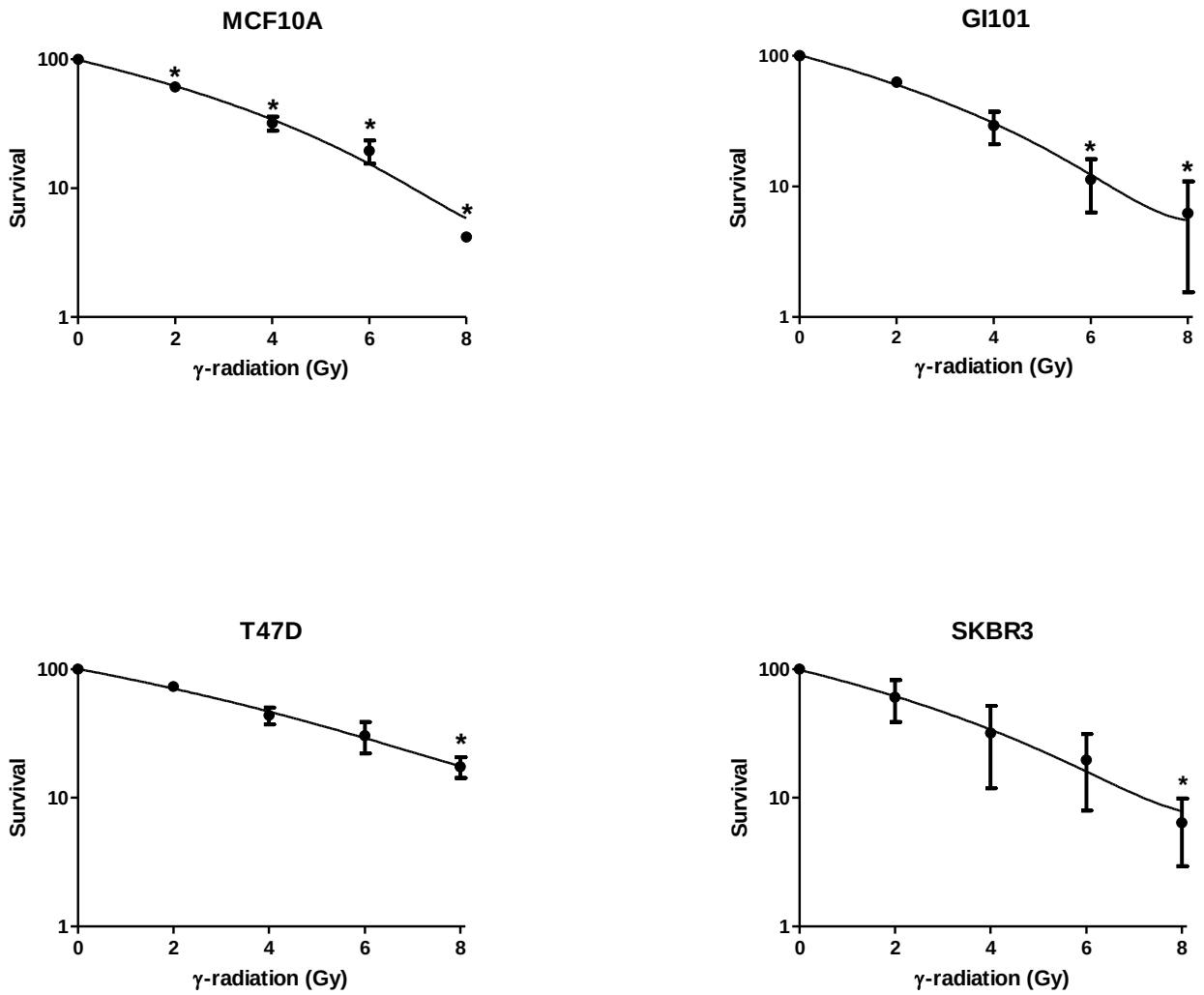

Figure 3.2. Average clonogenic survival for MCF10A, GI101, T47D and SKBR3 decreasing with increasing dose of gamma radiation. Cell lines were harvested and diluted to 1000 cells per ml (for 0Gy and 2Gy), 1500 cells per ml (for 4Gy) and 2000 cells per ml (for 6Gy and 8Gy) in 10ml medium and exposed to gamma radiation in 2Gy fractions. Cells were plated, incubated at 37˚C, 5% CO_2 for two weeks, fixed with 100% IMS and stained with methylene blue solution. . Survival graphs show average of n=3 independent experiments. Students paired T-Test was used to determine statistically significant in percentage survival between control and treated cells *P<0.05.

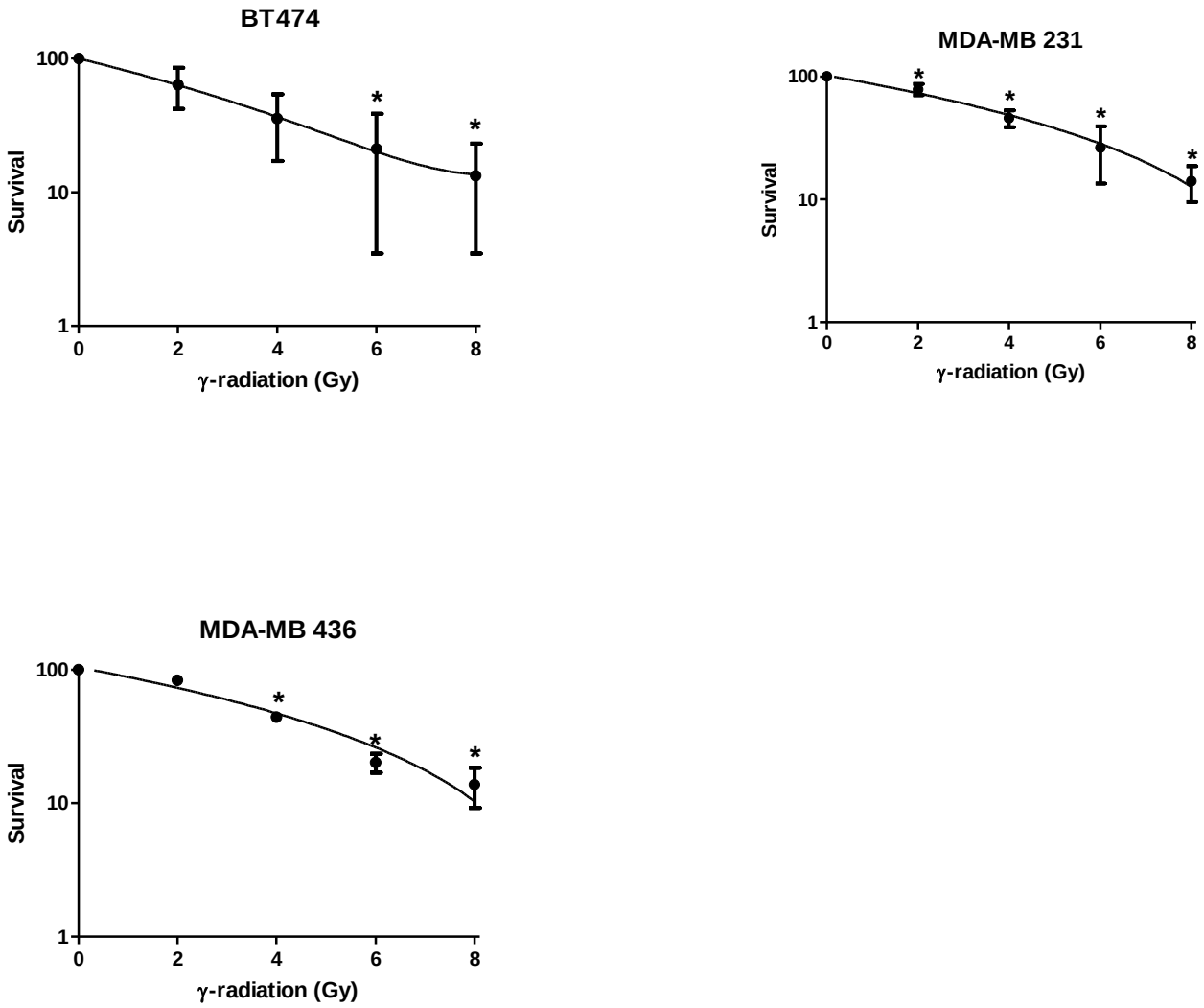

Figure 3.3. Average clonogenic survival for BT474, MDA-MB 231 and MDA-MB 436 cell lines decreases with increasing dose of gamma radiation. Cell lines were harvested and diluted to 1000 cells per ml (for 0Gy and 2Gy), 1500 cells per ml (for 4Gy) and 2000 cells per ml (for 6Gy and 8Gy) in 10ml medium and exposed to gamma radiation in 2Gy fractions. Cells were plated, incubated at 37˚C, 5% CO_2 for two weeks, fixed with 100% IMS and stained with methylene blue solution. Survival graphs show average of n=3 independent experiments. Students paired T Test was used to determine statistically significant in percentage survival between control and treated cells *P<0.05.

The T47D cell line had one of the highest survival rates at both 8Gy (17.5% +/- 7.8 standard deviation) and 2Gy (73.4% +/- 14.8 standard deviation) as shown in Figure 3.2 indicating increased radiotherapy resistance. GI101 seems to be more radiosensitive with average survival percentage of 62.9% +/- 5.1 standard deviation at 2Gy and 6.2% +/- 4.7 standard deviation at 8Gy (Figure 3.2).

The triple negative cell lines, MDA-MB 231 and MDA-MB 436 express differing levels of Brk . Both of these cell lines show survival rate at 2Gy with average percentage survival at 78.8% +/- 8.2 standard deviation for MDA-MB 231 cell line and 83.4% +/- 6.5 standard deviation for the MDA-MB 436 cell line. In addition, average percentage survival at 8Gy showed survival at 14.13% +/- 4.6 standard deviation for MDA-MB 231 (Figure 3.3) and 12.6% +/- 4.64 standard deviation for MDA-MB 436 cell line (Figure 3.3).

The HER2 positive cell lines BT474 and SKBR3 both express Brk, although at varying levels. They show a steady decrease with increasing radiation dose as with all the other cell lines and a similar percentage survival at 2Gy, 4Gy and 6Gy (Figure 3.2 and 3.3). Percentage survival was 63.7% +/- 21.7 standard deviation at 2Gy radiation dose and at 13.3% +/- 9.8 standard deviation at 8Gy dose. SKBR3 cell line may be more radiosensitive than the BT474 cell line, average percentage survival at 2Gy showed percentage survival at 60.7% +/- 21.8 standard deviation and for 8Gy at6.4% (+/- 2.5 standard deviation).

3.3.2 Brk expression does not directly affect clonogenic survival of breast cancer cell lines.

It has previously been shown that T47D cells express a high amount of Brk (Barker, Jackson and Crompton, 1997) whereas GI101 express a moderate amount. The difference in clonogenic survival may be due to different Brk expression levels. To further elucidate the effect of Brk expression on radio-sensitivity, the MDA-MB 468 and MDA-MB 157 cell lines which do not inherently express Brk, were used for transfection. These cells had previously been transfected with wild type (WT) Brk, kinase inactive Brk (KM) and an empty vector (VEC) (Harvey *et al.*, 2009), and expression was confirmed by western blotting (Figure 3.4A). Cell lines were harvested and lysed in 2X SDS-PAGE loading buffer, transferred onto nitrocellulose membrane before blocking with 5% Milk-TBST and incubating with IC-100 Brk primary antibody overnight. Anti-β actin was used as the loading control. Transfection with Brk (either wild type or kinase inactive) did not statistically alter the survival of MDA-MB-468 cells (Figure 3.4B). Since conventional schedules of radiotherapy in a clinical setting involve fractionated doses of 1.8-2Gy per fraction for a total of 40-50Gy (Plataniotis, 2010), the clonogenic survival at 2Gy (SF2 survival) was calculated.

Figure 3.4A shows Brk expression in the three variant transfected cell lines of MDA-MB 468 and MDA-MB 157. In the MDA-MB 468 VEC cell line, there was reduced clonogenic survival compared to the other two variants, however overall there was no statistically significant variation between these cell lines (Figure 3.4B). MDA-MB 157 VEC cell line appears (Figure 3.4C) to have lower overall survival rate after γ-radiation suggesting it is more sensitive to radiotherapy compared to MDA-MB 157 Brk KM and WT variants. ANOVA analysis shows a statistically significant difference between the three variants (ANOVA ($F(2,6) = 23.572$, $P = 0.001$). Clonogenic survival rate at 8Gy was as low as 3.42% for MDA -MB 157 VEC in comparison to 9.7% for MDA-MB 157 Brk WT cell line and 6.6% for MDA-MB 157 Brk KM.

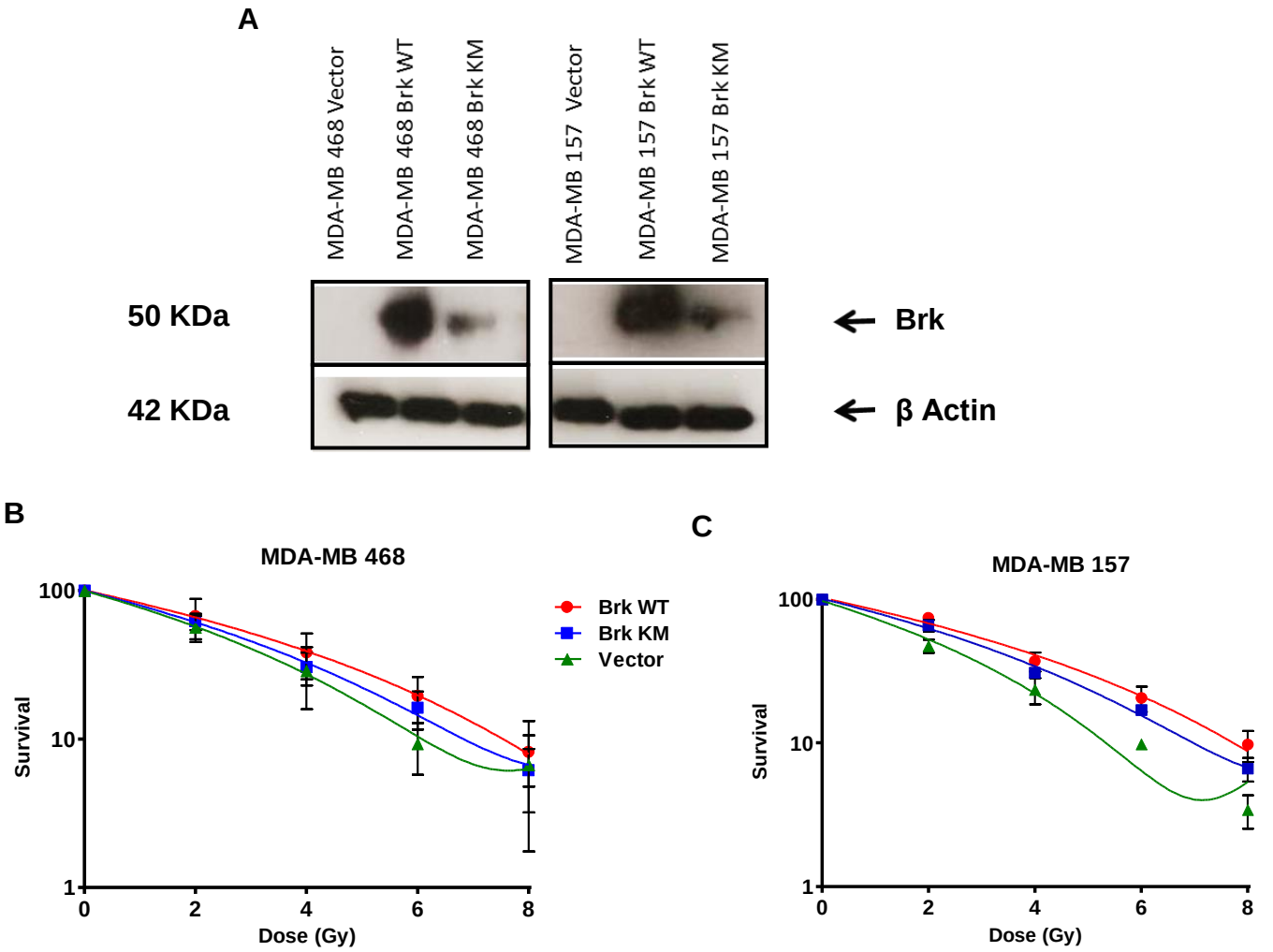

Figure 3.4 No significant difference in clonogenic survival in correlation with Brk expression was observed in both transfected cell lines. Brk expression for both cell line variants is shown in Figure 3.4A and clonogenic survival is shown in Figure 3.4B and 3.4C. Cell lines were harvested and diluted to 1000 cells per ml (for 0Gy and 2Gy), 1500 cells per ml (for 4Gy) and 2000 cells per ml (for 6Gy and 8Gy) and exposed to gamma radiation in 2Gy fractions. Cells were plated, incubated at 37˚C, 5% CO_2 for two weeks, fixed with 100% IMS and stained with methylene blue solution before counting number of colonies formed. Western blots were performed using whole lysates. Equal volume of lysates were loaded on a stacking gel and a 12% resolving gel was used. The proteins were then electro-blotted onto nitrocellulose membrane in 1x Towbin transfer buffer 1 hour at 300 volts and 400mAps. Membranes were blocked in 5% non-fat skimmed milk/TBS-T before incubating with primary antibodies overnight. The membranes were then washed with 1x TBST and incubated with the appropriate secondary antibody for 1 hour. Bands corresponding to Brk were detected after primary incubation with Brk antibody (ICR100- (Kamalati *et al.*, 1996)) and primary β actin (loading control) antibody (Abcam). Protein bands were detected using chemiluminescent substrates Coumaric acid (0.0148g/ml) and luminol (0.0443g/ml) and 1:1000 dilution of H_2O_2 in 100mM Tris pH 7.0. Mean survival from n=3 experiments is plotted with error bars representing standard deviation. ANOVA testing was performed to test significant variance between the three variants for each cell line.

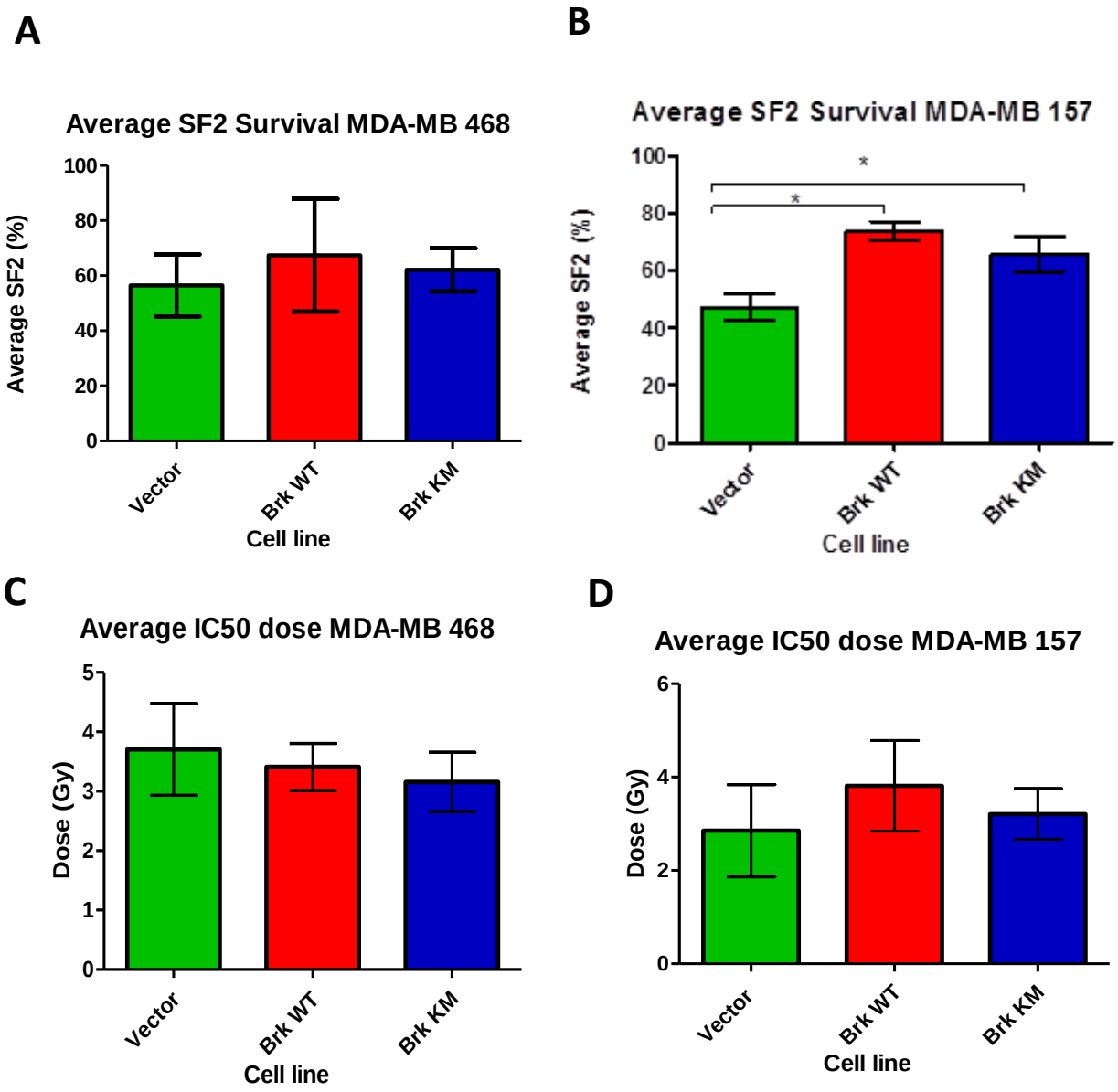

Figure 3.5 Statistically significant difference was observed for SF2 values between Brk WT and Brk KM in MDA-MB 157 cell line. Figure 3.5 A and B shows SF2 survival (survival at 2Gy dose) for MDA-MB 468 and MDA-MB 157 cell line variants respectively. Figure 3.5 C and D show the IC50 doses (IC50 indicates dose at which 50% of cell death occurs) for MDA-MB 468 and MDA-MB 157 cell line variants respectively. Cell lines were harvested and diluted to 1000 cells per ml (for 0Gy and 2Gy), 1500 cells per ml (for 4Gy) and 2000 cells per ml (for 6Gy and 8Gy) and exposed to gamma radiation. Cells were plated, incubated for two weeks and stained with methylene blue solution before counting number of colonies formed Mean SF2 survival and IC50 values from n=3 independent experiments are plotted with error bars representing standard deviation. ANOVA statistical test was used to detect significant variance between the three variants for each cell line. Students T Test was used to determine significant difference between vector and Brk WT or vector and Brk KM cell lines, *P<0.05.

No significant difference between all three variants was observed when comparing SF2 survival (ANOVA (F (2,6) = 0.449, *P* = 0.658). This suggests that high or over expression of Brk may not influence the clonogenic survival of MDA-MB-468 cells in comparison to Brk-KM and empty vector cell lines (Figure 3.5A). The SF2 values (Figure 3.5A) for MDA-MB 468 Brk WT was 67.4% (+/- 20.4 standard deviation), for MDA-MB 468 Brk KM it was 62.1% (+/- 7.8 standard deviation) and for MDA-MB 468 Vector it was 62.24% (+/- 18.53 standard deviation). Overall, there was an approximate 1.1-fold increase in SF2 survival rate between Vector only and Brk-WT cell lines. Statistically there was no significant difference observed between MDA-MB 468 Brk WT and MDA-MB 468 Vector cell lines for SF2 survival (*P*= 0.4606) which indicates Brk expression may not be linked to radiotherapy sensitivity. The SF2 values for all three variants in MDA-MB 157 cell line showed increased variance with significantly increased percentage survival for the Brk WT cell line compared to vector only cell line whereas this difference is not statistically significant in MDA-MB 468 cell line (Figure 3.5B). SF2 value for MDA-MB 157 VEC was at 54.5%, for MDA-MB 157 Brk WT it was at 76.2% and for Brk-KM variant it was at 65.8%. SF2 survival for Brk WT and Brk KM variants show statistically significant difference when compared to vector only (*P*<0.05). This suggests Brk expression may have some influence on radio-sensitivity with increased percentage survival observed in Brk expressing cells compared to the MDA-MB 157 vector cell line. The IC50 doses for all three variants for both MDA-MB 468 and MDA-MB 157 cell lines are shown in Figure 3.5C and there was no statistically significant difference between the three variants.

3.3.3 Brk expression in relation to 2Gy survival

3.3.3.1 Brk expression is induced after γ-irradiation

Previously, exposure to γ-radiation induced Brk expression in intestinal crypt epithelial cells (Haegebarth *et al.*, 2009); however, this has not been investigated in breast cancer cell lines. I sought to determine if Brk expression was induced after exposure to 2Gy γ-radiation dose in breast cancer cell lines. T47D, GI101 and SKBR3 cell lines, representative of high, moderate and low Brk expression levels, were chosen for these studies. Cell lines were exposed to 2Gy dose of γ-radiation as previously described (Chapter 2, section 2.2.6). Protein lysates were collected as described in Chapter 2, section 2.2.9at 4, 6, 24 and 48 hours post exposure to radiation and western blots were performed (Chapter 2, section 2.2.15). Figure 3.6 shows an induction in Brk expression levels over time in all cell lines examined. T47D cell line showed moderate induction of Brk with the greatest difference observed at 48 hours post treatment compared to the control lysate. GI101 cell line had the most induction of Brk at 6 hours post treatment compared to control lysate and remained at similar levels at 24 and 48 hours post radiation. The greatest induction of Brk was observed in the SKBR3 cell line, with the highest levels observed at 48 hours post radiation compared to control (Time 0) lysate. Overall, this suggests Brk is induced after exposure to γ-radiation in response to DNA damage, similar to the intestinal crypt epithelial cells.

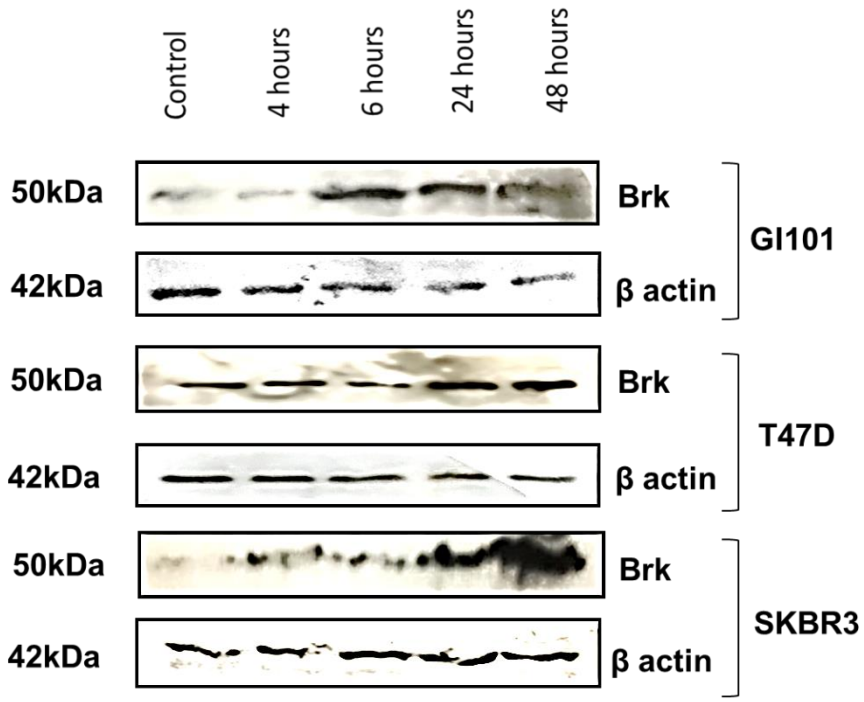

Figure 3.6 Brk is induced in response to DNA damage after exposure to γ-radiation.Cell lines were plated in 90mm petri dishes and exposed to 2Gy γ-radiation described in section 2.2.6.1 in Materials and Methods before preparing whole lysates at 4, 6, 24 and 48 hours post irradiation along with a control lysate. Equal volume of lysates were loaded on a stacking gel and a 12% resolving gel was used. The proteins were then electro-blotted onto nitrocellulose membrane in 1x Towbin transfer buffer 1 hour at 300 volts and 400mAps. Membranes were blocked in 5% non-fat skimmed milk/TBS-T before incubating with primary antibodies overnight. The membranes were then washed with 1x TBST and incubated with the appropriate secondary antibody for 1 hour. Bands corresponding to Brk were detected after primary incubation (1:100 dilution) with Brk antibody (ICR100- (Kamalati et al., 1996)) and primary β actin (loading control, 1:1000 dilution) antibody (Abcam). Protein bands were detected using chemiluminescent substrates Coumaric acid (0.0148g/ml) and luminol (0.0443g/ml) and 1:1000 dilution of H2O2 in 100mM Tris pH 7.0. N=3.

3.3.3.2 Brk expression in relation to SF2 survival rates

As Brk expression was induced in breast cancer cell lines, to assess if endogenous Brk expression may influence survival; survival at the 2Gy radiation dose (SF2) in a wider panel of cell lines was assessed in relation to Brk expression. Observing Brk expression and SF2 survival, a clear pattern does not emerge (Figure 3.7). Although statistical significance is seen between the SF2 survival rates for all cell lines (ANOVA ($F(8,19) = 3.239$, $P = 0.017$), this does not relate directly with Brk expression levels. This suggests differences in SF2 survival rates are not directly due to levels of Brk expression. BT474 and T47D cell lines express the highest levels of Brk and have some of the highest SF2 values along with the triple negative cell lines MDA-MB 231 and MDA-MB 436. T47D had a higher SF2 value and lower Brk expression compared to BT474 which had higher Brk expression but lower SF2 value. The results are not consistent for the rest of the cell lines. In comparison to the highest SF2 values (Figure 3.7) for triple negative cell lines MDA-MB-436 at 79.27% and MDA-MB-231 at 78.9%; the lowest SF2 values were for MCF10A at 57.65%, SKBR3 value at 61.31% and GI101 at 63.37%. BT474 had intermediate SF2 value at 63.73%.

It should be noted that although there might not be a direct association between SF2 survival and Brk expression; 4 out of the 5 cell lines (GI101, BT474, T47D, MDA-MB 436) with highest SF2 values show moderate to high Brk expression compared to the lower end of the SF2 survival rates which show no or low expression of Brk.

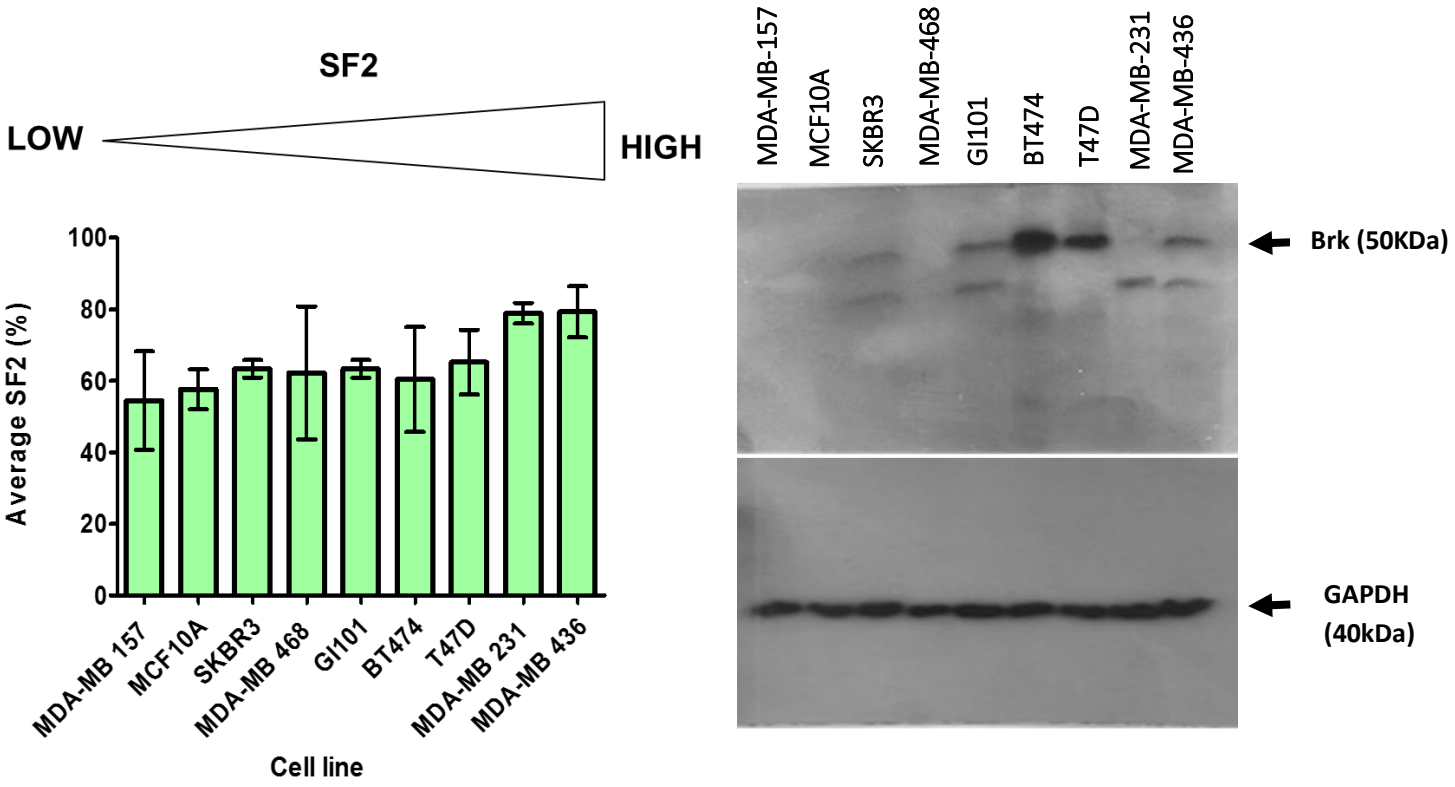

Figure 3.7 SF2 survival which indicates clonogenic survival at 2Gy dose varies between the breast cancer cell lines. Cell lines were harvested and diluted to 1000 cells per ml (for 0Gy and 2Gy), 1500 cells per ml (for 4Gy) and 2000 cells per ml (for 6Gy and 8Gy) in 10ml medium and exposed to gamma radiation in 2Gy fractions. Cells were plated, incubated at 37˚C, 5% CO2 for two weeks, fixed with 100% IMS and stained with methylene blue solution. Western blots were performed using whole lysates for all three variants of both transfected cell lines. Equal volume of lysates were loaded on a stacking gel and a 12% resolving gel was used. The proteins were then electro-blotted onto nitrocellulose membrane in 1x Towbin transfer buffer 1 hour at 300 volts and 400mAps. Membranes were blocked in 5% non-fat skimmed milk/TBS-T before incubating with primary antibodies overnight. The membranes were then washed with 1x TBST and incubated with the appropriate secondary antibody for 1 hour. Bands corresponding to Brk were detected after primary incubation with 1:100 diltuion of Brk antibody (ICR100- (Kamalati et al., 1996)) and primary Anti-GAPDH (Abcam) antibody as the loading control (1:1000 dilution). Protein bands were detected using chemiluminescent substrates Coumaric acid (0.0148g/ml) and luminol (0.0443g/ml) and 1:1000 dilution of H2O2 in 100mM Tris pH 7.0. Mean SF2 survival from n=3 experiments is plotted with error bars representing standard deviation, (ANOVA ($F(8,19) = 3.239$, $P = 0.017$).

3.3.4 IC50 survival and Brk expression

Although there was no clear association between Brk expression and 2Gy survival, there might be some significance when looking at IC50 (IC50 indicates dose at which 50% of cell death occurs) values and Brk expression. IC50 was determined using Excel. Brk expression in relation with IC50 dose, from lowest to highest is shown in Figure 3.8. Interestingly, the cell lines with higher Brk expression (BT474 and T47D) had higher IC50 values whereas cell lines with moderate to little Brk expression such as MCF10, GI101 and SKBR3 had lower IC50 values in comparison. However, ANOVA analysis showed no significant difference between average IC50 values for all cell lines (ANOVA ($F(8,17) = 2.312$, $P = 0.070$).

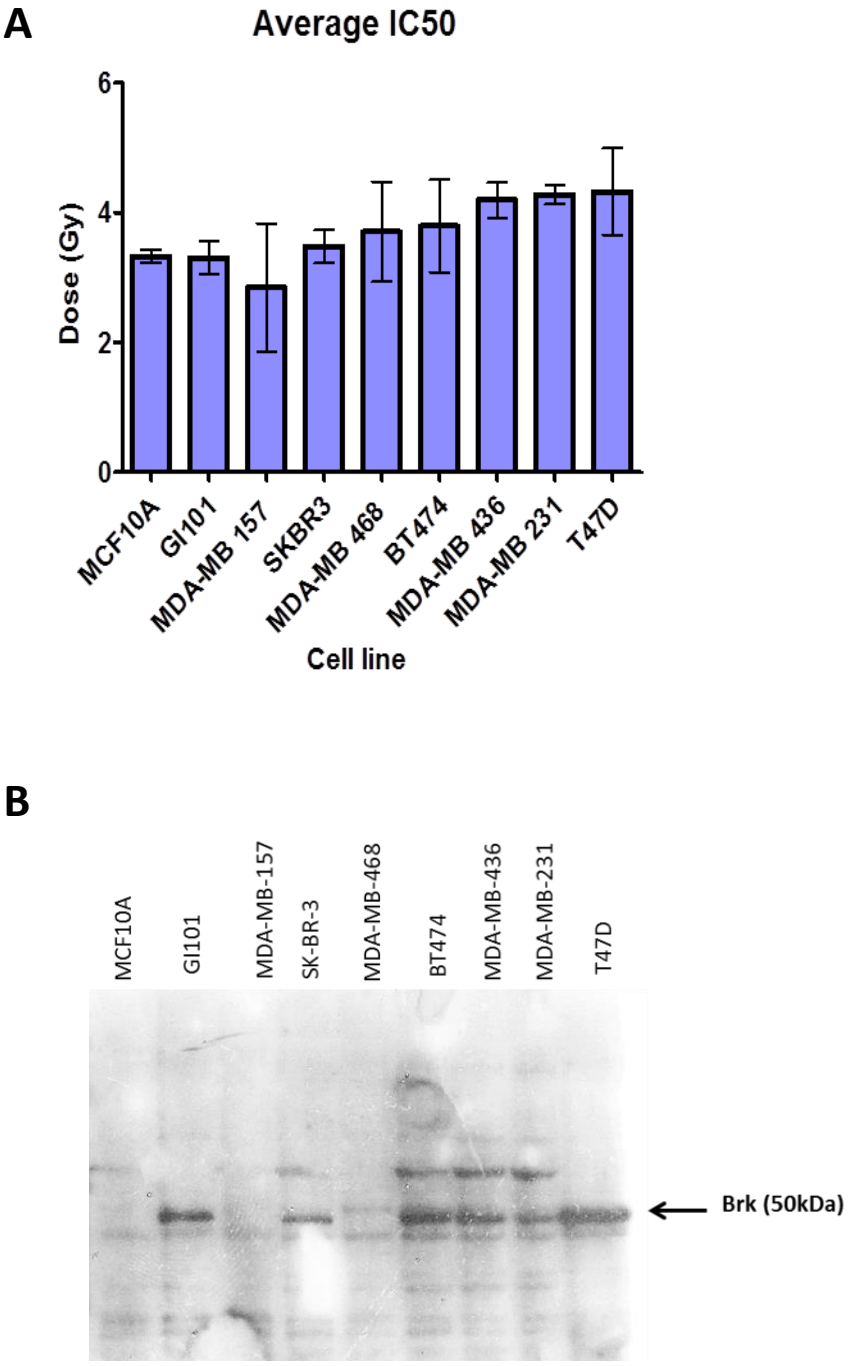

Figure 3.8 IC50 doses for 2 Gy survival, which indicates the dose at which there is a 50% reduction in survival at 2Gy dose varies between the breast cancer cell lines. Clonogenic assays were carried out as described in Figure 3.7. IC50s of 2Gy survival were determined (Figure 3.8A). Western blots were performed as described in Figure 3.7. using whole lysates for all cell lines, n=3 (Figure 3.8B). . Mean survival from n=3 experiments is plotted with error bars representing standard deviation, (ANOVA ($F(8,17) = 2.312$, $P = 0.070$).

3.3.5 γ-H2AX foci induction for different subtypes of breast cancer

To further examine Brk's role in radiotherapy, its potential role in DNA repair kinetics was investigated. Since it was originally hypothesised that Brk may be involved in sensitizing breast cancer cell lines to radiation, an involvement in DNA repair may demonstrate a potential mechanism by which it may do this. The induction of γ-H2AX post irradiation was assessed via immunocytochemistry using γ-H2AX antibody and the number of foci analysed with flow cytometry before quantification with Imagesteam IDEAS software. Originally the method of DNA double strand break detection was first introduced by Bonner and colleagues in 1999, which showed visual formation of γ-H2AX at the chromosomal sites of DNA double strand breaks (Rogakou *et al.*, 1999). Further studies indicated measuring γ-H2AX at various times up to 24 hours post radiation has proven to be a reliable technique to measure DNA double strand breaks (DSB) (Olive and Banáth, 2009; Bourton *et al.*, 2012, 2013). Cell lines representative of different subtypes (BT474, MDA-MB 436 and GI101) of breast cancer with various levels of Brk expression were selected to detect differences in DNA repair via gamma H2AX DNA repair assays. Cell lines were exposed to 2Gy gamma radiation and then processed at 30 mins, 3 hours, 5 hours and 24 hours post irradiation to assess DNA repair ability. Image flow cytometry was carried out using ImagestreamX system (Amnis Inc) with quantification of foci from 10,000 cells.

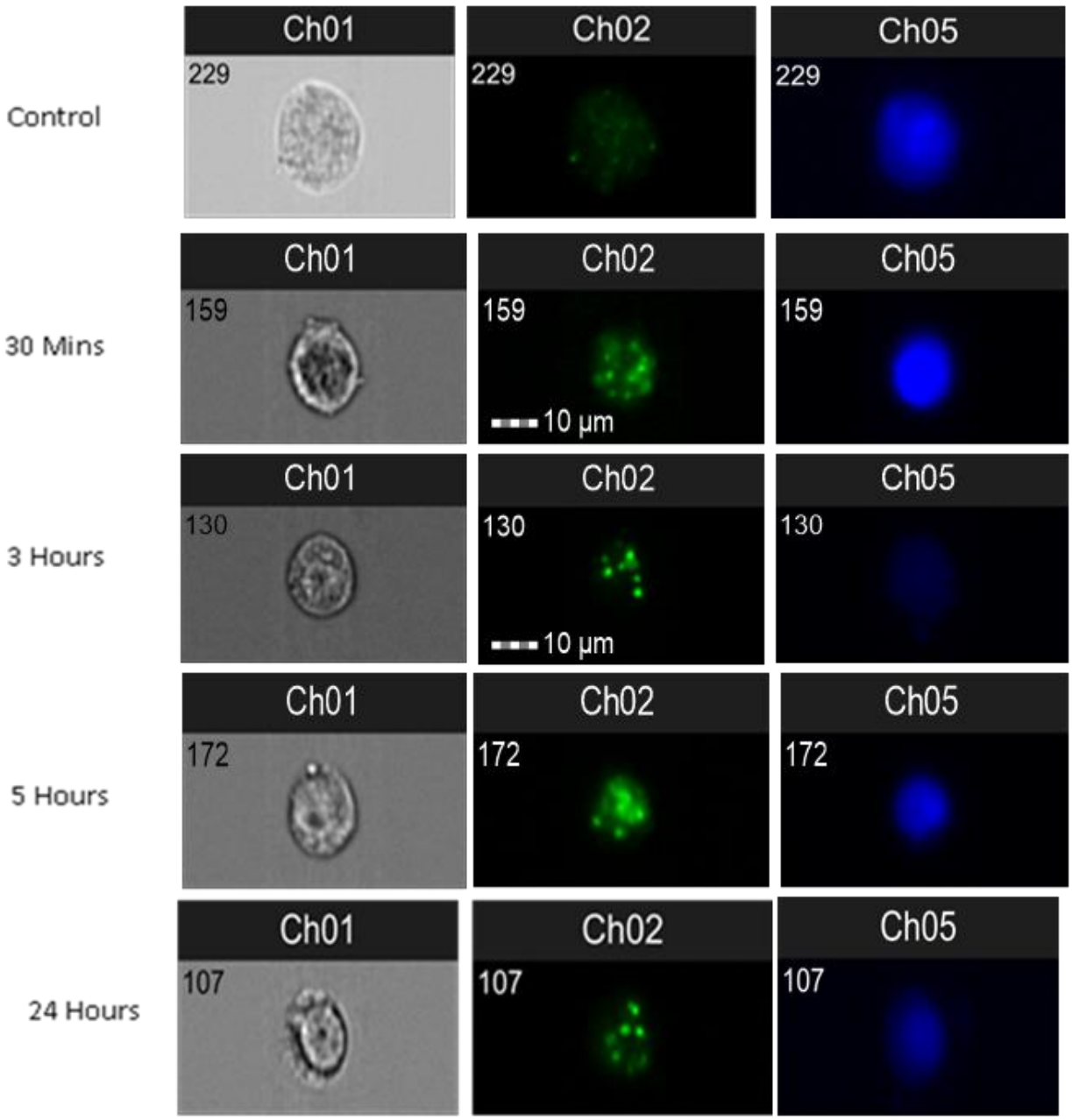

Figure 3.9 Representative image of gamma H2AX foci staining of BT474 cell line. The time interval of 30 minutes post irradiation showed the most intense fluorescence and highest count of H2AX foci being induced. This decreased gradually over time. Ch01 shows brightfield channel, ch02 shows H2AX foci induction and Ch05 shows DRAQ5 nuclear staining.

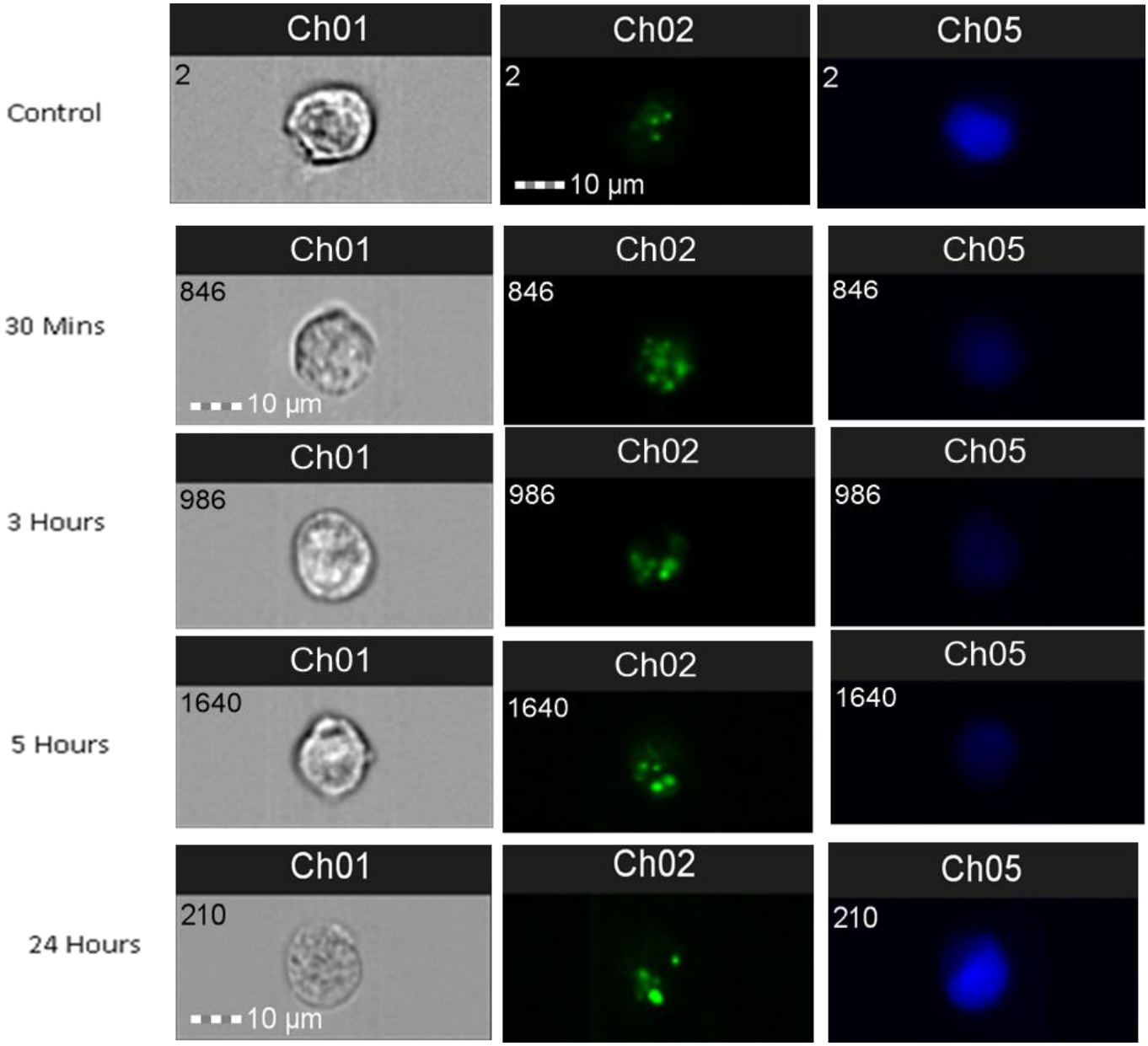

Figure 3.10 Representative image of gamma H2AX foci staining of MDA-MB 436 cell line. The time interval of 30 minutes post irradiation showed the most intense fluorescence and highest count of H2AX foci being induced. This decreased gradually over time. Ch01 shows brightfield channel, ch02 shows H2AX foci induction and Ch05 shows DRAQ5 nuclear staining

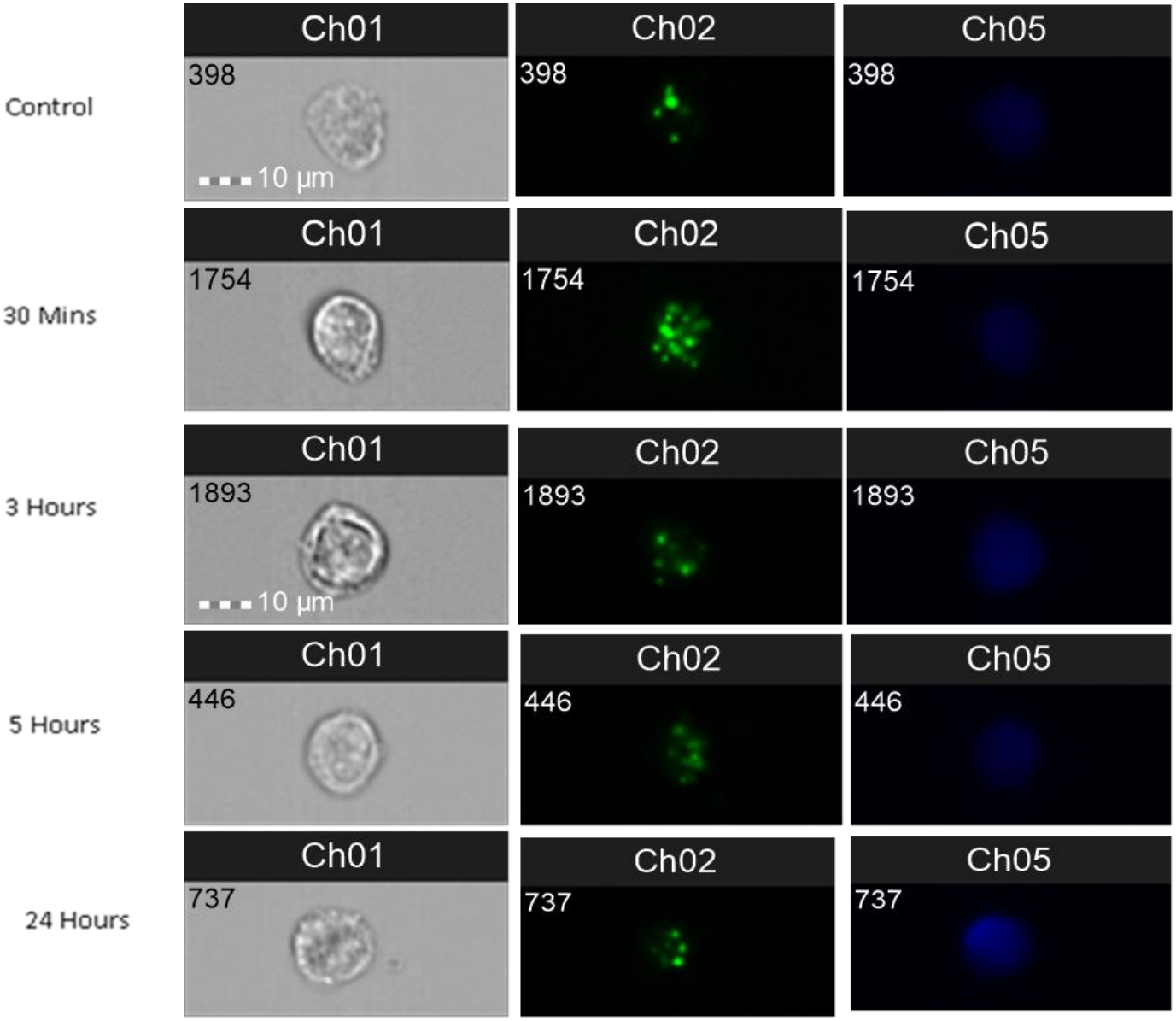

Figure 3.11 Representative image of gamma H2AX foci staining of GI101 cell line. The time interval of 30 minutes post irradiation showed the most intense fluorescence and highest count of H2AX foci being induced. This decreased gradually over time. Ch01 shows brightfield channel, ch02 shows H2AX foci induction and Ch05 shows DRAQ5 nuclear staining.

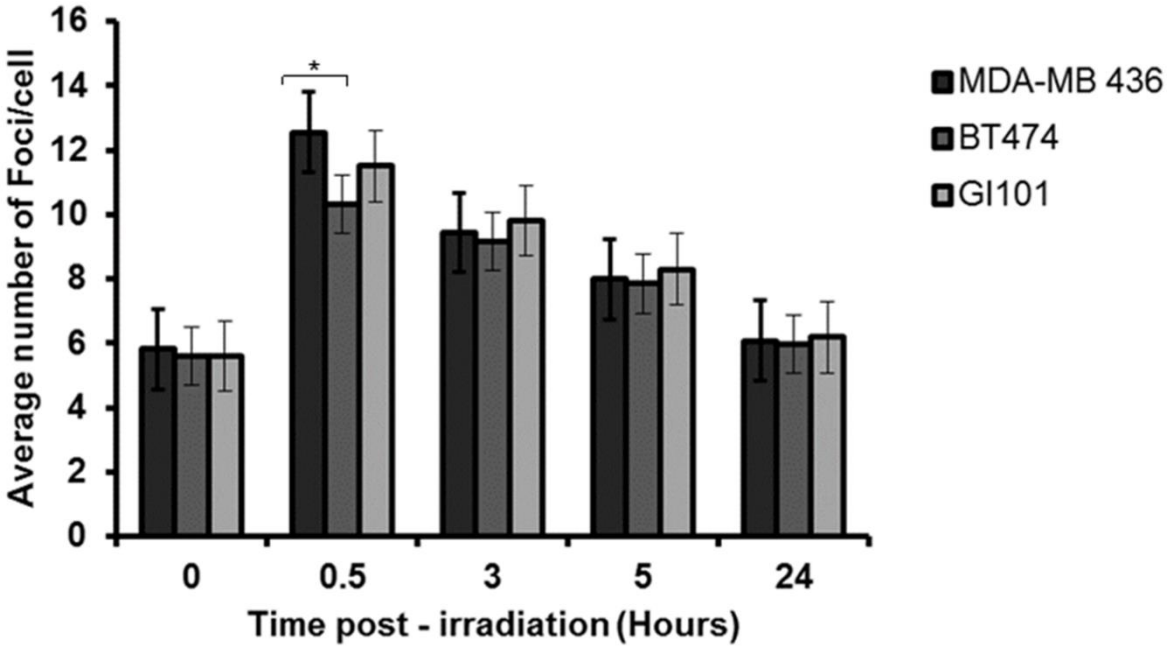

Figure 3.12 γ-H2AX assay for MDA-MB 436, BT474 and GI101 cell lines indicate little difference in DNA repair kinetics. After exposure to 2Gy γ- radiation, cell lines were harvested after various time points for kinetic analysis of DSB repair using H2AX foci induction. Each cell had untreated control and H2AX foci induction measured at 0.5, 3,5 and 24 hours post radiation treatment. Mean H2AX induction from n=3 experiments is plotted with error bars representing standard deviation, Students T Test was used to compare H2AX induction post treatment between each of the cell lines and time points, *P<0.05.

A representative image for H2AX foci staining is shown in Figure 3.9 for the BT474 cell line. Figures 4.10 and 4.11 show γ-H2AX staining for MDA-MB 436 and GI101 cell lines respectively. The data in Figure 3.12 shows the induction of gamma H2AX foci in MDA-MB-436, BT474 and GI101 cell lines. After irradiation, the DNA damage response is amplified with phosphorylation of many H2AX molecules at the double strand break sites at the 30-minute (Rogakou *et al.*, 1999; Marková, Schultz and Belyaev, 2007; Mariotti *et al.*, 2013; Ji *et al.*, 2017). Gradually, number of cells with phosphorylated H2AX are reduced as the number of cells repairing is lowered returning towards near un-irradiated levels at 24 hours. As previously shown Brk expression levels are quite high in BT474 and lower for GI101 cell line and as Brk increases resistance to radiotherapy as originally thought, there should be increasing amount of γ-H2AX phosphorylation at DNA double strand break sites occurring and with higher intensity compared to cell lines with lower Brk expression. The highest number of foci and with the most intense fluorescence was seen at 30 minutes post irradiation and gradually the number of H2AX foci decreased over time to near control levels. Looking at γ-H2AX foci induction 30 minutes post radiation for BT474 and GI101, there seems to be no significant difference (P= 0.0723), however there is a significant difference when comparing BT474 and MDA-MB-436 cell line (P= 0.0312). Nonetheless, this does not correspond to Brk expression levels in each cell line and the difference may be due to other factors. There was also no further difference in repair kinetics over the 24 hour time period.

3.3.6 γ-H2AX foci induction for MDA-MB 468 and MDA-MB 157 cell lines

In order to assess whether Brk directly influenced DNA repair in breast cancer cell lines, induction of γ-H2AX was measured in the two Brk transfected cell lines: MDA-MB 468 and

MDA-MB 157 (Figure 3.13). The greatest induction and highest fluorescent intensity was seen 30 minutes post irradiation for all three variants of both cell lines before H2AX foci levels returned to near normal levels after 24 hours. Although there appears to be higher induction of gH2AX in MDA-MB 468 Brk WT 30 minutes post radiation, it is not significant when compared to MDA-MB 468 Vector cell line ($P<0.05$). In contrast, the MDA-MB 157 Brk WT cell lines shows show reduced levels of H2AX foci in comparison to MDA-MB 157 Vector cell line ($P<0.05$). This suggests Brk may not have a direct role in DNA repair process of breast cancer cell lines. Additional data, from independent studies (Emma Bourton -Brunel University) which support my studies, show inconsistent induction of H2AX in both MDA-MB 468 and MDA-MB 157 cell lines respectively (data not shown). No significant difference in H2AX foci induction was observed 30 minutes post radiation between MDA-MB 468 Brk WT and Vector cell lines ($P<0.05$) as well as between MDA-MB 157 Brk WT and Vector cell lines ($P<0.05$).

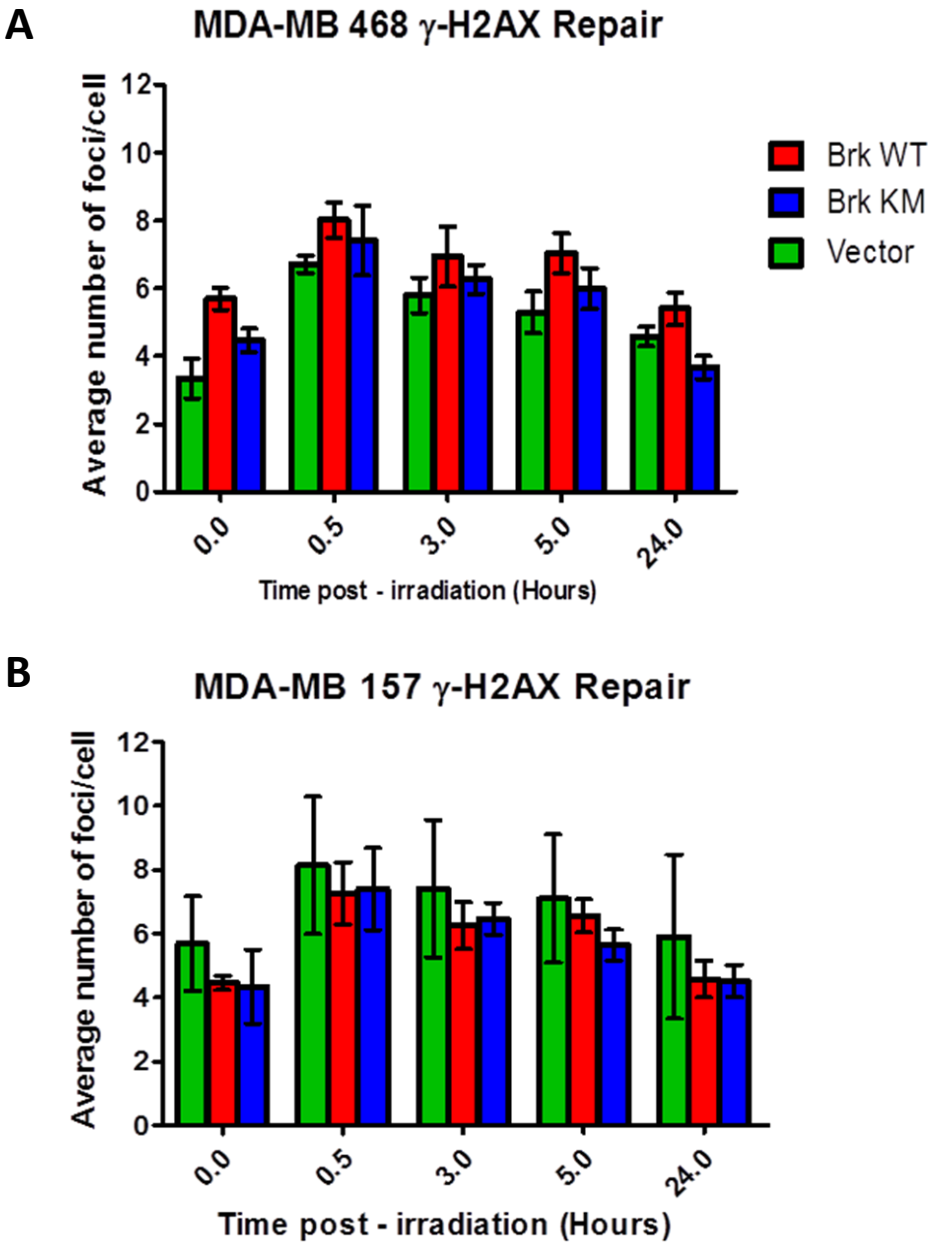

Figure 3.13 γ-H2AX DNA Repair Kinetics for MDA-MB 468 (A) and MDA-MB 157 (B) show no variation. Cell lines were exposed to 2 Gy gamma radiation before the number of cells with double strand breaks were measured based on γ-H2AX induction at 0.5, 3, 5 and 24 hours post treatment. 10,000 cells were analysed for the presence of γ-H2AX foci in each sample along with a control sample and compensation samples. No statistical significance was seen 30 minutes post radiation with the highest induction of γ-H2AX for MDA-MB 468 Brk WT and Vector cell lines (p value 0.0965) as well as between MDA-MB 157 Brk WT and Vector cell lines (*P*= 0.1701). Mean H2AX induction from n=3 experiments are plotted with error bars representing standard deviation. ANOVA statistical test was done to detect significant variance between the three variants for each cell line. Students T Test was used to determine significant difference between vector and Brk WT or vector and Brk KM cell lines. No statistical difference was determined for both transfected cell lines.

3.3.7 Total ATM and ATM phosphoserine794 levels in cells before and after exposure to 2Gy gamma radiation

To date, there are no direct relationships reported between Brk and DNA repair after γ-radiation within breast cancer cells. Since ATM regulates cell cycle checkpoints after double strand breaks, a functional connection between total ATM and phosphorylated ATM with Brk expression was investigated by immunological staining of total and phosphorylated ATM followed by analysis by Imagestream IDEAs analysis software. Breast cancer cell lines MDA-MB-468 Brk WT, Brk KM and Vector only as well as MDA-MB 157 Brk WT, Brk KM and Vector only were exposed as previously described (Chapter 2, section 2.2.6) to 2Gy of γ-radiation before cells were stained with the appropriate total and phospho-ATM antibodies (Chapter 2, section 2.1.4). The relative fluorescence intensity of untreated cells was compared with irradiated cells. Statistical significance was determined between Brk-WT-Brk -KM cell lines as well as between Brk WT-Vector and Brk KM-vector cell lines and additionally between control and irradiation cells. Figure 3.14 shows a representative image of ATM staining.

Figure 3.15 A and B show total ATM relative fluorescence for MDA-MB 468 and MDA-MB 157 cell lines respectively. Total ATM relative fluorescence intensity for MDA-MB 468 Brk WT cell line was 0.84 compared to 0.92 for MDA-MB-468 Brk KM and 1.02 for MDA-MB 468 Vector. Although there was reduction in total ATM for Brk-WT and Brk-KM, the difference between the three variants as well as between the un-irradiated controls does not appear to be significant. In MDA-MB-157 cell line when comparing total ATM fluorescence intensity between MDA-MB 157 Brk WT cell line and MDA-MB 157 Vector only cell line there is no significant difference. Although, there are lower total ATM levels seen in MDA-MB 157 Brk KM cell line (0.8 relative fluorescence) compared to vector only cell line (0.98), however this is also not statistically significant.

Figure 3.16A and B show relative fluorescence of phosphoserine ATM for MDA-MB 468 and MDA-MB 157 cell lines. Looking at phosphorylation of ATM of the two transfected cell lines, MDA-MB 468 Brk WT and MDA-MB 468 Brk KM, there is little difference between the two cell lines as well as little difference between control and irradiated cells. No statistically significant difference was shown between all three variants in MDA-MB 468 cell lines. However, there was significant reduction in phospho-ATM in MDA-MB 468 vector cell line when exposed to 2Gy radiation compared to control cells (P=0.04). For MDA-MB 157 Brk WT and Brk KM cell lines, a decline in active ATM was observed and an increase observed in MDA-MB-157 Vector only cell line, however there was no statistical significance.

Overall there are no changes observed in total ATM protein expression in breast cancer cell lines in relation to Brk expression nor any significant changes in response to 2Gy gamma radiation. Although there is a reduction in phospho-ATM levels in MDA-MB 468 vector cell line in response to gamma radiation this was not confirmed in MDA-MB 157 vector cell line.

.

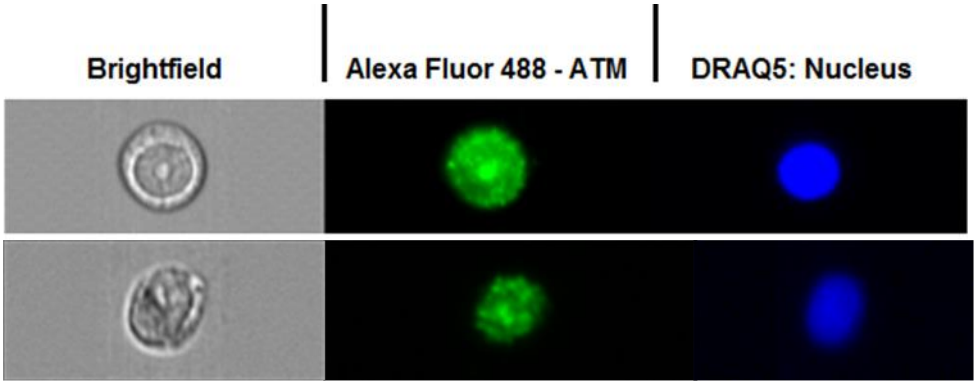

Figure 3.14 Representative image of total ATM (upper panel) and phosphorylated ATM (lower panel). Breast cancer cell lines; MDA-MB 468 Brk WT, Brk KM, vector a well as cell lines; MDA-MB 157 Brk WT, Brk KM were exposed to 2Gy gamma radiation. For detection of total and phosphorylated ATM protein levels, cells were labelled with primary antibody (1.500) diluted in blocking buffer and incubated for 24 hours at 4˚C. Mouse monoclonal antibody ATM for C-terminal region (ECM Biosciences) was used for total ATM detection and rabbit polyclonal for phosphorylated serine794 of the ATM protein (ECM Biosciences) to detect phosphorylated ATM. After washes, cells (except D5 compensation cells) were stained with rabbit anti-mouse or goat anti-rabbit secondary antibody solutions containing Alexa Fluor488 IgG (diluted to 1:1000 in blocking buffer) to detect total and phosphorylated ATM levels respectively. Cells were incubated for 1 hour at room temperature, washed with wash buffer and left overnight at 4˚C in Accumax solution. D5 solution was added to each sample except Alexa Fluor488 compensation cells and cells were analysed using the Imagestream (Amins).

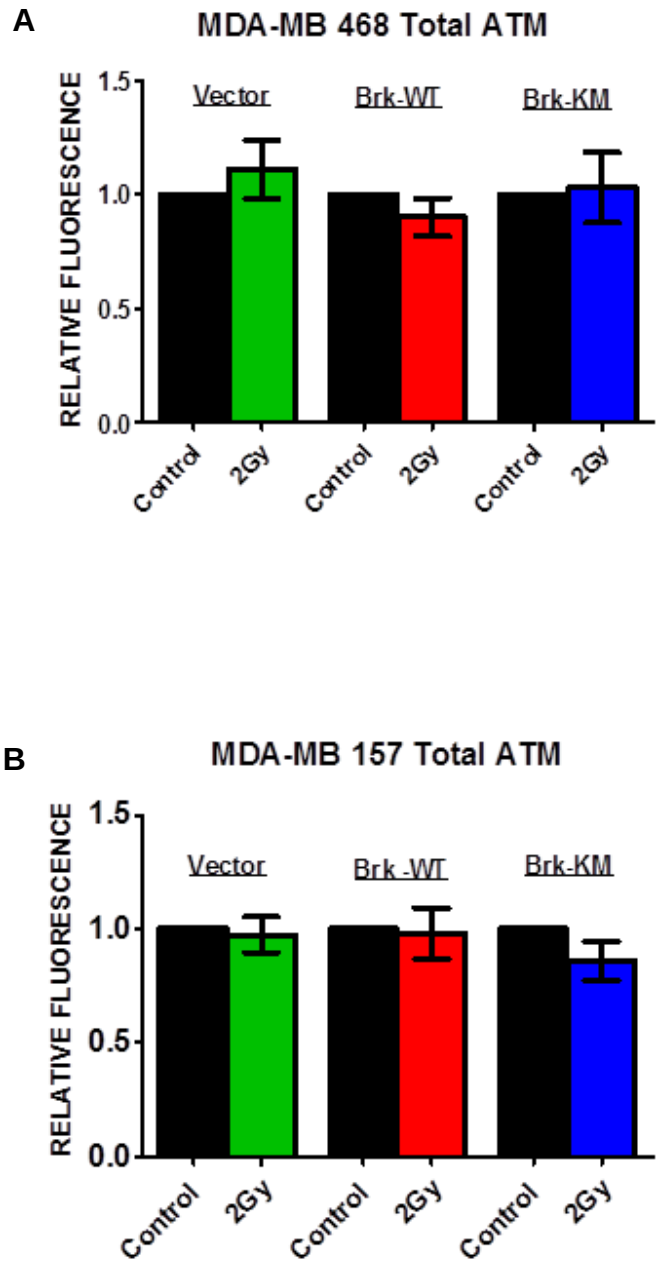

Figure 3.15 Relative fluorescence intensity of breast cancer cell lines for total ATM are unchanged compared to control cells. Cells were exposed to 2Gy gamma radiation and stained with mouse monoclonal ATM (C-terminal) antibody (1:500 dilution in blocking buffer) and fluorescence intensity of ATM staining in cells determined using Ideas software (Amins). A) MDA-MB 468 Brk WT, Brk KM, vector cell lines showing fluorescence intensity of total ATM protein B) MDA-MB 157 Brk WT, Brk KM and vector cell lines showing relative fluorescence intensity of total ATM protein. Students T Test was used to assess statistical significance between control and irradiated cells, n=3.

A

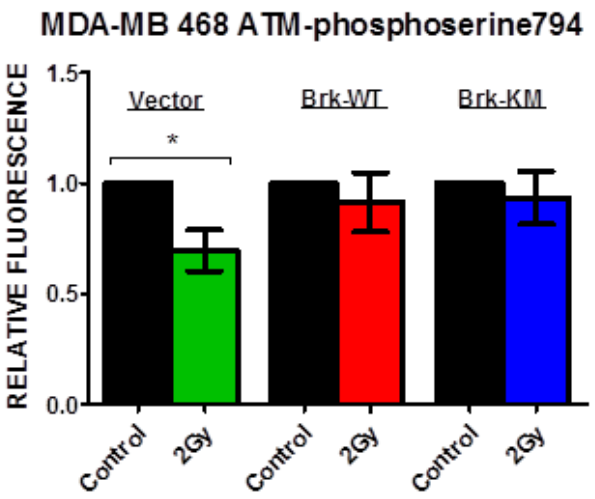

B

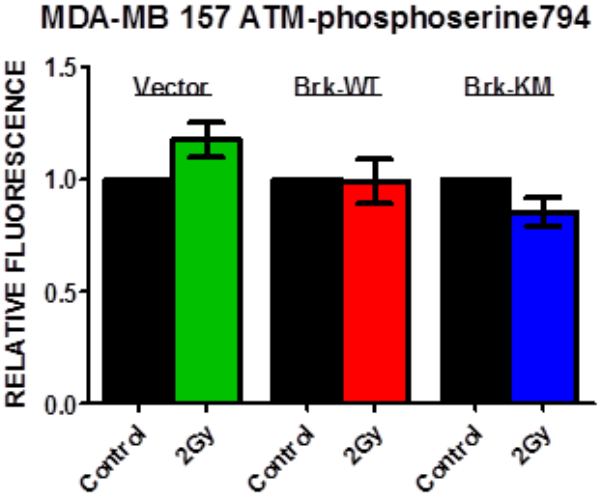

Figure 3.16 Relative fluorescence intensity of breast cancer cell lines for phosphorylated ATM are unchanged compared to control cells. Cells were exposed to 2Gy gamma radiation and stained with rabbit polyclonal ATM (Ser-794), phospho-specific (1:500 dilution in blocking buffer) and fluorescence intensity of phospho-ATM staining in cells determined using Ideas software (Amins). A) Shows MDA-MB 468 Brk WT, Brk KM, vector cell lines fluorescence intensity of phospho-ATM vector cells. B) Shows MDA-MB 157 Brk WT, Brk KM and vector cell lines difference in relative fluorescence intensity of phospho-ATM protein. Students T Test was used to assess statistical significance, n=3.

3.4 Discussion

In this chapter, the studies sought to determine the link between radio-sensitivity and Brk expression levels. I proposed that cell lines which had high Brk expression may also show increased sensitivity of breast cancer cell lines to radiotherapy. Brk may affect breast cancer cell line sensitivity to radiotherapy via deregulation of the DNA repair pathway. More specifically I sought to determine if there was any direct interaction between Brk and the ATM pathway by which Brk may affect breast cancer cell sensitivity to radiotherapy as Brk expression leads to increased ErbB signalling via P13K/Akt, which is an activator of the mTOR pathway and increased levels of mTOR are linked to down-regulation of ataxia telangiectasia mutated protein (ATM) (Kamalati et al., 1996; Shen and Houghton, 2013). Suppression of ATM, therefore, may increase cancer cell sensitivity to radiotherapy.

Previous studies have shown Brk may reduce sensitivity of breast cancer cell lines to chemotherapy as well as tyrosine kinase inhibitors (Xiang *et al.*, 2008). This indicates that Brk may have some role in relation to treatment responses. Furthermore, Brk is induced in response to DNA damage by gamma radiation (Haegebarth et al., 2009) in intestinal crypt epithelial cells. My studies show for the first time that Brk is also induced in breast cancer cells (Figure 3.7) in response to γ-radiation and that induction of Brk was not cell line (or subtype) specific. Interestingly the induction of Brk is delayed in response to γ-radiation as there were higher Brk levels at the later time points (Figure 3.6). Other studies have shown in the MDA-MB 231 cell line, Brk protein levels are rapidly induced within 5 minutes in response to hypoxia (Pires et al; 2014) and also show a delayed induction of Brk protein in hypoxic conditions (4 hours) (Anderson et al; 2013). The delayed induction coincided with induction of HIF1α whereas in the Pires study, Brk protein induction appeared to be independent of HIF1α suggesting other mechanisms are responsible for the early induction

of Brk. Brk protein levels are induced at 6 hours post gamma radiation in intestinal crypt epithelial cells (Haegebarth et al, 2009). These studies suggest early or late Brk induction variation may be dependent on other signalling pathways and further investigations may show the mechanism of Brk induction in response to radiotherapy in breast cancer cell lines. It was hypothesized that Brk increases sensitivity, however my studies suggest, that despite being induced, Brk may not play a direct role in the sensitization of breast cancer cell lines to radiotherapy. The clonogenic assays show a decrease in colony formation after exposure to increasing doses of gamma radiation, although this may be dose dependent and not due to Brk expression levels. Variation in SF2 (survival rate after exposure to 2Gy) values were observed between all cell lines with statistical significance ($P = 0.017$) but there was no direct association with Brk expression levels. However, although no direct association was seen with Brk expression; 4 out of the 5 cell lines (GI101, BT474, T47D, MDA-MB 436) with highest SF2 values also showed moderate to high Brk expression levels suggesting increased resistance.

Histone 2AX (H2AX) is a variant of the H2A protein family which function as vital components of the histone octamer in nucleosomes for the localisation and recruitment of DNA repair proteins (Kuo and Yang, 2008). H2AX has proven to be a key component in DNA damage response and is rapidly phosphorylated at the sites of double strand break after exposure to exogenous stimuli such as ionising radiation (Kuo and Yang, 2008). γ-H2AX assay, which has proven to be a more sensitive technique (Rothkamm and Lobrich, 2003), than comet assays and pulsed-field gel electrophoresis (PFGE) (Sharma, Singh and Almasan, 2012) was performed to investigate whether Brk influenced DNA repair of breast cancer cell lines. DNA repair was assessed in GI101 (a metastatic model), MDA-MB-436 (a triple negative cell line) and BT474 (HER2 positive cell line). No clear difference in γ-H2AX foci induction was observed post treatment between the three cell lines. Although there was statistical

difference observed in foci induction between BT474 and MDA-MB 436 cell lines at 30 minutes post exposure to γ-radiation (P<0.05), overall there was little statistically significant as well as biologically relevant difference noticeable between the three cell lines . It could be said that the BT474 cell line which shows high Brk expression levels with moderate SF2 survival rate (Figure 3.8) as well as lowest induction of γ-H2AX foci at 30 minutes; may suggest a role for Brk in protecting cells from cell death in response to γ-radiation or DNA damage thus increasing radio-sensitivity. However, other cell lines such as the GI101 cell line also has a similar SF2 survival rate to the BT474 cell line but lower Brk expression levels thus indicating Brk may not have any direct influence in radio-sensitivity. This was further investigated in the three variants of MDA-MB 468 and MDA-MB 157 cell lines (Brk-WT, Brk-KM and vector). The γ-H2AX assays comparing the three variants of Brk negative cell lines MDA-MB 468 and MDA-MB 157 do not suggest any clear role for Brk in DNA damage response, suggesting Brk may not directly affect radio-sensitivity (Figure 3.13). Nonetheless, the vector only cell line had marginally lower induction of H2AX foci for all time points in MDA-MB 468 compared to MDA-MB 468 Brk WT and Brk KM cells although not significantly different. However, this was not confirmed in the MDA-MB 157 cells. It should be of note, the γ-H2AX assay does not specifically detect only radiation induced DSB due to endogenous levels of DNA damage such as replication induced DSBs (Banáth, MacPhail and Olive, 2004; Kuo and Yang, 2008). Furthermore, although there are advantages of live cell imaging, often there are limitations involving signal background due to high level of expression resulting in high background level of foci (reviewed in Vignard, Mirey and Salles, 2013). Additional DBS repair markers along with γ-H2AX foci such as the p53 binding protein, MDC1 and RAD50 (Xu and Stern, 2003; Yuan and Chen, 2010) may offer a more accurate representation and confirmation of DSBs in the cell lines studied. Other limitations include reduced accuracy

due to lower resolution as compared to *in situ* fluorescence microscopy thus reducing number of observable foci (Bourton *et al.*, 2012).

Since the ATM protein phosphorylates the H2AX molecules (Burma *et al.*, 2001) upon double strand break indication, a potential association between total ATM and phospho-ATM 794 with Brk may provide further insight into the DNA repair process and thus the radio sensitivity of breast cancer cell lines (Burma *et al.*, 2001). Since, it was hypothesised that increased levels of Brk may cause cancer cells to be more radio sensitive by affecting DNA repair process via the ATM pathway, the levels of ATM in Brk WT cell lines compared to Brk KM and vector only cell lines could be significantly altered. However, my analysis of total ATM protein expression in both MDA-MB 468 and MDA-MB 157 cell lines showed little change from the control. Although there is a reduction in phospho-ATM levels in MDA-MB 468 vector cell line in response to gamma radiation suggesting Brk negative cell lines are more sensitive to radiation, this was not confirmed in MDA-MB 157 vector cell line which showed higher phospho-ATM expression in comparison indicating this difference might be cell line specific and not directly related to Brk expression.

Brk has been shown to interact with a wide variety of substrates (reviewed in Harvey and Burmi, 2011), and its function may change in different cellular conditions. Depending on the activation of different signalling pathways in the various cell lines, and their receptor status, Brk's influence in these cell lines may be altered. This may explain some of the discrepancies as it has been reported that the MDA-MB-468 cell line has a high level of EGFR and thus has a high level of EGF signalling (Filmus *et al.*, 1987), therefore the effects seen with transfected Brk may not be as pronounced.

It should be noted that Brk-targeted therapy which may be a kinase inhibitor may not rely on a specific cell cycle phase. However, since it is involved in cell cycle progression as it

promotes cell progression from resting phase to S phase, a Brk-targeted therapy could be utilised to prevent cell cycle progression (Chan and Nimnual, 2010). However, this could affect the efficacy of chemotherapy or radiotherapy which are cell cycle dependent. Since Brk promotes cell proliferation and, in addition, protects cancer cells from cell death, it could reduce the overall effect of radiotherapy thus it must be decided if a potential Brk targeted therapy will be useful before or after radiotherapy.

The main conclusions of this chapter show there is no consistent alterations in determining radio-sensitivity of breast cancer cell lines expressing Brk. This was confirmed in breast cancer cell lines expressing either wild type (Brk-WT), kinase mutant Brk (Brk KM) as well as a vector only cell line. Furthermore, investigations in DNA double strand break repair showed no differences between all three variants of MDA-MB 468 and MDA-MB 157 cell lines thus suggesting there are no significant differences in the repair kinetics of breast cancer cell lines in relation to Brk expression status. In addition, this chapter revealed there was no functional link between Brk expression and ATM activity as minor changes were observed of total and phosphorylated ATM protein levels in Brk WT, Brk KM and vector only cell lines. Overall these investigations suggest Brk does not affect radiation sensitivity directly nor is the effect of Brk on radiation responses mediated through DNA double strand break repair and other mechanisms may be involved.

4.0 Chapter 4: Examining the potential of Brk inhibition in breast cancer cell lines

4.1 Introduction

Despite improvements in treatment of breast cancer with adjuvant chemotherapy, there is still a need for novel breast cancer therapies. Treatment of the majority of invasive and higher grade/stage cancers is heavily chemotherapy based (Lee and Newman, 2007; Roche and Vahdat, 2011) thus the significance of how Brk may influence breast cancer cell sensitivity to chemotherapy agents as well as other drug-based treatments needs to be understood. Previous studies have shown that Brk may contribute towards influencing chemotherapeutic sensitivity in breast cancer (Burmi *et al.*, 2009; Harvey *et al.*, 2009). The mechanism proposed involves Brk altering the ratios of anti and pro-apoptotic proteins; Bcl-$_{XL}$ and Bcl-$_{XS}$ respectively, in respect of Bcl-$_{XL}$. Suppression of Brk in T47D breast cancer cells, which are representative of Luminal A breast cancer subtype, significantly increased sensitivity to chemotherapeutic drugs paclitaxel and doxorubicin, however this was not studied in triple negative breast cancers (Burmi *et al.*, 2009). The anti-apoptotic protein Bcl-$_{XL}$ is associated with chemotherapeutic resistance (Gul, Basaga and Kutuk, 2008) and reduced levels of Brk protein resulted in reduced levels of Bcl-$_{XL}$ protein and thus increased sensitivity to chemotherapy (Harvey *et al.*, 2009). Furthermore, breast cancer cells treated with methotrexate and 5-flurouracil showed decreased apoptosis due the inhibition by Bcl-$_{XL}$ *in vitro* and *in vivo*. Based on these studies, it is expected a Brk targeted therapy would modulate chemotherapeutic drug response.

4.1.1 Brk and targeted therapy

A number of Brk's functions are dependent on its kinase domain, including anchorage independent growth as well as regulation of certain cell death features (reviewed in Harvey and Burmi, 2011). Brk-negative breast cancer cells transfected with kinase inactive Brk

showed similar levels of suspension-induced cell death compared to cells transfected with the vector whereas cells transfected with wild type Brk had almost a 50% reduction in suspension-induced cell death, indicating a protective role for Brk's kinase activity in cancer cell death (Harvey *et al.*, 2009). This is further supported by another study which observed Brk downregulation increased apoptosis of breast as well as ovarian cancer cells which were deprived of matrix attachment whereas overexpression of Brk resulted in increased survival (Irie *et al.*, 2010). In addition, Brk's kinase activity is also required for migration and invasion of breast cancer cells. Brk was shown to significantly promote tyrosine phosphorylation of paxillin, which was not observed in cells that were transfected with kinase mutant Brk indicating dependency on Brk's catalytic activity (Chen *et al.*, 2004). Furthermore, overexpression of Brk but not kinase mutant Brk indicated a 2.3-fold elevation of Rac1 activity (Chen *et al.*, 2004). Brk kinase activity is also dependent for the phosphorylation of a number of cellular proteins (including KAP3A) which was not observed in cells transfected with kinase inactive Brk (Lukong and Richard, 2008). Furthermore, Brk's kinase activity is essential for its association with ARAP1 in an EGF/EGFR dependent manner (Kang *et al.*, 2010). This interaction results in enhanced EGFR signalling and inhibition of EGFR downregulation through phosphorylation of ARAP1 in breast cancer cells thus oncogenic functions of Brk expression cells are increased (Kang *et al.*, 2010). Taken together these studies provide support for inhibiting kinase activity of Brk which may offer some clinical benefit via inhibition of these processes especially when used in combination with current breast cancer therapies (reviewed in Harvey and Burmi, 2011).

Overexpression of Brk has previously shown to confer resistance to Lapatinib, the dual inhibitor for HER2 and (EGFR), with Brk as studied by Xiang and colleagues (Xiang *et al.*, 2008). The *ptk6* gene can be coamplified with the *HER2* gene and the Brk protein is associated with the HER2 protein which prolongs activation of the Ras/MAPK pathway which

in turn promotes cell proliferation (Xiang *et al.*, 2008). HER2-induced cell proliferation as measured by changes in cell numbers was shown to be dependent on Brk kinase activity. In addition, MCF10A cells expressing HER2 chimera were transfected with a kinase-dead version of Brk which significantly inhibited HER2 induced BrdU incorporation in comparison to cells transfected with wild type Brk (Xiang *et al.*, 2008). Furthermore, coexpression of Brk with HER2 within the MCF10A cells, in comparison to MCF10A cells expressing only the HER2 chimera, increased the concentration of Lapatinib that was required to inhibit HER2 induced proliferation; this suggests Brk reduces Lapatinib efficacy. This study, however, did not test this effect within breast cancer cells which endogenously overexpress HER2 nor if co-treatment with a Brk inhibitor could potentially reduce cell proliferation. Furthermore, downregulation of Brk in Lapatinib resistant breast cancer cells resulted in an induction in apoptosis (Park *et al.*, 2015). Interestingly, another study investigating the simultaneous knockdown of Brk and HER2 expression in Lapatinib and Trastuzumab resistant cancer cells did not show induction of cell death although there was significant reduction in cancer cell proliferation as well as reduced levels of tumour growth *in vivo* (Ludyga *et al.*, 2013). Nonetheless, both studies suggest inhibition of Brk and HER2 kinase activity in combination may offer an effective treatment modality. Thus, my studies hypothesise that, due to the interactions between Brk and HER2 as well as EGFR, inhibition of Brk using current small molecule inhibitors in combination with Lapatinib may offer a more effective reduction in cancer cell proliferation than either agent alone.

4.1.2 Brk and endocrine therapy

Over 70% of breast cancers diagnosed express the oestrogen receptor (ER) or/and the progesterone receptor (PR) and grow in the presence of oestrogen (Ito *et al.*, 2017). Recently, Brk has been shown to increase growth and survival of ER positive luminal breast cancer cells including those that have acquired resistance against endocrine therapies (Ito *et al.*, 2017). Downregulation of Brk in 3D Matrigel cultures resulted in the inhibition of growth of two ER+ breast cancer cell lines; T47D and MCF7 as well as variants of these cell line that were tamoxifen resistant. Thus, Brk promotes cancer cell growth even in the presence of tamoxifen. In addition, there was evidence to suggest downregulation of Brk induced apoptosis of MCF7 and T47D, tamoxifen-resistant cells, indicating a potential role for Brk in endocrine therapy resistance Although this study has not highlighted whether Brk inhibition would potentiate the effects of Tamoxifen; there is convincing evidence for the role Brk plays in tamoxifen resistance and the need for a Brk-targeted therapy, especially in patients with resistance to current endocrine therapies. My investigations using a Brk inhibitor in combination with Tamoxifen treatment on ER+ cell lines may offer further insight and support for a Brk targeted therapy. I hypothesise that, due to the proliferative role of Brk in ER+ breast cancer cells, a combination of Tamoxifen and Brk inhibition would result in reduced breast cancer cell proliferation.

4.1.3 Brk Inhibitors

There is a lack of development of Brk inhibitors, therefore no suitable agents have been identified to investigate the clinical benefits of Brk inhibition thus far. Although a few have been in development, they have yet to be completely investigated i*n vitro* and i*n vivo*. A specific inhibitor for Brk could reduce cancer cell proliferation for a number of cancers (such

as breast, colon and prostate cancers) and I predict that it could sensitize tumours to other therapies and potentially as a consequence prevent metastasis. However, Brk's kinase independent functions, which includes promotion of breast cancer cell proliferation, will need consideration (Harvey and Crompton, 2003). In addition, unpublished data has shown breast tumour xenograft growth is independent of Brk kinase activity. Therefore, a more desirable therapeutic intervention may involve protein-protein disruptions for a better therapeutic benefit.

The first inhibitor specific for Brk was discovered in 2011 as part of a focused library screening against the Brk enzyme (Zeng *et al.*, 2011). The results showed the imidazol (1,2-α) pyrazin-8-amine series of compounds as desirable and potent Brk kinase inhibitors. Compound 21a showed an IC50 (half maximal inhibitory concentration) value of 10nM with mouse pharmacokinetics providing a Cmax value of 17.9μM at 30 minutes after injection of 30mg/kg intra-peritoneal (Zeng *et al.*, 2011). Although bioavailability for compound 21a was only 5.8%, it may prove to be an important compound to evaluate *in vivo* Brk inhibitor activity. Further investigations with imidazol (1,2-α) pyrazin-8-amines show co-crystal structure of Brk kinase domain with an inhibitor from the imidazo[1,2-a]pyrazine- 8-amine series and IC50 at 80nM measured as percentage of Poly (G:T) using ADP-Glo assay kit (Thakur *et al.*, 2017). Further studies have yet to be carried out *in vitro* to show the inhibitory effects within breast cancers, however thus far they have shown to bind to the ATP pocket of Brk and are highly potent as well as have moderate to high cellular activity (Zeng *et al.*, 2011).

The discovery of 4-anilino α-carbolines further indicated that a Brk targeted therapy is a viable treatment option (Mahmoud *et al.*, 2014). The serine/threonine kinase, Haspin, has been shown to phosphorylate histone H3 in mitosis thus showing its potential as a target for anti-cancer drug treatment (Cuny *et al.*, 2012). From this, came the discovery of β carbolines as potential protein kinase inhibitors including for Haspin (Bain *et al.*, 2007). This provided a

rationale to investigate α-carbolines as potential kinase inhibitors. After chemical synthesis, the most active and potent Brk inhibitor identified was compound 4f which was tested for growth inhibition (GI) in three breast cancer cell lines producing GI50 value of 0.99μM in MCF7 cell line, 1.02μM in HS-578/T cells and 1.58μM in BT-549 cell line (Mahmoud *et al.*, 2014). Further studies with 4-anilino α-carbolines derivatives known as MK138 and MK150 also indicated reduced activity of STAT3, a signalling molecule downstream of Brk, with increasing concentration of both derivatives in T47D breast cancer cell line (Oelze *et al.*, 2015). In addition, inhibition of Brk with either 100nM of MK138 or MK150 induced cell death under loss of adherence conditions. Further studies using these inhibitors have not been published to date thus there is limited information regarding their potential as therapeutic agents for breast cancer.

More recently, a novel drug known as XMU-MP-2 was identified as a potential Brk inhibitor (Jiang *et al.*, 2017). XMU-MP-2 is a small molecule Brk kinase activity inhibitor which targets the ATP-binding site and has shown efficacy in inhibiting cell proliferation of oncogenic Brk-transformed Ba/F3 cells and Brk-overexpressing breast cancer cells *in vitro* and *in vivo* (Jiang *et al.*, 2017). This drug was highly selective for Brk when screened against 28 other kinases and has shown to be more potent compared to compound 4f. However, it should be noted this was investigated using the cell line Ba/F3, a murine interleukin 3 dependent pro-B cell line which was transfected with Brk.

Another set of Brk inhibitors recently identified include the pyrazolopyrimidines PP1 and PP2 (Shim, Kim and Lee, 2017), using an ELISA based *in vitro* kinase assay system for Brk. The most potent inhibitors identified along with PP1 and PP2 were the Lck inhibitor. IC50 values for PP1 included 230nM, for PP2 was 50nM and for Lck inhibitor, it was 60nM (Shim, Kim and Lee, 2017). These were also highly selective for Brk when tested against a panel of kinases including Src family of kinases. STAT3 activity was also significantly reduced with

increasing concentration of PP1 and Lck inhibitors in HEK 293 cell line (Shim, Kim and Lee, 2017). Furthermore, Brk inhibition with PP1 and PP2 reduced Brk-mediated proliferation of T47D breast cancer cell line and although this was also observed when using the Lck inhibitor, this effect was also seen in a Brk-independent manner when using the Lck inhibitor suggesting it is not specific as PP1 and PP2 when inhibiting Brk. Further *in vitro* and *in vivo* studies using PP1 and PP2 have yet to be performed. A summary of all Brk inhibitors is shown in Table 4.1.

Table 4.1 Summary of Brk inhibitors

Brk Inhibitor	First discovered	Summary of inhibitor
Compound 21a	2011 (Zeng et al., 2011)	Imidazol (1,2-α) pyrazin-8-amine compound with IC50 of 10nM, Cmax value of 17.9μM at 30 minutes after injection of 30mg/kg intra-peritoneal.
Compound 4f	2014 (Mahmoud et al., 2014)	A β carboline compound, GI50 value of 0.99μM in MCF7 cell line, 1.02μM in HS-578/T cells and 1.58μM in BT-549 cell line
MK138 and MK150 (Derivatives of Compound 4f)	2015 (Oelze et al., 2015)	Both inhibitors showed reduced activity of STAT3, a signalling molecule downstream of Brk. Inhibition of Brk with either 100nM of MK138 or MK150 induced cell death under loss of adherence conditions.
XMU-MP-2	2017 (Jiang et al., 2017)	Targets ATP binding site and reduces cell proliferation of oncogenic Brk-transformed Ba/F3 cells and Brk-overexpressing breast cancer cells *in vitro* and *in vivo.*
PP1, PP2 and Lck	2017 (Shim, Kim and Lee, 2017)	These are pyrazolopyrimidines with IC50 values for PP1 at 230nM, for PP2 at 50nM and for Lck inhibitor at 60nM. STAT3 activity was also significantly reduced with

		increasing concentration of PP1 and Lck inhibitors in HEK 293 cell line.

Considering the proliferating role of Brk in cancer cells as well as its role in tumorigenesis (reviewed in Harvey and Burmi, 2011), Brk inhibition using a novel inhibitor is expected to reduce Brk phosphorylation and subsequently decreased phosphorylation of its downstream signalling molecule, STAT3 (Liu *et al.*, 2006; Weaver and Silva, 2007; Gierut *et al.*, 2011). This is important as STAT3 is regarded as an oncogene, with tyrosine phosphorylation of STAT3 linked to breast cancer development (Gierut *et al.*, 2011). Activation of STAT3 by Brk may contribute towards cell transformation and uncontrolled growth in early stages of breast cancer. Brk also mediates STAT3 regulation in established tumours (Liu *et al.*, 2006), and constitutive activation of Brk accelerated cell migration and tumour growth *in vivo* (Miah, Martin and Lukong, 2012).

4.2 Aims and Objectives

Aims:

There have been a lack of studies investigating the potential of Brk inhibition in breast cancer cells. In this chapter the main aims were to investigate the potential of Brk inhibition as a monotherapy and in combination with standard breast cancer therapies as well as the effect on downstream signalling in response to Brk inhibition. Considering the proliferating role of Brk in cancer cells as well as its role in tumorigenesis (reviewed in Harvey and Burmi, 2011), Brk inhibition using a novel inhibitor is expected to reduce Brk phosphorylation and subsequently decreased phosphorylation of its downstream signalling molecule, STAT3 (Liu *et al.*, 2006; Weaver and Silva, 2007; Gierut *et al.*, 2011). In addition, Brk inhibition is hypothesised to reduce breast cancer cell line viability as well as modulate the response to standard breast cancer therapies including Taxol, Doxorubicin, Lapatinib and Tamoxifen.

The objectives were:

- To investigate the effect on cell viability of breast cancer cells using the novel Brk inhibitor known as Compound 4f (Mahmoud *et al.*, 2014) through MTT assays as a monotherapy as well as in combination with breast cancer therapies; Taxol, Doxorubicin, Lapatinib and Tamoxifen.

- To investigate the effect on Brk activity including the activity of its downstream signalling molecule STAT3, as well as determine levels of ALT-PTK6 protein in response to Compound 4f treatment over a 48-hour time period in breast cancer cell lines.

4.3 Results

4.3.1 Effect on breast cancer cell viability using a novel Brk inhibitor, Compound 4f.

I sought to investigate the effect of Brk inhibition on cell viability using the Brk inhibitor, Compound 4f. Considering the role that Brk plays in promoting proliferation of cancer cells (Kamalati et al 1996, 2000, Xiang et al 2008, Shen et al 2008, Ostrander et al 2007), inhibition of Brk's kinase function may prove to be an effective treatment modality. To elucidate the role Brk inhibition may have on breast cancer cell viability, cells were treated with a novel Brk inhibitor known as Compound 4f. The MTT (3-(4,5-dimethylthiazol-2-yl)-2,5-diphenyltetrazolium bromide) assay is a widely used colorimetric technique for measurement of cell proliferation and cytotoxicity (Liu et al, 1997). Breast cancer cells were plated in a 96 well plate at a seeding density of 5 $x10^3$ per well in replicates of six wells and left to incubate at 37˚C and 5% CO_2 overnight before treating with the compound. Cells were treated either with dimethyl sulfoxide (DMSO) as the control or the following concentrations of Compound 4f: 0.625µM, 1.25µM, 2.5µM, 5µM, 10µM and 20µM. The 96 well plates were incubated at 37˚C and 5% CO_2 for a total of 7 days with fresh media and compound added every 2/3 days. After which, MTT reagent/media mixture was added to each well and left to incubate as before for 2 hours before adding 0.04M HCL isopropanol to solubilize the formazan. Absorbance was measured at wavelengths 570nm and 620nm to determine cell viability. Cell viability was calculated as percentage of control for all graphs shown in this chapter and XY scatter graphs were produced to determine relationship between dose and cell viability. Correlation statistical analysis was performed for all graphs using Graphpad prism 5 to determine Spearman rho correlation coefficient (denoted as r_s value), as well as the statistical significance of correlation (*p* value).

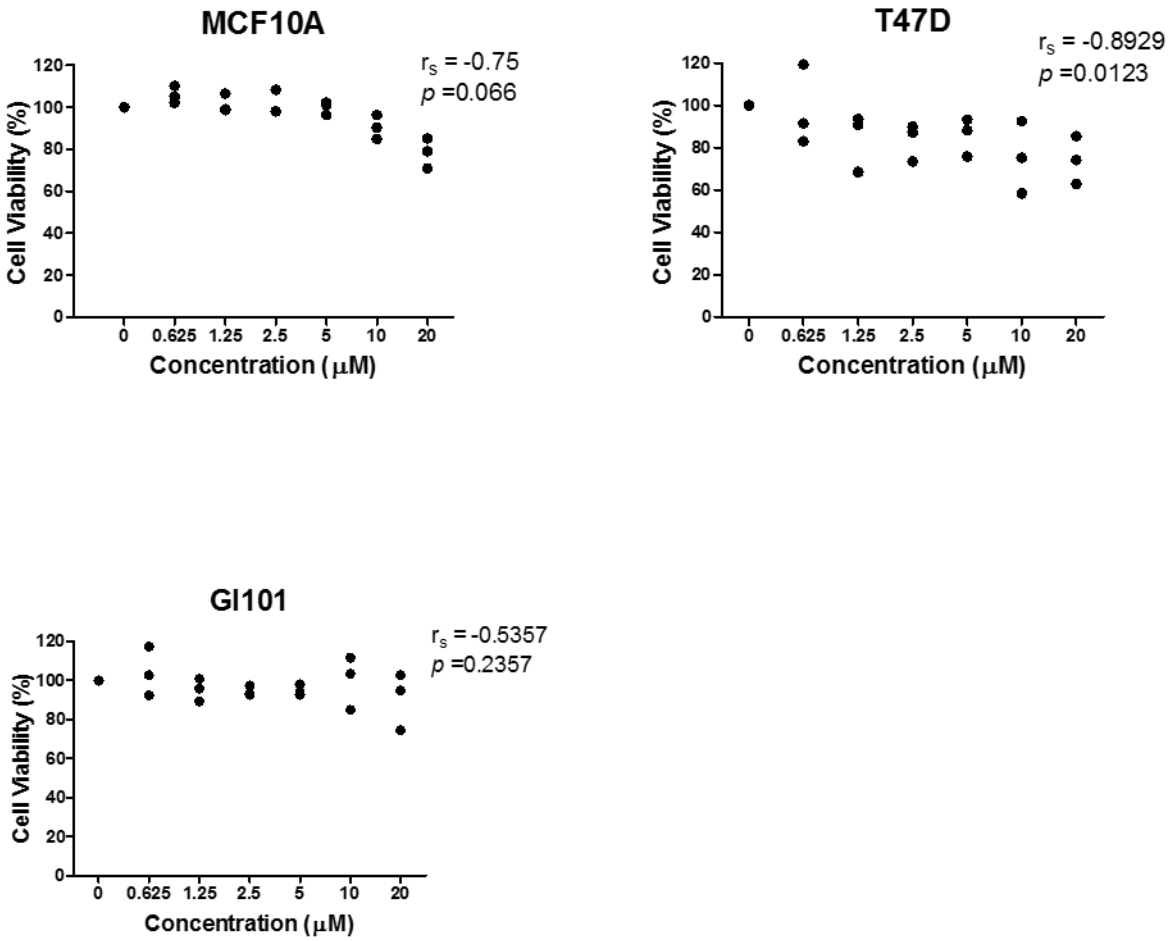

Figure 4.1 Statistically significant reduction is observed after Brk inhibition using a novel Brk inhibitor, Compound 4f for MCF10A, GI101 and T47D cell lines. MTT assays were performed to determine cell viability. Cells were seeded and allowed to adhere overnight in 96 wells plates before treatment with a range of doses (0-20μM) with the Brk inhibitor, Compound 4f. The cells were left in incubation (37˚C, 5% CO2) for 7 days. Fresh media and drug were added every 2/3 days. After which, MTT reagent was added to the wells and left in incubation for 2 hours before solubilisation with 0.04M HCL isopropanol. The absorbance at wavelengths 570 for MTT and 620nm (background) were determined and cell proliferation calculated as percentage of control. XY scatter graphs show each data point as a dot and correlation statistics determined using Graphpad software. Spearman rho correlation coefficient (rs), and two tailed p values for statistically significant correlation were determined, p <0.05 is significant, n=3.

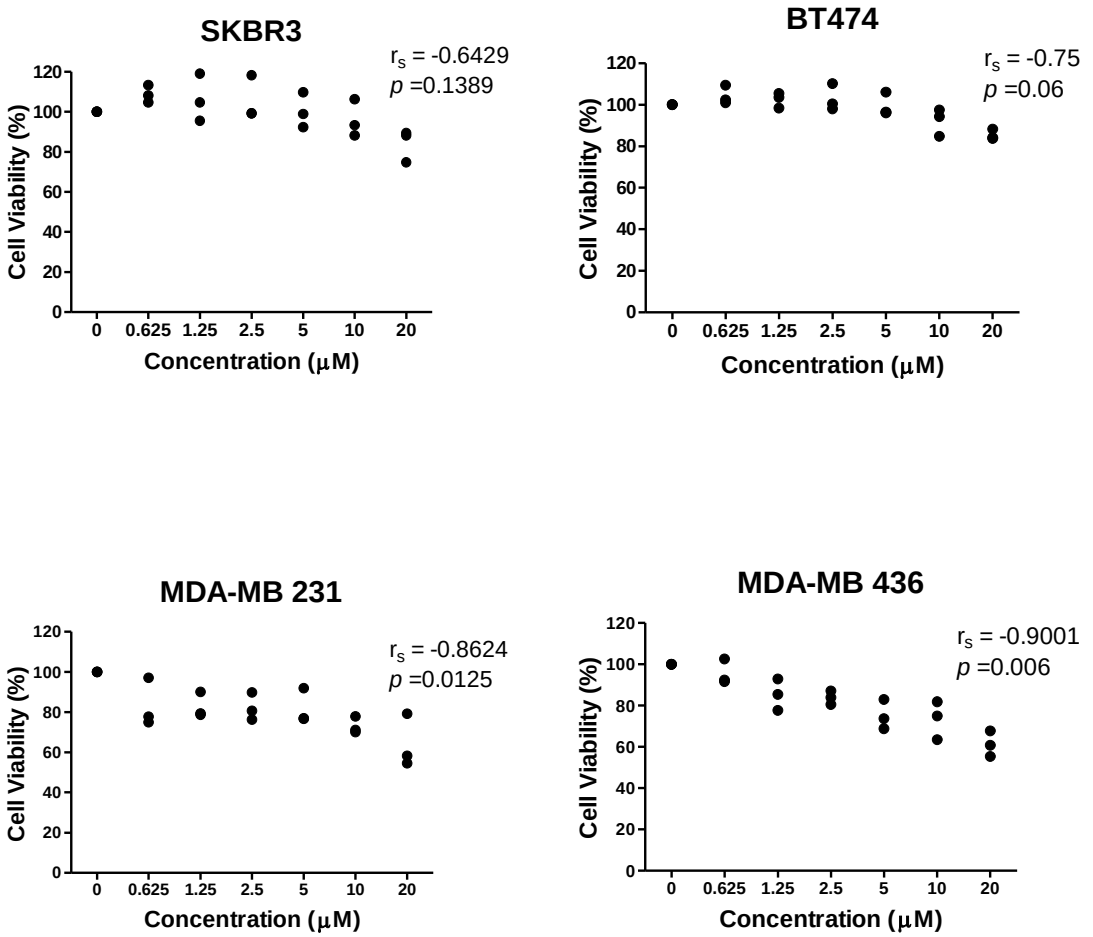

Figure 4.2 Statistically significant reduction in cell proliferation is observed for SKBR3, BT474, MDA-MB 231 and MDA-MB 436 cell lines after Compound 4f treatment. MTT assays were performed to determine cell viability. Cells were seeded and allowed to adhere overnight in 96 wells plates before treatment with a range of doses (0-20μM) with the Brk inhibitor, Compound 4f. The cells were left in incubation (37˚C, 5% CO2) for 7 days. Fresh media and drug were added every 2/3 days. After which, MTT reagent was added to the wells and left in incubation for 2 hours before solubilisation with 0.04M HCL isopropanol. The absorbance at wavelengths 570 for MTT and 620nm (background) were determined and cell proliferation calculated as percentage of control. XY scatter graphs show each data point as a dot and correlation statistics determined using Graphpad software. Spearman rho correlation coefficient (r_s), and two tailed p values for statistically significant correlation were determined, p <0.05 is significant, n=3.

The MCF10A cell line does show some reduction in cell proliferation with 78.4% (+/- 7.22 standard deviation) percentage cell viability at the highest (20µM) concentration of the compound. T47D cell line which expresses high levels of Brk protein, shows a reduction to 74.2% (+/- 11.3 standard deviation) with 20µM of compound 4f whereas GI101 which expresses moderate levels of the Brk protein shows 90.8% (+/- 14.6 standard deviation) at the same concentration. The HER2 positive cell lines; SKBR3 and BT474 show an average reduction in cell proliferation to 84.2% (+/- 8.1 standard deviation) and 85.4% (+/- 2.5 standard deviation) respectively at the 20µM concentration. Within the triple negative breast cancer cell lines; MDA-MB 231 and MDA-MB 436 there is a reduction to 69.6% (+/- 15.6 standard deviation) and 61.3% (+/- 6.19 standard deviation) respectively. For the MCF10A cell line, the Spearman rho correlation coefficient (r_s) value of -0.75 suggests a negative correlation with increasing dose and reducing cell viability in response to Brk inhibition, although this correlation is not statistically significant (p=0.66). For T47D, the r_s value is -0.8929 with a statistically significant correlation (p =0.0123) observed between cell viability and Brk inhibition. In contrast, GI101 cell line shows no statistical significance in correlation between Brk inhibition and cell viability (p =0.2357) and the r_s value of -0.5357 shows relatively weaker correlation. The r_s value of -0.6429 and -0.75 for SKBR3 and BT474 respectively show a correlation between reducing cell viability and increasing drug concentration. Both these HER2 positive cell lines, however showed statistically no significant correlation (p=0.1389 and p=0.06 respectively) as shown in Figure 4.2. The r value of -0.8624 and -0.9001 show a strong negative correlation in cell viability after treatment with compound 4f in the triple negative cell lines MDA-MB 231 and MDA-MB 436 respectively (Figure 4.2). The correlation is also statistically significant with p values of 0.0125 and 0.006 for MDA-MB 231 and MDA-MB 436 respectively. Overall majority of the cell lines displayed a dose dependent relationship between compound 4f and reducing cell viability except for

the GI101 cell line, which showed the weakest correlation that was not statistically significant. The cell lines, T47D, MDA-MB 231, MDA-MB 436 showed the strong inverse correlation between Brk inhibition and cell viability compared to the other cell lines. There was statistical significance observed suggesting there was a correlation between the cell viability and Brk inhibition. It should be noted, however that although there is a correlation observed between decreasing cell viability with increasing compound 4f concentration for these cell lines, the correlation analysis does not imply causation. The statistical significance does not necessarily indicate biological relevance and observing the graphs, the reduction in cell viability in response to Brk inhibition with compound 4f does not reach IC50 (half maximal inhibitory concentration) value even with a higher concentration of 20µM for all cell lines suggesting the low potency of the inhibitor. This suggests that Brk inhibition may not an effective monotherapy in these breast cancer cell lines. .

4.3.2 Combination treatment using compound 4f and chemotherapy agents, Taxol and Doxorubicin in breast cancer cell lines.

Treatment of majority of cancers including breast cancer is heavily chemotherapy based thus the significance of how Brk may influence breast cancer cell sensitivity to chemotherapy agents needs to be understood. In particular, chemotherapy remains the choice of treatment for triple negative breast cancer (reviewed in Collignon *et al.*, 2016). Therefore, I determined the efficacy of Taxol and Doxorubicin in two triple negative breast cancer cell lines; MDA-MB 231 and MDA-MB 436. I then sought to determine the difference in cell viability with Brk inhibitor treatment in combination with Taxol or Doxorubicin. The effect of Brk inhibition on the activity of its downstream signalling molecule, STAT3 was determined through western blots as well as determination of total and phospho-Brk activity and the levels of ALT-PTK6, the short isoform of full length Brk. As before the cell lines were plated in a 96 well plate at

a seeding density of 5 x10^3 per well and left to incubate at 37˚C and 5% CO2 overnight before treating with the either Taxol or Doxorubicin. Cells were treated either with dimethyl sulfoxide (DMSO) as the control or the following concentrations of each agent: 0.16µM, 0.3125µM, 0.625µM, 1.25µM, 2.5µM and 5µM. For the combination treatments, all cells were treated in addition with Compound 4f at a concentration of 5µM. The 96 well plates were left in incubation at 37˚C and 5% CO2 for a total of 7 days before processing as previously stated. Cell viability was calculated as percentage of control for all graphs. Graphs were plotted as scatter plots with mean and error bar showing standard deviation using Graphpad Prism 5 software. IC50 values showing half maximal inhibitory concentration were determined using Excel. Cells were treated with 5µM of compound 4f and protein lysates were collected at 0, 4, 6, 24 and 48 hours post treatment. Western blots were performed to determine levels of total Brk, phosphorylated Brk (p-Brk), total STAT3, phosphorylated STAT3 (p-STAT3) with β actin as the loading control as per the method in section 2.2.9and 2.2.4 in Chapter 2: Materials and Methods. Additionally, levels of ALT-PTK6 protein, the short isoform of full length Brk were determined.

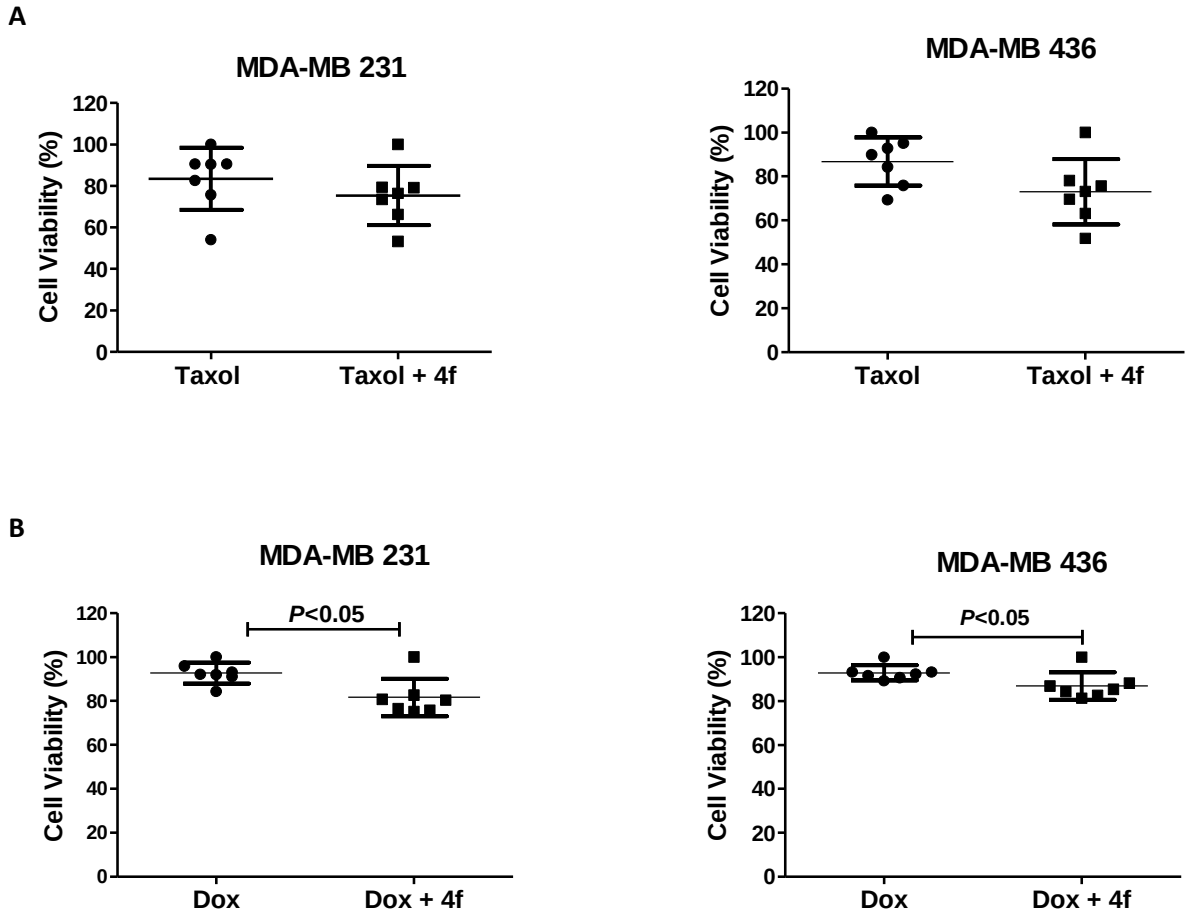

Figure 4.3 Brk modulates Taxol (Tax) and Doxorubicin (Dox) response in triple negative breast cancer cell lines: MDA-MB 231 and MDA-MB 436. Cell lines were plated in a 96 well plate at a seeding density of 5 x10^3 per well and left to incubate at 37˚C and 5% CO2 overnight before treating with the either Taxol or Doxorubicin. Cells were treated either with dimethyl sulfoxide (DMSO) as the control or the following concentrations of each agent: 0.16µM, 0.3125µM, 0.625µM, 1.25µM, 2.5µM and 5µM. For the combination treatments, all cells were treated in addition with Compound 4f at a concentration of 5µM. The 96 well plates were incubated at 37˚C and 5% CO2 for a total of 7 days with fresh media and compound added every 2/3 days. After which, MTT reagent/media mixture was added to each well and left to incubate as before for 2 hours before adding 0.04M HCL isopropanol to solubilize the formazan. Absorbance was measured at wavelengths 570nm and 620nm to determine cell viability. Scatter plots show mean (line in the middle) and error bars show standard deviation, n= 3. Students T Test indicates statistical significance with $P<0.05$ as significant.

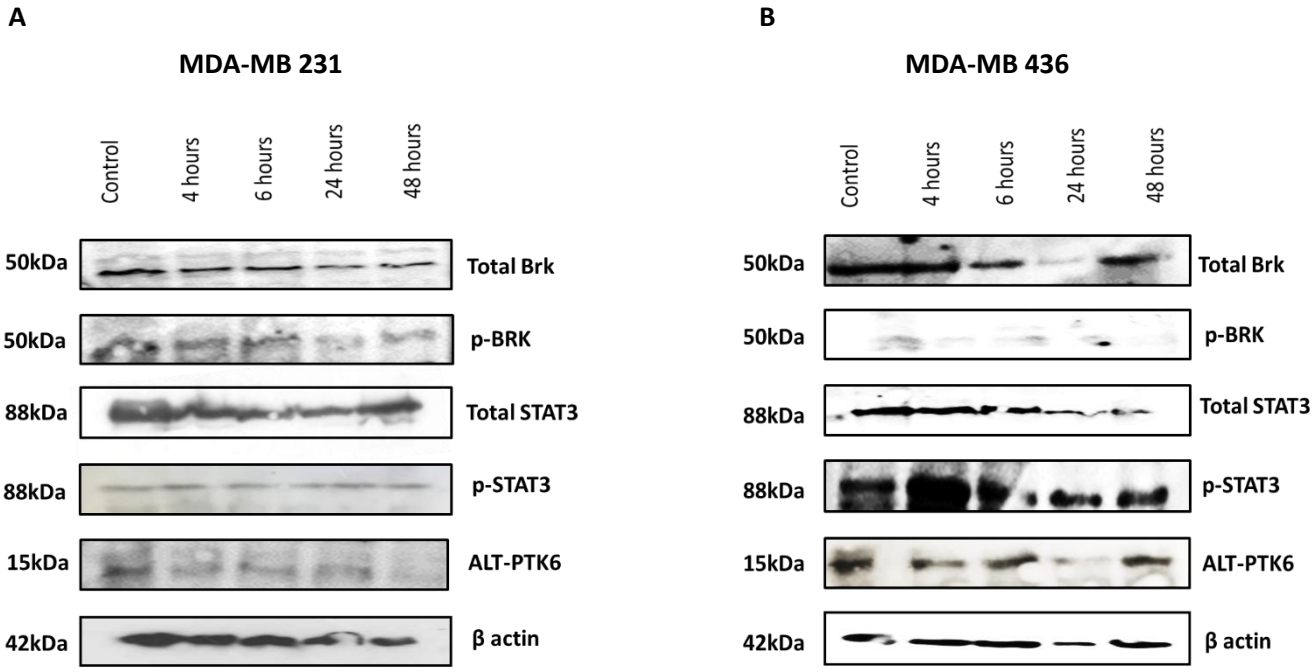

Figure 4.4 Western blots show an overall reduction in total and phosphorylated Brk in triple negative cell lines after Brk inhibition. Western blots were performed in A) MDA-MB 231 and B) MDA-MB 436 cell lines to show total and phosphorylated Brk (p-Brk) protein expression, total and phosphorylated STAT3 (p-STAT3) protein expression, ALT-PTK6 expression and β actin was used as loading control. Cells were lysed with 2x SDS-PAGE loading buffer, 100µl of lysis buffer was used per 1 million cells. Equal volume of lysates were loaded on a stacking gel and a 12% or 10% resolving gel was used. The proteins were then electro-blotted onto nitrocellulose membrane in 1x Towbin transfer buffer 1 hour at 300 volts and 400mAps. Membranes were blocked in 5% non-fat skimmed milk/TBS-T before incubating with primary antibodies overnight. The membranes were then washed with 1x TBST and incubated with the appropriate secondary antibody for 1 hour. Protein expression was detected with appropriate primary and secondary antibodies (Chapter 2: Materials and Methods, section 2.1.4., Table 5). Protein bands were detected using chemiluminescent substrates Coumaric acid (0.0148g/ml) and luminol (0.0443g/ml). N=3.

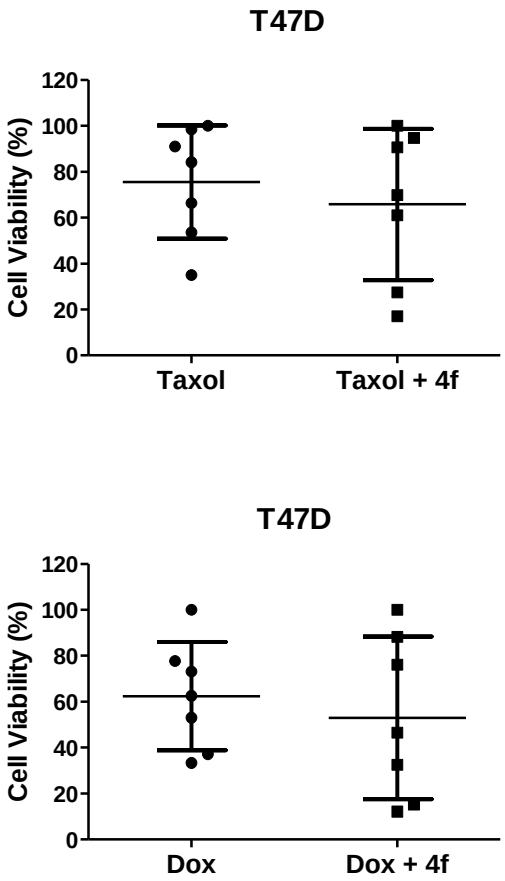

Figure 4.5 Shows difference in cell proliferation of T47D cell line is observed with Brk inhibition in combination with Taxol or Doxorubicin (Dox). Cell lines were plated in a 96 well plate at a seeding density of 5 x103 per well and left to incubate at 37˚C and 5% CO2 overnight before treating with the either Taxol or Doxorubicin. Cells were treated either with dimethyl sulfoxide (DMSO) as the control or the following concentrations of each agent: 0.16µM, 0.3125µM, 0.625µM, 1.25µM, 2.5µM and 5µM. For the combination treatments, all cells were treated in addition with Compound 4f at a concentration of 5µM. The 96 well plates were incubated at 37˚C and 5% CO2 for a total of 7 days with fresh media and compound added every 2/3 days. After which, MTT reagent/media mixture was added to each well and left to incubate as before for 2 hours before adding 0.04M HCL isopropanol to solubilize the formazan. Absorbance was measured at wavelengths 570nm and 620nm to determine cell viability. Scatter plots show mean (line in the middle) and error bars show standard deviation, n= 3. Students T Test indicates statistical significance with, $P<0.05$ is significant.

Figure 4.3 indicates modest reduction in cell viability for both triple negative breast cancer cell lines in response to either Paclitaxel (Taxol) or doxorubicin treatment only. Observing the intermediate dose of 0.625µM, average cell viability using Taxol only treatment was 90.5% (+/- 8.4 standard deviation) compared to average cell viability of 79.4% (+/- 7.5 standard deviation) for Taxol with compound 4f within MDA-MB 231 cell line. At the same concentration for MDA-MB 231 with Doxorubicin, cell viability was at 92% (+/- 2.6 standard deviation) compared to 76.4% (+/- 5.5 standard deviation) in combination with compound 4f. A cell line representative of Luminal A (T47D) was used due to its increased sensitivity to the chemotherapy agents in comparison to the two triple negative cell lines. A clear reduction in cell viability was observed in response to both Taxol and Doxorubicin treatment. IC50 concentration for treatment with Taxol and Taxol in combination with 4f was determined with Excel and showed concentrations of 1.95µM and 1.76µM respectively. For Doxorubicin treatment, the IC50 concentration was 2.49µM and for combination with 4f the IC50 was 0.89µM. The IC50 value for combination treatment shows a lower concentration suggesting combination treatment may be more effective than using Doxorubicin as a monotherapy. Overall, although statistically significant difference was observed, in comparison to treatment with either chemotherapy agent, there was greater reduction in cell viability with co-treatment using compound 4f (Figure 4.5).

Figure 4.4 shows the protein levels in MDA-MB 231 and MDA-MB 436 cell lines, after treatment with compound 4f, of total Brk, phosphorylated Brk (Tyr342) as well as phosphorylation of the downstream substrate, STAT3 as a marker of altered Brk activity. Total levels of Brk in MDA-MB 231 gradually decrease 24 hours post treatment before reaching near control levels at 48 hours post treatment. Levels of phosphorylated Brk (p-Brk) are also decreased over time compared to control lysate and STAT3 activity (p-STAT3) increases 4 hours post treatment before decreasing and remaining relatively constant at 6, 24 and 48

hours post treatment. For the first time, ALT-PTK6 protein expression was also detected in this cell line which decreased over time. In comparison, in MDA-MB 436 cells, total Brk protein expression and p-Brk levels are reduced gradually 4, 6, 24 and 48 hours post treatment along with total STAT3 and p-STAT3 levels (Figure 4.4). For the first time, protein expression of the short isoform, ALT-PTK6 was detected in the MDA-MB 436 cell line and some reduction was observed at 24 hours post treatment.

4.3.3 Combination treatment using compound 4f and the small molecule inhibitor, Lapatinib in HER2 positive breast cancer cell lines.

In addition to investigating whether Brk modulates chemotherapeutic response in breast cancer cell lines, I also sought to determine if Brk modulates response to targeted therapies. Since Brk, EGFR and HER2 interactions have previously been documented (Kamalati *et al.*, 1996, 2000; Born *et al.*, 2005; Aubele *et al.*, 2007, 2010; Xiang *et al.*, 2008; Li *et al.*, 2012; Ai *et al.*, 2013; Ludyga *et al.*, 2013); a Brk targeted therapy may prove to be beneficial. Briefly, lapatinib is a dual kinase inhibitor of HER2 and EGFR activity and its efficacy is reduced in HER2-trasnfected mammary epithelial cells with increased levels of Brk (Xiang *et al.*, 2008). This suggests potential for a novel Brk inhibitor treatment to be used in combination with lapatinib for a greater clinical benefit, especially in patients who have acquired resistance to lapatinib. The effect of Brk inhibition on the activity of its downstream signalling molecule, STAT3 was determined in HER2 positive cell lines through western blots as well as determination of total and phospho-Brk activity and the activity of HER2 protein. SKBR3 and BT474 cell lines were plated in a 96 well plate at a seeding density of 5 $x10^3$ per well as described previously and treated with either with dimethyl sulfoxide (DMSO) as the control or

the following concentrations of Lapatinib: 0.312µM, 0.625µM, 1.25µM, 2.5µM, 5µM and 10µM. For combination treatment, cells were treated with 5µM of Compound 4f. The 96 well plates were left in incubation and processed as previously stated. Cell viability was calculated as percentage of control for all graphs. Western blots were carried out to determine levels of total Brk, phosphorylated Brk (p-Brk), total STAT3 and phosphorylated STAT3 (p-STAT3) as well as total and phosphorylated HER2 levels with β actin as the loading control as per the method in section 2.2.9 and 2.2.11 in Chapter 2: Materials and Methods.

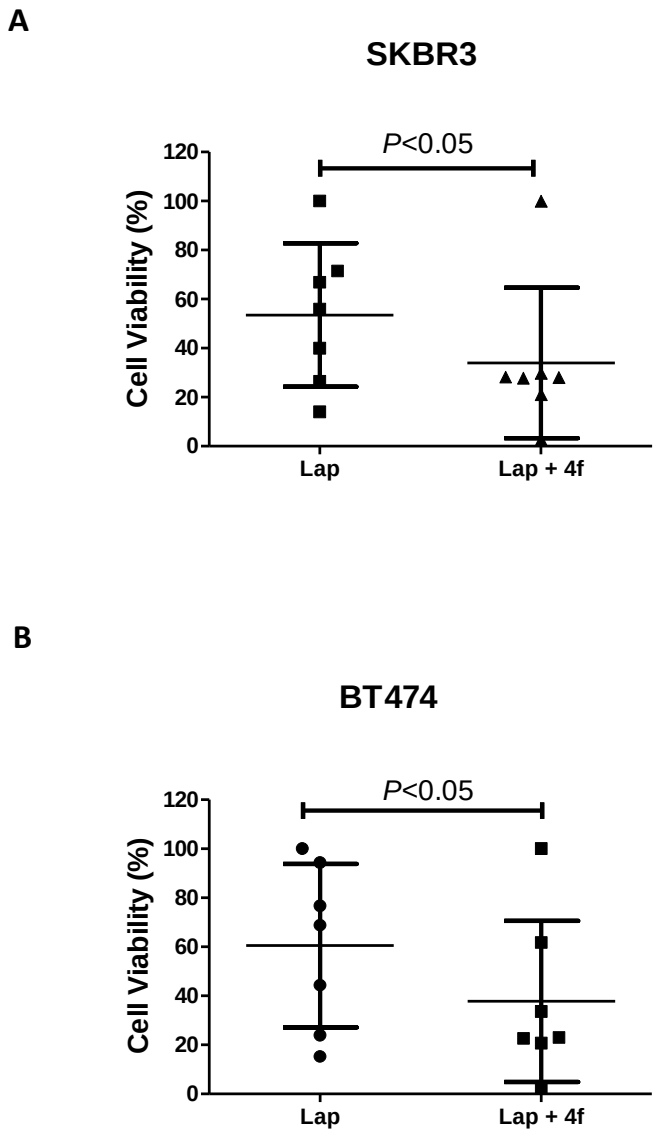

Figure 4.6 Brk modulates Lapatinib response in HER2 positive breast cancer cell lines: SKBR3 and BT474. SKBR3 (A) and BT474 (B) cell lines were plated in a 96 well plate at a seeding density of 5 x10^3 per well and treated with either with dimethyl sulfoxide (DMSO) as the control or the following concentrations of Lapatinib: 0.312µM, 0.625µM, 1.25µM, 2.5µM, 5µM and 10µM. For combination treatment, cells were treated with 5µM of Compound 4f. The 96 well plates were incubated at 37˚C and 5% CO2 for a total of 7 days with fresh media and compound added every 2/3 days. After which, MTT reagent/media mixture was added to each well and left to incubate as before for 2 hours before adding 0.04M HCL isopropanol to solubilize the formazan. Absorbance was measured at wavelengths 570nm and 620nm to determine cell viability. Scatter plots show mean (line in the middle) and error bars show standard deviation, n= 3. Students T Test indicates statistical significance with P<0.05 as significant.

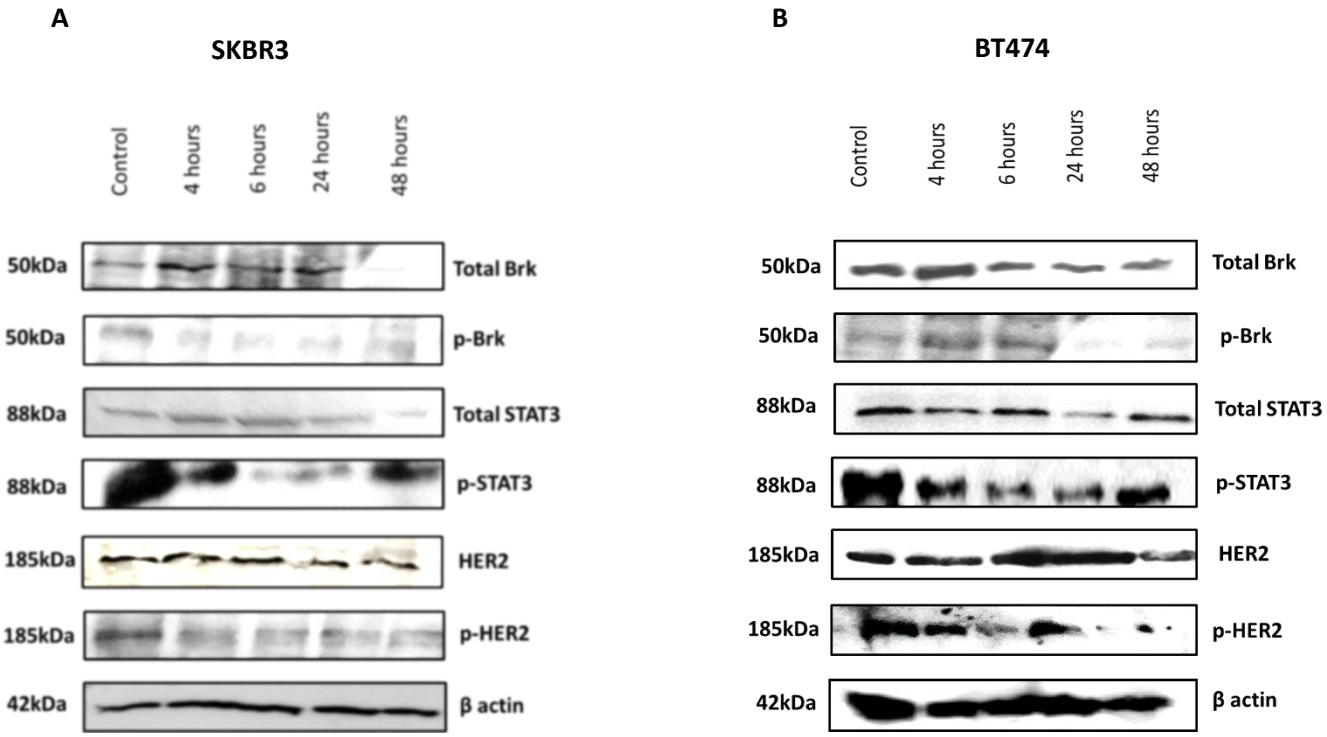

Figure 4.7 Western blots show an overall reduction in total and phosphorylated Brk in HER2 positive breast cancer cell lines after Brk inhibition. Western blots were performed in A) SKBR3 and B) BT474 cell lines to show total and phosphorylated Brk (p-Brk) protein expression, total and phosphorylated STAT3 (p-STAT3) protein expression and and β actin was used as loading control. Cells were lysed with 2x SDS-PAGE loading buffer, 100µl of lysis buffer was used per 1 million cells. Equal volume of lysates were loaded on a stacking gel and a 12% or 10% resolving gel was used. The proteins were then electro-blotted onto nitrocellulose membrane in 1x Towbin transfer buffer 1 hour at 300 volts and 400mAps. Membranes were blocked in 5% non-fat skimmed milk/TBS-T before incubating with primary antibodies overnight. The membranes were then washed with 1x TBST and incubated with the appropriate secondary antibody for 1 hour. Protein expression was detected with appropriate primary and secondary antibodies (Chapter 2: Materials and Methods, section 2.1.4., Table 5). Protein bands were detected using chemiluminescent substrates Coumaric acid (0.0148g/ml) and luminol (0.0443g/ml). N=3.

My investigations show significant reduction in cell viability for both HER2 positive breast cancer cell lines (SKBR3, *P*=0.023 and BT474, *P*=0.019) when a Brk inhibitor is used in combination with targeted therapy, lapatinib in comparison to either inhibiting Brk alone or using lapatinib alone (Figure 4.6A). Observing the lower concentrations, there is an average reduction to 61.74% (+/- 10.6 standard deviation) at the 0.312µM concentration for the combination treatment compared to an average reduction to 94.31% (+/- 5.5 standard deviation) with lapatinib only in the BT474 cell line. A greater reduction in cell viability was observed in the SKBR3 cell line, with an average reduction in cell proliferation to 71.4% (+/- 2.5 standard deviation) at the 0.312µM concentration for lapatinib treatment alone compared to 28.03% (+/- 9.7 standard deviation) for combination treatment with compound 4f. This is an approximate 2.5-fold reduction in cell viability.

Figure 4.7 shows an increase in protein levels of total Brk in the SKBR3 cell line at 4 hours post treatment with compound 4f before a reduction at 48 hours post treatment. Phospho-Brk activity is also reduced post treatment with compound 4f. Total STAT3 levels remain relatively constant before a reduction 48-hour post treatment. Phosphorylated STAT3 (p-STAT3) is reduced 4, 6, 24 and 48 hours post treatment compared to control levels. Interestingly, p-STAT3 levels are the lowest at 6 and 24 hours post treatment before increasing at 48 hours post treatment. There seems to be no observable change in HER2 levels. Figure 4.7B also shows protein levels of total Brk in BT474 cell line, which are increased 4 hours post treatment with compound 4f before reducing 6, 24 and 48 hours post treatment. Phospho-Brk (p-BRK) levels increase 4 and 6 hours post treatment relative to control levels before reducing 24 and 48 hours post treatment. Total STAT3 levels remain relatively constant post treatment with compound 4f, except at 24 hours post treatment where there is a reduction. STAT3 phosphorylation (p-STAT3) is reduced at all time points post treatment and starts to recover by 48 hours. HER2 levels appear to be relatively constant

with very modest increase 6 and 24 hours post treatment. In comparison phosphorylated HER2 (p-HER2) levels are decreased overall for both cell lines.

4.3.4 Combination treatment using compound 4f and endocrine therapy, Tamoxifen.

It has been previously documented there is a strong correlation between high expression of PTK6 and positive oestrogen receptor (ER+) status within breast tumours (Zhao *et al.*, 2003). Higher levels of PTK6 expression within ER+ breast cancers was also associated with adverse patient outcomes (Irie *et al.*, 2010). In addition, p38 MAPK, a mediator of MEF2 activation, cyclin D1 up regulation and involved in increased cell migration in response to ErbB signalling is a substrate of Brk (J H Ostrander *et al.*, 2007), with high levels of active phosphorylated p38 MAPK significantly correlated with elevated levels of HER2 and increased Tamoxifen resistance (Gutierrez *et al.*, 2005). More recently, Brk/PTK6 has been shown to enhance the growth of ER+ breast cancer cells basally as well as in oestrogen deprived conditions, and in the presence of Tamoxifen, further indicating a role for Brk in drug resistance (Ito *et al.*, 2017). These studies suggest targeting PTK6 for inhibition would potentially increase sensitivity of breast cancer cells to Tamoxifen and other endocrine therapies as well as overcome potential mechanism of drug resistance. I sought to determine sensitivity of ER+ breast cancer cells to Tamoxifen in combination with Brk inhibition. The effect of Brk inhibition on the activity of its downstream signalling molecule, STAT3 was determined in this luminal A breast cancer subtype cell line through western blots as well as determination of total and phospho-Brk activity, levels of the oestrogen receptor and the levels of ALT-PTK6, the short isoform of full length Brk. T47D cells were plated as before but, due to presence of low levels of oestrogen and to remove endogenous serum steroids,

phenol red free growth media supplemented with 10% charcoal stripped foetal bovine serum (FBS) was used. Cells were treated either with dimethyl sulfoxide (DMSO) as the control or the following concentrations of Tamoxifen: 0.312µM, 0.625µM, 1.25µM, 2.5µM, 5µM and 10µM. The cells were additionally treated with 5µM of compound 4f in combination therapy. The cells were processed as mentioned previously. Cell viability was calculated as percentage of control for all graphs. Western blots were performed as per the method in section 2.2.9 and 2.2.11 in Chapter 2: Materials and Methods.

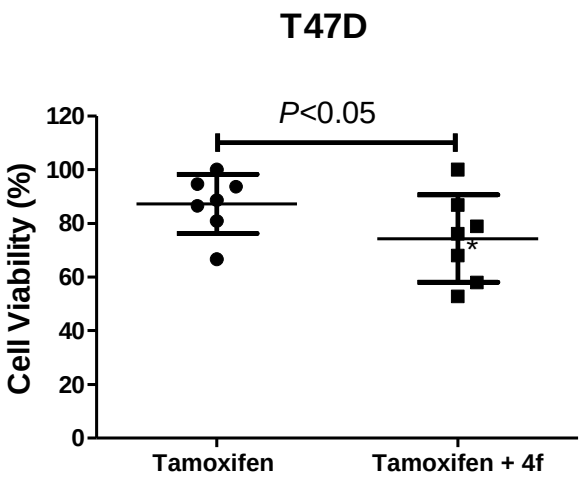

Figure 4.8 Brk modulates endocrine therapy, Tamoxifen response in ER+ breast cancer cell line T47D. Cells were cultured in phenol red free growth media supplemented with 10% charcoal stripped foetal bovine serum. Cells were plated in a 96 well plate at a seeding density of 5 x10^3 per well and treated either with dimethyl sulfoxide (DMSO) as the control or the following concentrations of Tamoxifen: 0.312µM, 0.625µM, 1.25µM, 2.5µM, 5µM and 10µM. The cells were additionally treated with 5µM of compound 4f in combination therapy. The 96 well plates were incubated at 37˚C and 5% CO2 for a total of 7 days with fresh media and compound added every 2/3 days. After which, MTT reagent/media mixture was added to each well and left to incubate as before for 2 hours before adding 0.04M HCL isopropanol to solubilize the formazan. Absorbance was measured at wavelengths 570nm and 620nm to determine cell viability. Scatter plots show mean (line in the middle) and error bars show standard deviation, n= 3. Students T Test indicates statistical significance with P<0.05 as significant.

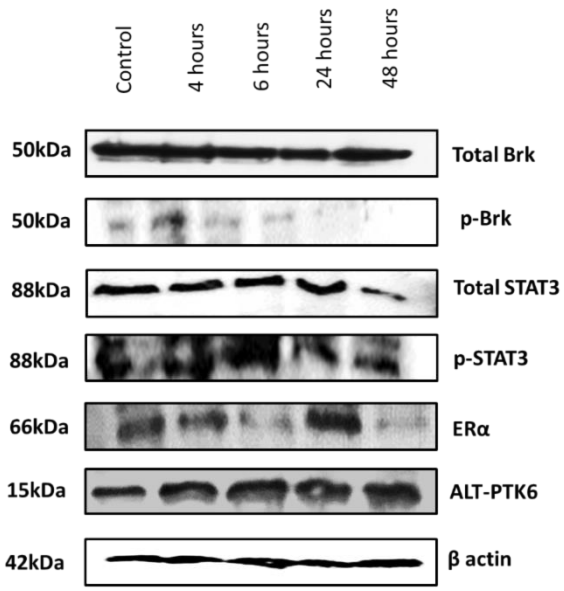

Figure 4.9 Relative expression ratios of ALT-PTK6 to PTK6 after compound 4f treatment some show some variation. Western blots were performed in T47D cell line to show total and phosphorylated Brk (p-Brk) protein expression, total and phosphorylated STAT3 (p-STAT3) protein expression and and β actin was used as loading control. Cells were lysed with 2x SDS-PAGE loading buffer, 100µl of lysis buffer was used per 1 million cells. Equal volume of lysates were loaded on a stacking gel and a 12% or 10% resolving gel was used. The proteins were then electro-blotted onto nitrocellulose membrane in 1x Towbin transfer buffer 1 hour at 300 volts and 400mAps. Membranes were blocked in 5% non-fat skimmed milk/TBS-T before incubating with primary antibodies overnight. The membranes were then washed with 1x TBST and incubated with the appropriate secondary antibody for 1 hour. Protein expression was detected with appropriate primary and secondary antibodies (Chapter 2: Materials and Methods, section 2.1.4., Table 5). Protein bands were detected using chemiluminescent substrates Coumaric acid (0.0148g/ml) and luminol (0.0443g/ml). N=3.

Treatment with Tamoxifen, the selective oestrogen receptor modulator (SERM), shows relative sensitivity of T47D cell line, a luminal A subtype of breast cancer (Figure 4.8). There is an average reduction in cell viability to 66.6% (+/- 10.9 standard deviation) at the highest concentration of 10µM when using Tamoxifen alone. In comparison, there is an average reduction to 52.8% (+/- 5.6 standard deviation) when treated in combination with compound 4f at the same concentration. A greater reduction is observed at the lower end doses, for example, at the concentration of 5µM, there was an average reduction in cell viability to 80.9% (+/- 6.1 standard deviation) using Tamoxifen only compared to 58% (+/- 5.2 standard deviation) when used in combination with the Brk inhibitor. Overall, there is statistically significant difference between Tamoxifen as a single agent and Tamoxifen in combination with compound 4f (P=0.004).

Figure 4.9 shows western blots for total Brk, phosphorylated Brk (p-Brk), total STAT3, phosphorylated STAT3 (p-STAT3), oestrogen receptor alpha (ERα) and the short isoform of full length Brk, ALT-PTK6. The western blot showed little difference in total Brk levels after treatment with 5µM of compound 4f, although there appears to be a reduction in Brk activity (p-Brk) levels at 6, 24 and 48 hours post treatment. There is reduction in total STAT3 and p-STAT3 levels relative to control levels at 48 hours post treatment. Oestrogen receptor alpha (ERα) levels showed a reduction at 6 and 48 hours post treatment compared to control levels. Interestingly ALT-PTK6 protein expression appeared to increase 4, 6, 24 and 48 hours post treatment after Brk inhibition.

4.4 Discussion

The studies in this chapter are some of the first to investigate the potential role of a novel Brk inhibitor in modulating breast cancer cell response to various anticancer drugs currently used in the treatment of breast cancer patients. These include chemotherapeutic agents Paclitaxel (Taxol) and Doxorubicin, small molecule inhibitor Lapatinib and endocrine therapy, Tamoxifen (Early Breast Cancer Trialists' Collaborative Group (EBCTCG), 2005; Mamounas *et al.*, 2005; Ogawa and Lindquist, 2018). Due to the role of Brk in promoting tumour cell proliferation including anchorage independent growth in breast cancer cells (Kamalati *et al.*, 1996; J H Ostrander *et al.*, 2007; Harvey *et al.*, 2009; Chan and Nimnual, 2010), I hypothesised a potential Brk inhibitor would decrease proliferation as well as sensitise breast cancer cells to these treatments. Using a novel Brk inhibitor known as compound 4f (Mahmoud *et al.*, 2014), I first sought to determine the effect on cell viability of breast cancer cell lines (Figures 4.1 and 4.2). There was reduction in cell viability observed with increasing concentration of compound 4f at low doses for majority of the breast cancer cell lines, especially at the mid to high end (5-20µM) of the drug concentrations used compared to untreated control cells. The greatest reduction in cell viability with compound 4f treatment was observed mainly in the triple negative cell lines (Figure 4.2). It should be noted that although there is some statistical significance observed with compound 4f treatment, the biological relevance of this may be small as overall the cell lines did not reach an IC50 (half maximal (50%) inhibitory concentration) value with Brk inhibition. The IC50 values are commonly used as a measure of a drug's efficacy (Aykul and Martinez-Hackert, 2016). In addition, the sample size of n=3 is small and a bigger sample may increase the power of any statistical analysis. The variations in cell viability for all cell lines upon Brk inhibition may be dependent on the levels of Brk expression. Observing Brk expression levels in the cell lines

that were used, MDA-MB 231 and MDA-MB 436 cell lines show moderate levels of Brk expression, T47D and BT474 cell lines show high Brk expression, GI101 and SKBR3 show lower Brk expression. In relation to efficacy to compound 4f, there is no clear pattern with Brk expression as cell lines with low and high Brk expression levels show similar sensitivity whereas the two triple negative cell lines which show moderate levels of Brk show the greatest sensitivity to compound 4f. This may suggest additional factors may influence cell line sensitivity to Brk inhibitor, for example, expression of other breast cancer receptors including: HER2, ER, PR and EGFR, within each cell line. Furthermore, due to the triple negative cell lines lacking HER2, ER and PR, and the role these receptors play in cell proliferation (Fanelli *et al.*, 1996; Conley *et al.*, 2016), inhibiting Brk may therefore reduce the number of signalling pathways by which the cancer cells are able to continue cell proliferation thus indicating reduced cell viability. I then further sought to determine if Brk modulated chemotherapeutic response in triple negative breast cancers (Figure 4.3). Triple negative breast cancers (TNBCs) showing chemo-sensitivity to anthracyclines (Doxorubicin) and taxanes (Taxol), indicate an overall survival which remains poor (O'Reilly *et al.*, 2015). In addition, chemo-resistance accounts for 90% of drug failures for metastatic cancers (Longley and Johnston, 2005) and there are a number of mechanism which induce chemo-resistance in TNBC including mutations in DNA repair enzymes, alterations in genes involved in apoptosis as well as due to overexpression of β tubulin III subunit which induces resistance to Taxol (Tommasi *et al.*, 2007). In addition, patients with triple negative breast cancer (TNBC) have limited therapeutic options and most do not respond to current endocrine or targeted therapies, thus there is a need for novel therapies for this subgroup of patients (Tomao *et al.*, 2015). Moreover, TNBC has become an attractive area of research within oncology and continuous understanding of its molecular characteristics would identify novel targets and allow for investigations of their therapeutic potential (Tomao *et al.*, 2015). Since

other breast molecular markers (ER, HER and PR) are absent in TNBC but Brk expression is present in triple negative cancers; any potential therapy targeting Brk inhibition may also be beneficial to TNBC patients. Thus, I sought to determine if compound 4f would reduce breast cancer cell viability in combination with standard of care chemotherapy agents Taxol or Doxorubicin within triple negative breast cancer cell lines. Overall, Taxol or Doxorubicin treatment resulted in reduction in cell viability of both of the triple negative cell lines MDA-MB 231 and MDA-MB 436 (Figure 4.3). These results showed both cell lines were more sensitive to Taxol and Doxorubicin as monotherapies compared to the Brk inhibitor, compound 4f alone. Thus suggesting, Brk kinase inhibition may not be effective as a monotherapy. Although it should be noted the two cell lines (MDA-MB 231 and MDA-MB 436) also express epidermal growth factor receptor (EGFR) and Brk association with EGFR leading to cell proliferation even in the absence of epidermal growth factor has previously been shown (Kamalati *et al.*, 1996). Brk also potentiates EGFR signalling by inhibiting the downregulation of EGFR and thus prolonging EGFR signalling (Kang *et al.*, 2012; Li *et al.*, 2012; Kang and Lee, 2013). EGFR signalling has shown to increase cancer cell proliferation and survival (reviewed in Kim and Muller, 1999). However, co-treatment with compound 4f and either Taxol or Doxorubicin indicated reduction in cell viability compared to either chemotherapy agent on its own, although this was not significantly different with Taxol treatment. This indicates inhibition of Brk kinase activity may improve the sensitivity of triple negative breast cancers to chemotherapy agents, Taxol and Doxorubicin.

In addition to cell viability for both triple negative cell lines, protein expression of Brk and Brk activity (p-Brk) as well as activity of its downstream signalling molecule signal transducer and activator of transcription 3 (STAT3) was determined after treatment with the Brk inhibitor, compound 4f over a 48-hour time period (Figure 4.4). STAT3 is a substrate of Brk and is involved in a number of cellular process including cell proliferation, migration and survival in

breast cancers (Liu *et al.*, 2006; Weaver and Silva, 2007). Brk has also shown to be auto-phosphorylated in its activation loop, most likely at Tyr-342 as well as additional sites at lower levels (Qiu and Miller, 2002; Castro and Lange, 2010). Thus, I hypothesised inhibition of Brk kinase domain would also result in reduced total Brk expression levels as well as reduced total and phosphorylated levels of STAT3. Overall there is a reduction in total Brk expression over time post treatment with compound 4f as well as a reduction in Brk activity within the MDA-MB 231 cell line. However total STAT3 protein expression as well as activity (p-STAT3) remain relatively unchanged. Within the MDA-MB 436 cell line, there is relative reduction in total Brk protein expression as well as Brk activity including reduced STAT3 activity post treatment with compound 4f. STAT3 activation has been linked to all subtypes of breast cancer especially the more aggressive types and thus its activation is important for survival of triple negative breast cancers (Marotta *et al.*, 2011; Walker and Frank, 2015). The difference observed with total STAT3 and phospho-STAT3 levels between the two cell lines after Brk inhibition may be explained due to increased levels of STAT3 gene within MDA-MB 231 cell line as well as increased number of STAT3 binding sites which is specific for the MDA-MB 231 cell line (McDaniel et al., 2017). Since STAT3 has a prominent role in TNBC migration and invasion leading to metastasis, inhibition of Brk as an upstream regulator of STAT3, may have potential to reduce these oncogenic functions in the TNBC subtype (Jackson and Lozano, 2017). Both cell lines also expresses low levels of ALT-PTK6, which is the short isoform of full length Brk. ALT-PTK6 has been proposed to act as a competitive inhibitor of full length Brk as well as negatively regulate cell growth in prostate cancer cells and increasing levels of transfected ALT-PTK6 within HEK293 cells showed reducing levels of Brk proportionally (Brauer *et al.*, 2011; Harvey and Burmi, 2011). However, little else is known regarding its role in breast cancer. ALT-PTK6 expression remains relatively unchanged within MDA-MB 436 cell lines (Figure 4.4B) after treatment with the Brk inhibitor.

Although there is a reduction at 24 hours post treatment, this may be explained due to lower loading as the β actin levels as the loading control are lower than the other samples. In the MDA-MB 231 cell line, interestingly ALT-PTK6 levels reduce over time with Brk inhibition. This may be due to the concurrently reducing levels of the full length form. Any Brk targeted therapy may have potential effects on the short isoform due to interactions of Brk with RNA binding proteins such as Sam68, SLM1 and SLM2 which regulate the splicing process (Brauer *et al.*, 2011). Thus, a reduction in Brk levels may also result in reduced ALT-PTK6 protein. Alternatively, ALT-PTK6 itself has shown to associate with Sam68 thus it may regulate its own splicing. In other cellular contexts, a reduction in Brk may shift the balance in favour of ALT-PTK6 for any SH3 binding partners of Brk and thus result in reduced Brk at the membrane and more localisation of Brk in the nucleus, where it has shown to have growth inhibitory functions (Brauer *et al.*, 2011). However, there appears to be minor change in ALT-PTK6 expression within the MDA-MB 436 cell line, indicating compound 4f does not affect ALT-PTK6 protein levels and thus would not negatively affect its potential role as a negative regulator of growth in breast cancer cells.

To further elucidate the role of Brk in modulating breast cancer cell response to current breast cancer therapies, I sought to determine if Brk decreased cell viability in combination with targeted therapy, Lapatinib within two HER2 positive cell lines: SKBR3 and BT474. Both cell lines showed high sensitivity to lapatinib as a monotherapy (Figure 4.6). Co-treatment with compound 4f, however, resulted in a reduction of cell viability to an average of less than 3% at the dose of 10µM for both cell lines. Significant difference was observed between lapatinib as a single agent and in combination with compound 4f (P=0.023 for SKBR3 and P=0.019 for BT474). These results are further supported by other *in vitro* studies which have shown simultaneous knock down of HER2 and Brk leads to significant reduction in cell proliferation (Ludyga *et al.*, 2013). Overall, there is a reduction in protein expression of Brk

as well as Brk activity with compound 4f treatment in both cell lines as well as reduced levels of total STAT3 and p-STAT3 activity (Figure 4.7B). Due to Brk and HER2 co-expression (Ludyga *et al.*, 2013), Brk inhibition may result in downregulation of HER2 activity. However, there appears to little observable change in HER2 levels. In comparison, overall there is a clear reduction in p-HER2 levels for both cell lines indicating Brk inhibition results in a reduction in HER2 activity. Previous studies have shown comparable results for Brk inhibition in HER2 positive cell lines. siRNA knockdown of PTK6 in breast cancer cell lines including a trastuzumab resistant cell line JIMT-1, showed little change in HER2 and HER2 protein expression whereas phosphorylated HER2, levels were reduced (Ludyga *et al.*, 2011). Taken together, these results suggest inhibition of Brk and HER2 in combination may offer a more effective alternative therapy than to use either as a monotherapy.

I next sought to determine the role of Brk in sensitizing breast cancer cells to endocrine therapy, more specifically Tamoxifen. Tamoxifen is a selective oestrogen receptor modulator (SERM) that binds to the oestrogen receptor and functions by antagonizing the effects of oestrogens (Abdulkareem and Zurmi, 2012). It has shown clinical efficacy in combination with other chemotherapy drugs for the treatment of early as well as advanced breast cancer (Clemons, Danson and Howell, 2002). However, some tumours do not show any response to Tamoxifen and some will eventually acquire resistance through various mechanisms including mutation or loss of oestrogen receptors, impaired co activator signalling and altered Tamoxifen metabolism (Ali and Coombes, 2002; Abdulkareem and Zurmi, 2012). Tamoxifen resistance is also linked to increased insulin growth factor (IGF)-1 signalling through the IGF-1 receptor (IGF-1R) and cross talks with oestrogen receptor (Parisot *et al.*, 1999). Thus, breast cancer cells with resistance to Tamoxifen indicate upregulation of IGF-1R. There have been few published studies investigating the role between Brk and endocrine therapies. However Brk has been shown to co-precipitate with IGF-1R and regulate IGF-1 induced

anchorage independent survival, inhibition of Brk may therefore sensitise breast cancer cell lines to Tamoxifen treatment and overcome a potential resistance mechanism (Irie *et al.*, 2010). Elevated levels of PTK6 transcript have also been associated with adverse outcomes for oestrogen receptor (ER) positive subset of patients (Irie *et al.*, 2010). This was further confirmed more recently, when the Irie group showed that breast cancer patients with positive oestrogen receptor status and higher relative expression of PTK6 transcript had poorer overall survival (Ito et al., 2017). Brk and oestrogen receptor interactions have also been shown to indicate a rationale for Brk as a positive prognostic marker despite being overexpressed in high grade tumours as the oestrogen receptor is associated with positive prognosis and increased disease free survival (Harvey *et al.*, 2009).

My studies show a proportionate reduction in cell viability with increasing concentration of Tamoxifen in ER positive breast cancer cell line T47D (Figures 4.8). There is also a significant difference between co-treatment with compound 4f for T47D cell line compared to Tamoxifen treatment alone (P=0.004). Protein expression of total Brk is relatively unchanged to control levels after treatment with compound 4f (Figure 4.9). However, Brk activity is reduced at 6, 24 and 48 hours post treatment compared to control levels, thus indicating reduction in active Brk in the oestrogen receptor positive cell line. Total STAT3 levels remain relatively unchanged until 48 hours post treatment where there is a reduction compared to control levels as well as very moderate reduction in p-STAT3 levels. Interestingly, oestrogen receptor alpha (ERα) levels vary with compound 4f treatment. ERα levels are relatively similar to control levels 4 hours post treatment then reduced 6 hours post treatment before increasing 24 hours post treatment and subsequently decreasing 48 hours post treatment. Nonetheless, there is an overall reduction in oestrogen receptor levels as well as reduced Brk activity, indicating Brk inhibition modulates breast cancer cell response to endocrine therapies, potentially via downregulation of oestrogen receptor although this needs further

validation. In addition, ALT-PTK6 protein expression was increased in response to Brk inhibition over the time period. A reduction in Brk activity shows reduced interaction with its downstream substrates and considering that ALT-PTK6 may compete for Brk's SH3 binding partners, reduced Brk activity may therefore result in increased ALT-PTK6 levels at the protein level. Although there was an increase in ALT-PTK6 protein expression within the T47D cell line and a decrease in the MDA-MB 231 cell line, this may be due to the expression levels of Brk and ALT-PTK6. Considering the low level of ALT-PTK6 expression in the MDA-MB 231 cell line, additionally inhibiting Brk may reduce the production of the alternatively spliced isoform due to Brk's interaction with proteins involved in alternative splicing. However, this effect is not as pronounced in the T47D cell line due to the much higher level of ALT-PTK6. Recently, Brk overexpression has shown to enhance growth of ER positive breast cancer cells including in oestrogen deprived conditions as well as in the presence of Tamoxifen (Ito *et al.*, 2017). ER positive breast cancer cell lines, MCF7 and T47D were stably expressed with activated Brk which was enough to enhance growth of these cell lines thus suggesting a role for Brk in promoting ER positive breast cancer growth basally as well as under oestrogen deprived conditions (Ito *et al.*, 2017). Downregulation of Brk impaired growth and induced apoptosis in both Tamoxifen sensitive and resistant breast cancer cells *in vivo* as well as *in vitro* (Ito *et al.*, 2017). Thus, my studies with compound 4f corroborate results with Brk inhibition in ER positive breast cancer cells.

Overall, my studies provide insight to the potential of Brk targeted therapy. Brk modulates response of breast cancer cells to a number of commonly used treatment modalities in breast cancer including Paclitaxel (Taxol), Doxorubicin, Lapatinib as well as endocrine therapy, Tamoxifen. The co-treatments with Brk also indicate significant reduction in cell viability at lower doses. There are number of issues with current breast cancer therapies including an increasing number of patients treated using anthracyclines and taxanes in the adjuvant

setting have shown to present with metastatic disease (Hassan et al., 2010). Resistance to these therapies, including to hormone and targeted therapies, remains a major challenge to overcome (Hussain et al., 2005). In addition, there are a number of acute, immediate and long-term toxicities associated with many chemotherapeutic agents used in breast cancer therapy, including cardiac toxicities with anthracycline based regimens (Bird and Swain, 2008), an increased relative risk of secondary cancers by 22% (Schaapveld et al., 2008), increased risk of cognitive impairment as well as neurotoxicity by 20-30% (Azim et al., 2011). Thus, there is a need for novel breast cancer therapies that, when used in combination with existing drugs, could allow for increased efficacy at potentially lower doses, thereby reducing side effects. My investigations indicate Brk as a monotherapy may not be effective to reduce breast cancer cell viability, however there is potential for Brk inhibitors to be used in combination with other treatments. Nonetheless, it should be noted that the overall very moderate reduction in cell viability using compound 4f alone may be due to the actual inhibitor. At the time of these studies, a Brk inhibitor was not commercially available. Thus my studies utilised a novel Brk kinase inhibitor known as compound 4f as developed by Hilgeroth and group (Mahmoud *et al.*, 2014). There are also few published studies investigating the role of compound 4f as well as its potency in inhibiting Brk *in vivo* as well as i*n vitro*. In addition, through personal communication with other research groups working with Brk, we discovered compound 4f was not found to be a particularly stable drug once it is in solution thus this will affect its activity and potency. A more potent version of compound 4f or another more potent inhibitor for Brk may indicate a more effective reduction in cell viability as a monotherapy as well as in combination therapy.

The main conclusions from this chapter were that Brk as a monotherapy may not be effective, however, there is potential in combination with other breast cancer treatments. There was a correlation between Brk inhibition and reducing cell viability, however it should be noted that

this does not imply compound 4f was the only cause of the reduction in cell viability and other factors may be involved including breast cancer receptor status and stability of the compound. In addition, it should be noted although there was some significant correlation observed, the biological relevance of this may not be substantial due to low efficacy of the inhibitor. Furthermore, the specificity of the inhibitor to target Brk was not evaluated in this study and will need consideration in any future studies using this inhibitor.

5.0 Chapter 5: Investigating the ratios of *ALT-PTK6* to *PTK6* transcripts in breast cancer cell lines and tissues

5.1 Introduction

The *ptk6* gene comprises of 8 exons which span 10kb, and fluorescent *in situ* hybridization (FISH) studies indicate its localisation to chromosome 20q13.6 (Mitchell *et al.*, 1997). Alternative splicing of the *PTK6* transcript produces a separate mRNA sequence encoding the truncated protein *ALT-PTK6* (alternative PTK6 isoform), which shares the first 77 amino acids and SH3 domain with the full length protein (Mitchell *et al.*, 1997). Both transcripts were shown to be co-expressed in prostate and colon cancer primary cell lines and human prostate tumour and normal tissue (Brauer *et al.*, 2011). Tyner and group also revealed potential functions of the short isoform (Brauer *et al.*, 2011). Ectopic expression of ALT-PTK6 was shown to enhance repression of β-catenin/TCF transcription, which is involved in the WNT pathway and enhances cancer growth, (Palka-Hamblin *et al.*, 2010; Brauer *et al.*, 2011). PC3 prostate cancer cell lines with induced ALT-PTK6 expression also had reduced proliferation and colony formation compared to controls without ALT-PTK6 induction (Brauer *et al.*, 2011). In addition, ALT-PTK6 may enhance the nuclear functions of Brk and previous studies have indicated subcellular localisation of Brk significantly influenced its ability to regulate β-catenin transcriptional activity (Palka-Hamblin *et al.*, 2010; Brauer *et al.*, 2011). Furthermore, *PTK6* to *ALT-PTK6* mRNA expression ratios were shown to be higher in prostate tumour cells in comparison to normal prostate cells (Brauer *et al.*, 2011).

Co expression of the full length *PTK6* transcript and the alternative isoform have also been shown in breast cancer cell lines including T47D, SKBR3, BT474, MDA-MB 231 (Peng *et al.*, 2014). It was originally believed the *PTK6* was present in mainly breast cancer cell lines and breast cancer tissues and not in normal breast (Mitchell *et al.*, 1997). However, more recently Brk was detected in normal mammary tissue as well as in the non-transformed mammary gland epithelial cell line MCF10A (Peng *et al.*, 2014). Furthermore, protein expression of *ptk6*

was detected in the cytoplasm and nucleus of luminal and myoepithelial cells within the cores of mammary gland tissue from 27 patients (Peng *et al.*, 2014)

Interestingly, active Brk was not detected in epithelial cells of normal mammary glands, indicating perhaps Brk has kinase-independent functions in the normal mammary gland (Peng *et al.*, 2014). Studies have shown high expression of *PTK6* in high grade invasive ductal carcinomas compared to low or undetectable levels in low grade tumours; suggesting a negative correlation with patient survival outcomes and that *PTK6* expression levels may be used to determine prognosis (Harvey *et al.*, 2009; Irie *et al.*, 2010; Peng *et al.*, 2014). It should also be noted, other investigations have shown a positive correlation with high Brk expression and improved probability of distant recurrence free survival in breast cancer patient cohorts, although this was observed at the later months (240 months) (Born *et al.*, 2005; Aubele *et al.*, 2007). This was later confirmed in a different and smaller (n=80) patient cohort with Brk expression correlating with a good prognosis (P=0.018) (Aubele *et al.*, 2010). This contradiction may be due to the presence of other breast molecular markers such as ER, which has shown positive association with Brk expression and ER is a known positive prognostic indicator (reviewed in Taneja *et al.*, 2010).

My investigations focused on the detection and expression of full length *PTK6* transcript as well as the short isoform splice variant *ALT-PTK6* in a number of breast cancer cell lines at the basal level. Using qPCR allowed for the quantification of the relative expression ratios of both variants in comparison to full length *PTK6* at basal level, as well as in response to Brk inhibition using the compound 4f (Mahmoud *et al.*, 2014). Relative expression and expression ratios were also determined post treatment with a number of breast cancer anticancer agents including; Paclitaxel (Taxol), Doxorubicin, Lapatinib and Tamoxifen. Due to the role of ALT-PTK6 in negative regulation of cell growth as well as its role as a regulator of Brk activity and as a competitive inhibitor of Brk substrates; any reduction in Brk may shift

the balance in favour of ALT-PTK6 expression (Brauer *et al.*, 2011). Since ALT-PTK6 is proposed to be a negative regulator of Brk activity and higher *PTK6* mRNA expression is associated with poorer outcomes (Harvey *et al.*, 2009; Brauer *et al.*, 2011) it was predicted *ALT-PTK6* to *PTK6* ratios will be higher in cancerous tissues and reduced in normal/ low grade breast tumours and may associate with improved overall patient survival.

5.2 Aims and Objectives

Aims:

Previous studies have shown *PTK6* transcript is associated with adverse patient survival outcomes in breast cancer as well as expression of both *PTK6* and *ALT-PTK6* expression in a limited number of breast cancer cell lines. The aims of this chapter were to investigate the ratio of mRNA expression levels of *ALT-PTK6* and *PTK6* in breast cancer cell lines in response to Brk inhibition and standard breast cancer therapies. In addition, previous studies have not investigated the role of *ALT-PTK6* and *PTK6* transcripts in breast cancer tissue in relation to overall and disease free survival and it was hypothesised that *ALT-PTK6* to *PTK6* ratios will be higher in cancerous tissues/cell lines and reduced in normal/ low grade breast tumours/cell lines.

The objectives were:

- To determine expression of both full length *PTK6* transcript and the short splice variant; *ALT-PTK6* in breast cancer cell lines using Real Time-PCR.
- To quantify the relative mRNA expression and ratios of both *PTK6* transcripts in breast cancer cell lines at basal levels and before and after treatment with compound 4f as well as in response to standard breast cancer treatments: Taxol, Doxorubicin, Lapatinib as well as Tamoxifen.
- To determine *ALT-PTK6* to *PTK6* mRNA expression ratios in normal and tumour breast tissue samples in relation to overall and disease free survival.

5.3 Results

5.3.1 Determination of *PTK6* and *ALT-PTK6* expression in breast cancer cell lines using RT-PCR

I first sought to determine gene expression of *PTK6* as well as the short isoform *ALT-PTK6*. For reverse transcriptase PCR (RT-PCR), RNA was extracted from the cell lines and 200ng/µl concentration of RNA in a final volume of 20µl was reverse transcribed and the cDNA used as template for PCR. RT-PCR was performed in the following cell lines: MCF10A, GI101, T47D, SKBR3, BT474, MDA-MB 231 and MDA-MB 436. REDTaq Readymix PCR Reaction Mix with MgCI2 (Sigma-Aldrich) was prepared with either Brk primers (Sigma Aldrich) or loading control gene, β actin as described in Materials and Methodology (section 2.2.18). All experiments were carried out with three independent sets of RNA lysates. PCR products were visualised using the Gel Doc Imaging System (BioRad) and a representative image of the RT-PCR products is shown in Figure 5.1.

Expression of both *PTK6* (407 bp) and *ALT-PTK6* (285bp) was detected in most of the cell lines examined under basal conditions (Figure 5.1). Expression was not detected in the immortalised transformed cell line MCF10A as well as one of the triple negative cell lines, MDA-MB 231. High levels of expression were seen in GI101, T47D, SKBR3 and BT474 cell lines. The MDA-MB 436 cell line had moderate expression of the both *PTK6* and *ALT-PTK6* transcripts.

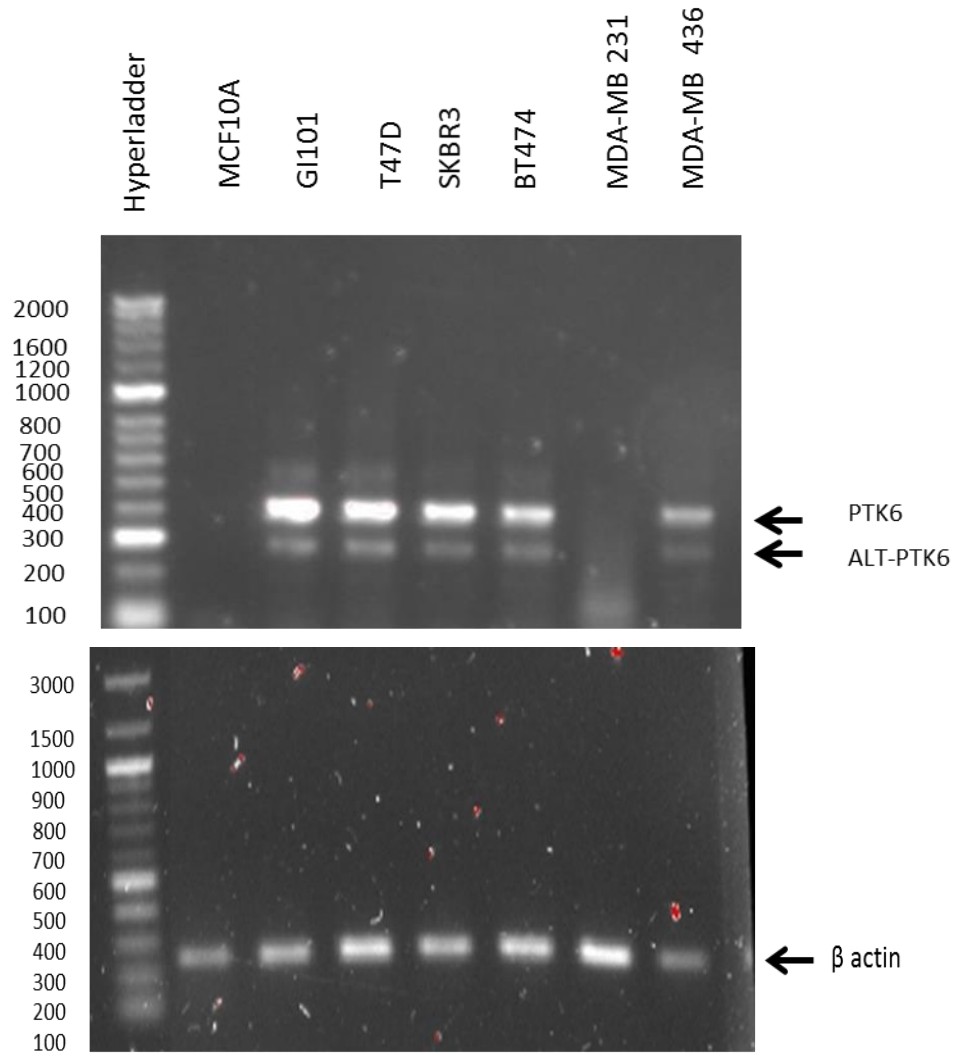

Figure 5.1 Representative RT-PCR showing basal expression of PTK6 and ALT-PTK6 (upper panel) as well as β actin as loading control (lower panel) in MCF10A, GI101, T47D, SKBR3, BT474, MDA-MB 231 and MDA-MB 436 cell lines. PTK6 and ALT-PTK6 are 407 and 285 bp respectively. β actin is 350bp. 1x of REDTaq Readymix PCR Reaction Mix with MgCI2 (Sigma-Aldrich), sterile distilled water, Forward Primer (1µM), Reverse Primer (1µM), cDNA (250ng/µl) were mixed together before running a RT-PCR reaction with β actin parameters: 35 cycles of denaturing at 95˚C for 30 seconds, primer annealing at 58˚C for 30 seconds and extensions at 72˚C for 45 seconds. The final step was at 72˚C for 10 minutes. The parameters for PTK6 RT-PCR were: 35 cycles of denaturing at 95˚C for 30 seconds, pimer annealing at 63˚C 30 seconds and extensions at 72˚C for 45 seconds and the final step was at 72˚C for 10 minutes. RT-PCR was performed on 3 independent sets of RNA.

5.3.2 Determination of reference genes with GeNORM analysis

Reverse transcriptase PCR (RT-PCR) only allows for detection or absence of gene expression with the endpoint of the experiments visualised as PCR bands and is, at best, semi-quantitative although there is no quantification of the expression levels measured during the exponential phase. Thus quantitative polymerase chain reaction (qPCR) is a better method which has proven to be more precise and makes quantification easier (Bonetta, 2005).

Before beginning analysis of target gene expression, it has become essential to decide the most stable reference genes expressed for all the cell lines used in the experimental conditions. This allows for a reliable qPCR experiment set up that is normalised to these reference genes and is compliant with the Minimum Information for Publication of Quantitative Real Time PCR experiments or the MIQE guidelines (Bustin *et al.*, 2009). This is particularly important when using a set of cell lines with high heterogeneity as is the case with breast cancer cell lines. Often a single reference gene is used for qPCR experiment normalisation, however normalisation against a single gene is considered unreliable due to a greater chance of introducing relatively large errors, whereas increasing the number of reference genes leads to greater resolution and increased accuracy (Kozera and Rapacz, 2013); therefore the optimal number and choice of reference genes needed to be determined (Vandesompele *et al.*, 2002; Bustin *et al.*, 2009).

In order to determine the reference genes to use with the following cell lines; MCF10A, GI101, T47D, SKBR3, BT474, MDA-MB 231 and MDA-MB 436, the GeNORM array kit for 12 reference genes was used (Primer Design). The geNORM kit contains a panel of either 6 or 12 candidate genes that are used to determine the optimal reference gene for the

experimental conditions. The relative expression of these genes is determined with quantitative PCR and the data analysed using the geNORM analysis software called qbase+ provided by Biogazelle. The reference genes included in the kit are shown in Table 2.12 (Chapter 2, section 2.2.16). The qPCRs were performed in duplicate wells for each reference gene and performed twice for control or basal and treated experimental conditions, with 5ng/µl of cDNA loaded in each well, according to the manufactures protocol. Primer Design do not disclose the primer sequences of their GeNORM analysis reference genes therefore once reference genes were determined via GeNORM analysis, primers for these genes of known sequence were designed and purchased from Sigma Aldrich. The qPCR data was analysed using qBase+ software (Biogazelle) as recommended by Primer Design for their GeNORM analysis kit.

The qBase+ software determines which genes to use as well as the optimal number of reference genes to use for the cell lines tested. Data analysis issues a geNORM M value for each of the 12 reference genes which indicates gene stability between the samples (Figure 5.2). The lower the M value the more stable the reference gene is. In addition to an M value, a bar graph indicating a V value was generated (Figure 5.3). This shows the levels of variation in reference gene stability with sequential addition of each candidate gene. This measure is known as ‘pairwise variation V’. The geNORM V value, in conjunction with the generated M values, suggests the optimal number of reference genes to use.

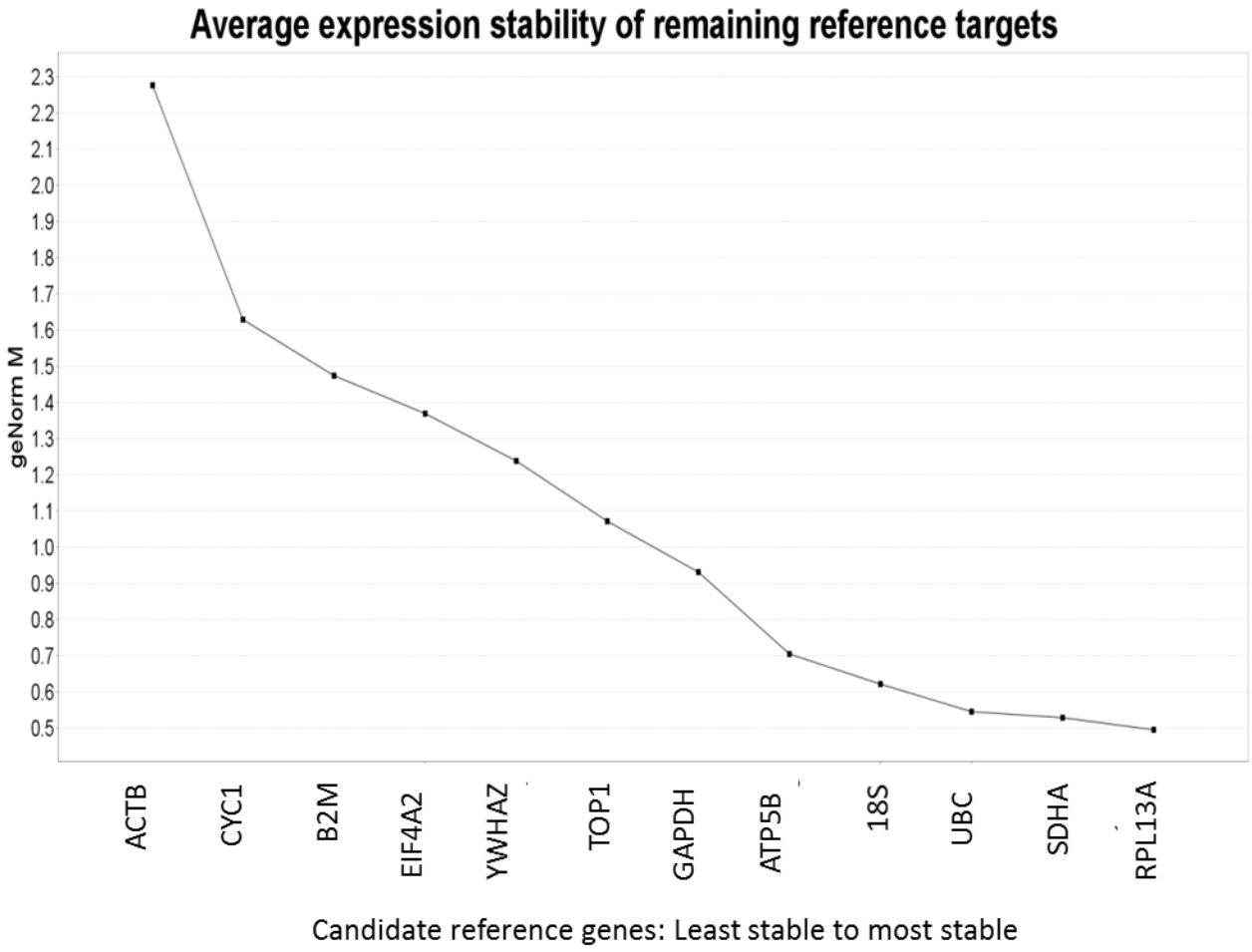

Figure 5.2 GeNORM 12 gene reference kit (Primer Design) was used to assess the stability of expression of 12 reference (housekeeping) genes in breast cancer cell lines. For each cell line, 5ng/µl of cDNA was used in duplicate wells in a 96 well plate and the data analysed using qBase+ software (Biogazelle). The software generated a geNORM M value for each reference gene indicating the stability of each gene. The lower the M value, the more stable the gene. The graph shows the least stable genes to the most stable genes from left to right. The two most stable genes were: *SDHA* and *RPL13A*.

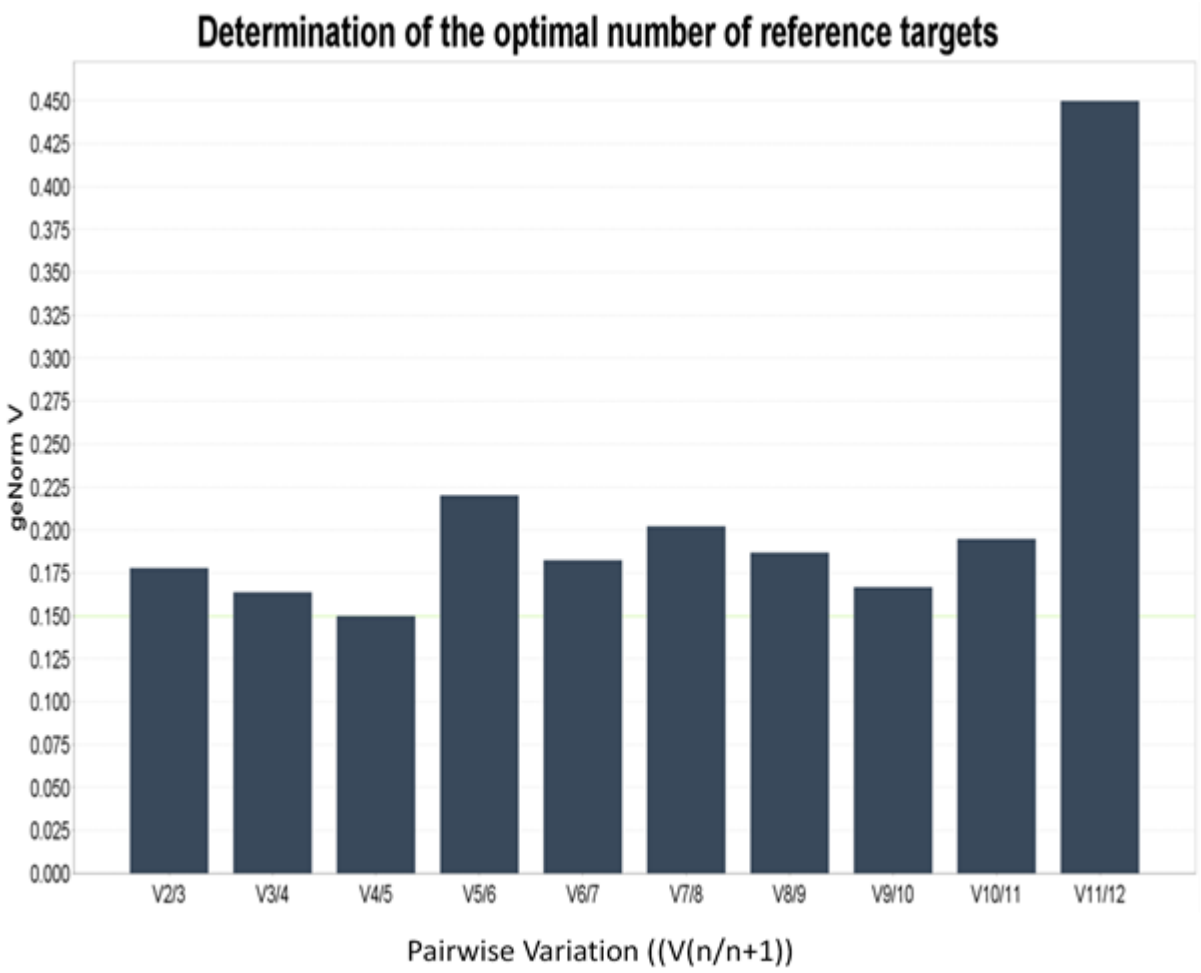

Figure 5.3 GeNORM 12 gene reference kit (Primer Design) was used to determine number of optimal reference genes. For each cell line, 5ng/µl of cDNA was used in duplicate wells in a 96 well plate and the data analysed using qBase+ software (Biogazelle). The software generated a geNORM V value indicating variability between successive sets of genes. A V value of 0.15 or lower indicates the optimal number of reference genes to used (indicated by green line). Optimal number of reference genes to use were 2-4 reference genes.

The qBase+ software recommends that anything below or equal to 1.0 for the value of M indicates a stable gene. The geNORM V value shows average variation of stability between successive genes, with the average geNORM V value of 0.15 or below as the recommended value for deciding the number of reference genes to use. Therefore, the optimal number of 2-4 reference genes to use was indicated and the four most stable reference genes recommended to use are as follows: 18S, UBC, *SDHA* and *RPL13A*. The qbase+ manual

states: “The proposed 0.15 value must not be taken as a too strict cut off” and the number of reference genes was the recommendation, and since the MIQE guidelines suggest at least two reference genes to be used and the use of only one reference gene is not acceptable in addition to the third and fourth most stable genes (UBS and 18S respectively) beginning to incline in the gene stability graph (Figure 5.2); I decided to use the two most stable genes; Succinate Dehydrogenase complex flavoprotein subunit A (*SDHA*) and Ribosomal protein L13a (*RPL13A*) as the reference genes (Bustin *et al.*, 2009; Kałużna, Kuras and Puławska, 2017). The *SDHA* gene encodes a catalytic subunit of the succinate-ubiquinone oxidoreductase complex which is involved in the mitochondrial respiratory chain and the *RPL13A* gene encodes a member of the L13p family of ribosomal proteins.

5.3.3 Determination of *PTK6* and *ALT-PTK6* mRNA expression in breast cancer cell lines and mRNA expression ratios of *ALT-PTK6* to *PTK6* at basal level.

There are no commercially available primers for the *PTK6* or the short isoform *ALT-PTK6* thus custom primers were designed for both transcripts by Primer Design. Primers were designed to specifically detect the full-length isoform, *PTK6*. Primers were also designed that detected the short isoform, *ALT-PTK6*, however due to issues with the primer specificity Primer Design were unable to design primers which only detected the short isoform. Primers that were able to detect the short isoform, were also able to detect the full-length isoform. *ALT-PTK6* expression was therefore determined from subtraction from the full-length values. Previous studies have not used qPCR to evaluate levels of *ptk6* transcripts in breast cancer cell lines, although there are higher *PTK6* to *ALT-PTK6* ratios in prostate cancer cell lines as well as in higher grade prostate tumours compared to normal tissue and low grade tumours

(Brauer *et al.*, 2011). However, within breast cancer tissues, although *ALT-PTK6* transcript levels were not investigated, Brk mRNA expression was detected in 85% of breast tumours and shown to be overexpressed in tumour samples compared to normal mammary tissues (Harvey *et al.*, 2009). To further elucidate the significance of *ALT-PTK6* expression within breast cancer cell lines, I determined ratios of *ALT-PTK6* to *PTK6* under normal growth conditions. In addition, ALT-PTK6 protein expression was determined by western blotting as previously described (Chapter 2, section 2.2.11) with an anti-Brk polyclonal antibody N-Terminal (Abcam). In order to confirm the PCR band sizes of the primers purchased, I performed reverse transcriptase PCR and agarose gel electrophoresis (Figure 5.4). I then performed qPCRs on cDNA from the following breast cancer cell lines: MCF10A, GI101, T47D, SKBR3, BT474, MDA-MB 231 and MDA-MB 436. PrecisionPLUS MasterMix premixed with SYBRgreen (Primer Design) was prepared with either transcript's primer mixes (300nM final concentration) (Primer Design) and RNase/DNase free water per manufacturers protocol. The qPCR was carried out on the Applied Biosystems Quantstudio 7 Flex Real-Time PCR machine. The qPCRs were prepared in duplicate well using three 3 independent sets of RNAs for each cell line. The reference genes used for normalisation were *SDHA* and *RPL13A*. These were determined and validated by geNORM analysis as performed in section 5.3.2. The geNORM analysis shows the number of reference genes and the most stable genes to use for the experimental conditions (Adeola, 2018) It has been suggested use of more than one reference gene as internal control for normalisation might generate more reliable results (Adeola, 2018). qPCR analysis was performed using the average CT (Cycle Threshold) values obtained after each run. This value is determined as the number of cycles required for the fluorescent signal to exceed the background (threshold) levels and is proportional to amount of target gene expressed in the sample. These CT values were first normalised by calculating the difference between gene of interest and reference gene before

determining the ΔCT values which were normalised to control untreated samples (Livak and Schmittgen, 2001). Using this ΔCT value, the relative quantification (RQ) value was obtained. This indicates the amplification of the target gene relative to the untreated samples, which were used as endogenous control for all experimental conditions. Graphs show average relative quantification of either transcript in breast cancer cells, with error bars showing standard deviation. Additionally, mean RQ values for *ALT-PTK6* expression over mean RQ values of *PTK6* only expression (*ALT-PTK6/PTK6*) were determined to show *ALT-PTK6* to *PTK6* ratios in the breast cancer cell lines.

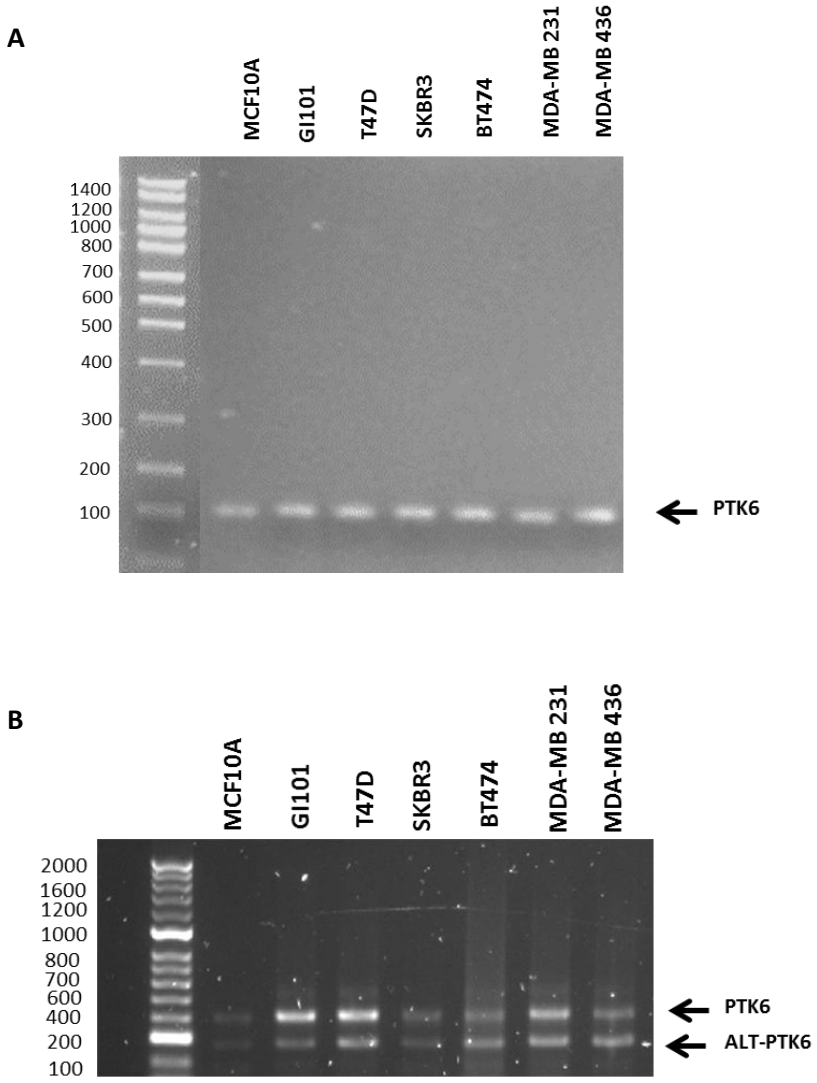

Figure 5.4 Confirmation of A) PTK6 only and B) expression of both transcripts (PTK6 and ALT-PTK6) using custom designed primers. Reverse transcriptase-PCR was performed to detect end point bands using custom designed primers for PTK6 only transcript and primers to detect both isoforms. RNA was extracted using RNeasy Plus Mini Spin Kit (Qiagen), cDNA synthesised using SuperScript II Reverse Transcriptase Kit (Invitrogen) before reverse transcription PCR using REDTaq® ReadyMix™ PCR Reaction Mix (Invitrogen) was performed.

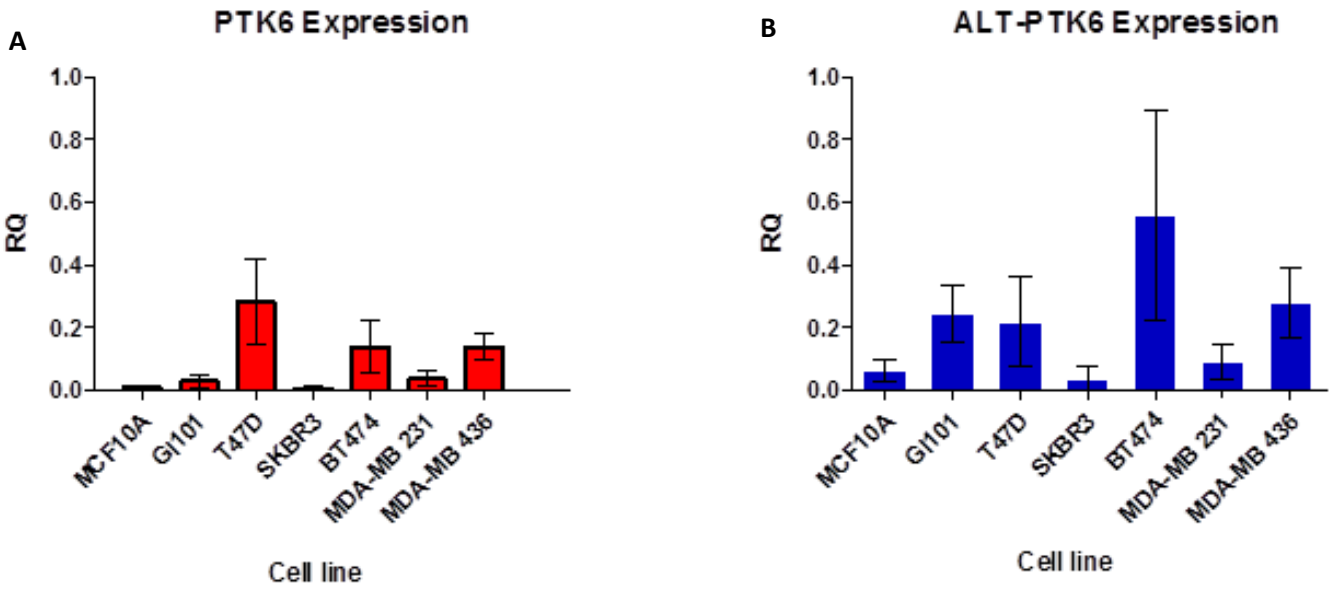

Figure 5.5 Relative expression of PTK6 and ALT-PTK6 is varied between cell lines at basal conditions. PrecisionPLUS MasterMix with ROX at a lower level premixed with SYBRgreen (10µl), primer mix (1µl), RNase/DNase Free water, cDNA (5µl) were mixed. The experimental parameters were 40x cycles of enzyme activation for 2 minutes at 95˚C and denaturation for 10 seconds at 95˚C. Data was analysed by calculating average Cycle Threshold (CT) of both isoforms and normalised to average CT values of reference genes: *SDHA* and *RPL13A*. This gave the delta CT (ΔCT) value which was used to calculate relative quantification (RQ) as follows: $RQ = 2^{-\Delta\Delta CT}$. Figure 5.5A shows relative expression of PTK6 of breast cancer cell lines (ANOVA $F(6,13)=11.16$, $P= 0.0002$). Figure 5.5B shows relative expression for ALT-PTK6 (ANOVA $F(6,13)=4.318$, $P =0.0130$). qPCRs were performed using n=3 independent sets of RNA for all cell lines with error bars representing standard deviation. Statistical variance between cell lines was determined with ANOVA test.

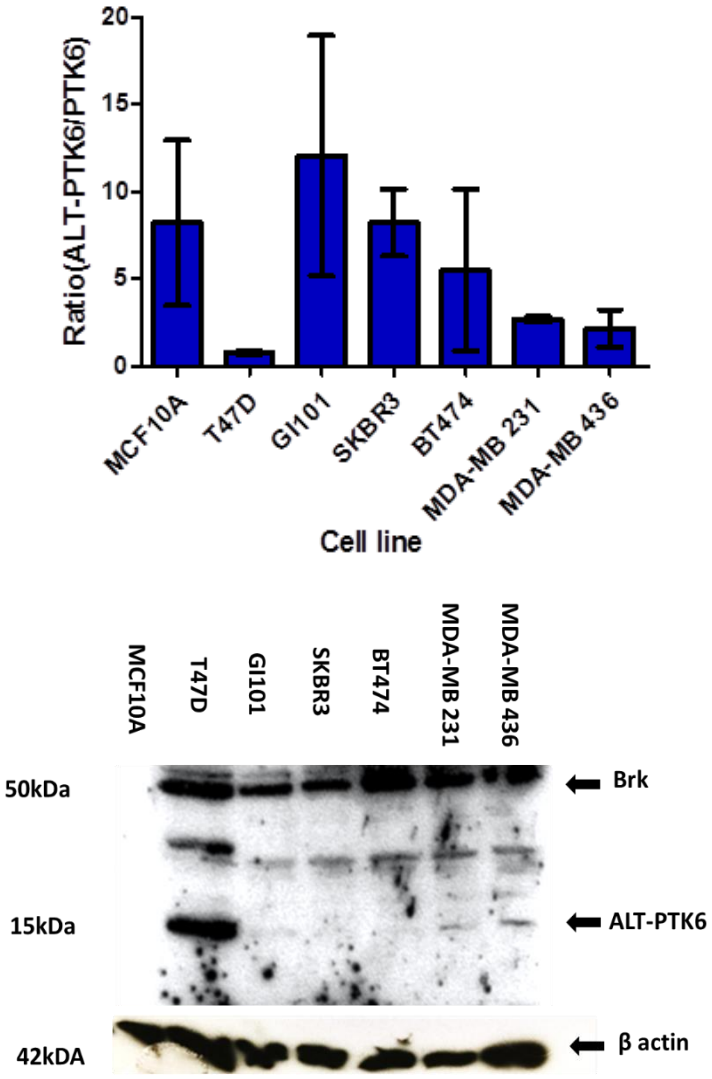

Figure 5.6 Relative ratio of ALT-PTK6 to PTK6 after at basal levels show higher levels of ALT-PTK6 transcript in non-tumourigenic cell line and mostly in hormone positive breast cancer cells. PrecisionPLUS MasterMix with ROX at a lower level premixed with SYBRgreen (10µl), primer mix (1µl), RNase/DNase Free water, cDNA (5µl) were mixed. The experimental parameters were 40x cycles of enzyme activation for 2 minutes at 95˚C and denaturation for 10 seconds at 95˚C. Data was analysed by calculating average Cycle Threshold (CT) of both isoforms and normalised to average CT values of reference genes: *SDHA* and *RPL13A*. This gave the delta CT (ΔCT) value which was used to calculate relative quantification (RQ) as follows: RQ= $2^{-\Delta\Delta CT}$. Results were used to determine mean ratios of *ALT-PTK6/PTK6*. Western blot (n=3) using anti-Brk polyclonal antibody N-Terminal (Abcam) was performed to determine ALT-PTK6 protein expression as well as Brk expression levels. qPCRs were performed using n=3 independent sets of RNA for all cell lines with error bars representing standard deviation. ANOVA statistical analysis was carried out to demonstrate variation (ANOVA $F(6,14)=3.601$, $P=0.023$).

Relative expression of the *PTK6* transcript (Figure 5.4A) and *ALT-PTK6* (Figure 5.5B) show variation between the cell lines. The T47D cell line showed the highest mean relative expression (RQ=0.18 +/- 0.05 S.D) with the HER2 positive cell line SKBR3 (RQ=0.003 +/- 0.002 S.D) showing the least relative expression of *PTK6* full-length transcript. Statistical analysis with ANOVA testing between the cell lines (ANOVA $F(6,13)=11.16$, $P= 0.0002$) showed highly significant variation of *PTK6* between all the breast cancer cell lines. mRNA expression of *ALT-PTK6* was highest in SKBR3 with an RQ value of 0.15 (+/- 0.02 S.D) compared to the lowest RQ value of 0.018 +/- 0.012 S.D for the MCF10A cell line. Statistical analysis with ANOVA testing between the cell lines showed significant variation of expression (ANOVA $F(6,13)=4.318$, $P =0.0130$). For *PTK6* transcript, the cell lines with high RQ values (T47D, MDA-MB 436, BT474) all show high or moderate Brk expression at the protein level in comparison to GI101, MDA-MB 231 and MCF10A which show low levels of Brk protein expression.

Overall, the cell lines with the most expression of the full-length form were the luminal A subtype cell line T47D, HER2 positive cell line BT474 and the triple negative cell line MDA-MB 436. The cell lines with highest *ALT-PTK6* expression were BT474, MDA-MB 436, GI101 and T47D. It appears expression of *ALT-PTK6* transcript may not be cell type specific, nor limited to cancerous cells and is expressed at varying levels in the breast cancer cell lines.

Figure 5.6 shows *ALT-PTK6/PTK6* ratios at basal levels for the breast cancer cell lines. Overall, cell lines with higher *ALT-PTK6* to *PTK6* ratio were MCF10A, GI101 and the HER2 positive cell lines (SKBR3 and BT474). In comparison, lower ratios were observed in the T47D cell line and the two triple negative cell lines (MDA-MB 231 and MDA-MB 436). ANOVA testing shows significant variation in in *ALT-PTK6/PTK6* ratios (ANOVA $F(6,14)=3.601$, $P =0.023$). Protein expression of *ALT-PTK6* was confirmed in the T47D cell line and was detected at low levels in MDA-MB 231 and MDA-MB 436 cell lines.

5.3.4 Determination of *ALT-PTK6* to *PTK6* mRNA expression ratios in breast cancer cell lines after Brk inhibition.

Transcript levels of *ptk6* isoforms have not been investigated especially in response to Brk inhibition within breast cancer cell lines. It has previously been suggested *ptk6* may potentially regulate its own expression due to its impact on alternative splicing via its substrates that include a number of RNA binding proteins such as Sam68, SLM1 and SLM2 as well as polypyrimidine tract-binding protein-associated splicing factor (PSF) which are all involved in regulating splicing (Derry et al., 2000; Haegebarth et al., 2004; Lukong, Huot and Richard, 2009; Brauer et al., 2011). Thus, I next sought to assess whether expression of the *ptk6* variants at the mRNA level are affected with inhibition of Brk after treatment with 5μM of Compound 4f. Due to inhibition of Brk, it is expected there will be a reduction in the full length *PTK6* transcript, which may favour up-regulation of the shorter isoform, *ALT-PTK6*. Additionally, ratios of *ALT-PTK6/PTK6* transcripts within the breast cancer cell lines in response to Brk inhibition were calculated. Ratios were determined within the control (untreated) cells as well as the treated cells.

Cells were seeded at 200,000 cells per well in a 6 well plate and treated with 5μM of the Brk inhibitor. Cell lysates were taken at the following time points along with untreated controls: 0, 2 hours, 4 hours, 8 hours, 24 hours and 48 hours. For RNA extraction, the RNeasy Mini Spin Column kit from Qiagen was used to elute high quality and yield of RNA free of contamination as described in Materials and Methods (Chapter 2, section 2.2.16). cDNA was prepared using SuperScript II Reverse Transcriptase (Invitrogen) kit and PrecisionPLUS MasterMix with ROX at a lower level premixed with SYBRgreen (Primer Design) was prepared with primer mixes for either transcript along with the primers for two reference

genes, *SDHA* and *RPL13A*. Each master mix for each gene was pipetted in duplicate in a 96 well plate and 5µl of cDNA was pipetted using sterile filter tips as per manufacturer's protocol. The Applied Biosystems Quantstudio 7 Flex Real-Time PCR machine was used, and qPCRs were carried out using 3 sets of independent RNA. Data was analysed using the QuantStudio™ Software V1.3—for QuantStudio™ 6 and 7 Flex and ViiA™ 7 Real-Time PCR software (Applied Biosystems).

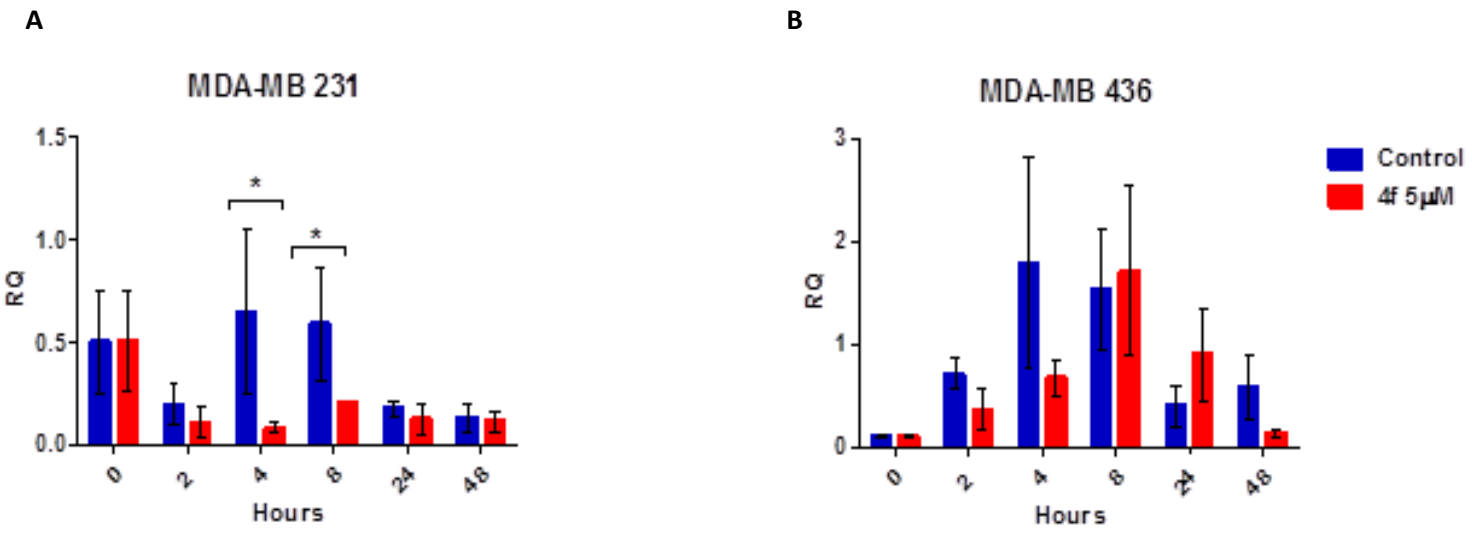

Figure 5.7 qPCR showing relative mRNA expression of PTK6 after compound 4f treatment shows decrease in MDA-MB 231 cells and little change in MDA-MB 436 cells. Cells were seeded at 200,000 cells per well in a 6 well plate and treated with compound 4f (5µM). Cells were harvested for RNA at the following time points along with untreated controls: 0, 2 hours, 4 hours, 8 hours, 24 hours and 48 hours. cDNA was prepared using SuperScript II reverse transcriptase. PrecisionPLUS MasterMix with ROX at a lower level premixed with SYBRgreen (10µl), primer mix (1µl), RNase/DNase Free water, cDNA (5µl) were mixed. The experimental parameters were 40x cycles of enzyme activation for 2 minutes at 95˚C and denaturation for 10 seconds at 95˚C. Data was analysed by calculating average Cycle Threshold (CT) of both isoforms and normalised to average CT values of reference genes: *SDHA* and *RPL13A*. This gave the delta CT (ΔCT) value which was used to calculate relative quantification (RQ) as follows: RQ= 2-ΔΔCT. Results show PTK6 relative expression in control, untreated (blue) and treated cells (red) in MDA-MB 231 cell line (A) and MDA-MB 436 cell line (B). qPCRs were performed using 3 independent sets of RNA for all cell lines with error bars representing standard deviation. ANOVA statistical analysis was performed to demonstrate variation within control cells as well as within treated groups. Students T Test was used to assess significant difference between each control and treated time points, * $P<0.05$.

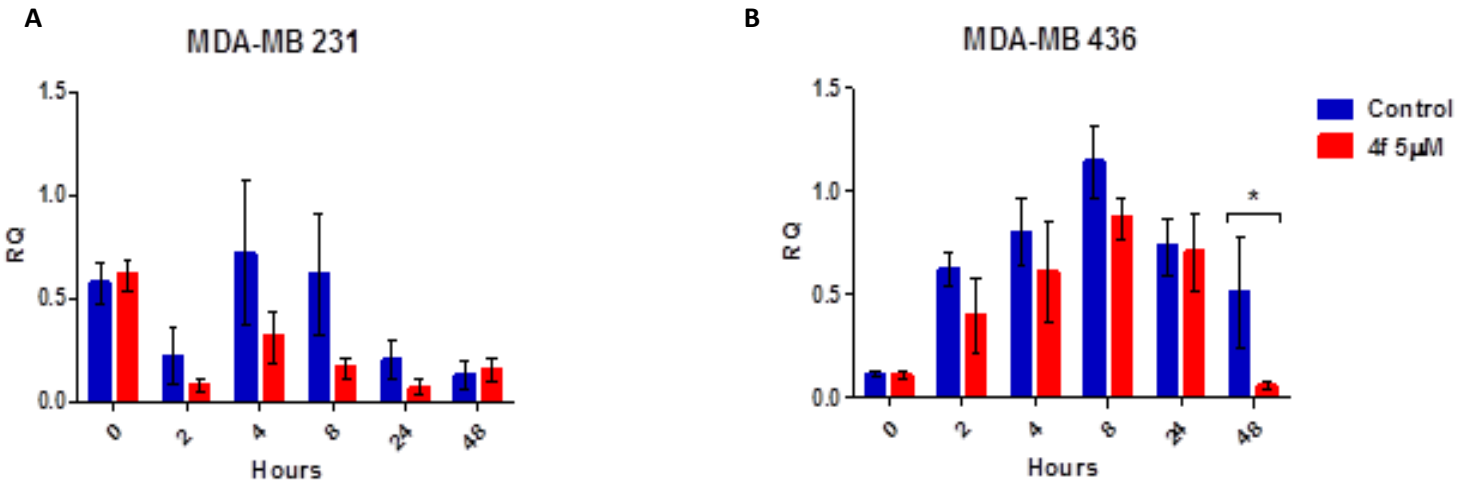

Figure 5.8 qPCR showing relative mRNA expression of ALT-PTK6 after compound 4f treatment shows minor change in MDA-MB 231 cells and a reduction in MDA-MB 436 at 48 hours. Cells were seeded at 200,000 cells per well in a 6 well plate and treated with compound 4f (5µM). Cells were harvested for RNA at the following time points along with untreated controls: 0, 2 hours, 4 hours, 8 hours, 24 hours and 48 hours. cDNA was prepared using SuperScript II reverse transcriptase. PrecisionPLUS MasterMix with ROX at a lower level premixed with SYBRgreen (10µl), primer mix (1µl), RNase/DNase Free water, cDNA (5µl) were mixed. The experimental parameters were 40x cycles of enzyme activation for 2 minutes at 95˚C and denaturation for 10 seconds at 95˚C. Data was analysed by calculating average Cycle Threshold (CT) of both isoforms and normalised to average CT values of reference genes: *SDHA* and *RPL13A*. This gave the delta CT (ΔCT) value which was used to calculate relative quantification (RQ) as follows: $RQ = 2^{-\Delta\Delta CT}$. Results show PTK6 relative expression in control, untreated (blue) and treated cells (red) in MDA-MB 231 cell line (A) and MDA-MB 436 cell line (B). qPCRs were performed using 3 independent sets of RNA for all cell lines with error bars representing standard deviation. ANOVA statistical analysis was performed to demonstrate variation within control cells as well as within treated groups. Students T Test was used to assess significant difference between each control and treated time points, * $P<0.05$. qPCRs were performed using 3 independent sets of RNA for all cell lines with error bars representing standard deviation.

The triple negative cell line MDA-MB 231 *PTK6* mRNA expression shows an increase over time before decreasing at 24 and 48 hours (Figure 5.7A) within the untreated control group (ANOVA F(4,10) =3.699, *P* = 0.042). There seems to be no significant difference in *PTK6* expression within the treated group (ANOVA F(4,10) =0.74, *P* = 0.586). Nonetheless, there is statistically significant reduction observed at 4 and 8 hours post treatment with compound 4f when compared to untreated control cells at the same time points. Overall, MDA-MB 231 cells treated with compound 4f show lower levels of *PTK6* mRNA expression overtime compared to untreated control cells.

Within MDA-MB 436 cells, *PTK6* expression shows a similar pattern within the control group and treated group (Figure 5.7B). Overall, there seems to be no statistical difference within the control group (ANOVA F(4,10) =3.213, *P* = 0.061). There was greater statistically significant difference within the treated group (ANOVA F(4,10) =4.409, *P* = 0.026). There were reduced level of *PTK6* mRNA expression compared to control cells at 2 and 4 and 48 hour time points, although this is not statistically significant.

ALT-PTK6 mRNA expression decreases over time post treatment compared to control cells in the MDA-MB 231 cell line (Figure 5.8A). Although there was no statistically significant reduction within the treated group (ANOVA F(4,10) =1.589, *P* = 0.251), overall there are reduced levels of *ALT-PTK6* compared to control cells. mRNA expression levels of *ALT-PTK6* in MDA-MB 436 cells show a significant difference within the treated group (ANOVA F(4,10) =10.593, *P* = 0.001) as seen in Figure 5.8B. Overall there was a reduction in expression in treated cells compared to control cells, with statistically significant difference at 48 hours post treatment.

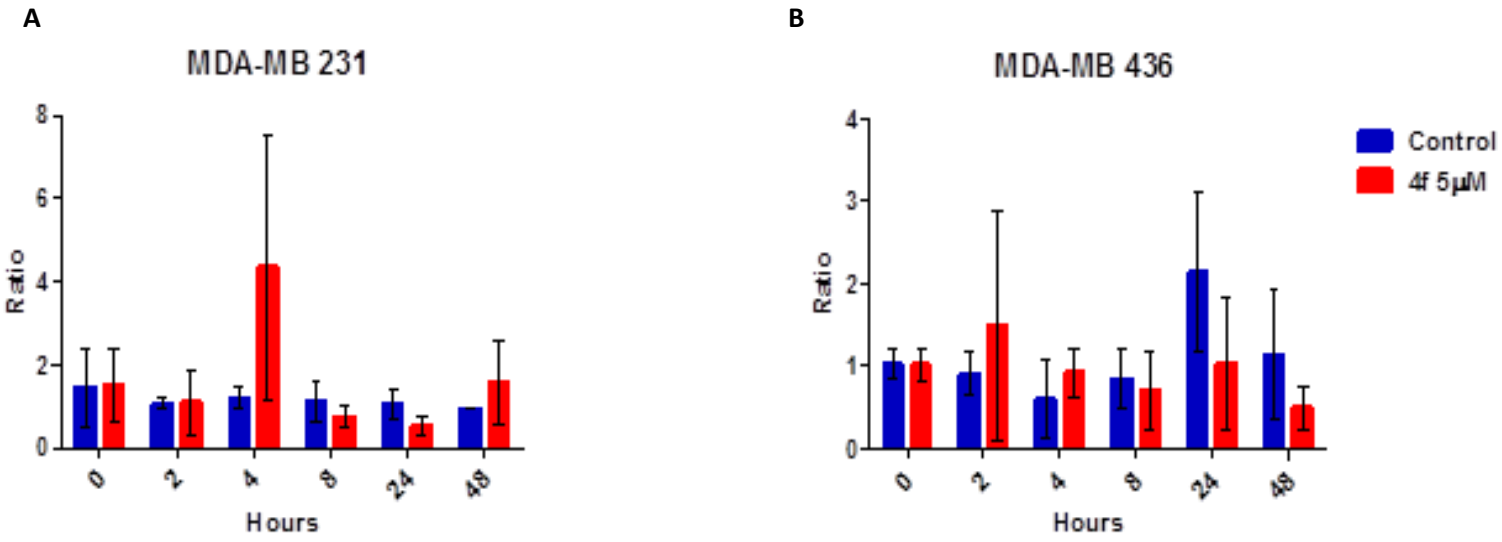

Figure 5.9 Relative expression ratios of ALT-PTK6 to PTK6 after compound 4f treatment show little difference compared to control ratios. Cells were seeded at 200,000 cells per well in a 6 well plate and treated with compound 4f (5µM). Cells were harvested for RNA at the following time points along with untreated controls: 0, 2 hours, 4 hours, 8 hours, 24 hours and 48 hours. cDNA was prepared using SuperScript II reverse transcriptase. PrecisionPLUS MasterMix with ROX at a lower level premixed with SYBRgreen (10µl), primer mix (1µl), RNase/DNase Free water, cDNA (5µl) were mixed. The experimental parameters were 40x cycles of enzyme activation for 2 minutes at 95˚C and denaturation for 10 seconds at 95˚C. Data was analysed by calculating average Cycle Threshold (CT) of both isoforms and normalised to average CT values of reference genes: *SDHA* and *RPL13A*. This gave the delta CT (ΔCT) value which was used to calculate relative quantification (RQ) as follows: RQ= 2-ΔΔCT. Ratios were determined from mean RQ values of ALT-PTK6/PTK6. Results show ALT-PTK6/PTK6 ratios in control, untreated (blue) and treated cells (red) in MDA-MB 231 cell line (A) and MDA-MB 436 cell line (B).. qPCRs were performed using 3 independent sets of RNA for all cell lines with error bars representing standard deviation. ANOVA statistical analysis was performed to demonstrate variation within control cells as well as within treated groups. Students T Test was used to assess significant difference between each control and treated time points, * $P<0.05$.

ALT-PTK6 to *PTK6* ratios were relatively unchanged after compound 4f treatment compared to control cells in the MDA-MB 231 cell line (Figure 5.9A). Although there was higher ALT-*PTK6* to *PTK6* ratio at 4 hours post treatment, overall no statistically significant variance was observed within the control group (ANOVA $F(5,12) = 0.417$, $P = 0.828$) and treated group (ANOVA $F(5,12) = 2.734$, $P = 0.071$).

Within the MDA-MB 436 cell line, ratio of *ALT-PTK6* to *PTK6* ratios were also relatively unchanged after compound 4f treatment compared to control cells (Figure 5.9B). There were no statistically significant variance shown in *ALT-PTK6 /PTK6* ratios within control group (ANOVA $F(5,12) = 2.577$, $P = 0.083$) and treated group (ANOVA $F(5,12) = 0.705$, $P = 0.631$).

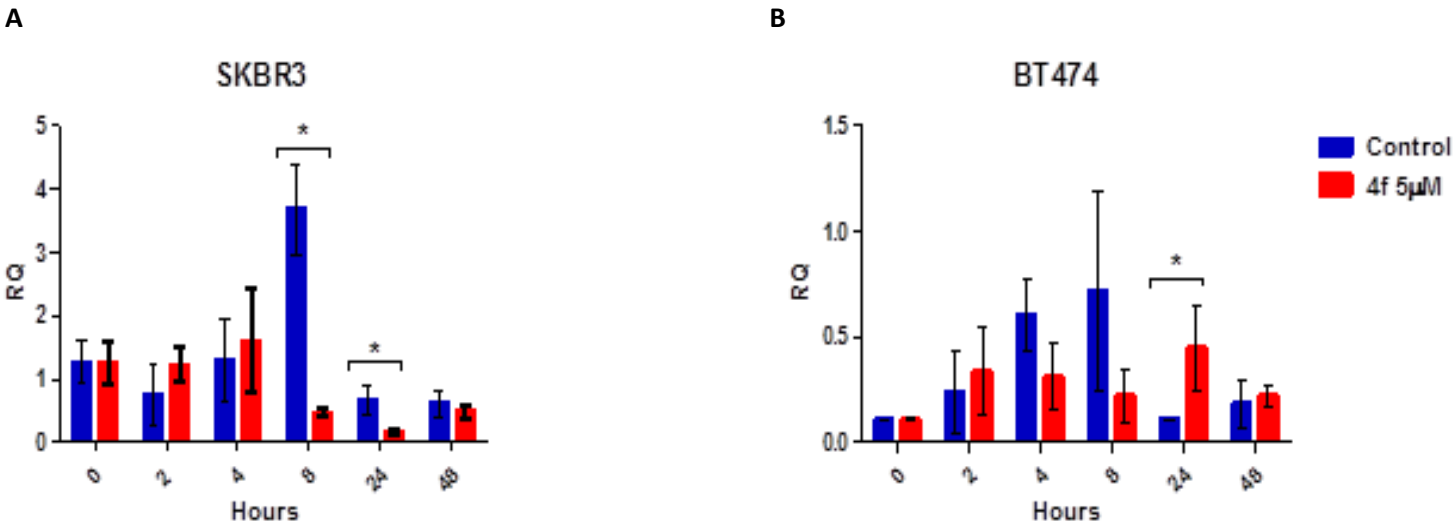

Figure 5.10 qPCR showing relative mRNA expression of PTK6 after compound 4f treatment shows decrease in SKBR3 cells and increase in BT474 cells. Cells were seeded at 200,000 cells per well in a 6 well plate and treated with compound 4f (5µM). Cells were harvested for RNA at the following time points along with untreated controls: 0, 2 hours, 4 hours, 8 hours, 24 hours and 48 hours. cDNA was prepared using SuperScript II reverse transcriptase. PrecisionPLUS MasterMix with ROX at a lower level premixed with SYBRgreen (10µl), primer mix (1µl), RNase/DNase Free water, cDNA (5µl) were mixed. The experimental parameters were 40x cycles of enzyme activation for 2 minutes at 95˚C and denaturation for 10 seconds at 95˚C. Data was analysed by calculating average Cycle Threshold (CT) of both isoforms and normalised to average CT values of reference genes: *SDHA* and *RPL13A*. This gave the delta CT (ΔCT) value which was used to calculate relative quantification (RQ) as follows: RQ= 2-ΔΔCT. Results show PTK6 relative expression in control, untreated (blue) and treated cells (red) in SKBR3 cell line (A) and BT474 cell line (B). qPCRs were performed using 3 independent sets of RNA for all cell lines with error bars representing standard deviation. ANOVA statistical analysis was performed to demonstrate variation within control cells as well as within treated groups. Students T Test was used to assess significant difference between each control and treated time points, * P<0.05.

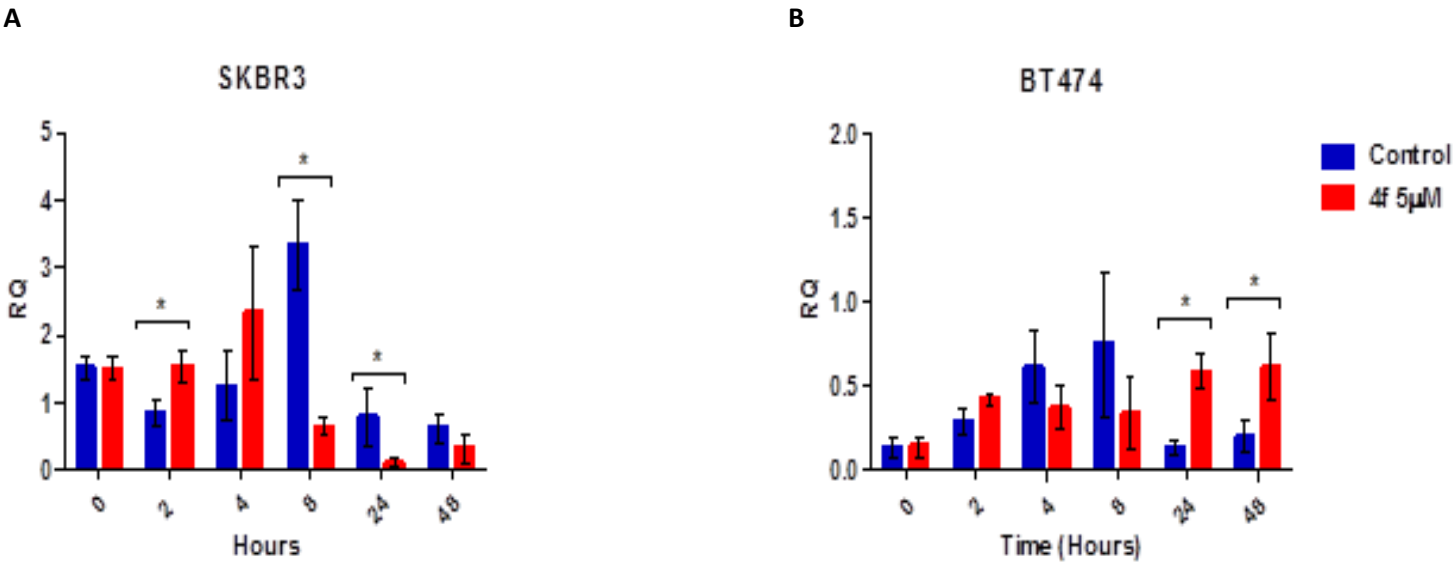

Figure 5.11 qPCR showing relative mRNA expression of ALT-PTK6 after compound 4f treatment shows overall reduction in SKBR3 cells and increase in BT474 cells. Cells were seeded at 200,000 cells per well in a 6 well plate and treated with compound 4f (5µM). Cells were harvested for RNA at the following time points along with untreated controls: 0, 2 hours, 4 hours, 8 hours, 24 hours and 48 hours. cDNA was prepared using SuperScript II reverse transcriptase. PrecisionPLUS MasterMix with ROX at a lower level premixed with SYBRgreen (10µl), primer mix (1µl), RNase/DNase Free water, cDNA (5µl) were mixed. The experimental parameters were 40x cycles of enzyme activation for 2 minutes at 95˚C and denaturation for 10 seconds at 95˚C. Data was analysed by calculating average Cycle Threshold (CT) of both isoforms and normalised to average CT values of reference genes: *SDHA* and *RPL13A*. This gave the delta CT (ΔCT) value which was used to calculate relative quantification (RQ) as follows: RQ= 2-ΔΔCT. Results show PTK6 relative expression in control, untreated (blue) and treated cells (red) in SKBR3 cell line (A) and BT474 cell line (B). qPCRs were performed using 3 independent sets of RNA for all cell lines with error bars representing standard deviation. ANOVA statistical analysis was performed to demonstrate variation within control cells as well as within treated groups. Students T Test was used to assess significant difference between each control and treated time points, * P<0.05.

PTK6 expression in SKBR3 cell line (Figure 5.10A) showed a marked decrease at 8 and 24 hours post treatment compared to control cells ($P<0.05$). Overall there was a clear decrease in *PTK6* expression over time in response to compound 4f treatment (ANOVA $F(4,10) = 7.282$, $P = 0.005$).

BT474 cell line showed an increase in relative *PTK6* expression (Figure 5.10B) levels at 2,4 and 8 hours within the control group before decreasing at 24 and 48 hours (ANOVA $F(4,10) = 3.814$, $P = 0.039$). Overall, there was significant induction in *PTK6* expression at 24-hour post treatment ($P<0.05$) compared to control cells with little change at other time points.

Expression levels of *ALT-PTK6* transcript were significantly higher within in the SKBR3 cell line (Figure 5.11A) at 2 hours post treatment compared to control cells; however overall there was reduction with statistically significant difference at 8 and 24 hours post treatment ($P<0.05$). On the other hand, *ALT-PTK6* expression increased overtime in response to Brk inhibition within the BT474 cell line (Figure 5.11B), with significant difference observed at 24 and 48 hours post treatment compared to control cells ($P<0.05$). ANOVA statistical analysis does not show statistical difference within the treated group time points (ANOVA $F(4,10) = 2.092$, $P = 0.157$).

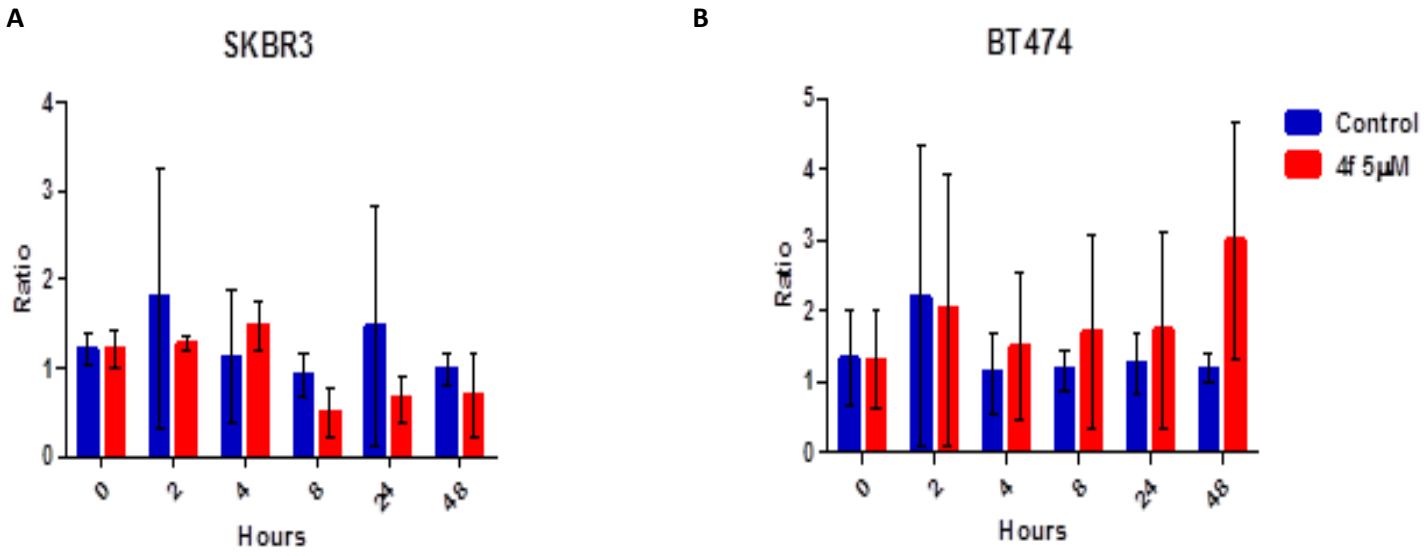

Figure 5.12 Relative expression ratios of ALT-PTK6 to PTK6 after compound 4f treatment are unchanged compared to control in HER2 positive breast cancer cell lines. Cells were seeded at 200,000 cells per well in a 6 well plate and treated with compound 4f (5µM). Cells were harvested for RNA at the following time points along with untreated controls: 0, 2 hours, 4 hours, 8 hours, 24 hours and 48 hours. cDNA was prepared using SuperScript II reverse transcriptase. PrecisionPLUS MasterMix with ROX at a lower level premixed with SYBRgreen (10µl), primer mix (1µl), RNase/DNase Free water, cDNA (5µl) were mixed. The experimental parameters were 40x cycles of enzyme activation for 2 minutes at 95˚C and denaturation for 10 seconds at 95˚C. Data was analysed as previously described and results were used to determine mean ratios of ALT-PTK6 over PTK6. Results show ALT-PTK6/PTK6 ratios in control, untreated (blue) and treated cells (red) in SKBR3 cell line (A) and BT474 cell line (B). qPCRs were performed using 3 independent sets of RNA for all cell lines with error bars representing standard deviation. ANOVA statistical analysis was carried out to demonstrate variation within control and treated groups. Students T Test was used to assess significant difference between each control and treated time points, *P<0.05.

Within the HER2 positive cell line, SKBR3 no statistically significant difference in *ALT-PTK6* to *PTK6* ratios (Figure 5.12A) were observed between control and treated groups. However, overall there were reduced ratios of *ALT-PTK6* to *PTK6* in the treated group (2, 8, 24 and 48 hours post treatment) compared to control cells.

Little difference is observed in *ALT-PTK6* to *PTK6* ratios after compound 4f treatment compared to control cells in BT474 cell line (Figure 5.12B). There are no statistically significant variance observed within the control (ANOVA $F(5,12) = 0.556$, $P = 0.732$) and treated groups (ANOVA $F(5,12) = 0.534$, $P = 0.747$). Although not significant, there appear to be higher *ALT-PTK6* levels in this cell line after compound 4f.

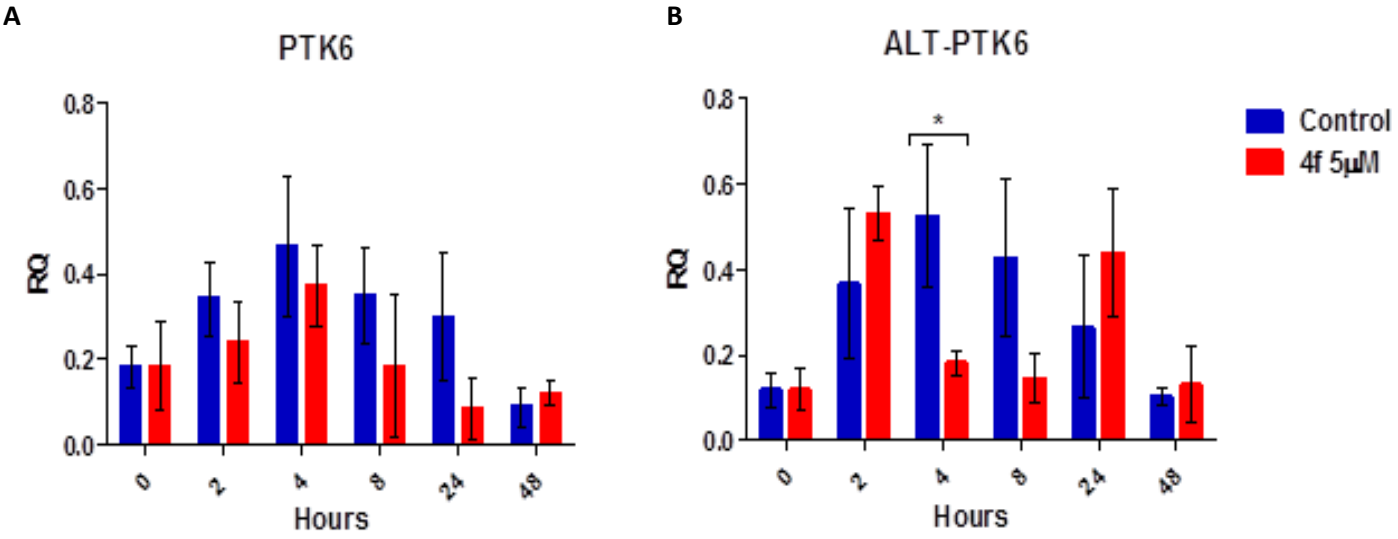

Figure 5.13 qPCR showing A) unchanged relative mRNA expression of PTK6 in T47D cells and B) reduction at 4 hours post treatment in ALT-PTK6 expression (B). Cells were seeded at 200,000 cells per well in a 6 well plate and treated with compound 4f (5µM). Cells were harvested for RNA at the following time points along with untreated controls: 0, 2 hours, 4 hours, 8 hours, 24 hours and 48 hours. cDNA was prepared using SuperScript II reverse transcriptase. PrecisionPLUS MasterMix with ROX at a lower level premixed with SYBRgreen (10µl), primer mix (1µl), RNase/DNase Free water, cDNA (5µl) were mixed. The experimental parameters were 40x cycles of enzyme activation for 2 minutes at 95˚C and denaturation for 10 seconds at 95˚C. Data was analysed by calculating average Cycle Threshold (CT) of both isoforms and normalised to average CT values of reference genes: *SDHA* and *RPL13A*. This gave the delta CT (ΔCT) value which was used to calculate relative quantification (RQ) as follows: $RQ = 2^{-\Delta\Delta CT}$. Results show PTK6 (A) expression and ALT-PTK6 (B) expression in control (blue) and treated cells (red). qPCRs were performed using 3 independent sets of RNA for all cell lines with error bars representing standard deviation. ANOVA statistical analysis was carried out to demonstrate variation within control and treated groups. Students T Test was used to assess significant difference between control and treated time points, $*P<0.05$.

T47D cells showed moderate increase in *PTK6* expression after 4 hours post treatment compared to 0 and 2 hours but began to gradually reduce over time compared to control cells (Figure 5.13A). Statistically *PTK6* expression within the treated group (ANOVA $F(4,10) = 8.692$, $P = 0.003$) showed significant difference. *ALT-PTK6* expression showed there was a significant difference within the treated group as seen in Figure 5.14B (ANOVA $F(4,10) = 15.27$, $P = 0.0002$). mRNA Expression, although was increased initially (2 hours post treatment), it began to decline over time (4 and 8 hours). The main statistical difference showed reduction at 4 hours ($P<0.05$) post treatment compared to control samples.

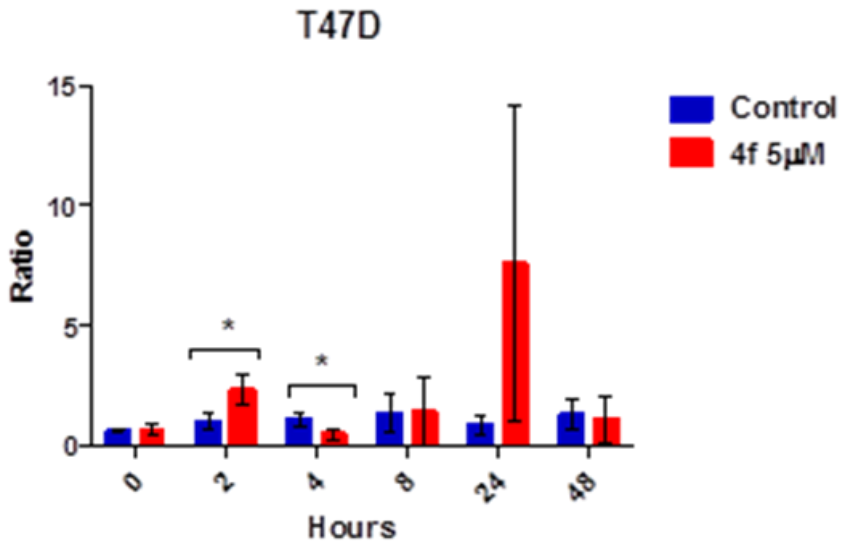

Figure 5.14 Relative expression ratios of ALT-PTK6 to PTK6 after compound 4f treatment show some variation. Cells were seeded at 200,000 cells per well in a 6 well plate and treated with compound 4f (5µM). Cells were harvested for RNA at the following time points along with untreated controls: 0, 2 hours, 4 hours, 8 hours, 24 hours and 48 hours. cDNA was prepared using SuperScript II reverse transcriptase. PrecisionPLUS MasterMix with ROX at a lower level premixed with SYBRgreen (10µl), primer mix (1µl), RNase/DNase Free water, cDNA (5µl) were mixed. The experimental parameters were 40x cycles of enzyme activation for 2 minutes at 95˚C and denaturation for 10 seconds at 95˚C. Data was analysed by calculating average Cycle Threshold (CT) of both isoforms and normalised to average CT values of reference genes: *SDHA* and *RPL13A*. This gave the delta CT (ΔCT) value which was used to calculate relative quantification (RQ) as follows: RQ= 2-ΔΔCT. The results were used to determine mean ratios of ALT-PTK6 over PTK6. Results show ALT-PTK6/PTK6 mRNA ratios for T47D cell line. qPCRs were performed using 3 independent sets of RNA for all cell lines with error bars representing standard deviation. ANOVA statistical analysis was carried out to demonstrate variation within control and treated groups. Students T Test was used to assess significant difference between each control and treated time points, *P<0.05.

Figure 5.14 showed the T47D cell line had no statistically significant variance in *ALT-PTK6* to *PTK6* ratios within the control group (ANOVA F(5,12) =0.999, *P* = 0.459) as well as no statistically significant variance within treated group (ANOVA F(5,12) =2.797, *P*= 0.067). However, *ALT-PTK6* to *PTK6* ratios were initially higher at 2 hours post treatment with compound 4f, before significantly decreasing at 4 hours post treatment (*P*<0.05).

5.3.5 mRNA expression of both isoforms and *ALT-PTK6* to *PTK6* ratios in breast in breast cancer cell lines after Taxol and Doxorubicin treatment (5μM).

It is worth investigating the alterations in *PTK6* and *ALT-PTK6* transcript levels in response to chemotherapeutic agents because as previously mentioned, breast cancer treatment is heavily chemotherapy based and thus potential effect on both isoforms in response to common chemotherapy agents, Paclitaxel/Taxol (Tax) and Doxorubicin (Dox) needs to be examined. Taxol functions as a taxane which are a group of chemotherapy agents that disrupt microtubule formation leading to arrest in mitosis (reviewed in Weaver, 2014). These have been used as first line treatment for triple negative breast cancer (TNBC) subtypes of which MDA-MB 231 and MDA-MB 436 cell lines are representative of (reviewed in Mustacchi and De Laurentiis, 2015). Doxorubicin, an anthracycline, causes DNA intercalation and also disrupts topoisomerase II mediated DNA repair eventually leading to DNA damage and apoptosis (reviewed in Thorn *et al.*, 2011). Doxorubicin has shown to be effective in TNBC and there is also evidence for using both chemotherapy drugs in combination therapy for triple negative breast cancers (reviewed in Isakoff, 2010).

The triple negative breast cancer cell lines, MDA-MB 231 and MDA-MB 436 were seeded as before and treated with either 5μM of Taxol or Doxorubicin. For RNA extraction, the RNeasy Mini Spin Column kit from Qiagen was used to elute high quality and yield of RNA free of contamination as described in Materials and Methods (Chapter 2, section 2.2.16). cDNA was prepared using SuperScript II Reverse Transcriptase (Invitrogen) kit and qPCR performed using PrecisionPLUS MasterMix with ROX at a lower level premixed with SYBRgreen (Primer Design) with primer mixes for either transcript along with the primers for two reference genes, *SDHA* and *RPL13A*. Each master mix for each gene was pipetted in duplicate in a 96 well plate and 5μl of cDNA was pipetted using sterile filter tips as per manufacturer's protocol. The Applied Biosystems Quantstudio 7 Flex Real-Time PCR machine was used, and qPCRs were carried out using 3 sets of independent RNA. Data was analysed using the QuantStudio™ Software V1.3—for QuantStudio™ 6 and 7 Flex and ViiA™ 7 Real-Time PCR software (Applied Biosystems). Ratios of *ALT-PTK6* to *PTK6* transcripts within the breast cancer cell lines in response to Taxol or Doxorubicin were also calculated.

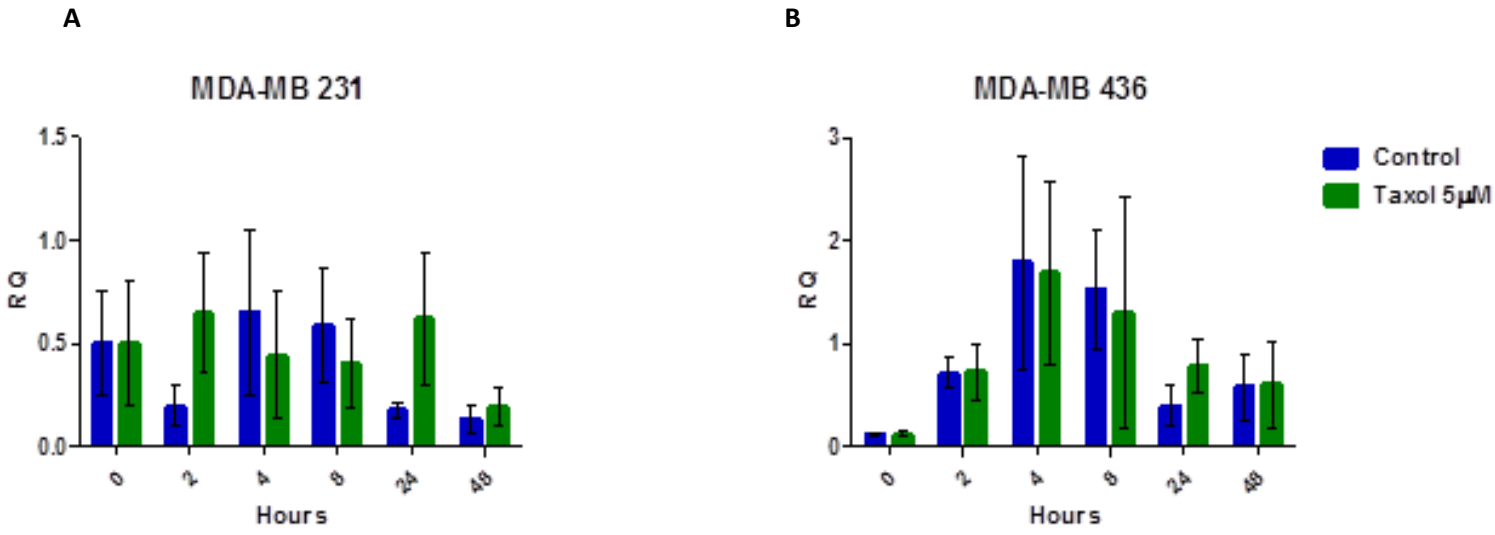

Figure 5.15 No significant change in PTK6 expression in response to Taxol (5µM) treatment in triple negative breast cancer cell lines. Cells were seeded at 200,000 cells per well in a 6 well plate and treated with Taxol (5µM). Cells were harvested for RNA at the following time points along with untreated controls: 0, 2 hours, 4 hours, 8 hours, 24 hours and 48 hours. cDNA was prepared using SuperScript II reverse transcriptase. PrecisionPLUS MasterMix with ROX at a lower level premixed with SYBRgreen (10µl), primer mix (1µl), RNase/DNase Free water, cDNA (5µl) were mixed. The experimental parameters were 40x cycles of enzyme activation for 2 minutes at 95˚C and denaturation for 10 seconds at 95˚C. Data was analysed by calculating average Cycle Threshold (CT) of both isoforms and normalised to average CT values of reference genes: *SDHA* and *RPL13A*. This gave the delta CT (ΔCT) value which was used to calculate relative quantification (RQ) as follows: RQ= 2-ΔΔCT. Results show PTK6 relative expression in control, untreated (blue) and treated cells (green) in MDA-MB 231 cell line (A) and MDA-MB 436 cell line (B). qPCRs were performed using 3 independent sets of RNA for all cell lines with error bars representing standard deviation. ANOVA statistical analysis was performed to demonstrate variation within control cells as well as within treated groups. Students T Test was used to assess significant difference between each control and treated time points, * $P<0.05$.

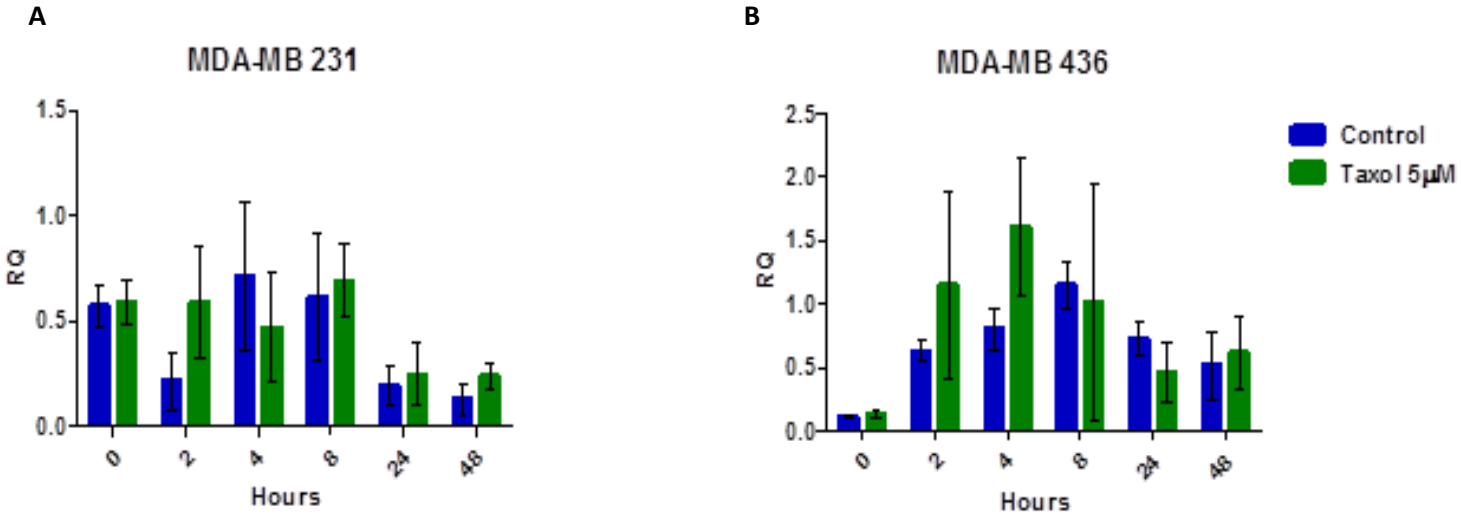

Figure 5.16 No significant change in expression of ALT-PTK6 in response to Taxol (5µM) treatment in triple negative breast cancer cell lines. Cells were seeded at 200,000 cells per well in a 6 well plate and treated with Taxol (5µM). Cells were harvested for RNA at the following time points along with untreated controls: 0, 2 hours, 4 hours, 8 hours, 24 hours and 48 hours. cDNA was prepared using SuperScript II reverse transcriptase. PrecisionPLUS MasterMix with ROX at a lower level premixed with SYBRgreen (10µl), primer mix (1µl), RNase/DNase Free water, cDNA (5µl) were mixed. The experimental parameters were 40x cycles of enzyme activation for 2 minutes at 95˚C and denaturation for 10 seconds at 95˚C. Data was analysed by calculating average Cycle Threshold (CT) of both isoforms and normalised to average CT values of reference genes: *SDHA* and *RPL13A*. This gave the delta CT (ΔCT) value which was used to calculate relative quantification (RQ) as follows: RQ= 2-ΔΔCT. Results show PTK6 relative expression in control, untreated (blue) and treated cells (green) in MDA-MB 231 cell line (A) and MDA-MB 436 cell line (B). qPCRs were performed using 3 independent sets of RNA for all cell lines with error bars representing standard deviation. ANOVA statistical analysis was performed to demonstrate variation within control cells as well as within treated groups. Students T Test was used to assess significant difference between each control and treated time points, * P<0.05.

MDA-MB 231 cell lines showed moderate response when treated with Taxol (Figure 5.15A), there was no significant difference in expression levels for PTK6 mRNA expression within the treated group (ANOVA F(4,10) =1.518, *P* = 0.269) as well as no significant difference between control and treated cells. However, there is an overall reduction in PTK6 expression over time in response to Taxol. For MDA-MB 436 cells, PTK6 expression was increased in response to Taxol treatment over time (Figure 5.16B), however little significant difference in response to Taxol treatment compared to control cells was observed. Within the treated group there was also little variation in PTK6 expression levels (ANOVA F(4,10) =1.113, *P* = 0.403).

ALT-PTK6 expression after Taxol treatment showed similar levels as control group in MDA-MB-231 cell line (Figure 5.16A) and showed no significant difference within treated group (ANOVA F(4,10) =3.427, *P* = 0.052). Overall, lower expression of both isoforms was observed overtime but there was no statistically significant difference between control and treated cells. Expression of *ALT-PTK6* did not differ significantly after Taxol treatment compared to control cells in MDA-MB 436 cell line (Figure 5.16B) and variation within the treated group did not statistically differ (ANOVA F(4,10) =1.19, *P* = 0.373). Statistical analysis did not reveal any significance between control and treated cells for MDA-MB 436 cell line. Overall it appears expression of *PTK6* isoforms are not significantly altered in response to Taxol treatment in MDA-MB 231 and MDA-MB 436 breast cancer cell lines.

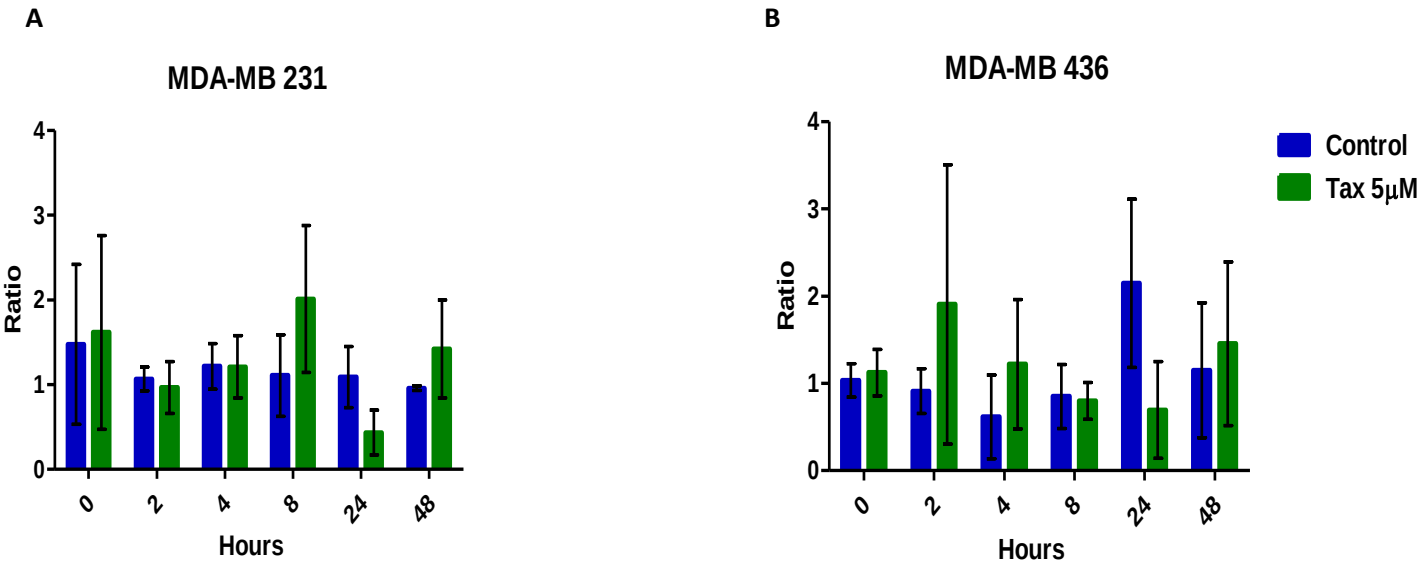

Figure 5.17 Relative ratio of *ALT-PTK6* to *PTK6* after Taxol treatment shows little difference compared to control cells in triple negative breast cancer cell lines. Cells were seeded at 200,000 cells per well in a 6 well plate and treated with Taxol (5µM). Cells were harvested for RNA at the following time points along with untreated controls: 0, 2 hours, 4 hours, 8 hours, 24 hours and 48 hours. cDNA was prepared using SuperScript II reverse transcriptase. PrecisionPLUS MasterMix with ROX at a lower level premixed with SYBRgreen (10µl), primer mix (1µl), RNase/DNase Free water, cDNA (5µl) were mixed. The experimental parameters were 40x cycles of enzyme activation for 2 minutes at 95˚C and denaturation for 10 seconds at 95˚C. Data was analysed by calculating average Cycle Threshold (CT) of both isoforms and normalised to average CT values of reference genes: *SDHA* and *RPL13A*. This gave the delta CT (ΔCT) value which was used to calculate relative quantification (RQ) as follows: RQ= 2-ΔΔCT. Ratios were determined from mean RQ values of ALT-PTK6/PTK6. Results show *ALT-PTK6/PTK6* ratios in control, untreated (blue) and treated cells (green) in MDA-MB 231 cell line (A) and MDA-MB 436 cell line (B).. qPCRs were performed using 3 independent sets of RNA for all cell lines with error bars representing standard deviation. ANOVA statistical analysis was performed to demonstrate variation within control cells as well as within treated groups. Students T Test was used to assess significant difference between each control and treated time points, * $P<0.05$.

MDA-MB 231 cell line shows relatively unchanged *ALT-PTK6* to *PTK6* ratios in Figure 5.17A between control and treated cells. There was no statistical variance observed within the treated group (ANOVA F(5,12) =2.224, *P* = 0.119). For the MDA-MB 436 cell line, *ALT-PTK6* to *PTK6* ratios (Figure 5.18B), there was no statistically significant difference between control and treated groups and no significant variation was observed within the treated group (ANOVA F(5,12) =0.712, *P* = 0.626). Overall, there was no statistically significant difference in the triple negative cell lines, in response to Taxol treatment for *ALT-PTK6/PTK6* ratios.

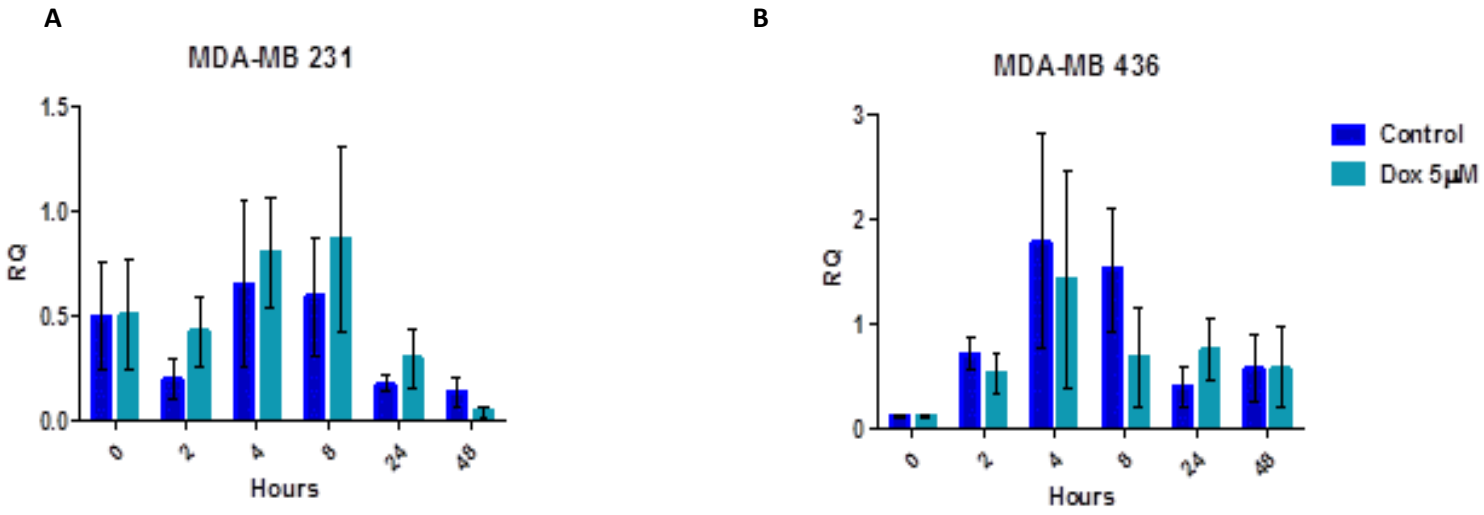

Figure 5.18 No significant change in PTK6 expression in response to Doxorubicin (Dox) at 5µM concentration in triple negative breast cancer cell lines. Cells were seeded at 200,000 cells per well in a 6 well plate and treated with Dox (5µM). Cells were harvested for RNA at the following time points along with untreated controls: 0, 2 hours, 4 hours, 8 hours, 24 hours and 48 hours. cDNA was prepared using SuperScript II reverse transcriptase. PrecisionPLUS MasterMix with ROX at a lower level premixed with SYBRgreen (10µl), primer mix (1µl), RNase/DNase Free water, cDNA (5µl) were mixed. The experimental parameters were 40x cycles of enzyme activation for 2 minutes at 95˚C and denaturation for 10 seconds at 95˚C. Data was analysed by calculating average Cycle Threshold (CT) of both isoforms and normalised to average CT values of reference genes: *SDHA* and *RPL13A*. This gave the delta CT (ΔCT) value which was used to calculate relative quantification (RQ) as follows: $RQ = 2^{-\Delta\Delta CT}$. Results show PTK6 relative expression in control, untreated (blue) and treated cells (light blue) in MDA-MB 231 cell line (A) and MDA-MB 436 cell line (B). qPCRs were performed using 3 independent sets of RNA for all cell lines with error bars representing standard deviation. ANOVA statistical analysis was performed to demonstrate variation within control cells as well as within treated groups. Students T Test was used to assess significant difference between each control and treated time points, * $P<0.05$.

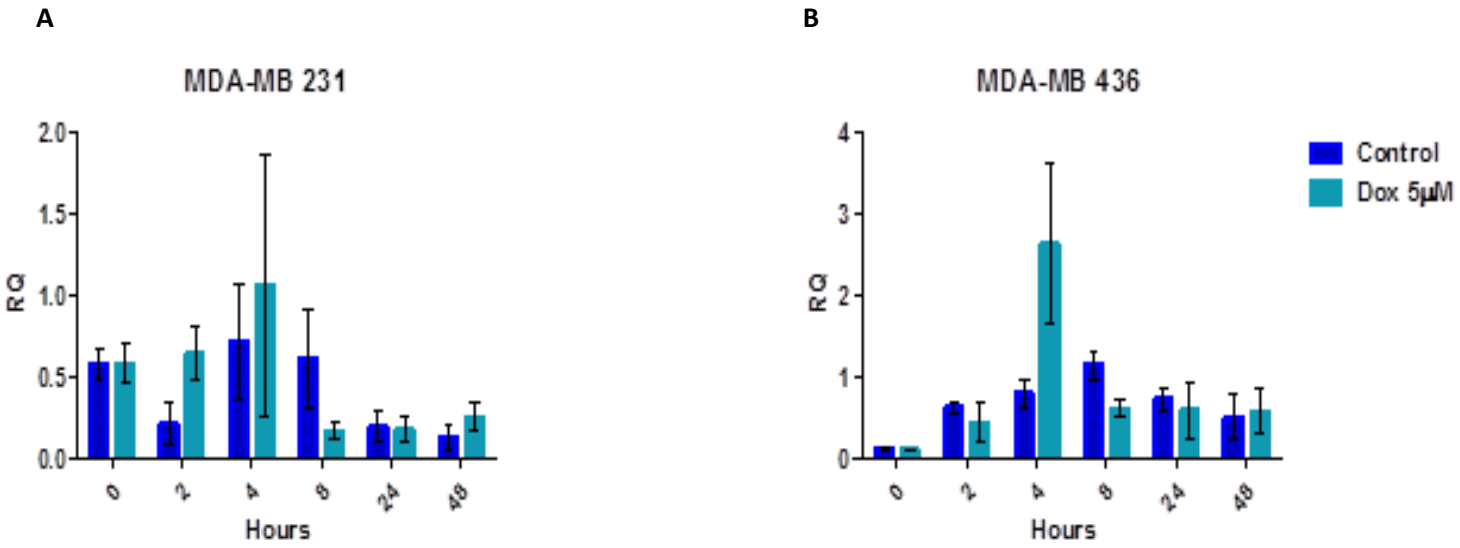

Figure 5.19 ALT-PTK6 mRNA expression levels remain relatively unchanged in MDA-MB 231 and MDA-MB-436 cell lines in response to Doxorubicin (Dox) treatment (5µM). Cells were seeded at 200,000 cells per well in a 6 well plate and treated with Dox (5µM). Cells were harvested for RNA at the following time points along with untreated controls: 0, 2 hours, 4 hours, 8 hours, 24 hours and 48 hours. cDNA was prepared using SuperScript II reverse transcriptase. PrecisionPLUS MasterMix with ROX at a lower level premixed with SYBRgreen (10µl), primer mix (1µl), RNase/DNase Free water, cDNA (5µl) were mixed. The experimental parameters were 40x cycles of enzyme activation for 2 minutes at 95˚C and denaturation for 10 seconds at 95˚C. Data was analysed by calculating average Cycle Threshold (CT) of both isoforms and normalised to average CT values of reference genes: *SDHA* and *RPL13A*. This gave the delta CT (ΔCT) value which was used to calculate relative quantification (RQ) as follows: RQ= 2-ΔΔCT. Results show ALT-PTK6 relative expression in control, untreated (blue) and treated cells (light blue) in MDA-MB 231 cell line (A) and MDA-MB 436 cell line (B). qPCRs were performed using 3 independent sets of RNA for all cell lines with error bars representing standard deviation. ANOVA statistical analysis was performed to demonstrate variation within control cells as well as within treated groups. Students T Test was used to assess significant difference between each control and treated time points, * $P<0.05$.

Observing the MDA-MB 231 cell line, overall there is a reduction in *PTK6* expression (Figure 5.18A) in response to Doxorubicin. However there does not seem to be a significant difference in expression between control and treated cells. ANOVA testing showed no statistically significant variation within treated group (ANOVA $F(4,10) = 1.518$, $P = 0.269$).

PTK6 expression is generally increased in the MDA-MB 436 cell line within both the control and treated groups overtime. However, there was no statistically significant difference between control and cells treated with Dox treatment (Figure 5.18B).

A similar pattern is seen for *ALT-PTK6* mRNA expression levels in MDA-MB 231 as with *PTK6* expression (Figure 5.19A). Although not statistically significant, compared to control cells, there is an overall reduction in expression levels in the treated cells. Interestingly, *ALT-PTK6* levels are largely increased at 4 hours post treatment in MDA-MB 436 cell lines before remaining relatively unchanged at 24 and 48 hours compared to control samples (Figure 5.19B). However, no significant difference was seen when treated cells were compared to control cells.

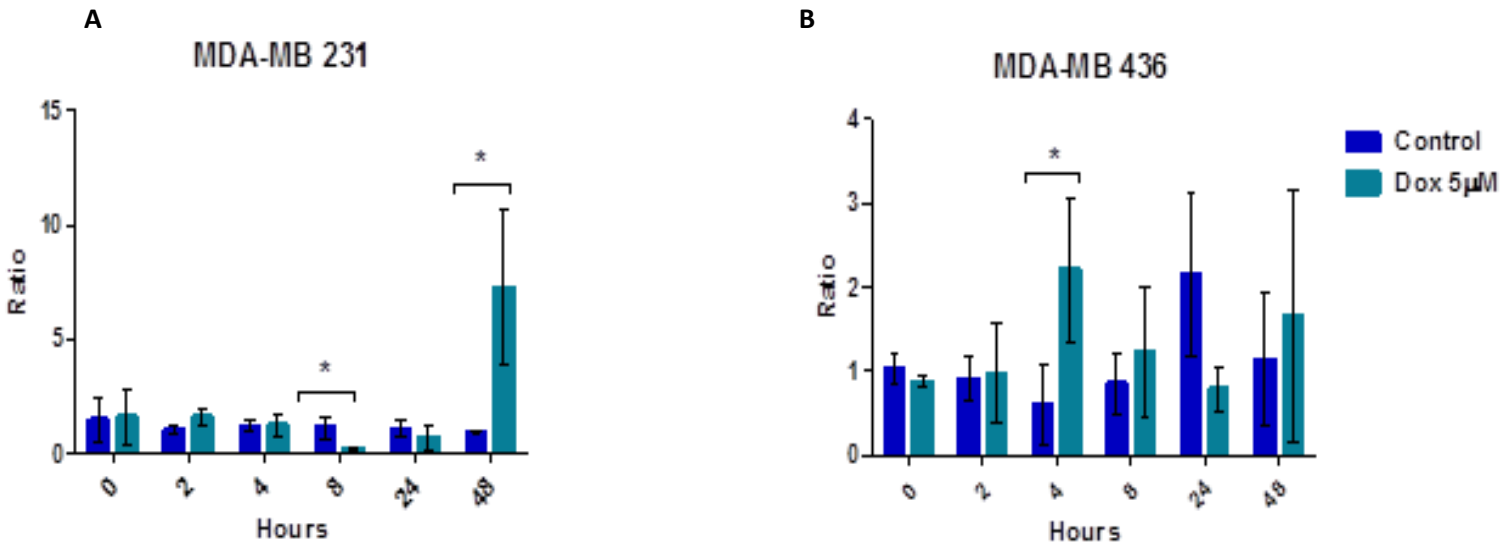

Figure 5.20 Relative ratio of ALT-PTK6 to PTK6 after Doxorubicin (Dox) treatment shows variation in triple negative cell lines MDA-MB 231 and MDA-MB 436. Cells were seeded at 200,000 cells per well in a 6 well plate and treated with Taxol (5µM). Cells were harvested for RNA at the following time points along with untreated controls: 0, 2 hours, 4 hours, 8 hours, 24 hours and 48 hours. cDNA was prepared using SuperScript II reverse transcriptase. PrecisionPLUS MasterMix with ROX at a lower level premixed with SYBRgreen (10µl), primer mix (1µl), RNase/DNase Free water, cDNA (5µl) were mixed. The experimental parameters were 40x cycles of enzyme activation for 2 minutes at 95˚C and denaturation for 10 seconds at 95˚C. Data was analysed by calculating average Cycle Threshold (CT) of both isoforms and normalised to average CT values of reference genes: *SDHA* and *RPL13A*. This gave the delta CT (ΔCT) value which was used to calculate relative quantification (RQ) as follows: RQ= 2-ΔΔCT. Ratios were determined from mean RQ values of ALT-PTK6/PTK6. Results show ALT-PTK6/PTK6 ratios in control, untreated (blue) and treated cells (green) in MDA-MB 231 cell line (A) and MDA-MB 436 cell line (B).. qPCRs were performed using 3 independent sets of RNA for all cell lines with error bars representing standard deviation. ANOVA statistical analysis was performed to demonstrate variation within control cells as well as within treated groups. Students T Test was used to assess significant difference between each control and treated time points, * $P<0.05$.

For Doxorubicin treatment in MDA-MB 231 cells, *ALT-PTK6* to *PTK6* ratios showed variation (Figure 5.20A) with significantly reduced *ALT-PTK6* to *PTK6* ratios at 8 hours before significant increase at 48 hours post treatment. Significant variation was observed in the treated groups for *ALT-PTK6* and *PTK6* ratios (ANOVA $F(5,12) = 8.97$, $P = 0.001$).

For Doxorubicin treatment in MDA-MB 436 cells, ratios of *ALT-PTK6* to *PTK6* (Figure 5.20B) showed higher levels in treated cells compared to control cells at 4 hours post treatment ($P<0.05$). However, ratios remain relatively unchanged at the other time points. Variance analysis showed no statistical difference within the treated group for *ALT-PTK6/PTK6* ratios (ANOVA $F(5,12) = 0.97$, $P= 0.473$).

Overall, there are higher *ALT-PTK6* to *PTK6* ratios in both the triple negative cell lines in response to Dox treatment compared to control cells with significance at 48 hours post treatment for MDA-MB 231 cell line and 4 hours post treatment in the MDA-MB 436 cell line.

5.3.6 mRNA expression of both isoforms and *ALT-PTK6* to *PTK6* ratios in breast in breast cancer cell lines after Lapatinib treatment (2.5μM).

In addition to examining the changes in *PTK6* and *ALT-PTK6* expressions in response to chemotherapy agents, I also investigated the expression of both isoforms in response to targeted therapy, Lapatinib. This is important as *ptk6* gene and *HER2* have previously shown to be co-expressed and cooperation between the two increases proliferative potential of HER2 positive cancers (Xiang *et al.*, 2008). In addition, co-expression of Brk with HER2 has shown to increase resistance to lapatinib as higher concentrations of the drug were needed in Brk positive cells to reduce cellular proliferation (Xiang *et al.*, 2008). Thus, due to the

involvement of Brk in HER2 signalling, lapatinib could potentially impact mRNA expression of *PTK6* transcripts.

The HER2 positive cell lines, SKBR3 and BT474 were seeded as before and treated with 2.5μM of lapatinib. For RNA extraction, the RNeasy Mini Spin Column kit from Qiagen was used to elute high quality and yield of RNA free of contamination as described in Materials and Methods (Chapter 2, section 2.2.16). cDNA was prepared using SuperScript II Reverse Transcriptase (Invitrogen) kit and qPCR performed using PrecisionPLUS MasterMix with ROX at a lower level premixed with SYBRgreen (Primer Design) with primer mixes for either transcript along with the primers for two reference genes, *SDHA* and *RPL13A*. Each master mix for each gene was pipetted in duplicate in a 96 well plate and 5μl of cDNA was pipetted using sterile filter tips as per manufacturer's protocol. The Applied Biosystems Quantstudio 7 Flex Real-Time PCR machine was used, and qPCRs were carried out using 3 sets of independent RNA. Data was analysed using the QuantStudio™ Software V1.3—for QuantStudio™ 6 and 7 Flex and ViiA™ 7 Real-Time PCR software (Applied Biosystems). Additionally, ratios of *ALT-PTK6* to *PTK6* transcript within the breast cancer cell lines in response to Lapatinib treatment were calculated. Ratios were determined within the control (untreated) cells as well as the treated cells.

A

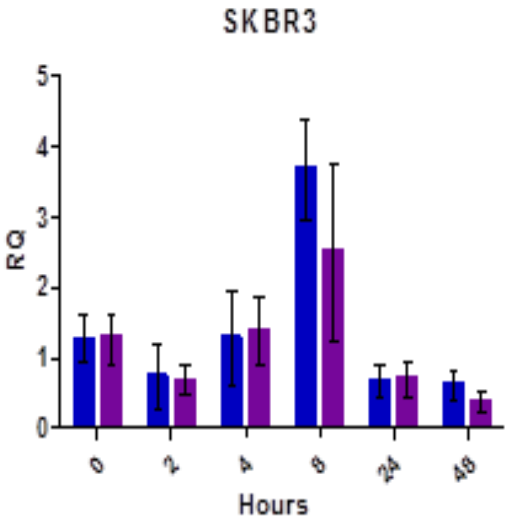

B

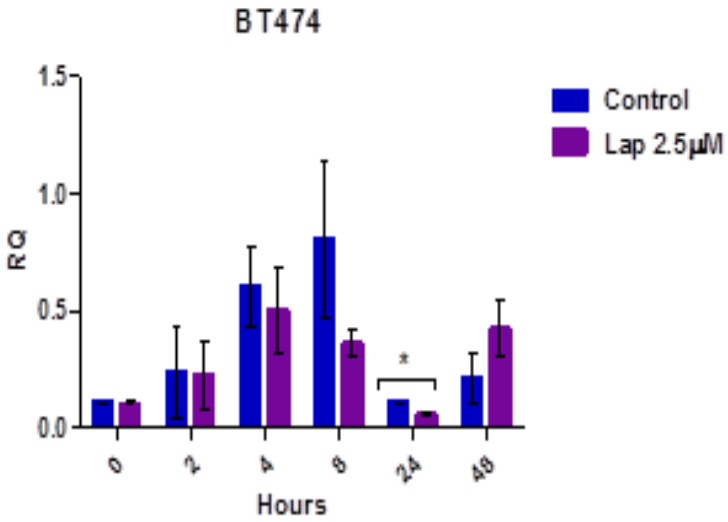

Figure 5.21 Lapatinib (Lap) treatment (2.5μM) decreases PTK6 expression in MDA-MB 231 with some increase in MDA-MB 436 cells. Cells were seeded at 200,000 cells per well in a 6 well plate and treated with Lap (2.5μM). Cells were harvested for RNA at the following time points along with untreated controls: 0, 2 hours, 4 hours, 8 hours, 24 hours and 48 hours. cDNA was prepared using SuperScript II reverse transcriptase. PrecisionPLUS MasterMix with ROX at a lower level premixed with SYBRgreen (10μl), primer mix (1μl), RNase/DNase Free water, cDNA (5μl) were mixed. The experimental parameters were 40x cycles of enzyme activation for 2 minutes at 95˚C and denaturation for 10 seconds at 95˚C. Data was analysed by calculating average Cycle Threshold (CT) of both isoforms and normalised to average CT values of reference genes: *SDHA* and *RPL13A*. This gave the delta CT (ΔCT) value which was used to calculate relative quantification (RQ) as follows: RQ= 2-ΔΔCT. Results show PTK6 relative expression in control, untreated (blue) and treated cells (purple) in SKBR3 cell line (A) and BT474 cell line (B). qPCRs were performed using 3 independent sets of RNA for all cell lines with error bars representing standard deviation. ANOVA statistical analysis was performed to demonstrate variation within control cells as well as within treated groups. Students T Test was used to assess significant difference between each control and treated time points, **P*<0.05.

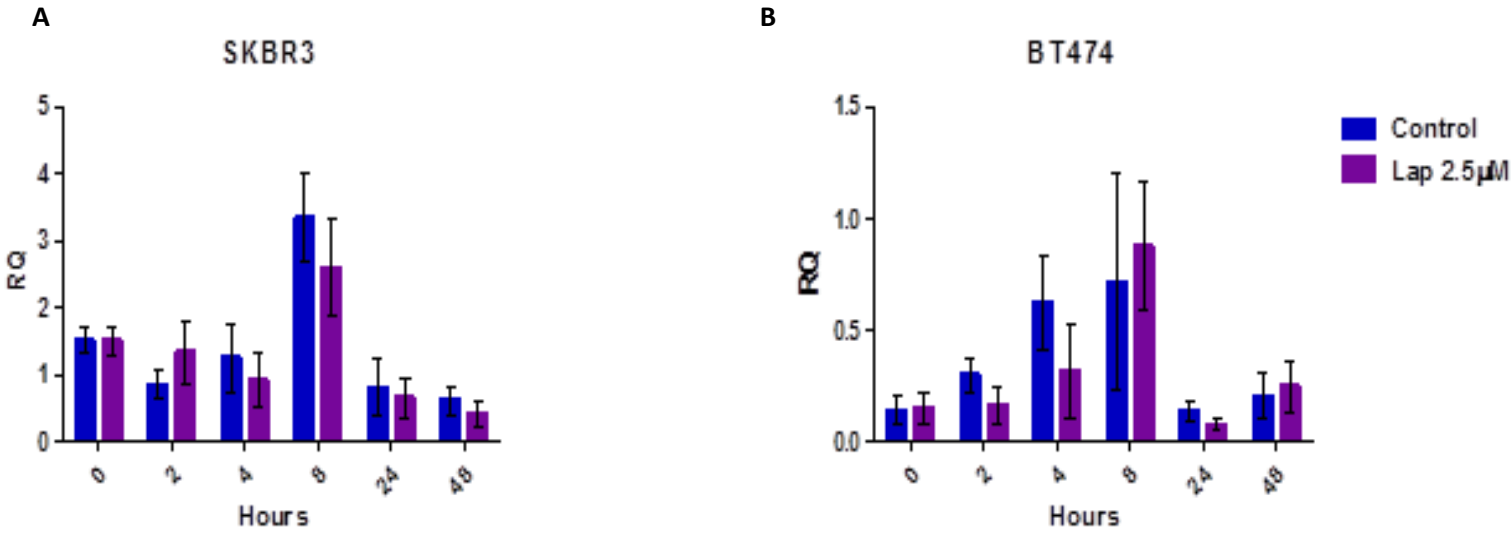

Figure 5.22 Lapatinib (Lap) treatment (2.5μM) does not significantly alter mRNA expression of ALT-PTK6 in HER2 positive cell lines. Cells were seeded at 200,000 cells per well in a 6 well plate and treated with Lap (2.5μM). Cells were harvested for RNA at the following time points along with untreated controls: 0, 2 hours, 4 hours, 8 hours, 24 hours and 48 hours. cDNA was prepared using SuperScript II reverse transcriptase. PrecisionPLUS MasterMix with ROX at a lower level premixed with SYBRgreen (10μl), primer mix (1μl), RNase/DNase Free water, cDNA (5μl) were mixed. The experimental parameters were 40x cycles of enzyme activation for 2 minutes at 95˚C and denaturation for 10 seconds at 95˚C. Data was analysed by calculating average Cycle Threshold (CT) of both isoforms and normalised to average CT values of reference genes: *SDHA* and *RPL13A*. This gave the delta CT (ΔCT) value which was used to calculate relative quantification (RQ) as follows: RQ= 2-ΔΔCT. Results show ALT-PTK6 relative expression in control, untreated (blue) and treated cells (purple) in SKBR3 cell line (A) and BT474 cell line (B). qPCRs were performed using 3 independent sets of RNA for all cell lines with error bars representing standard deviation. ANOVA statistical analysis was performed to demonstrate variation within control cells as well as within treated groups. Students T Test was used to assess significant difference between each control and treated time points, * $P<0.05$.

SKBR3 cell line showed relatively unchanged levels of the full-length transcript *PTK6* in response to lapatinib treatment (2.5μM) as shown in Figure 5.21A. There was greater statistical variance shown within the treated group (ANOVA F(5,12) =5.178, P = 0.009), as expression decreased over time. Although there was statistically significant reduction in *PTK6* levels at 24 hours post treatment (P<0.05), overall expression was increased over time in the BT474 cell line (Figure 5.21B). ANOVA testing revealed significant variance of *PTK6* expression within the treated group (ANOVA F(5,12) =7.952, P = 0.002).

ALT-PTK6 expression in the SKBR3 cell line showed similar pattern as expression of *PTK6* and there was no statistically significant difference between control and treated cells (Figure 5.22A). Overall, there was a decrease in expression over time and variance analysis within the treated group showed statistical significance (ANOVA F(5,12) =10.092, P = 0.001).

Within the BT474 cell line, overall there were no statistically significant differences observed in *ALT-PTK6* expression between control and treated cells in response to lapatinib treatment (Figure 5.22B). However, overall there was an increase in expression over time, with ANOVA statistical analysis showing significant difference between the time points within the treated group (ANOVA F(5,12) =10.257, P = 0.001).

Overall, within the SKBR3 cell line, lapatinib treatment reduces expression of both isoforms, however this was not statistically significant compared to control cells. Although there is significant reduction in *PTK6* expression within the BT474 cell line at 24 hours post treatment with lapatinib, there are no significant differences at the other time points between control and treated cells.

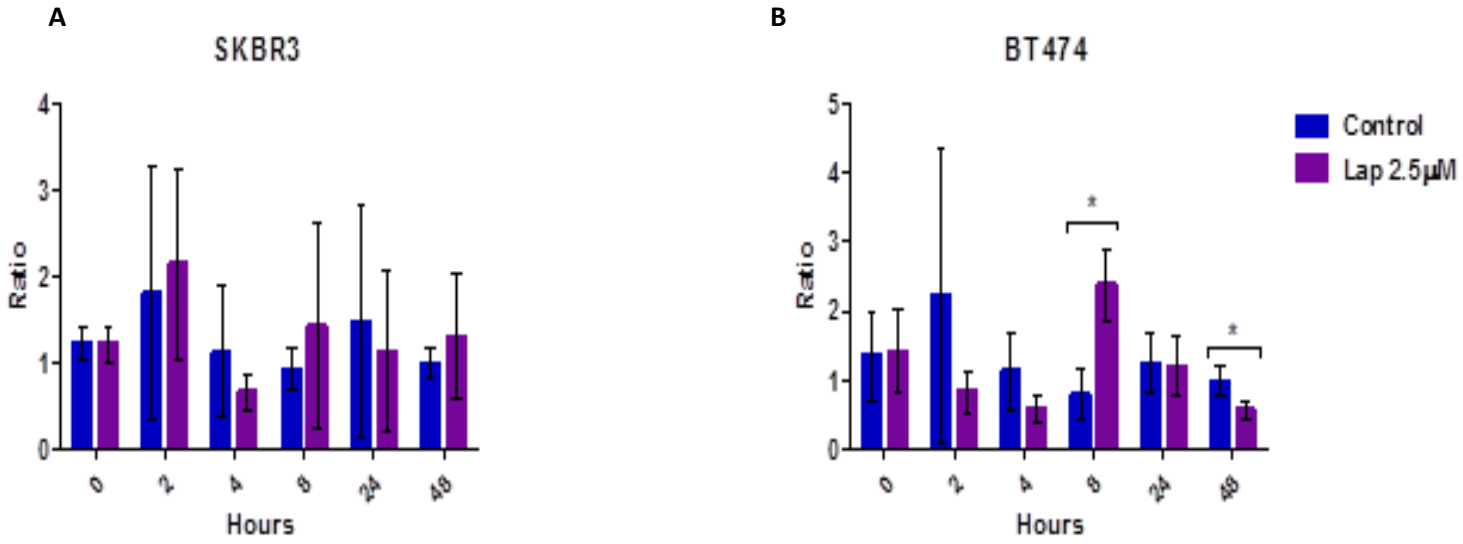

Figure 5.23 Relative *ALT-PTK6/PTK6* ratios are unchanged in response to Lapatinib (Lap) treatment in SKBR3 cells but there is some variation in the BT474 cell line. Cells were seeded at 200,000 cells per well in a 6 well plate and treated with Lap (2.5µM). Cells were harvested for RNA at the following time points along with untreated controls: 0, 2 hours, 4 hours, 8 hours, 24 hours and 48 hours. cDNA was prepared using SuperScript II reverse transcriptase. PrecisionPLUS MasterMix with ROX at a lower level premixed with SYBRgreen (10µl), primer mix (1µl), RNase/DNase Free water, cDNA (5µl) were mixed. The experimental parameters were 40x cycles of enzyme activation for 2 minutes at 95˚C and denaturation for 10 seconds at 95˚C. Data was analysed by calculating average Cycle Threshold (CT) of both isoforms and normalised to average CT values of reference genes: *SDHA* and *RPL13A*. This gave the delta CT (ΔCT) value which was used to calculate relative quantification (RQ) as follows: RQ= 2-ΔΔCT. Ratios were determined from mean RQ values of *ALT-PTK6/PTK6*. Results show *ALT-PTK6/PTK6* ratios in control, untreated (blue) and treated cells (purple) in SKBR3 cell line (A) and BT474 cell line (B). qPCRs were performed using 3 independent sets of RNA for all cell lines with error bars representing standard deviation. ANOVA statistical analysis was performed to demonstrate variation within control cells as well as within treated groups. Students T Test was used to assess significant difference between each control and treated time points, * P<0.05.

Ratios of *ALT-PTK6* to *PTK6* were relatively unchanged in SKBR3 cell line (Figure 5.23A) in response to lapatinib treatment compared to the untreated control cells. There were no statistically significant variations observed within control (ANOVA F(5,12) =0.413, *P* = 0.083) and treated group (ANOVA F(5,12) =1.063, *P* = 0.427) for ALT-PTK6/PTK6 ratios. Overall *ALT-PTK6* to *PTK6* ratios were reduced compared to control cells after lapatinib treatment (Figure 5.23B) in the BT474 cell line. Although there were higher *ALT-PTK6* to *PTK6* ratios at 8 hours post treatment suggesting induction of *ALT-PTK6* transcript, the ratios were lower at the other time point and were significantly lower compared to control cells after 48 hours of lapatinib treatment. There was statistically significant variance within the treated group (ANOVA F(5,12) =5.562, *P* = 0.007).

In summary, ratios of *ALT-PTK6* to *PTK6* were not statistically different in control and treated cells in response to lapatinib treatment at 2.5μM concentration within the SKBR3 cell line. For BT474 cell line, there are lower ratios of *ALT-PTK6* to *PTK6* overall in response to lapatinib with significance at 48 hours post treatment.

5.3.7 mRNA expression of both isoforms and *ALT-PTK6* to *PTK6* ratios in breast in breast cancer cell line after Tamoxifen treatment (5μM).

I next sought to determine alterations in mRNA expression of both *PTK6* isoforms in response to endocrine therapy using Tamoxifen (5μM) which has not been previously investigated. As a large majority of diagnosed breast cancers are oestrogen receptor (ER) expressing (and/or progesterone receptor expressing) and are stimulated via interaction with oestrogen (reviewed in Zhang *et al.*, 2014) and treated with oestrogen targeting therapies including the selective oestrogen receptor modulator (SERM) Tamoxifen; potential consequences on *PTK6* and *ALT-PTK6* mRNA levels in response to these treatments need to be determined. Furthermore, studies have shown there is high expression of *PTK6* transcript in breast cancers that are ER positive (Irie *et al.*, 2010; Peng *et al.*, 2014).

ER positive cell line, T47D was seeded as before and treated with 5μM of Tamoxifen. For RNA extraction, the RNeasy Mini Spin Column kit from Qiagen was used to elute high quality and yield of RNA free of contamination as described in Materials and Methods (Chapter 2, section 2.2.15.2). cDNA was prepared using SuperScript II Reverse Transcriptase (Invitrogen) kit and qPCR performed using PrecisionPLUS MasterMix with ROX at a lower level premixed with SYBRgreen (Primer Design) with primer mixes for either transcript along with the primers for two reference genes, *SDHA* and *RPL13A*. Each master mix for each gene was pipetted in duplicate in a 96 well plate and 5μl of cDNA was pipetted using sterile filter tips as per manufacturer's protocol. The Applied Biosystems Quantstudio 7 Flex Real-Time PCR machine was used, and qPCRs were carried out using 3 sets of independent RNA. Data was analysed using the QuantStudio™ Software V1.3—for QuantStudio™ 6 and 7 Flex and ViiA™ 7 Real-Time PCR software (Applied Biosystems). Additionally, ratios of *ALT-PTK6*

to *PTK6* transcripts within the breast cancer cell lines in response to Tamoxifen were calculated. Ratios were determined within the control (untreated) cells as well as the treated cells

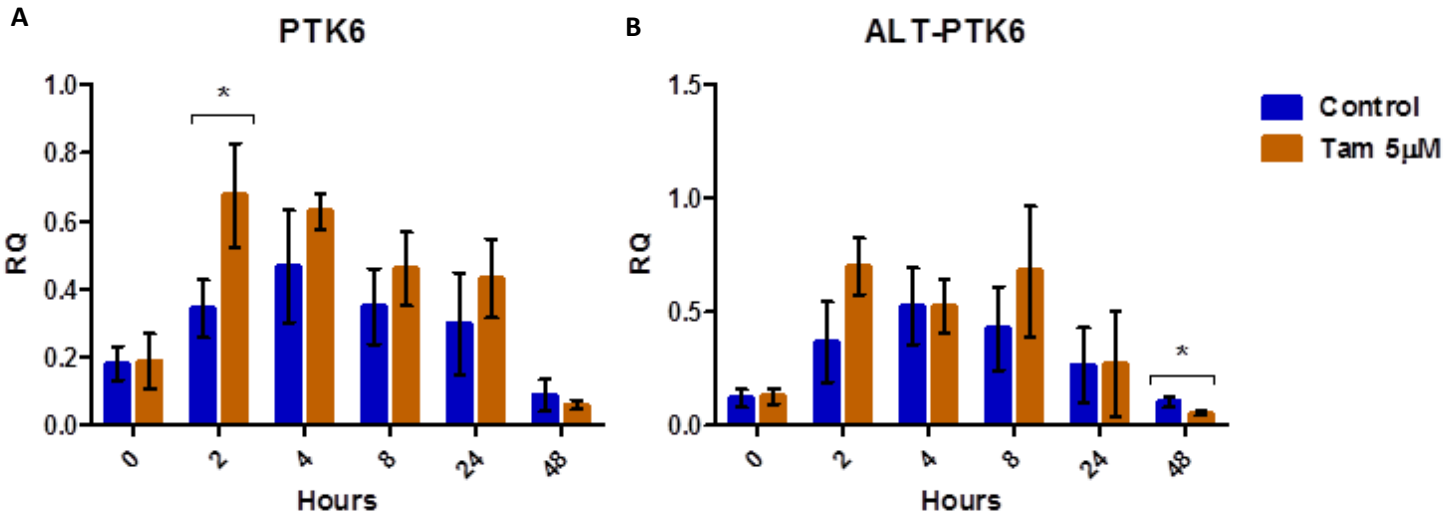

Figure 5.24 Tamoxifen (Tam) treatment shows A) increase in levels of PTK6 and (B) increase in ALT-PTK6 before significant reduction at 48 hours post treatment. Cells were seeded at 200,000 cells per well in a 6 well plate and treated with Tam (5µM). Cells were harvested for RNA at the following time points along with untreated controls: 0, 2 hours, 4 hours, 8 hours, 24 hours and 48 hours. cDNA was prepared using SuperScript II reverse transcriptase. PrecisionPLUS MasterMix with ROX at a lower level premixed with SYBRgreen (10µl), primer mix (1µl), RNase/DNase Free water, cDNA (5µl) were mixed. The experimental parameters were 40x cycles of enzyme activation for 2 minutes at 95˚C and denaturation for 10 seconds at 95˚C. Data was analysed by calculating average Cycle Threshold (CT) of both isoforms and normalised to average CT values of reference genes: *SDHA* and *RPL13A*. This gave the delta CT (ΔCT) value which was used to calculate relative quantification (RQ) as follows: RQ= 2-ΔΔCT. Results show PTK6 (A) and ALT-PTK6 (B) relative expression in control, untreated (blue) and treated cells (brown) in the T47D cell line. qPCRs were performed using 3 independent sets of RNA for all cell lines with error bars representing standard deviation. ANOVA statistical analysis was performed to demonstrate variation within control cells as well as within treated groups. Students T Test was used to assess significant difference between each control and treated time points, * $P<0.05$.

PTK6 expression appeared to increase in response to Tamoxifen treatment (5μM) in comparison to control cells in T47D cell line (Figure 5.24A), with significantly higher *PTK6* levels in treated cells at 2 hours ($P<0.05$). In addition, there was statistical variance observed within the treated group (ANOVA $F(5,12) = 19.932$, $P<0.001$). However, overtime *PTK6* expression is reduced 48 hours post treatment compared to expression at the 0-hour timepoint. Similarly, *ALT-PTK6* expression, although not statistically significant, is higher compared to control cells (Figure 5.24B). There was a significant reduction at 48 hours post treatment compared to control cells ($P<0.05$). Statistically significant variance within the treated group was observed (ANOVA $F(5,12) = 8.655$, $P = 0.001$).

Overall, initially there was induction of *PTK6* expression in the T47D cell line in response to Tamoxifen treatment (5μM) but this was reduced overtime. *ALT-PTK6* expression was higher in treated cells compared to control cells until at 48 hours post treatment were there was significant reduction.

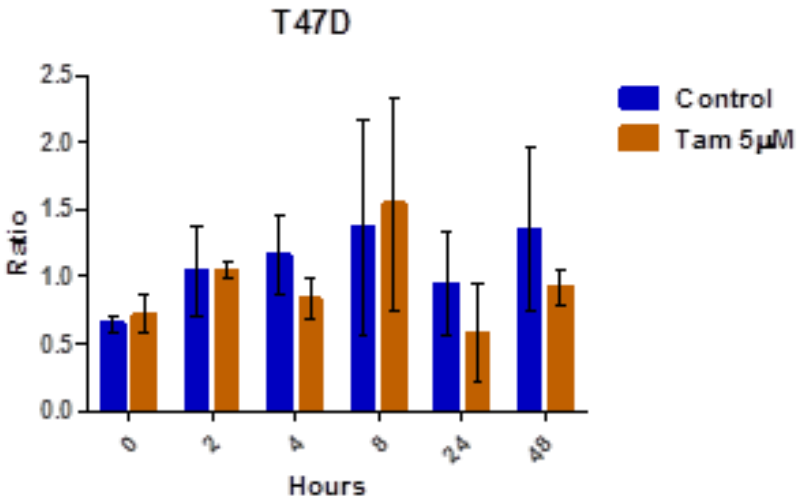

Figure 5.25 Relative ALT-PTK6/PTK6 ratios are unchanged in response to Tamoxifen (Tam) treatment compared to control cells in T47D cell lines. Cells were seeded at 200,000 cells per well in a 6 well plate and treated with Tam (5µM). Cells were harvested for RNA at the following time points along with untreated controls: 0, 2 hours, 4 hours, 8 hours, 24 hours and 48 hours. cDNA was prepared using SuperScript II reverse transcriptase. PrecisionPLUS MasterMix with ROX at a lower level premixed with SYBRgreen (10µl), primer mix (1µl), RNase/DNase Free water, cDNA (5µl) were mixed. The experimental parameters were 40x cycles of enzyme activation for 2 minutes at 95˚C and denaturation for 10 seconds at 95˚C. Data was analysed by calculating average Cycle Threshold (CT) of both isoforms and normalised to average CT values of reference genes: *SDHA* and *RPL13A*. This gave the delta CT (ΔCT) value which was used to calculate relative quantification (RQ) as follows: $RQ= 2^{-\Delta\Delta CT}$. Ratios were determined from mean RQ values of ALT-PTK6/PTK6. Results show ALT-PTK6/PTK6 ratios in control, untreated (blue) and treated cells (brown) in the T47D cell line. qPCRs were performed using 3 independent sets of RNA for all cell lines with error bars representing standard deviation. ANOVA statistical analysis was performed to demonstrate variation within control cells as well as within treated groups. Students T Test was used to assess significant difference between each control and treated time points, * $P<0.05$.

Within the T47D cell line, there was no statistically significant differences observed in *ALT-PTK6/PTK6* ratios in response to Tamoxifen treatment (Figure 5.25). There was no statistically significant variance observed within the treated cells (ANOVA F(5,12) =2.65, P =0.077) suggesting little variation of *PTK6* transcripts in response to Tamoxifen.

5.3.8 mRNA expression analysis of *PTK6* and *ALT-PTK6* in breast cancer tissues

ALT-PTK6 mRNA expression has not been investigated until now in breast cancer tissue samples. Previous studies have shown expression of *PTK6* mRNA in normal non-neoplastic breast tissues as well as in breast tumour tissues (Zhao *et al.*, 2003; Born *et al.*, 2005; Aubele *et al.*, 2007, 2009; Harvey *et al.*, 2009), with higher expression in tumour cells which increases with increasing tumour grade (Harvey *et al.*, 2009; Irie *et al.*, 2010) suggesting *PTK6* expression is associated with adverse patient outcomes. Previously the *ALT-PTK6* protein has shown to negatively regulate Brk expression and is associated with reduced cancer cell proliferation (Brauer *et al.*, 2011). In addition, my investigations in *ALT-PTK6* to *PTK6* ratios within breast cancer cell lines showed higher ratio of *ALT-PTK6* to *PTK6* in non-cancerous breast cells and in breast cancer cell lines representative of breast cancer subtypes with better patient outcomes; therefore, it was predicted higher *ALT-PTK6/PTK6* ratios would be associated with better overall patient survival within breast cancer patients. *PTK6 and ALT-PTK6* mRNA expression levels were assessed in normal (n=33) and malignant (n=127) breast tissue samples using real time qPCR and correlated with conventional clinic-pathological parameters and clinical outcomes. Tissue samples with informed consent and ethical approval for the experiments were obtained as stated in (Wazir et al., 2013). Breast

cancer tissues and normal background tissue were collected and stored in -80˚C until commencement of study. The patient cohort has been part of a number of completed and on-going studies and the clinicopathological data describing the patient cohort is further described in (Wazir et al., 2013). Breast tissue samples were collected immediately after excision and RNA extracted before reverse transcription and determination of transcript levels with β-actin as the reference gene used for normalisation. It should be noted that the experimental work for this section was performed by the group's clinical collaborators and so the choice of reference genes for these investigations were out of our control. Transcript levels within the breast cancer tissues were compared in relation to the background normal breast tissues and analysed against the tumour node and metastasis (TNM) stage, nodal involvement, tumour grade and clinical outcome over a 10 year follow up period. Results below show Kaplan Meier survival curves with y-axis as the cumulative survival (probability) and the x-axis shows the timeframe. Statistical analysis to determine difference in survival distributions in relation to *PTK6* and *ALT-PTK6* transcript levels and ratios was determined at multiple levels using a number of statistical tests including Logrank (Mantel Cox) for significant difference between high and low *PTK6* expression in relation to overall survival at later time points with Breslow (generalized Wilcoxon) test showing significant difference at the earlier time points. The Tarone-Ware test was used to further assess distribution of overall survival with assumptions that there is identical distribution as well as equal variance. All three statistical tests are therefore presented.

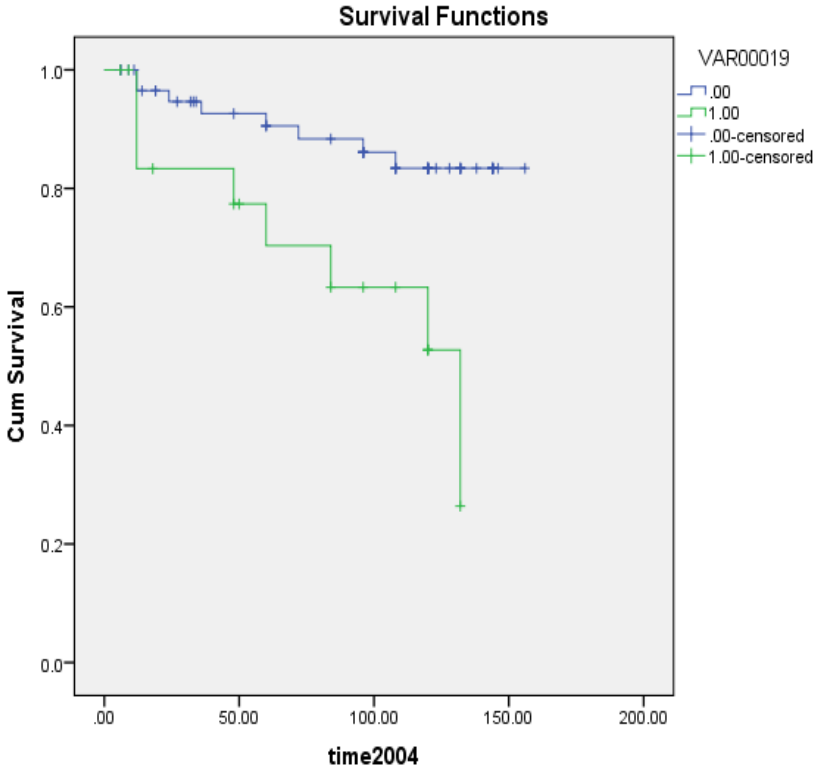

Overall Comparisons

	Chi-Square	Df	Sig.
Log Rank (Mantel-Cox)	8.600	1	.003
Breslow (Generalized Wilcoxon)	6.339	1	.012
Tarone-Ware	7.213	1	.007

Test of equality of survival distributions for the different levels of VAR00019.

Means and Medians for Survival Time

VAR00019	Mean[a]				Median			
	Estimate	Std. Error	95% Confidence Interval		Estimate	Std. Error	95% Confidence Interval	
			Lower Bound	Upper Bound			Lower Bound	Upper Bound
.00	139.600	5.515	128.791	150.408	.	.	.	.
1.00	97.292	12.077	73.621	120.964	132.000	25.888	81.259	182.741
Overall	131.451	5.594	120.487	142.415	.	.	.	.

a. Estimation is limited to the largest survival time if it is censored.

Figure 5.26 High mRNA expression of PTK6 in breast cancer tissues is associated with reduced overall survival. PTK6 transcript expression was determined in breast cancer tissue (n=127) in relation to the normal background tissue (n=33) using real time qPCR and correlated with conventional clinic-pathological parameters and clinical outcomes. Kaplan Meier curve shows high PTK6 (green) and low PTK6 (blue) levels in relation to overall survival over time. Statistical analysis was carried out using log rank (Mantel Cox), Breslow (generalized Wilcoxon) and Tarone-Ware to determine survival distributions in relation to PTK6 expression levels.

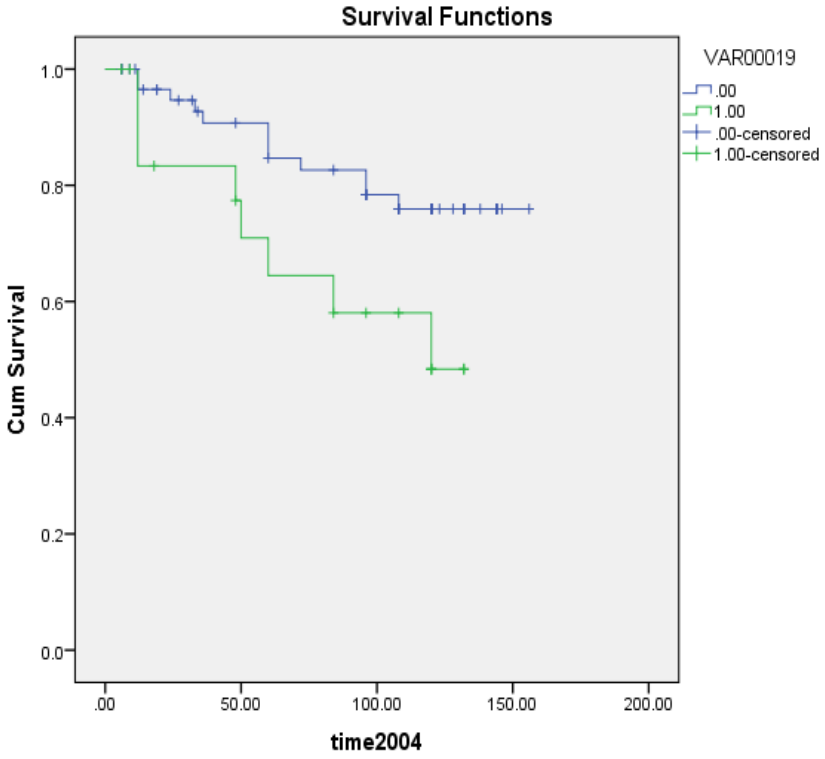

Overall Comparisons

	Chi-Square	df	Sig.
Log Rank (Mantel-Cox)	4.517	1	.034
Breslow (Generalized Wilcoxon)	4.488	1	.034
Tarone-Ware	4.505	1	.034

Test of equality of survival distributions for the different levels of VAR00019.

Means and Medians for Survival Time

VAR00019	Mean[a]				Median			
	Estimate	Std. Error	95% Confidence Interval		Estimate	Std. Error	95% Confidence Interval	
			Lower Bound	Upper Bound			Lower Bound	Upper Bound
.00	132.496	6.200	120.343	144.648	.	.	.	.
1.00	92.813	11.417	70.436	115.191	120.000	.	.	.
Overall	125.752	5.965	114.061	137.443	.	.	.	.

a. Estimation is limited to the largest survival time if it is censored.

Figure 5.27 High mRNA expression of PTK6 in breast cancer tissues is associated with reduced disease-free survival. PTK6 transcript expression was determined in breast cancer tissue (n=127) in relation to the normal background tissue (n=33) using real time qPCR and correlated with conventional clinic-pathological parameters and clinical outcomes. Kaplan Meier curve shows high PTK6 (green) and low PTK6 (blue) levels in relation to disease free survival over time. Statistical analysis was carried out using log rank (Mantel Cox), Breslow (generalized Wilcoxon) and Tarone-Ware to determine survival distributions in relation to PTK6 expression levels.

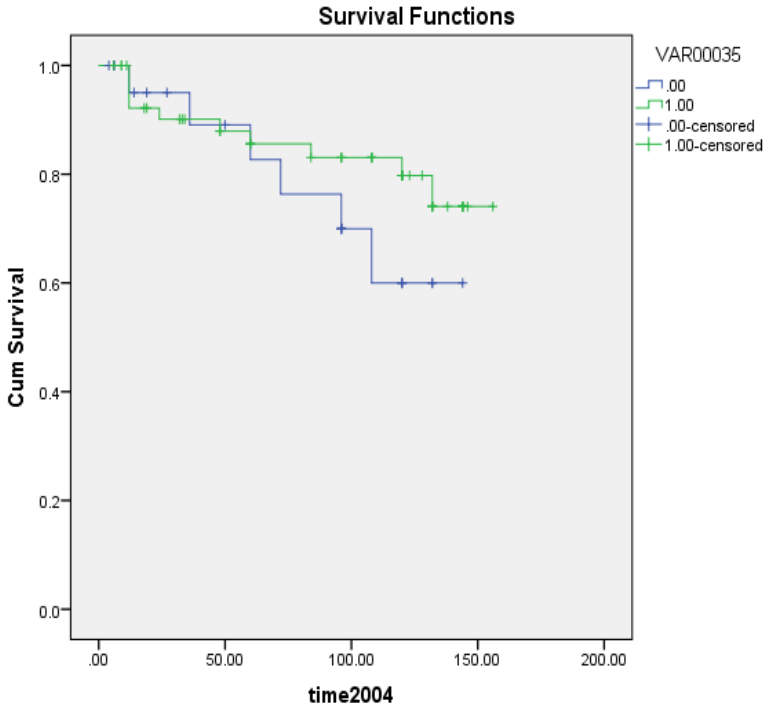

Overall Comparisons

	Chi-Square	df	Sig.
Log Rank (Mantel-Cox)	1.153	1	.283
Breslow (Generalized Wilcoxon)	.639	1	.424
Tarone-Ware	.915	1	.339

Test of equality of survival distributions for the different levels of VAR00035.

Means and Medians for Survival Time

VAR00035	Mean[a]				Median			
	Estimate	Std. Error	95% Confidence Interval		Estimate	Std. Error	95% Confidence Interval	
			Lower Bound	Upper Bound			Lower Bound	Upper Bound
.00	114.411	10.272	94.277	134.545	.	.	.	.
1.00	133.032	6.747	119.808	146.256	.	.	.	.
Overall	130.029	5.876	118.512	141.547	.	.	.	.

a. Estimation is limited to the largest survival time if it is censored.

Figure 5.28 High mRNA expression of ALT-PTK6 in breast cancer tissues is associated with improved overall survival. ALT-PTK6 transcript expression was determined in breast cancer tissue (n=127) in relation to the normal background tissue (n=3) using real time qPCR and correlated with conventional clinic-pathological parameters and clinical outcomes. Kaplan Meier curve shows high ALT-PTK6 (green) and low ALT-PTK6 (blue) levels in relation to overall survival over time. Statistical analysis was carried out using log rank (Mantel Cox), Breslow (generalized Wilcoxon) and Tarone-Ware to determine survival distributions in relation to ALT-PTK6 expression levels.

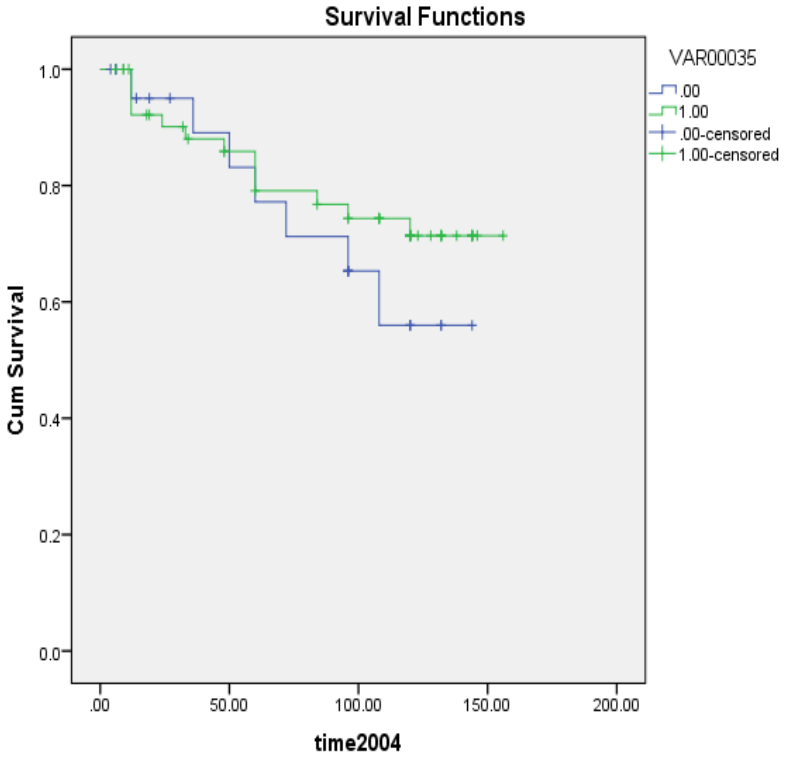

Overall Comparisons

	Chi-Square	df	Sig.
Log Rank (Mantel-Cox)	.734	1	.392
Breslow (Generalized Wilcoxon)	.329	1	.566
Tarone-Ware	.514	1	.474

Test of equality of survival distributions for the different levels of VAR00035.

Means and Medians for Survival Time

VAR00035	Mean[a]				Median			
	Estimate	Std. Error	95% Confidence Interval		Estimate	Std. Error	95% Confidence Interval	
			Lower Bound	Upper Bound			Lower Bound	Upper Bound
.00	109.935	10.599	89.161	130.708	.	.	.	.
1.00	126.414	7.312	112.082	140.746	.	.	.	.
Overall	123.929	6.255	111.668	136.190	.	.	.	.

a. Estimation is limited to the largest survival time if it is censored.

Figure 5.29 High mRNA expression of ALT-PTK6 in breast cancer tissues is associated with improved disease-free survival. ALT-PTK6 transcript expression was determined in breast cancer tissue (n=127) in relation to the normal background tissue (n=33) using real time qPCR and correlated with conventional clinic-pathological parameters and clinical outcomes. Kaplan Meier curve shows high ALT-PTK6 (green) and low ALT-PTK6 (blue) levels in relation disease free survival over time. Statistical analysis was carried out using log rank (Mantel Cox), Breslow (generalized Wilcoxon) and Tarone-Ware to determine survival distributions in relation to ALT-PTK6 expression levels.

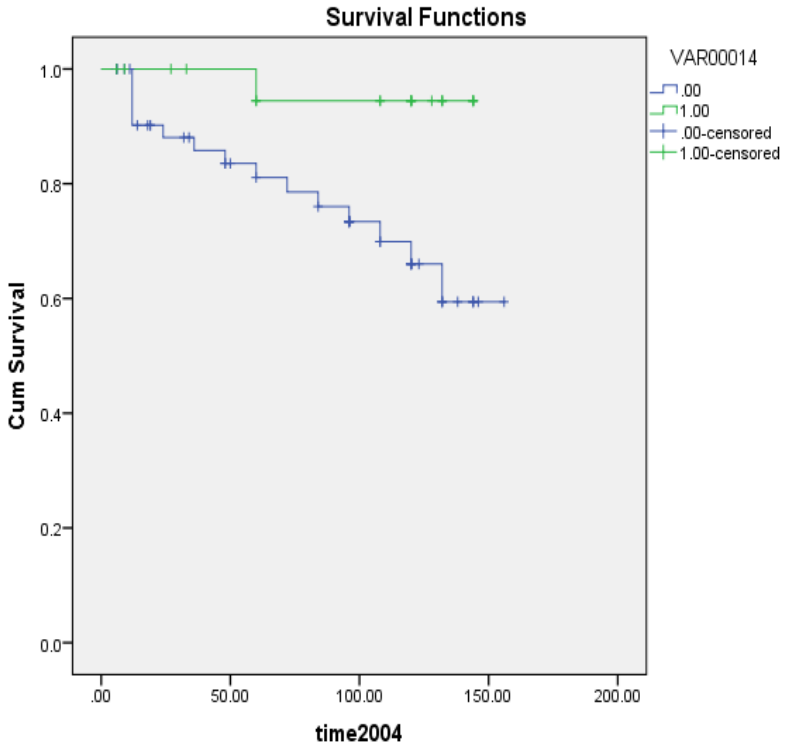

Overall Comparisons

	Chi-Square	df	Sig.
Log Rank (Mantel-Cox)	5.360	1	.021
Breslow (Generalized Wilcoxon)	4.730	1	.030
Tarone-Ware	5.071	1	.024

Test of equality of survival distributions for the different levels of VAR00014.

Means and Medians for Survival Time

VAR00014	Mean[a]				Median			
	Estimate	Std. Error	95% Confidence Interval		Estimate	Std. Error	95% Confidence Interval	
			Lower Bound	Upper Bound			Lower Bound	Upper Bound
.00	121.357	7.657	106.349	136.364	.	.	.	.
1.00	139.333	4.535	130.444	148.222	.	.	.	.
Overall	130.029	5.876	118.512	141.547	.	.	.	.

a. Estimation is limited to the largest survival time if it is censored.

Figure 5.30 High ALT-PTK6/PTK6 ratios in breast cancer tissues are associated with improved overall survival. ALT-PTK6 and PTK6 transcript expression was determined in breast cancer tissue (n=127) in relation to the normal background tissue (n=33) using real time qPCR and correlated with conventional clinic-pathological parameters and clinical outcomes. Kaplan Meier curve shows high ALT-PTK6/PTK6 ratio (green) and low ALT-PTK6/PTK6 ratio (blue) levels in relation to overall survival over time. Statistical analysis was carried out using log rank (Mantel Cox), Breslow (generalized Wilcoxon) and Tarone-Ware to determine survival distributions in relation to ALT-PTK6/PTK6 ratios levels.

Kaplan Meier curves are used to determine the estimate probability of overall or disease free survival over a 10 year time period in relation to *PTK6* and *ALT-PTK6* expression levels. The median copy number of full-length transcript (*PTK6*) was higher in breast cancer tissues compared to normal breast tissue and increased with increasing tumour grade (364 vs 13 for TNM3 vs TNM1 respectively, *P*=0.019 and 374 vs 23 for TNM3 vs TNM2 respectively, *P*=0.0244). Figures 5.26 and 5.27 show higher *PTK6* expression correlates with decreased overall survival as well as decreased disease-free survival compared to cancers with lower *PTK6* expression respectively. Figures 5.28 and 5.29 show higher *ALT-PTK6* levels in breast cancer are associated with improved overall and disease-free survival respectively. As previously determined (Zhao *et al.*, 2003; Irie *et al.*, 2010), high Brk expression was associated with oestrogen receptor positivity (*P*=0.061). Furthermore, high *PTK6* transcript levels were present for patients who developed recurrence (*P*=0.03) as well as patients who died of breast cancer (*P*=0.003). Interestingly, *ALT-PTK6* levels were higher in normal breast tissue compared to malignant breast tissue and also decreased with increasing tumour grade. Comparing high and low *ALT-PTK6/PTK6* ratios (Figure 5.30), a significant difference was observed; higher *ALT-PTK6/PTK6* ratios were associated with longer overall survival (*P*=0.021, logrank test).

5.4 Discussion

My studies confirm the expression of *PTK6* (407bp) within breast cancer cell lines as well as mRNA expression of *ALT-PTK6* (285bp), as shown in Figure 5.1. The alternatively spliced *PTK6* transcript (*ALT-PTK6*) was first identified in the T47D breast cancer cell line during the characterisation and chromosome mapping of the Brk gene (Mitchell et al., 1997). *ALT-PTK6* has a 122 base pair deletion at the 3' of the SH3 coding region with a novel proline rich sequence at the C-terminal and is 134 amino acids long which encodes a 15KDa protein (Mitchell et al., 1997). Although previous groups have shown mRNA expression of *PTK6* in breast cancer cell lines (Barker, Jackson and Crompton, 1997), expression of *ALT-PTK6* mRNA was not previously investigated. Breast cancer cell lines T47D, MDA-MB 436 and BT474 showed the highest *PTK6* expression. Each cell line is representative of a different breast cancer subtype; Luminal A (T47D), triple negative (MDA-MB 436) and Luminal B/HER2 positive (BT474) breast cancer, suggesting high expression of *PTK6* is not limited to a single subtype. Furthermore, the cell lines with low *PTK6* transcript expression include MCF10A and SKBR3 which is consistent with Tyner and group findings (Peng et al., 2014). These variations may be dependent on the expression of molecular markers in the breast cancer, for example, high Brk expression has been shown in over 80% of Luminal A (ER negative, PR positive and HER2 negative) and) and Luminal B (ER positive, PR negative or low and HER2 negative) breast cancers (Peng et al., 2014). Overall, majority of the breast cancer cell lines showed much greater *PTK6* transcript expression compared to the non-cancerous cell line MCF10A, which is consistent with previous reports (Peng *et al.*, 2014). My polymerase chain reaction (PCR) experiments corroborate the detection of *ALT-PTK6* expression within SKBR3, BT474 and T47D breast cancer cell lines and additionally within GI101 and MDA-MB 436 with other studies (Peng et al., 2014). Overall, there was higher

PTK6 expression and lower *ALT-PTK6* expression within the breast cancer cell lines compared to MCF10A cell line (Figure 5.1). *ALT-PTK6* transcript has further been detected in prostate and colon cancer cell lines thus far (Brauer et al., 2011) suggesting *ALT-PTK6* is not limited to a specific cancer type. Although *ALT-PTK6* expression was also shown in normal prostate cells (Brauer et al., 2011), interestingly no *PTK6* or *ALT-PTK6* transcripts were detected in the immortalised non-tumorigenic cell line MCF10A in my PCR experiments using standard PCR (Figure 5.1). In addition, no *PTK6* or *ALT-PTK6* expression was detected in the triple negative cell line, MDA-MB 231 using standard PCR. However, this is in contrast to Tyner and group which showed *PTK6* mRNA expression in MCF10A cell line as well as expression of both transcripts in MDA-MB 231 cell line (Peng et al., 2014). This discrepancy may be due to the different experimental conditions and set of primers used in the studies as well as lower levels of *PTK6* and *ALT-PTK6* transcripts in the cell lines. Quantitative PCR (qPCR) is a more sensitive and reliable method that is able to detect very low amounts of target DNA (reviewed in Rocha et al., 2015), further experiments were carried out using quantitative PCR. The expression of *PTK6* and *ALT-PTK6* transcripts were thus detectable using qPCR in the breast cancer cell lines including MCF10A and MDA-MB 231 (Figure 5.5). Previously it had been reported, *PTK6* expression was not detectable in normal mammary tissues, however since *PTK6* mRNA expression was detectable in the non-transformed mammary epithelial cell line MCF10A, this lead to investigations of *PTK6* expression in normal mammary tissue and thus confirmation that the *PTK6* transcript was expressed in normal mammary tissue (Peng et al., 2014). In addition to *PTK6* expression, expression of *ALT-PTK6* transcript was also detectable in MCF10A cell line (Figures 5.5). There was higher *ALT-PTK6* expression within MCF10A cell line compared to *PTK6* transcript, although this is contrary to Tyner and group which showed very low levels of *ALT-PTK6* transcript although this may be due to the volume of cDNA input and method of detection (Peng et al., 2014).

ALT-PTK6 transcript has previously been detected in normal human prostate and colon cells (Brauer et al., 2011) and now in the non-transformed mammary epithelial cell line MCF10A, suggesting *ALT-PTK6* transcript expression is also not limited to only cancerous cells. This is of interest as ALT-PTK6 protein has been shown to enhance the nuclear functions of Brk and negatively regulate cell proliferation in cancer cells (Brauer et al., 2011); thus, any Brk-therapy which disrupts the SH3 domain will need consideration for potential consequences of *PTK6* and *ALT-PTK6* expression in normal tissues, considering both isoforms contain functioning SH3 domains.

Interestingly, ratios of *ALT-PTK6* to *PTK6* transcripts (Figure 5.6) were higher in mainly breast molecular marker expressing cell lines (ER/PR/HER2) and the non-cancerous MCF10A cell line compared to cell lines representative of triple negative breast cancers. ER expression has also shown to be a positive prognostic factor in breast cancer (Ademuyiwa *et al.*, 2013). In addition, studies have shown a positive association with *PTK6* mRNA levels in breast tumours and positive oestrogen receptor status and HER2 expression (Zhao *et al.*, 2003; Born *et al.*, 2005). If higher *ALT-PTK6* expression is detected in breast cancer cells expressing higher levels of ER, this could suggest there is potentially more than one mechanism for improved breast cancer prognosis. Furthermore, triple negative breast cancers are linked with an overall poorer survival compared to hormone expressing breast cancers including HER2 positive breast cancers (Caggiano, Bauer and Parise, 2011). Although ALT-PTK6 protein expression was detectable in MDA-MB 231 and MDA-MB 436, this was at a low level compared to T47D, a luminal A subtype of breast cancer (Figure 5.6). Since elevated levels of *PTK6* transcript are detected with increasing tumour grade in breast cancers as well as higher levels of *PTK6* transcript compared to *ALT-PTK6*, this suggests higher *ALT-PTK6/PTK6* ratios may be associated with less aggressive and low-grade tumours.

My studies are some of the first to investigate the consequence of Brk inhibition on both *PTK6* transcripts. Using a novel Brk inhibitor, compound 4f (5μM), the ratio of *ALT-PTK6/PTK6* transcripts was determined using qPCR after treatment along with control untreated samples. Ratios of *ALT-PTK6* to *PTK6* showed variation from cell line to cell line. Table 5.1 shows the cell lines in order of high to low ratios of *ALT-PTK6/PTK6*. However, generally with higher *PTK6* mRNA levels, there was conversely lower *ALT-PTK6* in comparison and *vice versa*. Within the MDA-MB 231 cell line, representative of triple negative breast cancer, *ALT-PTK6/PTK6* ratios increased at 4 hours and 48 hours post treatment. In the MDA-MB 436 cell line, there was a moderate increase in *ALT-PTK6/PTK6* ratios at 2, 4 and 24 hours post treatment compared to at 0 hours. Although these were not statistically significant, the higher ALT-PTK6 levels may suggest Brk inhibition results in reduced levels of *PTK6* transcript which may shift the balance in favour of *ALT-PTK6* expression.

Table 5.1 High to Low *ALT-PTK6/PTK6* transcript ratios

High to Low ALT-PTK6/PTK6 expression ratios (Basal)
GI101
MCF10A
SKBR3
BT474
MDA-MB 231
MDA-MB 436
T47D

As breast cancer treatment is heavily chemotherapy based, the effect on both *PTK6* transcripts was investigated. Generally, *PTK6* expression (Figure 5.16) and *ALT-PTK6* expression (Figure 5.17) as well as ratios (Figure 5.18) did not statistically differ significantly compared to control untreated cells in MDA-MB 231 and MDA-MB 436 cell lines in response to Taxol suggesting Taxol does not significantly alter *PTK6* transcript ratios in these cell lines. Previous studies have shown hypoxia inducible factor alpha (HIFα) protein expression is induced in response to Paclitaxel/Taxol (Samanta et al., 2014). Hypoxia inducible factors are mediators of transcriptional responses to hypoxia and are involved in many cellular functions within cancer cells leading to progression and metastasis (Semenza, 2010). HIFα subunits are overexpressed in breast cancers especially in triple negative breast cancers (Yamamoto et al., 2008) and indicate higher risk of metastasis (Dales et al., 2005). Hypoxia has shown to counteract Taxol-induced apoptosis in breast cancer cell lines including MDA-MB 231 suggesting potential mechanism of chemotherapeutic resistance (Notte et al., 2013). Since Brk is co-expressed with HIF-1α (Regan Anderson et al., 2013), the total effect of Taxol on *PTK6* transcripts may not be as pronounced in the triple negative cell lines compared to the luminal A T47D cell line which appear to be more sensitive to chemotherapy agents (Figure 4.5, Chapter 4). It should be noted, however, that other studies have shown Brk expression is induced prior to induction of HIF-1α suggesting that Brk expression is independent of HIF-1α and that there are alternative mechanisms that are HIF-independent which mediate Brk protein expression (Pires *et al.*, 2014).

Interestingly within MDA-MB 231 cell line there were significantly lower *ALT-PTK6/PTK6* ratios in response to doxorubicin compared to untreated control cells at 8 hours post treatment (Figure 5.21A), however at 48 hours post treatment there were significantly higher *ALT-PTK6/PTK6* ratios in comparison. MDA-MB 436 cell line also shows generally higher *ALT-PTK6/PTK6* ratios with significantly higher ratios at 4 hours post treatment in response

to doxorubicin (Figure 5.21B). Previously, Brk has shown to be induced in response to DNA damage via gamma irradiation or doxorubicin (Haegebarth et al., 2009; Gierut et al., 2012) albeit in colon cancer cells. Thus, the initial induction of *PTK6* mRNA expression may be in response to the DNA damage by doxorubicin. In addition, hepatocyte growth factor (HGF) which is involved in protecting cancer cells against cytotoxicity and apoptosis induced by DNA damage (including doxorubicin) is an upstream activator of Brk in breast cancer cells (Fan et al., 2005; Castro and Lange, 2010) further indicating a potential mechanism by which Brk levels may increase in response to doxorubicin. The reduction of full length transcript and induction of *ALT-PTK6* at the later time points may suggest increased number of apoptotic cells resulting due to doxorubicin treatment over time leading to reduced levels of PTK6 and concurrently higher *ALT-PTK6* transcript levels. Previous studies have shown as ALT-PTK6 levels are increased, Brk levels are reduced (Brauer et al., 2011). Furthermore, as ALT-PTK6 levels increase, interaction with Brk with other proteins may reduce due to the two isoforms competing via their SH3 domains as well as reduction of Brk phosphorylation by other kinases if they interact via the SH3 domain. In addition, ALT-PTK6 also associates with β-catenin which is also a substrate of Brk (Brauer et al., 2011). β catenin/WNT signalling has extensively been examined in breast cancer tumorigenesis and metastasis (Wang et al., 2015) and has shown to be involved in cell migration as well as chemo-resistance of triple negative breast cancers i*n vitro* (Xu et al., 2015) suggesting ALT-PTK6 and β catenin interactions may have some role in chemotherapy response. As increasing amounts of ALT-PTK6 protein in transfected prostate cancer cells enhanced repression of β catenin and T-cell factor (TCF) transcriptional target proteins, Cyclin D and c-Myc (Brauer et al., 2011) and increasing levels of ALT-PTK6 resulted in reduced cell proliferation, it may be a point of interest that ALT-PTK6 could sensitise cancer cells to chemotherapy via repression of β catenin/WNT signalling and reduced cellular proliferation. However, Brk and ALT-PTK6

interactions with this signalling pathway will need further validation in breast cancer cells. Furthermore, as ALT-PTK6 may decrease cell proliferation and chemotherapy targets mainly rapidly dividing cells, this could result in reduced sensitivity to chemotherapeutic agents and indicate a potential mechanism that confers resistance.

Brk inhibition in the HER2 positive cell lines showed significant reduction in *PTK6* transcript levels compared to control cells in SKBR3 and *ALT-PTK6* to *PTK6* ratios, however showed no meaningful change between treated and control cells in both cell lines. Although no statistical significance was observed, there are generally higher *ALT-PTK6/PTK6* ratios in response to Brk treatment in BT474 cell line compared to control cells. *ALT-PTK6/PTK6* ratios in response to lapatinib within HER2 positive cell line SKBR3 (Figure 5.24A) were not statistically significantly different compared to ratios in untreated control cells. In BT474 cell line, *ALT-PTK6/PTK6* ratios (Figure 5.24B) show higher *ALT-PTK6* to *PTK6* transcript at 8 hours before significant reduction at 48 hours post treatment compared to ratios in control cells. Studies have shown *ptk6* gene is coamplified with *erB2* gene and promotes cell proliferation as well as confers resistance to HER targeted therapies such as lapatinib (Xiang et al., 2008). Downregulation of Brk has shown to sensitize breast cancer cells to lapatinib by enhancement of Bim expression via p38 activation (Park et al., 2015). My results show overall *ALT-PTK6/PTK6* ratios decrease in BT474 cell line in response to lapatinib but remain relatively unchanged in SKBR3 cell line. As lapatinib resistance has been linked to Brk, high *PTK6* levels were expected in response to lapatinib treatment. Taken together, these results support combination treatment with Brk inhibition and HER2 targeted therapy would significantly reduce cancer cell viability as shown in Figure 4.6 (Chapter 4, section 4.3.3). In addition, these results along with results shown in chapter 4, section 4.3.3, show HER2 positive cell lines appear to be more sensitive to Brk inhibition than triple negative breast cancers.

Although not statistically significant, *PTK6* levels are reduced with Brk inhibition compared to control cells in T47D cell line. Overall, *ALT-PTK6/PTK6* ratios are generally increased with Brk inhibition compared to control cells. T47D cell line did not significantly alter ALT-*PTK6/PTK6* ratios (Figure 5.26), suggesting Tamoxifen does not directly influence *PTK6* and *ALT-PTK6* ratios. *PTK6* transcript expression remains more dominant compared to *ALT-PTK6* in this cell line. Brk inhibition with Tamoxifen treatments have shown strong synergism in ER positive breast cancers (Jiang et al., 2017). It has been now reported Brk is involved in promoting survival and growth of endocrine therapy (Tamoxifen) resistant breast cancer cells (Ito et al., 2017) and downregulation of Brk promoted apoptosis of ER positive breast cancer cells including in tamoxifen-resistant cells. My results corroborate this as *PTK6* expression is not significantly altered in the presence of Tamoxifen thus breast cancer cells will continue to proliferate via Brk signalling. Table 5.2 shows the summary description of all *ALT-PTK6/PTK6* expression ratios in response to Brk inhibition and breast cancer therapies.

Table 5.2 Summary of *ALT-PTK6/PTK6* mRNA expression ratios in response to Brk inhibition and other breast cancer therapies.

Cell line	Brk inhibition	Taxol treatment	Doxorubicin treatment	Lapatinib treatment	Tamoxifen treatment
MDA-MB 231	No change between control and treated cells observed.	No change between control and treated cells observed.	Ratios reduce at 8hrs post treatment and significantly increase at 48hrs post treatment. No changes observed at other time points.		
MDA-MB 436			Ratios increase at 4hrs post treatment compared to control. No other changes observed at other time points.		
SKBR3	No change between control and treated cells observed			No change between control and treated cells observed	
BT474				Ratios increase at 8hrs post treatment compared to control cells and decrease at 48hrs post treatment. No other changes observed at other time points.	
T47D	Ratios increase at 2hrs after treatment before decreasing at 4hrs after treatment compared to control cells. No difference observed at other time points.				No change between control and treated cells observed

Previous studies have shown expression of *PTK6* mRNA in normal non-neoplastic breast tissues as well as in breast tumour tissues (Zhao et al., 2003; Born et al., 2005; Aubele et al., 2007, 2009; Harvey et al., 2009), with higher expression in tumour cells which increases with increasing tumour grade (Harvey et al., 2009; Irie et al., 2010). *PTK6* to *ALT-PTK6* ratios have also been shown to be higher in prostate cancer tissues compared to normal or low-grade tumour prostate tissue (Brauer et al., 2011). However, expression ratios of *ALT-PTK6* to *PTK6* have yet to be investigated in breast cancer tissue samples. Brk expression has shown to be associated with increasing tumour grade and adverse patient outcomes (Harvey et al., 2009; Irie et al., 2010) and ALT-PTK6 is associated with inhibition of Brk phosphorylation and reduced cancer cell proliferation as well as reduced levels with higher grade tumours in prostate tissues; thus higher *ALT-PTK6/PTK6* ratios may indicate potentially better prognosis and overall survival in breast cancer tumours. In addition, my *in vitro* studies show higher *ALT-PTK6/PTK6* ratios in non-cancerous cell line as well as in cell lines representative of breast cancer subtypes which are less aggressive and have a better prognosis (Lumina A/B). Investigation of *ALT-PTK6* and *PTK6* transcripts in normal and malignant breast tissue showed increasing levels of *PTK6* transcript with increasing tumour grade and reduced overall survival as well as disease free survival compared to breast cancer tissues with lower *PTK6* levels (Figures 5.27 and 5.28). Conversely, higher *ALT-PTK6* transcript levels were associated with improved overall and disease-free survival and decreased with increasing tumour grade (Figures 5.29 and 5.30) which corroborate my experiments in the cell lines. Additionally, higher *ALT-PTK6/PTK6* ratios significantly correlated with longer overall and disease-free survival (Figure 5.31) suggesting *ALT-PTK6* and *PTK6* ratios are important prognostic predictors of disease free and overall survival in breast cancers. This further validates an inverse relationship between both transcripts in breast cancer cells. This could have a potential impact on therapies targeting Brk inhibition

and investigations on ALT-PTK6 influence on Brk inhibition, especially in relation to localisation within breast cancers may offer further insight on the roles of ALT-PTK6 as previous groups have suggested ALT-PTK6 may be able to localise Brk to the nucleus and nuclear Brk has shown to have growth inhibitory functions, an inverse to cytoplasmic Brk which has oncogenic functions (Derry et al., 2003; Ie Kim and Lee, 2009; Brauer et al., 2011). It is worth mentioning that validation of *ALT-PTK6* and *PTK6* transcript ratios in breast cancer tissues in a larger cohort of patient samples may show further statistical as well as biological relevance.

The main conclusions of this chapter were that the *in vitro* investigations show higher levels of *ALT-PTK6/PTK6* ratios in non-cancerous cell line as well as in cell lines representative of breast cancer subtypes which are less aggressive and have a better prognosis (Lumina A/B) compared to triple negative breast cancer cell lines which have higher level of the *PTK6* transcript. There were no significant differences in *PTK6* and *ALT-PTK6* mRNA expression in response to standard breast cancer therapies suggesting these therapies do not affect Brk at the transcript level. Furthermore, expression of *ALT-PTK6* and *PTK6* transcripts in normal and malignant breast tissue showed increasing levels of *PTK6* transcript with increasing tumour grade and reduced overall survival as well as disease free survival compared to breast cancer tissues with lower *PTK6* levels. Conversely, there were higher levels of the short transcript, *ALT-PTK6* in normal and low grade breast cancer tissues. The expression ratios of *ALT-PTK6/PTK6* show higher ratios were associated with longer overall survival. These data suggest there is potential for *ALT-PTK6/PTK6* expression ratios to be used as prognostic factors to determine overall and disease free survival.

6.0 Chapter 6: General Discussion

Previous studies have not shown a direct association between radio-sensitivity and Brk expression in breast cancer cell lines nor any link between Brk and DNA repair after γ-radiation induced DNA damage in the context of breast cancer. This is important due to the use of radiotherapy and cytotoxic chemotherapeutic agents which function via inducing DNA damage in breast cancer treatments. I hypothesised, Brk positive breast cancer cell lines may be more susceptible to gamma radiation. Brk expression has shown to potentiate ErbB signalling via P13K/Akt, which is an activator of the mTOR pathway and increased levels of mTOR are linked to down-regulation of ataxia telangiectasia mutated protein (ATM) (Kamalati et al., 1996; Shen and Houghton, 2013). Downregulation of ATM may increase cancer cell sensitivity to radiotherapy as cancer cells have reduced repair capacity (Truman *et al.*, 2005; Hammond and Muschel, 2014).

Although my studies did not indicate a role for Brk in directly influencing radio-sensitivity of breast cancer cell lines, there was indication that cell lines with high SF2 survival rates (survival rate 2Gy dose) had moderate to higher Brk expression (Figure 3.7, Chapter 3). In addition, Brk was induced in response to gamma radiation showing an increase in Brk protein expression in response to DNA damage (Figure 3.6, Chapter 3). Further investigations using transfected cell lines expressing Brk WT, Brk KM and vector only in cell lines that were endogenously Brk negative (MDA-MB 468 and MDA-MB 157) showed increased radio-resistance in Brk WT and Brk KM cell lines (Figure 3.4, Chapter 3). Interestingly SF2 survival did show statistically significant higher survival rates for MDA-MB 157 Brk WT and Brk KM cell lines compared to MDA-MB 157 Vector cell line (Figure 3.5 Chapter 3). However, this was not confirmed in the MDA-MB 468 cell line which showed no statistically significant variation. The difference in part can be explained due to the activation of signalling pathways between the two cell lines as MDA-MB 468 shows considerably higher expression of EGFR in MDA-MB 468 cell line compared to MDA-MB 157 as well as mutations in the P13K/Akt

inhibitor PTEN (Bamford *et al.*, 2004; Burness, Grushko and Olopade, 2010), suggesting little impact by Brk within a cell line with already elevated EGFR signalling. Furthermore, there were no statistically significant differences in gamma H2AX DNA repair kinetics as well as no functional relationship with ATM activity in the MDA-MB 468 and MDA-MB 157 cell lines suggesting Brk expression may not directly influence radio-sensitivity through the ATM signalling pathway. Thus, radiotherapy remains a viable treatment option for breast cancer patients and Brk may not have a significant impact on sensitivity.

My studies of Brk influence on breast cancer sensitivity in response to common breast cancer therapies such as Taxol, Doxorubicin, Lapatinib as well as Tamoxifen showed significant reduction in cell proliferation in combination with Brk inhibition using a novel inhibitor, compound 4f (Figures 4.3, 4.5, 4.6, and 4.8, Chapter 4) suggesting Brk kinase inhibition as a combination therapy may prove to be a viable and effective treatment for the diverse subtypes of breast cancer. Although Brk did not show a direct role in sensitising breast cancer cell lines to radiotherapy, it was induced in response to radiation and since it modulates response to chemotherapeutic agents, patients undergoing treatments involving radiotherapy and chemotherapy in combination may benefit additionally with Brk inhibition. Further investigations *in vivo* will reveal the impact of Brk inhibition in mice models. In addition, although Brk inhibition using compound 4f did not significantly reduce breast cancer cell proliferation as a monotherapy, this does not suggest more potent Brk inhibitors will show improved efficacy. Irie and group have recently shown P21d, a variant of imidazo[1,2-a]pyrazin-8-amines (Zeng *et al.*, 2011) as a potent Brk kinase activity inhibitor in breast cancer cells (Ito *et al.*, 2016). P21d treatment showed downregulation of the SNAIL protein, restoration of E-cadherin expression as well as induction of anoikis and reduced metastasis in TNBC cells (Ito *et al.*, 2016). More recent development of Brk inhibitors include pyrazolopyrimidine (PP)1, PP2 and a lymphocyte-specific protein tyrosine kinase inhibitor

which show promise as selective kinase inhibitors of Brk activity with reduced phosphorylation of Brk substrate proteins including STAT3 (Shim, Kim and Lee, 2017). Further investigations *in vitro* and *in vivo* will shed light on the effectiveness of these inhibitors. However, identification of novel Brk inhibitors and continued investigations with Brk inhibitors show Brk kinase inhibition remains an area of interest.

Along with *PTK6*, an alternatively spliced Brk transcript was identified which was named originally as λm5 and much later coined as *ALT-PTK6* (Mitchell *et al.*, 1997; Brauer *et al.*, 2011). The short isoform has a 122 base pair deletion at the 3' end of the SH3 coding region thus it lacks a functional SH2 and tyrosine kinase domain but instead has a C-terminal proline rich sequence (Figure 1.1, Chapter 1). Thus far ALT-PTK6 expression has been shown in breast, colon and prostate cancer cells (Brauer *et al*., 2011; Mitchell et al, 1997). The exact role of this isoform in breast cancer has not been fully investigated previously. My investigations show ALT-PTK6 protein expression in T47D and low expression in the two triple negative cell lines, MDA-MB 231 and MDA-MB 436. Interestingly for MDA-MB 231 cell line, ALT-PTK6 protein levels appeared to reduce over time due to Brk inhibition suggesting Brk reduction may also affect the levels of ALT-PTK6. The potential mechanism for this may involve Brk's association with proteins that regulate alternative splicing such as sam68, SLM1 and SLM2. Due to reduced Brk activity, phosphorylation of downstream substrates is also reduced which may in consequence lead to reduced levels of the alternative isoform. This is of importance as any Brk targeted therapy may have potential effects on the short isoform due to interactions of Brk with these RNA binding proteins.

Previous studies have shown expression of *PTK6* mRNA in normal breast tissues as well as in breast tumour tissues (Zhao et al., 2003; Born et al., 2005; Aubele et al., 2007, 2009; Harvey et al., 2009), with higher expression in tumour cells which increases with increasing tumour grade (Harvey et al., 2009; Irie et al., 2010) suggesting *PTK6* expression is associated

with adverse patient outcomes. ALT-PTK6 has been proposed to potentially negatively regulate Brk expression and is associated with reduced cancer cell proliferation (Brauer *et al,* 2011). Moreover, the higher ratio of *ALT-PTK6* to *PTK6* expression in non-cancerous breast cells (MCF10A) and in breast cancer cell lines representative of breast cancer subtypes with better patient outcomes (Figure 5.5, Chapter 5); suggests higher *ALT-PTK6* to *PTK6* ratios would be associated with better overall patient survival within breast cancer patients. Indeed, *ALT-PTK6* expression was higher in normal breast tissue and low grade tumours and decreased with increasing tumour grade/stage, whereas *PTK6* expression conversely was higher in malignant tissue compared to normal breast tissue and increased with advancing tumour stage. Thus, suggesting a role for both transcripts in predicting breast cancer prognosis. This was confirmed with high *ALT-PTK6/PTK6* ratios significantly correlating with improved overall breast survival over a 10 year period (Figure 5.30, Chapter 5). These results confirm and corroborate the oncogenic role for *PTK6* in relation to poor prognosis in breast cancers (Harvey *et al.*, 2009; Irie *et al.*, 2010) and offer the potential of *ALT-PTK6/PTK6* mRNA expression ratio as a predictive prognostic marker. It should be noted, other groups have suggested a positive prognostic potential for *PTK6*, with high *PTK6* expression beyond 50-100 months correlating with improved probability of distant recurrence free survival (Aubele *et al.*, 2007). This discrepancy may be due to the association of Brk expression with the oestrogen receptor which is linked to positive prognosis in breast cancer (reviewed in Cao and Lu, 2016).

Breast cancer survival rates have doubled over the last 40 years and continue to improve (Cancer research UK, 2014), however breast cancer along with bowel and prostate cancers account for almost half of all cancer related deaths in the UK (Cancer research UK, 2014). In addition, incidence rates continue to increase, and breast cancer remains one of the most common cancers in the UK. Furthermore, chemotherapy and radiotherapy although continue

to be improved with advancing technology, still show severe adverse side effects (Erban and Lau, 2006; Azim *et al.*, 2011; Henson *et al.*, 2013; Sardar *et al.*, 2017). Hormonal therapies such as Tamoxifen, have been used for early stage and metastatic breast cancer since its license in 1972 (Smith, 2012). Although proven to be effective against pre-menopausal breast cancer, especially those that are oestrogen receptor positive, there are still many issues that need to be overcome, including the diverse adverse toxicities, development of secondary cancers, resistance against Tamoxifen and subsequent recurrence in some patients. Furthermore, this drug is only effective against oestrogen or progesterone receptor positive breast cancers thus making it unsuitable for other types of breast cancer such as HER2 positive/ER/PR negative and triple negative breast cancers (den Hollander, Savage and Brown, 2013). Treatments available for HER2 positive cancers include monoclonal antibodies such as Herceptin that binds to HER2 thus negatively effecting receptor function. Unfortunately the more advanced stages of breast cancer do not always respond to Herceptin therapy and those that do, often progress in 12 months from the start of the treatment (Fink and Chipuk, 2013). In addition resistance may occur due to the involvement of a number of signalling pathway molecules such as activation of the PI3K/AKT pathway, loss of PTEN and activation of PIK3CA (reviewed in Brauer and Tyner, 2010). The multiple issues with standard breast cancer therapies suggest a need for identifying novel therapeutic targets and continuous development of novel anticancer therapies.

Brk is expressed in a wide range of cancer types including in hormone negative breast cancers which lack targetable molecular markers such as ER/PR/HER2, thus making it an ideal candidate for therapeutic intervention (Barker, Jackson and Crompton, 1997; Brauer and Tyner, 2010). At the start of my PhD, there were few studies thoroughly investigating Brk's role in response to common breast cancer therapies as well as in response to novel Brk inhibitors. Little was known regarding the role of the short isoform, ALT-PTK6 in breast

cancer and to date there have been no published studies exploring the role of this transcript in breast cancer cell lines or breast cancer tissues especially in relation to the full-length transcript and its potential prognostic value.

Further consideration will also be needed for Brk and ALT-PTK6 localisation in the role of breast cancer pathogenesis as well in response to therapies as Brk has different functions in different tissue types and cellular compartments (discussed in Harvey and Burmi, 2011). Brk's role will greatly depend on the availability of different substrates in the cytoplasm, plasma membrane and nucleus. Studies have shown adding a myristoylation site to the N terminal of Brk, which it lacks, promotes Brk's oncogenic role by promoting proliferation and migration of HEK293 cells via localisation to the membrane, whereas trapping Brk in the nucleus with a nuclear localisation sequence (NLS) reversed these effects (Ie Kim and Lee, 2009). Moreover, normally Brk is active in differentiating, non-dividing epithelial cells in the small intestine where it is a negative regulator of growth, however, due to an external stimulus such as DNA damage by irradiation, Brk has shown to promote apoptosis (Haegebarth *et al.*, 2009). This shows Brk's differing role within the same tissue but in different conditions. In addition, ALT-PTK6 effects Brk's cellular localisation as increased expression of ALT-PTK6 resulted in decreased Brk at the membrane and an increase in nuclear Brk in transfected HEK293 cells (Brauer *et al.*, 2011). As Brk lacks an NLS and myristoylation site, it can be freely moving and difficult to track within the cell and the exact mechanism for Brk movement from one sub-cellular compartment to another is not fully understood. It may be due to Brk's interactions with its substrates which determine localisation. However, the discovery that ALT-PTK6 may influence Brk's localisation may offer an additional mechanism by which it changes location.

Overall Brk has shown to be an ideal therapeutic target in breast cancer especially as it is involved in various hallmarks of cancer as discussed in (Hanahan and Weinberg, 2011)

(Figure 6.1). Furthermore, Harvey and Burmi show the number of Brk substrates and protein interactions (Harvey and Burmi, 2011). However, since then more substrates, regulators and protein interactions of Brk have been identified which indicates the involvement of Brk in several signalling pathways which are dysregulated in cancer. Brk's therapeutic potential could also extend to non-small cell lung cancer, prostate and colon cancer therapy (Fan *et al.*, 2011; Zheng *Y* and Tyner *AL,* 2013; 2011; Gierut *et al.*, 2011). It was recognised as one of the tyrosine kinases expressed in breast cancer due to the immense interest in tyrosine kinase inhibitors (Meric *et al.*, 2002).

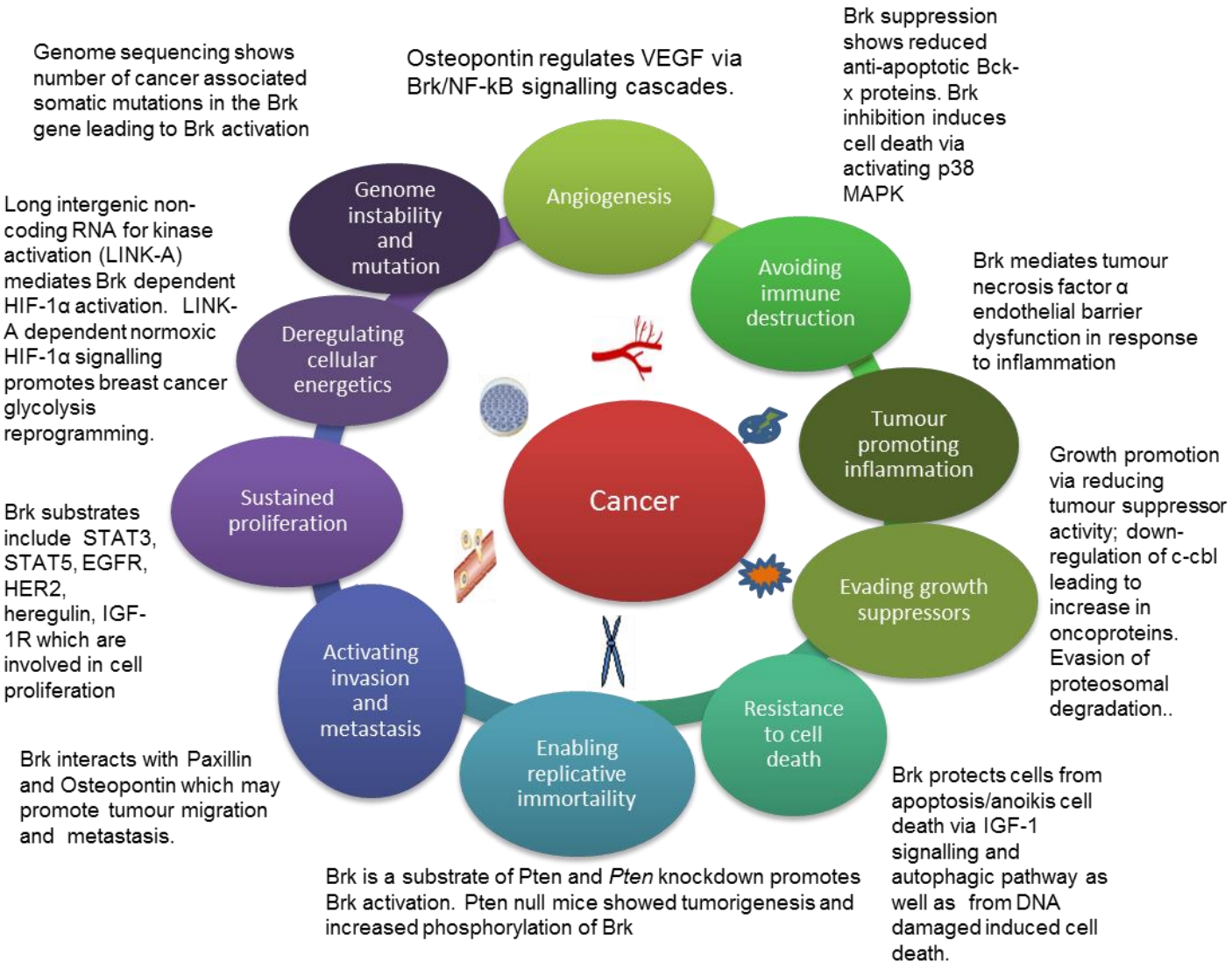

Figure 6.1 Breast tumour kinase and cancer hallmarks. Brk and cancer hallmarks. The original six cancer hallmarks described by Hannahan and Weinberg (2011) are illustrated along with a summary of Brk's role in their regulation. Brk: Breast tumour kinase (Figure adapted from: Hussain and Harvey, 2014).

It should be noted many of Brk's interactions require Brk's kinase domain whereas others may require protein-protein interactions and some through indirect association via a third party (reviewed in Harvey and Burmi, 2011). Therefore, Brk kinase-independent activity does need consideration when looking at tyrosine kinase inhibitors. Interfering with Brk's protein–protein interactions by disrupting its conformational activation may also be therapeutically effective, including disruptions in the SH2 and SH3 domains. However, tyrosine kinase inhibitors have in the past proven to be well tolerated with manageable side effects, selective and relatively effective in a range of cancers (Zhang, Yang and Gray, 2009). In addition, *PTK6*-null mice have shown to grow relatively healthily into adulthood indicating potential tolerability to Brk inhibitors in breast cancer patients (Haegebarth *et al.*, 2006). Many of Brk's activities involve its kinase catalytic domain including anchorage independent growth, EGFR signalling, cell migration and cell death (reviewed in Harvey and Burmi, 2011; Irie *et al.*, 2010). These properties still make tyrosine kinase inhibition an attractive prospect despite Brk's kinase independent functions. Furthermore, in comparison to HER2, EGFR, IGFR and p53, its expression is much higher in many types of breast cancer indicating targeting Brk may benefit a wider range of patients (Harvey and Crompton, 2004). The continuous development of Brk inhibitors will offer further insight into its therapeutic potential especially in relation to its short isoform expression as well as within other cancers.

6.1 Limitations

There were some limitations for the work presented in this thesis. Firstly, the cell line MCF10A although non-cancerous represented a non-tumorigenic immortalized epithelial cell and a normal breast cell line as a normal control was not used in my investigations. However, it should be noted, there are a lack of normal breast cells due to the difficulty in obtaining tissue samples to generate a stable cell line, in addition, MCF10A do exhibit some of the features for the normal breast epithelium including anchorage independent growth and dependence

on growth factors for proliferation. Further limitations included the *ALT-PTK6* custom designed primers with the qPCR work performed by our clinical collaborators, which were also able to weakly detect the full length form (*PTK6*) due to specificity issues. It may be that some levels of both *PTK6* and *ALT-PTK6* were detected in the cancer tissue samples and thus the results may not reflect the true expression of *ALT-PTK6* transcript in the breast cancer cell lines. It should be noted that a bigger sample size of normal and tumour breast tissues may offer more statistical power and validate the findings of the potential of *ALT-PTK6/PTK6* mRNA expression ratios in prognosis. Another limitation included the lack of commercially available Brk inhibitors at the time of my investigations. There are also few published studies investigating the role of compound 4f as well as its potency in inhibiting Brk i*n vitro*. There was limited information on the duration of effect of this compound as well as its stability over time. Recently, other Brk inhibitors have been identified which may prove to be more potent than compound 4f, such as a novel Brk kinase inhibitor known as XMU-MP-2 (Jiang *et al.*, 2017). This drug has shown to significantly inhibit proliferation in Brk transformed Ba/F3 and Brk overexpressing breast cancer cells (Jiang *et al.*, 2017). Other Brk inhibitors that have been identified through ELISA based *in vitro* kinase assay systems include pyrazolopyrimidines PP1 and PP2 (Shim, Kim and Lee, 2017). These inhibitors have shown reduced Brk mediated proliferation of T47D breast cancer cells as well as reduction in STAT3 activity (Shim, Kim and Lee, 2017). Further studies using these inhibitors will show the efficacy of these inhibitors as monotherapy in wide range of breast cancer cell lines as well as efficacy in combination with standard therapies. Furthermore, some reports have suggested toxicity of MTT as the formazan crystals may puncture the cell membrane, however this may be dependent on the concentration of MTT reagent (Lü *et al.*, 2012) and may be avoided by reducing the incubation time. Additional limitations included the lack of commercially available plasmid tagged differently to Brk with green fluorescent protein tag

(GFP-tag) for transfection of the short isoform, ALT-PTK6 in ALT-PTK6 negative cell lines to determine localisation of Brk. Localisation of Brk before and after treatment with radiotherapy may have shed further light on the role of Brk in radiotherapy. There were other limitations which included the use of the Imagestream flow cytometry, due to the low resolution and accuracy of the images obtained in the Brightfield channel. In comparison the confocal microscopy may have shown a greater resolution (x100 magnification) and accuracy although the Imagestream allowed for cells to be in suspension. Furthermore, the 'gating' of cells chosen for analysis can be subjective which may lead to a reduced sample size in addition to the many wash steps during the preparation of the sample.

6.2 Future work

It may be that a better understanding of Brk will require 3D culturing especially for investigating breast cancer transformation and migration/invasion as well as cell growth and proliferation. 3D culturing compared to 2D culturing has shown to better mimic *in vivo* conditions and maybe be more useful to further evaluate Brk's role in normal and malignant breast cells. Successful use of 3D culturing in addition to 2D culturing of breast cancer cells has even been used to evaluate breast cancer drug sensitivity and resistance as previously determined with HER2 targeted therapy neratinib and classical chemotherapy, Docetaxel (Qu *et al.*, 2015; Breslin and O'Driscoll, 2016). Future work would involve repeat of some of these investigations using a more stable and potent Brk inhibitor which may offer further evidence for the need for Brk inhibition in breast cancer. It may be that a closer look at interrupting protein-protein interactions will prove to be a better method of Brk inhibition especially considering that Brk has kinase independent functions. This protein-protein disruption may

be mediated via the SH2 and SH3 domains of Brk. This is supported by studies investigating the SH3 binding site which showed that the SH3 domain is important for substrate recognition and many of Brk substrates interact via the SH3 domain including sam68 (Qiu and Miller, 2004). It should be noted that ALT-PTK6 also contains an SH2 domain thus potential side effects of Brk inhibition on ALT-PTK6 will need to be considered. Protein-protein disruptions have previously shown to be ideal therapeutic targets and show promise in clinical trials (Fischer, Rossmann and Hyvönen, 2015)(Petta *et al.*, 2016).

It should be noted, Brk is involved in the deregulation of cell cycle progression, as with increasing Brk levels, there was reduced p27 expression, a cell cycle checkpoint inhibitor (Chan and Nimnual, 2010). Brk reduced cell proliferation within these cell lines suggesting the requirement of p27/Fox03a pathway to promote cell growth and a Brk-targeted therapy could be utilised to prevent cell cycle progression (Chan and Nimnual, 2010). Seeing as majority of chemotherapeutic agents as well as radiotherapy are cell cycle specific, the impact of Brk inhibition on cell cycle progression in response to chemotherapy or radiotherapy may indicate whether Brk targeted therapy will be more useful before or after radiotherapy or chemotherapy especially considering the proliferative role of Brk in cancer cells. The effect on ALT-PTK6 in response to DNA damage will need further investigation in relation to Brk expression. Exactly what happens to ALT-PTK6 expression in DNA damage needs further exploring especially if ALT-PTK6 reduces Brk proliferation and may confine Brk to the nucleus. The mRNA expression ratios of *ALT-PTK6* and *PTK6* will need further verification in other cancer types as well as correlated with the breast molecular markers in patient tissue samples as well as with the treatment modality as these may affect the ratios and thus the predictive potential of the transcripts for overall patient survival. Further *in vivo* studies evaluating Brk inhibition on normal breast cells as well as breast tumours as well as the effect of overexpressing *ALT-PTK6* transgene in a mice model concurrently or in tumour xenografts

may further confirm the negative growth regulatory role of ALT-PTK6. Further work may also involve investigations with other inhibitors (in combination with Brk inhibition) of signalling pathways that are deregulated in cancer such as mTOR inhibitors (e.g. Everolimus), P13K/Akt inhibitors (e.g. BKM120) as well as monoclonal antibodies (Herceptin) thus providing further overview and impact of Brk inhibition. Validation of *PTK6* transcript ratios and their potential as prognostic factors will need to be determined in other breast cancer patient cohorts as well as in larger tissue samples. Further work may also involve validation of Brk role in response to radiotherapy through determining localisation before and after treatment using tagged plasmids for transfection, especially if ALT-PTK6 plays a role in translocation of the full length form. This may include using genome editing technologies such as CRISPR-Cas9 if no suitable plasmids are available in the future in order assess the role of the short isoform. CRISPR-Cas9 allows for the insertion of a small sequence that encodes a specific tag into genes which in turn allows for the production of a protein as desired by the research and which will include the tag allowing for easier monitoring of the protein (Dewari *et al.*, 2018).

4.0 Chapter 9: Bibliography

Abdulkareem, I. and Zurmi, I. (2012) ‘Review of hormonal treatment of breast cancer’, *Nigerian Journal of Clinical Practice*, 15(1), p. 9. doi: 10.4103/1119-3077.94088.

Ademuyiwa, F. O. *et al.* (2013) ‘Time-trends in survival in young women with breast cancer in a SEER population-based study’, *Breast Cancer Research and Treatment*, 138(1), pp. 241–248. doi: 10.1007/s10549-013-2425-1.

Adeola, F. (2018) ‘Normalization of Gene Expression by Quantitative RT-PCR in Human Cell Line: comparison of 12 Endogenous Reference Genes.’, *Ethiopian journal of health sciences*. College of Public Health and Medical Sciences of Jimma University, 28(6), pp. 741–748. doi: 10.4314/ejhs.v28i6.9.

Ai, M. *et al.* (2013) ‘HER2 regulates Brk/PTK6 stability via upregulating calpastatin, an inhibitor of calpain’, *Cellular signalling*. Department of Experimental Therapeutics, The University of Texas MD Anderson Cancer Center, Houston, TX 77030, USA.: Elsevier Inc, 25(9), pp. 1754–1761. doi: 10.1016/j.cellsig.2013.05.010; 10.1016/j.cellsig.2013.05.010.

Ali, S. and Coombes, R. C. (2002) ‘ENDOCRINE-RESPONSIVE BREAST CANCER AND STRATEGIES FOR COMBATING RESISTANCE’, *Nature Reviews Cancer*, 2(2), pp. 101–112. doi: 10.1038/nrc721.

Allen, M. D. *et al.* (2011) ‘Clinical and functional significance of α9β1 integrin expression in breast cancer: a novel cell-surface marker of the basal phenotype that promotes tumour cell invasion.’, *The Journal of pathology*, 223(5), pp. 646–58. doi: 10.1002/path.2833.

Ankrapp, D. P., Bennett, J. M. and Haslam, S. Z. (1998) ‘Role of epidermal growth factor in the acquisition of ovarian steroid hormone responsiveness in the normal mouse mammary gland’, *Journal of Cellular Physiology*, 174(2), pp. 251–260. doi: 10.1002/(SICI)1097-4652(199802)174:2<251::AID-JCP12>3.0.CO;2-F.

Apostolou, P. and Fostira, F. (2013) ‘Hereditary breast cancer: the era of new susceptibility genes.’, *BioMed research international*. Hindawi, 2013, p. 747318. doi: 10.1155/2013/747318.

Arora, A. and Scholar, E. M. (2005) ‘Role of tyrosine kinase inhibitors in cancer therapy’, *The Journal of pharmacology and experimental therapeutics*. University of Nebraska College of Medicine, Department of Pharmacology and Experimental Neuroscience, 985800 Nebraska Medical Center, Omaha, NE 68198-5800, USA., 315(3), pp. 971–979.

doi: 10.1124/jpet.105.084145.

Athma, P., Rappaport, R. and Swift, M. (1996) ‘Molecular genotyping shows that ataxia-telangiectasia heterozygotes are predisposed to breast cancer.’, *Cancer genetics and cytogenetics*, 92(2), pp. 130–4. Available at: http://www.ncbi.nlm.nih.gov/pubmed/8976369 (Accessed: 12 October 2017).

Aubele, M. *et al.* (2007) ‘PTK (protein tyrosine kinase)-6 and HER2 and 4, but not HER1 and 3 predict long-term survival in breast carcinomas’, *British journal of cancer*. GSF-National Research Center for Environment and Health, Institute of Pathology, D-85764 Neuherberg, Germany. aubele@gsf.de, 96(5), pp. 801–807. doi: 10.1038/sj.bjc.6603613.

Aubele, M. *et al.* (2008) ‘Prognostic value of protein tyrosine kinase 6 (PTK6) for long-term survival of breast cancer patients’, *British journal of cancer*. Institute of Pathology, Helmholtz Centre Munich, German Research Centre for Environmental Health, Neuherberg D-85764, Germany. aubele@helmholtz-muenchen.de, 99(7), pp. 1089–1095. doi: 10.1038/sj.bjc.6604660; 10.1038/sj.bjc.6604660.

Aubele, M. *et al.* (2009) ‘Overexpression of PTK6 (breast tumor kinase) protein--a prognostic factor for long-term breast cancer survival--is not due to gene amplification’, *Virchows Archiv : an international journal of pathology*. Institute of Pathology, Helmholtz Zentrum Munchen, German Research Center for Environmental Health, 85764 Neuherberg, Germany. aubele@helmholtz-muenchen.de, 455(2), pp. 117–123. doi: 10.1007/s00428-009-0809-8; 10.1007/s00428-009-0809-8.

Aubele, M. *et al.* (2010) ‘In situ quantification of HER2-protein tyrosine kinase 6 (PTK6) protein-protein complexes in paraffin sections from breast cancer tissues’, *British journal of cancer*. Institute of Pathology, Helmholtz Zentrum Munchen, German Research Center for Environmental Health, D-85764 Neuherberg, Germany. aubele@helmholtz-muenchen.de, 103(5), pp. 663–667. doi: 10.1038/sj.bjc.6605836; 10.1038/sj.bjc.6605836.

Aykul, S. and Martinez-Hackert, E. (2016) ‘Determination of half-maximal inhibitory concentration using biosensor-based protein interaction analysis’, *Analytical Biochemistry*, 508, pp. 97–103. doi: 10.1016/j.ab.2016.06.025.

Azim, H. A. *et al.* (2011) ‘Long-term toxic effects of adjuvant chemotherapy in breast cancer’, *Annals of Oncology*. Oxford University Press, 22(9), pp. 1939–1947. doi: 10.1093/annonc/mdq683.

Bahmed, K. *et al.* (2011) 'End-processing during non-homologous end-joining: a role for exonuclease 1', *Nucleic Acids Research*, 39(3), pp. 970–978. doi: 10.1093/nar/gkq886.

Bain, J. *et al.* (2007) 'The selectivity of protein kinase inhibitors: a further update', *Biochemical Journal*, 408(3), pp. 297–315. doi: 10.1042/BJ20070797.

Bamford, S. *et al.* (2004) 'The COSMIC (Catalogue of Somatic Mutations in Cancer) database and website.', *British journal of cancer*. Nature Publishing Group, 91(2), pp. 355–8. doi: 10.1038/sj.bjc.6601894.

Ban, K. A. and Godellas, C. V (2014) 'Epidemiology of breast cancer', *Surgical oncology clinics of North America*. Elsevier, 23(3), pp. 409–422.

Banáth, J. P., MacPhail, S. H. and Olive, P. L. (2004) 'Radiation Sensitivity, H2AX Phosphorylation, and Kinetics of Repair of DNA Strand Breaks in Irradiated Cervical Cancer Cell Lines', *Cancer Research*, 64(19), pp. 7144–7149. doi: 10.1158/0008-5472.CAN-04-1433.

Barker, C. A. and Powell, S. N. (2010) 'Enhancing radiotherapy through a greater understanding of homologous recombination.', *Seminars in radiation oncology*. NIH Public Access, 20(4), p. 267–273.e3. doi: 10.1016/j.semradonc.2010.05.001.

Barker, K. T., Jackson, L. E. and Crompton, M. R. (1997) 'BRK tyrosine kinase expression in a high proportion of human breast carcinomas', *Oncogene*. Section of Cell Biology and Experimental Pathology, Institute of Cancer Research, Sutton, Surrey, UK., 15(7), pp. 799–805. doi: 10.1038/sj.onc.1201241.

Baselga, J. (2011) 'Targeting the phosphoinositide-3 (PI3) kinase pathway in breast cancer', *The oncologist*. Massachusetts General Hospital Cancer Center, Massachusetts General Hospital, Boston, Massachusetts 02114, USA. jbaselga@partners.org, 16 Suppl 1, pp. 12–19. doi: 10.1634/theoncologist.2011-S1-12; 10.1634/theoncologist.2011-S1-12.

Bender, L. M. and Nahta, R. (2008) 'Her2 cross talk and therapeutic resistance in breast cancer', *Frontiers in bioscience : a journal and virtual library*. Department of Pharmacology, School of Medicine, Winship Cancer Institute, Emory University, Atlanta, GA 30322-1013, USA., 13, pp. 3906–3912.

Berthois, Y., Katzenellenbogen, J. A. and Katzenellenbogen, B. S. (1986) 'Phenol red in tissue culture media is a weak estrogen: implications concerning the study of estrogen-

responsive cells in culture.', *Proceedings of the National Academy of Sciences of the United States of America*. National Academy of Sciences, 83(8), pp. 2496–500. Available at: http://www.ncbi.nlm.nih.gov/pubmed/3458212 (Accessed: 19 March 2018).

Bonetta, L. (2005) 'Prime time for real-time PCR', *Nature Methods*, 2(4), pp. 305–312. doi: 10.1038/nmeth0405-305.

Bonotto, M. *et al.* (2014) 'Measures of Outcome in Metastatic Breast Cancer: Insights From a Real-World Scenario', *The Oncologist*, 19(6), pp. 608–615. doi: 10.1634/theoncologist.2014-0002.

Born, M. *et al.* (2005) 'Simultaneous over-expression of the Her2/neu and PTK6 tyrosine kinases in archival invasive ductal breast carcinomas', *The Journal of pathology*. Institute of Pathology, GSF-National Research Centre for Environment and Health, D-85764 Neuherberg, Germany., 205(5), pp. 592–596. doi: 10.1002/path.1720.

Borrego-Soto, G. *et al.* (2015) 'Ionizing radiation-induced DNA injury and damage detection in patients with breast cancer', *Genetics and Molecular Biology*. Sociedade Brasileira de Genética, 38(4), pp. 420–432. doi: 10.1590/S1415-475738420150019.

Børresen, A. L. *et al.* (1992) 'Screening for germ line TP53 mutations in breast cancer patients.', *Cancer research*, 52(11), pp. 3234–6. Available at: http://www.ncbi.nlm.nih.gov/pubmed/1591732 (Accessed: 12 October 2017).

Bourton, E. C. *et al.* (2012) 'Multispectral imaging flow cytometry reveals distinct frequencies of γ-H2AX foci induction in DNA double strand break repair defective human cell lines', *Cytometry Part A*, 81A(2), pp. 130–137. doi: 10.1002/cyto.a.21171.

Bourton, E. C. *et al.* (2013) 'The PARP-1 Inhibitor Olaparib Causes Retention of γ-H2AX Foci in <i>BRCA</i>1 Heterozygote Cells Following Exposure to Gamma Radiation', *Journal of Cancer Therapy*. Scientific Research Publishing, 4(11), pp. 44–52. doi: 10.4236/jct.2013.411A006.

Brauer, P. M. *et al.* (2011) 'The alternative splice variant of protein tyrosine kinase 6 negatively regulates growth and enhances PTK6-mediated inhibition of beta-catenin', *PloS one*. Department of Biochemistry and Molecular Genetics, University of Illinois College of Medicine, Chicago, Illinois, United States of America., 6(3), p. e14789. doi: 10.1371/journal.pone.0014789; 10.1371/journal.pone.0014789.

Brauer, P. M. and Tyner, A. L. (2010) 'Building a better understanding of the intracellular tyrosine kinase PTK6 - BRK by BRK', *Biochimica et biophysica acta*. Department of Biochemistry and Molecular Genetics, University of Illinois at Chicago, Chicago, IL 60607, USA.: Elsevier B.V, 1806(1), pp. 66–73. doi: 10.1016/j.bbcan.2010.02.003; 10.1016/j.bbcan.2010.02.003.

Breslin, S. and O'Driscoll, L. (2016) 'The relevance of using 3D cell cultures, in addition to 2D monolayer cultures, when evaluating breast cancer drug sensitivity and resistance.', *Oncotarget*. Impact Journals, LLC, 7(29), pp. 45745–45756. doi: 10.18632/oncotarget.9935.

Brown, J. M. and Giaccia, A. J. (1998) 'The unique physiology of solid tumors: opportunities (and problems) for cancer therapy.', *Cancer research*, 58(7), pp. 1408–16. Available at: http://www.ncbi.nlm.nih.gov/pubmed/9537241 (Accessed: 30 January 2019).

Bucci, M. K., Bevan, A. and Roach, M. (2005) 'Advances in radiation therapy: conventional to 3D, to IMRT, to 4D, and beyond.', *CA: a cancer journal for clinicians*, 55(2), pp. 117–34. Available at: http://www.ncbi.nlm.nih.gov/pubmed/15761080 (Accessed: 14 January 2018).

Burma, S. *et al.* (2001) 'ATM phosphorylates histone H2AX in response to DNA double-strand breaks.', *The Journal of biological chemistry*, 276(45), pp. 42462–7. doi: 10.1074/jbc.C100466200.

Burmi, R. *et al.* (2009) 'Brk/PTK6 & Bcl-x Proteins Contribute to Reduced Sensitivity to Chemotherapy.', *Cancer Research*. American Association for Cancer Research, 69(24 Supplement), pp. 5068–5068. doi: 10.1158/0008-5472.SABCS-09-5068.

Burness, M. L., Grushko, T. A. and Olopade, O. I. (2010) 'Epidermal Growth Factor Receptor in Triple-Negative and Basal-Like Breast Cancer', *The Cancer Journal*, 16(1), pp. 23–32. doi: 10.1097/PPO.0b013e3181d24fc1.

Bustin, S. A. *et al.* (2009) 'The MIQE Guidelines: Minimum Information for Publication of Quantitative Real-Time PCR Experiments', *Clinical Chemistry*, 55(4), pp. 611–622. doi: 10.1373/clinchem.2008.112797.

Cailleau, R. *et al.* (1974) 'Breast tumor cell lines from pleural effusions.', *Journal of the National Cancer Institute*, 53(3), pp. 661–74. Available at: http://www.ncbi.nlm.nih.gov/pubmed/4412247 (Accessed: 25 April 2018).

Cailleau, R., Olivé, M. and Cruciger, Q. V (1978) 'Long-term human breast carcinoma cell

lines of metastatic origin: preliminary characterization.', *In vitro*, 14(11), pp. 911–5. Available at: http://www.ncbi.nlm.nih.gov/pubmed/730202 (Accessed: 25 April 2018).

Cancer Research UK (2014) *Breast cancer statistics | Cancer Research UK*. Available at: http://www.cancerresearchuk.org/health-professional/cancer-statistics/statistics-by-cancer-type/breast-cancer#heading-Zero (Accessed: 12 October 2017).

Cannan, W. J. and Pederson, D. S. (2017) 'Chromosome Break', *Reference Module in Life Sciences*. Elsevier. doi: 10.1016/B978-0-12-809633-8.06208-7.

Cao, S.-S. and Lu, C.-T. (2016) 'Recent perspectives of breast cancer prognosis and predictive factors.', *Oncology letters*. Spandidos Publications, 12(5), pp. 3674–3678. doi: 10.3892/ol.2016.5149.

Cariati, M., Marlow, R. and Dontu, G. (2011) 'Xenotransplantation of Breast Cancers', in *Methods in molecular biology (Clifton, N.J.)*, pp. 471–482. doi: 10.1007/978-1-61779-080-5_38.

Castro, N. E. and Lange, C. A. (2010) 'Breast tumor kinase and extracellular signal-regulated kinase 5 mediate Met receptor signaling to cell migration in breast cancer cells', *Breast cancer research : BCR*. Department of Pharmacology, University of Minnesota, 321 Church Street S.E., Minneapolis, MN 55455, USA., 12(4), p. R60. doi: 10.1186/bcr2622; 10.1186/bcr2622.

Chakraborty, G., Jain, S. and Kundu, G. C. (2008) 'Osteopontin promotes vascular endothelial growth factor-dependent breast tumor growth and angiogenesis via autocrine and paracrine mechanisms', *Cancer research*. National Center for Cell Science, Pune, India., 68(1), pp. 152–161. doi: 10.1158/0008-5472.CAN-07-2126; 10.1158/0008-5472.CAN-07-2126.

Challapalli, A., Carroll, L. and Aboagye, E. O. (2017) 'Molecular mechanisms of hypoxia in cancer.', *Clinical and translational imaging*. Springer, 5(3), pp. 225–253. doi: 10.1007/s40336-017-0231-1.

Chan, E. and Nimnual, A. S. (2010) 'Deregulation of the cell cycle by breast tumor kinase (Brk)', *International journal of cancer.Journal international du cancer*. Department of Pediatric Hematology/Oncology, State University of New York at Stony Brook, Stony Brook, New York 11794, USA., 127(11), pp. 2723–2731. doi: 10.1002/ijc.25263; 10.1002/ijc.25263.

Chanas-Sacré, G. *et al.* (1999) 'Identification of PSF, the polypyrimidine tract-binding protein-associated splicing factor, as a developmentally regulated neuronal protein', *Journal of Neuroscience Research*, 57(1), pp. 62–73. doi: 10.1002/(SICI)1097-4547(19990701)57:1<62::AID-JNR7>3.0.CO;2-Y.

Chang, M. (2012) 'Tamoxifen resistance in breast cancer.', *Biomolecules & therapeutics*. Korean Society of Applied Pharmacology, 20(3), pp. 256–67. doi: 10.4062/biomolther.2012.20.3.256.

Chen, H. Y. *et al.* (2004) 'Brk activates rac1 and promotes cell migration and invasion by phosphorylating paxillin', *Molecular and cellular biology*. Institute of Molecular Medicine, College of Medicine, National Taiwan University, Taipei, Taiwan., 24(24), pp. 10558–10572. doi: 10.1128/MCB.24.24.10558-10572.2004.

Chen, T. *et al.* (1999) 'A role for the GSG domain in localizing Sam68 to novel nuclear structures in cancer cell lines.', *Molecular biology of the cell*. American Society for Cell Biology, 10(9), pp. 3015–33. Available at: http://www.ncbi.nlm.nih.gov/pubmed/10473643 (Accessed: 23 April 2018).

Chen, Y.-C. *et al.* (2008) 'Activation of phosphoinositide 3-kinase by the NBS1 DNA repair protein through a novel activation motif', *Journal of Molecular Medicine*, 86(4), pp. 401–412. doi: 10.1007/s00109-008-0302-x.

Cho, N. L. *et al.* (2012) 'Global tyrosine kinome profiling of human thyroid tumors identifies Src as a promising target for invasive cancers', *Biochemical and biophysical research communications*. Department of Surgery, Brigham and Women's Hospital, Boston, MA 02115, USA. nlcho@partners.org: Elsevier Inc, 421(3), pp. 508–513. doi: 10.1016/j.bbrc.2012.04.034 [doi].

Claus, E. B., Risch, N. and Thompson, W. D. (1991) 'Genetic analysis of breast cancer in the cancer and steroid hormone study', *American Journal of Human Genetics*. Department of Epidemiology and Public Health, Yale University School of Medicine, New Haven, CT 06510., 48(2), pp. 232–242.

Clemons, M., Danson, S. and Howell, A. (2002) 'Tamoxifen ("Nolvadex"): a review.', *Cancer treatment reviews*. Elsevier, 28(4), pp. 165–80. doi: 10.1016/S0305-7372(02)00036-1.

Collaborative Group on Hormonal Factors in Breast Cancer, C. G. on H. F. in B. (2012) 'Menarche, menopause, and breast cancer risk: individual participant meta-analysis, including 118 964 women with breast cancer from 117 epidemiological studies.', *The Lancet. Oncology*. Elsevier, 13(11), pp. 1141–51. doi: 10.1016/S1470-2045(12)70425-4.

Collignon, J. *et al.* (2016) 'Triple-negative breast cancer: treatment challenges and solutions.', *Breast cancer (Dove Medical Press)*. Dove Press, 8, pp. 93–107. doi: 10.2147/BCTT.S69488.

Conley, S. J. *et al.* (2016) 'HER2 drives Mucin-like 1 to control proliferation in breast cancer cells', *Oncogene*. Nature Publishing Group, 35(32), pp. 4225–4234. doi: 10.1038/onc.2015.487.

Cortazar, P. *et al.* (2014) 'Pathological complete response and long-term clinical benefit in breast cancer: the CTNeoBC pooled analysis.', *Lancet (London, England)*. Elsevier, 384(9938), pp. 164–72. doi: 10.1016/S0140-6736(13)62422-8.

Cross, M. J. *et al.* (2003) 'VEGF-receptor signal transduction', *Trends in Biochemical Sciences*, 28(9), pp. 488–494. doi: 10.1016/S0968-0004(03)00193-2.

Cuny, G. D. *et al.* (2012) 'Structure–activity relationship study of beta-carboline derivatives as haspin kinase inhibitors', *Bioorganic & Medicinal Chemistry Letters*, 22(5), pp. 2015–2019. doi: 10.1016/j.bmcl.2012.01.028.

Dai, X. *et al.* (2016) 'Cancer Hallmarks, Biomarkers and Breast Cancer Molecular Subtypes', *Journal of Cancer*, 7(10), pp. 1281–1294. doi: 10.7150/jca.13141.

Dales, J.-P. *et al.* (2005) 'Overexpression of hypoxia-inducible factor HIF-1α predicts early relapse in breast cancer: Retrospective study in a series of 745 patients', *International Journal of Cancer*, 116(5), pp. 734–739. doi: 10.1002/ijc.20984.

Danforth Jr, D. N. (2013) 'Disparities in breast cancer outcomes between Caucasian and African American women: a model for describing the relationship of biological and nonbiological factors', *Breast cancer research*. BioMed Central, 15(3), p. 208.

Daoud, S. S., Leathers, C. W. and Hurst, J. M. (2002) 'p53 Expression, growth, and spontaneous metastasis of the human GI 101 breast carcinoma in athymic nude mice', *Journal of Experimental Therapeutics and Oncology*. Blackwell Science Inc, 2(2), pp. 121–127. doi: 10.1046/j.1359-4117.2002.01018.x.

Deakin, N. O. and Turner, C. E. (2008) ‘Paxillin comes of age’, *Journal of cell science*, 121(Pt 15), pp. 2435–2444. doi: 10.1242/jcs.018044.

Derry, J. J. *et al.* (2000) ‘Sik (BRK) phosphorylates Sam68 in the nucleus and negatively regulates its RNA binding ability’, *Molecular and cellular biology*. Departments of Molecular Genetics and Medicine, University of Illinois at Chicago, Chicago, Illinois 60607, USA., 20(16), pp. 6114–6126.

Derry, J. J. *et al.* (2003) ‘Altered localization and activity of the intracellular tyrosine kinase BRK/Sik in prostate tumor cells’, *Oncogene*. Department of Molecular Genetics, University of Illinois at Chicago, Chicago, IL 60607, USA., 22(27), pp. 4212–4220. doi: 10.1038/sj.onc.1206465.

Dewari, P. S. *et al.* (2018) ‘An efficient and scalable pipeline for epitope tagging in mammalian stem cells using Cas9 ribonucleoprotein.’, *eLife*. eLife Sciences Publications, Ltd, 7. doi: 10.7554/eLife.35069.

Dittmann, K. *et al.* (2017) ‘New roles for nuclear EGFR in regulating the stability and translation of mRNAs associated with VEGF signaling’, *PLOS ONE*. Edited by C. J. Wilusz, 12(12), p. e0189087. doi: 10.1371/journal.pone.0189087.

Dorgan, J. F. *et al.* (2001) ‘Serum hormones and the alcohol-breast cancer association in postmenopausal women.’, *Journal of the National Cancer Institute*, 93(9), pp. 710–5. Available at: http://www.ncbi.nlm.nih.gov/pubmed/11333294 (Accessed: 12 October 2017).

Dossus, L. and Benusiglio, P. R. (2015) ‘Lobular breast cancer: incidence and genetic and non-genetic risk factors’, *Breast Cancer Research*. BioMed Central, 17(1), p. 37.

Dunnwald, L. K., Rossing, M. A. and Li, C. I. (2007) ‘Hormone receptor status, tumor characteristics, and prognosis: a prospective cohort of breast cancer patients’, *Breast Cancer Research*, 9(1), p. R6. doi: 10.1186/bcr1639.

Early Breast Cancer Trialists’ Collaborative Group (EBCTCG) (2005) ‘Effects of chemotherapy and hormonal therapy for early breast cancer on recurrence and 15-year survival: an overview of the randomised trials’, *The Lancet*, 365(9472), pp. 1687–1717. doi: 10.1016/S0140-6736(05)66544-0.

Early Breast Cancer Trialists’ Collaborative Group (EBCTCG) *et al.* (2011) ‘Effect of radiotherapy after breast-conserving surgery on 10-year recurrence and 15-year breast

cancer death: meta-analysis of individual patient data for 10,801 women in 17 randomised trials.', *Lancet (London, England)*, 378(9804), pp. 1707–16. doi: 10.1016/S0140-6736(11)61629-2.

Easty, D. J. *et al.* (1997) 'Loss of expression of receptor tyrosine kinase family genes PTK7 and SEK in metastatic melanoma', *International journal of cancer.Journal international du cancer*. St. George's Hospital Medical School, London, UK., 71(6), pp. 1061–1065.

Eccles, S. A. *et al.* (2013) 'Critical research gaps and translational priorities for the successful prevention and treatment of breast cancer', *Breast cancer research : BCR*, 15(5), p. R92. doi: 10.1186/bcr3493.

El-Rifai, W. *et al.* (1998) 'Consistent genetic alterations in xenografts of proximal stomach and gastro-esophageal junction adenocarcinomas', *Cancer research*. Department of Medical Genetics, University of Helsinki, Finland., 58(1), pp. 34–37.

Engen, J. R. *et al.* (2008) 'Structure and dynamic regulation of Src-family kinases', *Cellular and Molecular Life Sciences*, 65(19), pp. 3058–3073. doi: 10.1007/s00018-008-8122-2.

Erban, J. K. and Lau, J. (2006) 'On the Toxicity of Chemotherapy for Breast Cancer—the Need for Vigilance', *JNCI: Journal of the National Cancer Institute*. Oxford University Press, 98(16), pp. 1096–1097. doi: 10.1093/jnci/djj338.

Eriksson, D. and Stigbrand, T. (2010) 'Radiation-induced cell death mechanisms', *Tumor Biology*, 31(4), pp. 363–372. doi: 10.1007/s13277-010-0042-8.

Eroles, P. *et al.* (2012) 'Molecular biology in breast cancer: Intrinsic subtypes and signaling pathways', *Cancer Treatment Reviews*, 38(6), pp. 698–707. doi: 10.1016/j.ctrv.2011.11.005.

Fan, C. *et al.* (2011) 'Detection of Brk expression in non-small cell lung cancer: clinicopathological relevance', *Tumour biology : the journal of the International Society for Oncodevelopmental Biology and Medicine*. Department of Pathology, First Affiliated Hospital and College of Basic Medical Sciences of China Medical University, 110001, Shenyang, China. fanchuifeng@yeah.net, 32(5), pp. 873–880. doi: 10.1007/s13277-011-0188-z; 10.1007/s13277-011-0188-z.

Fan, S. *et al.* (2005) 'Role of NF-κB signaling in hepatocyte growth factor/scatter factor-mediated cell protection', *Oncogene*, 24(10), pp. 1749–1766. doi: 10.1038/sj.onc.1208327.

Fanelli, M. A. *et al.* (1996) ‘Estrogen receptors, progesterone receptors, and cell proliferation in human breast cancer’, *Breast Cancer Research and Treatment*. Kluwer Academic Publishers, 37(3), pp. 217–228. doi: 10.1007/BF01806503.

Fearon, A. E., Gould, C. R. and Grose, R. P. (2013) ‘FGFR signalling in women’s cancers’, *The international journal of biochemistry & cell biology*. Centre for Tumour Biology, Barts Cancer Institute - A Cancer Research UK Centre of Excellence, Queen Mary University of London, John Vane Science Centre, Charterhouse Square, London EC1M 6BQ, United Kingdom. Electronic address: a.e.fearon@qmul.ac.uk.: Elsevier Ltd, 45(12), pp. 2832–2842. doi: 10.1016/j.biocel.2013.09.017; 10.1016/j.biocel.2013.09.017.

Feracci, M. *et al.* (2016) ‘Structural basis of RNA recognition and dimerization by the STAR proteins T-STAR and Sam68’, *Nature Communications*, 7, p. 10355. doi: 10.1038/ncomms10355.

Filmus, J. *et al.* (1987) ‘Epidermal growth factor receptor gene-amplified MDA-468 breast cancer cell line and its nonamplified variants’, *Molecular and cellular biology*, 7(1), pp. 251–257.

Fink, M. Y. and Chipuk, J. E. (2013) ‘Survival of HER2-Positive Breast Cancer Cells: Receptor Signaling to Apoptotic Control Centers’, *Genes & cancer*. Department of Biomedical Sciences, Long Island University Post, Brookville, NY, USA., 4(5–6), pp. 187–195. doi: 10.1177/1947601913488598; 10.1177/1947601913488598.

Fischer, G., Rossmann, M. and Hyvönen, M. (2015) ‘Alternative modulation of protein–protein interactions by small molecules’, *Current Opinion in Biotechnology*. Elsevier Current Trends, 35, pp. 78–85. doi: 10.1016/J.COPBIO.2015.04.006.

Fogh, J., Fogh, J. M. and Orfeo, T. (1977) ‘One hundred and twenty-seven cultured human tumor cell lines producing tumors in nude mice.’, *Journal of the National Cancer Institute*, 59(1), pp. 221–6. Available at: http://www.ncbi.nlm.nih.gov/pubmed/327080 (Accessed: 13 October 2017).

Fogh, J. and Trempe, G. (1975) ‘New Human Tumor Cell Lines’, in *Human Tumor Cells in Vitro*. Boston, MA: Springer US, pp. 115–159. doi: 10.1007/978-1-4757-1647-4_5.

Foulkes, W. D., Smith, I. E. and Reis-Filho, J. S. (2010) ‘Triple-Negative Breast Cancer’, *New England Journal of Medicine*. Massachusetts Medical Society , 363(20), pp. 1938–

1948. doi: 10.1056/NEJMra1001389.

Frisch, S. M. and Francis, H. (1994) ‘Disruption of epithelial cell-matrix interactions induces apoptosis’, *The Journal of cell biology*. La Jolla Cancer Research Foundation, California 92037., 124(4), pp. 619–626.

Giebeler, N. and Zigrino, P. (2016) ‘A Disintegrin and Metalloprotease (ADAM): Historical Overview of Their Functions.’, *Toxins*. Multidisciplinary Digital Publishing Institute (MDPI), 8(4), p. 122. doi: 10.3390/toxins8040122.

Gierut, J. *et al.* (2011) ‘Disruption of the mouse protein tyrosine kinase 6 gene prevents STAT3 activation and confers resistance to azoxymethane’, *Gastroenterology*. Department of Biochemistry and Molecular Genetics, University of Illinois at Chicago, Chicago, Illinois 60607, USA.: AGA Institute. Published by Elsevier Inc, 141(4), pp. 1371–80, 1380–2. doi: 10.1053/j.gastro.2011.06.071; 10.1053/j.gastro.2011.06.071.

Gierut, J. J. *et al.* (2012) ‘Targeting protein tyrosine kinase 6 enhances apoptosis of colon cancer cells following DNA damage’, *Molecular cancer therapeutics*. Department of Biochemistry and Molecular Genetics, University of Illinois College of Medicine, M/C 669, 900 South Ashland Avenue, Chicago, IL 60607, USA.: AACR, 11(11), pp. 2311–2320. doi: 10.1158/1535-7163.MCT-12-0009; 10.1158/1535-7163.MCT-12-0009.

Gutierrez, M. C. *et al.* (2005) ‘Molecular Changes in Tamoxifen-Resistant Breast Cancer: Relationship Between Estrogen Receptor, HER-2, and p38 Mitogen-Activated Protein Kinase’, *Journal of Clinical Oncology*, 23(11), pp. 2469–2476. doi: 10.1200/JCO.2005.01.172.

Haegebarth, A. *et al.* (2004) ‘The nuclear tyrosine kinase BRK/Sik phosphorylates and inhibits the RNA-binding activities of the Sam68-like mammalian proteins SLM-1 and SLM-2’, *The Journal of biological chemistry*. Departments of Biochemistry and Molecular Genetics, University of Illinois, Chicago, Illinois 60607, USA., 279(52), pp. 54398–54404. doi: 10.1074/jbc.M409579200.

Haegebarth, A. *et al.* (2006) ‘Protein tyrosine kinase 6 negatively regulates growth and promotes enterocyte differentiation in the small intestine’, *Molecular and cellular biology*. University of Illinois College of Medicine, Department of Biochemistry and Molecular Genetics, M/C 669, 900 S. Ashland Ave., Chicago, IL 60607, USA., 26(13), pp. 4949–4957. doi: 10.1128/MCB.01901-05.

Haegebarth, A. *et al.* (2009) ‘Induction of protein tyrosine kinase 6 in mouse intestinal crypt epithelial cells promotes DNA damage-induced apoptosis’, *Gastroenterology*. Department of Biochemistry and Molecular Genetics, University of Illinois at Chicago, Chicago, Illinois 60607, USA., 137(3), pp. 945–954. doi: 10.1053/j.gastro.2009.05.054; 10.1053/j.gastro.2009.05.054.

Haegebarth, A., Nunez, R. and Tyner, A. L. (2005) ‘The intracellular tyrosine kinase Brk sensitizes non-transformed cells to inducers of apoptosis’, *Cell cycle (Georgetown, Tex.)*. Department of Biochemistry and Molecular Genetics, University of Illinois, Chicago, Illinois, USA., 4(9), pp. 1239–1246.

Hainaut, P. (2013) ‘TP53: Coordinator of the Processes That Underlie the Hallmarks of Cancer’, in *p53 in the Clinics*. New York, NY: Springer New York, pp. 1–23. doi: 10.1007/978-1-4614-3676-8_1.

Hamajima, N. *et al.* (2002) ‘Alcohol, tobacco and breast cancer--collaborative reanalysis of individual data from 53 epidemiological studies, including 58,515 women with breast cancer and 95,067 women without the disease.’, *British journal of cancer*, 87(11), pp. 1234–45. doi: 10.1038/sj.bjc.6600596.

Hammond, E. M. and Muschel, R. J. (2014) ‘Radiation and ATM inhibition: the heart of the matter.’, *The Journal of clinical investigation*. American Society for Clinical Investigation, 124(8), pp. 3289–91. doi: 10.1172/JCI77195.

Hanahan, D. and Weinberg, R. A. (2011) ‘Hallmarks of cancer: the next generation.’, *Cell*, 144(5), pp. 646–74. doi: 10.1016/j.cell.2011.02.013.

Hartlerode, A. J. and Scully, R. (2009) ‘Mechanisms of double-strand break repair in somatic mammalian cells’, *Biochemical Journal*, 423(2), pp. 157–168. doi: 10.1042/BJ20090942.

Harvey, A. and Burmi, R. (2011) ‘Future Therapeutic Strategies: Implications for Brk Targeting’, in Gunduz, E. and Gunduz, M. (eds) *Breast Cancer - Current and alternative therapeutic modalities*, p. 413.

Harvey, A. J. *et al.* (2009) ‘Brk protects breast cancer cells from autophagic cell death induced by loss of anchorage’, *The American journal of pathology*. Brunel Institute for Cancer Genetics and Pharmacogenomics, Biosciences, School of Health Sciences and

Social Care, Brunel University, Kingston Lane, Uxbridge, Middlesex, United Kingdom. amanda.harvey@brunel.ac.uk, 175(3), pp. 1226–1234. doi: 10.2353/ajpath.2009.080811; 10.2353/ajpath.2009.080811.

Harvey, A. J. and Crompton, M. R. (2003) 'Use of RNA interference to validate Brk as a novel therapeutic target in breast cancer: Brk promotes breast carcinoma cell proliferation', *Oncogene*. School of Biological Sciences, Royal Holloway University of London, Egham, Surrey TW20 OEX, UK., 22(32), pp. 5006–5010. doi: 10.1038/sj.onc.1206577.

Harvey, A. J. and Crompton, M. R. (2004) 'The Brk protein tyrosine kinase as a therapeutic target in cancer: opportunities and challenges', *Anti-Cancer Drugs*. School of Biological Sciences, Royal Holloway University of London, Egham, Surrey TW20 0EX, UK., 15(2), pp. 107–111.

Hayes, D. F. and Thor, A. D. (2002) 'c-erbB-2 in breast cancer: development of a clinically useful marker', *Seminars in oncology*. University of Michigan Comprehensive Cancer Center, Department of Medicine, University of Michigan Medical Center, Ann Arbor, MI, USA.: Elsevier Science (USA), 29(3), pp. 231–245.

Hein, A. L., Ouellette, M. M. and Yan, Y. (2014) 'Radiation-induced signaling pathways that promote cancer cell survival (review).', *International journal of oncology*, 45(5), pp. 1813–9. doi: 10.3892/ijo.2014.2614.

Helt, C. E. *et al.* (2005) 'Ataxia telangiectasia mutated (ATM) and ATM and Rad3-related protein exhibit selective target specificities in response to different forms of DNA damage.', *The Journal of biological chemistry*, 280(2), pp. 1186–92. doi: 10.1074/jbc.M410873200.

Henderson, I. C. *et al.* (2003) 'Improved Outcomes From Adding Sequential Paclitaxel but Not From Escalating Doxorubicin Dose in an Adjuvant Chemotherapy Regimen for Patients With Node-Positive Primary Breast Cancer', *Journal of Clinical Oncology*, 21(6), pp. 976–983. doi: 10.1200/JCO.2003.02.063.

Henson, K. E. *et al.* (2013) 'Radiation-related mortality from heart disease and lung cancer more than 20 years after radiotherapy for breast cancer', *British Journal of Cancer*, 108(1), pp. 179–182. doi: 10.1038/bjc.2012.575.

Herschkowitz, J. I. *et al.* (2007) 'Identification of conserved gene expression features between murine mammary carcinoma models and human breast tumors', *Genome Biology*,

8(5), p. R76. doi: 10.1186/gb-2007-8-5-r76.

Herzog, B. *et al.* (2011) 'VEGF binding to NRP1 is essential for VEGF stimulation of endothelial cell migration, complex formation between NRP1 and VEGFR2, and signaling via FAK Tyr407 phosphorylation.', *Molecular biology of the cell*. American Society for Cell Biology, 22(15), pp. 2766–76. doi: 10.1091/mbc.E09-12-1061.

den Hollander, P., Savage, M. I. and Brown, P. H. (2013) 'Targeted Therapy for Breast Cancer Prevention'. Department of Clinical Cancer Prevention, The University of Texas MD Anderson Cancer Center , Houston, TX , USA., 3, p. 250.

Holliday, D. L. and Speirs, V. (2011) 'Choosing the right cell line for breast cancer research', *Breast Cancer Research*, 13(4), p. 215. doi: 10.1186/bcr2889.

Holmes, M. D. and Willett, W. C. (2004) 'Does diet affect breast cancer risk?', *Breast Cancer Research*, 6(4), p. 170. doi: 10.1186/bcr909.

Hong, E. *et al.* (2001) 'Complete sequence-specific 1H, 13C and 15N resonance assignments of the human PTK6 SH2 domain', *Journal of Biomolecular NMR*. Netherlands, 19(3), pp. 291–292.

Hurst, J. *et al.* (1993) 'A novel model of a metastatic human breast tumour xenograft line.', *British journal of cancer*. Nature Publishing Group, 68(2), pp. 274–6. Available at: http://www.ncbi.nlm.nih.gov/pubmed/8394103 (Accessed: 3 October 2017).

Hussain, H. A. and Harvey, A. J. (2014) 'Evolution of breast cancer therapeutics: Breast tumour kinase's role in breast cancer and hope for breast tumour kinase targeted therapy.', *World journal of clinical oncology*. Baishideng Publishing Group Inc, 5(3), pp. 299–310. doi: 10.5306/wjco.v5.i3.299.

Ie Kim, H. and Lee, S. T. (2009) 'Oncogenic functions of PTK6 are enhanced by its targeting to plasma membrane but abolished by its targeting to nucleus', *Journal of Biochemistry*. Department of Biochemistry, Yonsei University, Seoul, Republic of Korea., 146(1), pp. 133–139. doi: 10.1093/jb/mvp050; 10.1093/jb/mvp050.

Ignatiadis, M. *et al.* (2009) 'A Meta-Analysis of Gene Expression Profiling Studies Identifies Clinically Relevant Oncogenic Pathways in Basal-Like Breast Cancer.':, *Cancer Research*. American Association for Cancer Research, 69(24 Supplement), pp. 106–106. doi: 10.1158/0008-5472.SABCS-09-106.

Irie, H. Y. *et al.* (2010) 'PTK6 regulates IGF-1-induced anchorage-independent survival', *PloS one*. Department of Cell Biology, Harvard Medical School, Boston, Massachusetts, United States of America., 5(7), p. e11729. doi: 10.1371/journal.pone.0011729; 10.1371/journal.pone.0011729.

Irvin Jr, W., Muss, H. B. and Mayer, D. K. (2011) 'Symptom management in metastatic breast cancer', *The oncologist*. R.N., A.O.C.N., F.A.A.N., School of Nursing, Carrington Hall #7460, UNC-Chapel Hill, Chapel Hill, North Carolina 27599-7460, USA., 16(9), pp. 1203–1214. doi: 10.1634/theoncologist.2011-0159; 10.1634/theoncologist.2011-0159.

Isakoff, S. J. (2010) 'Triple-negative breast cancer: role of specific chemotherapy agents.', *Cancer journal (Sudbury, Mass.)*. NIH Public Access, 16(1), pp. 53–61. doi: 10.1097/PPO.0b013e3181d24ff7.

Ito, K. *et al.* (2016) 'PTK6 Inhibition Suppresses Metastases of Triple-Negative Breast Cancer via SNAIL-Dependent E-Cadherin Regulation', *Cancer Research*, 76(15), pp. 4406–4417. doi: 10.1158/0008-5472.CAN-15-3445.

Ito, K. *et al.* (2017) 'PTK6 regulates growth and survival of endocrine therapy-resistant ER+ breast cancer cells', *npj Breast Cancer*. Nature Publishing Group, 3(1), p. 45. doi: 10.1038/s41523-017-0047-1.

Jackson, J. G. and Lozano, G. (2017) 'TNBC invasion: downstream of STAT3.', *Oncotarget*. Impact Journals, LLC, 8(13), pp. 20517–20518. doi: 10.18632/oncotarget.15259.

Ji, J. *et al.* (2017) 'Phosphorylated fraction of H2AX as a measurement for DNA damage in cancer cells and potential applications of a novel assay.', *PloS one*. Public Library of Science, 12(2), p. e0171582. doi: 10.1371/journal.pone.0171582.

Jiang, J. *et al.* (2017) 'Targeting BRK-Positive Breast Cancers with Small-Molecule Kinase Inhibitors', *Cancer Research*, 77(1), pp. 175–186. doi: 10.1158/0008-5472.CAN-16-1038.

Juan, R. (2011) *Rosai and Ackerman's Surgical Pathology*. 10th edn. France: Elsevier.

Kałużna, M., Kuras, A. and Puławska, J. (2017) 'Validation of reference genes for the normalization of the RT-qPCR gene expression of virulence genes of Erwinia amylovora in apple shoots', *Scientific Reports*. Nature Publishing Group, 7(1), p. 2034. doi: 10.1038/s41598-017-02078-4.

Kamalati, T. *et al.* (1996) 'Brk, a breast tumor-derived non-receptor protein-tyrosine kinase,

sensitizes mammary epithelial cells to epidermal growth factor', *The Journal of biological chemistry*. Section of Cell Biology and Experimental Pathology, Institute of Cancer Research, Sutton, Surrey, United Kingdom., 271(48), pp. 30956–30963.

Kamalati, T. *et al.* (2000) 'Expression of the BRK tyrosine kinase in mammary epithelial cells enhances the coupling of EGF signalling to PI 3-kinase and Akt, via erbB3 phosphorylation', *Oncogene*. School of Biological Sciences, Royal Holloway, University of London, Egham, Surrey, UK., 19(48), pp. 5471–5476. doi: 10.1038/sj.onc.1203931.

Kaminska, M. *et al.* (2015) 'Breast cancer risk factors', *Przeglad menopauzalny = Menopause review*. Clinical Oncology Ward, St. John's Cancer Center, Lublin, Poland.; Clinical Oncology Ward, St. John's Cancer Center, Lublin, Poland.; Clinical Oncology Ward, St. John's Cancer Center, Lublin, Poland.; 2 Department of Gynecology, Medical Universi(TRUNCATED, 14(3), pp. 196–202.

Kang, S. A. *et al.* (2010) 'PTK6 inhibits down-regulation of EGF receptor through phosphorylation of ARAP1', *The Journal of biological chemistry*. Department of Biochemistry, College of Life Science and Biotechnology, Yonsei University, Seoul 120-749, Korea., 285(34), pp. 26013–26021. doi: 10.1074/jbc.M109.088971; 10.1074/jbc.M109.088971.

Kang, S. A. *et al.* (2012) 'Hsp90 rescues PTK6 from proteasomal degradation in breast cancer cells', *The Biochemical journal*. Department of Biochemistry, College of Life Science and Biotechnology, Yonsei University, Seoul 120-749, Korea., 447(2), pp. 313–320. doi: 10.1042/BJ20120803.

Kang, S. A. and Lee, S. T. (2013) 'PTK6 promotes degradation of c-Cbl through PTK6-mediated phosphorylation', *Biochemical and biophysical research communications*. Department of Biochemistry, College of Life Science and Biotechnology, Yonsei University, Seoul 120-749, Republic of Korea.: Elsevier Inc, 431(4), pp. 734–739. doi: 10.1016/j.bbrc.2013.01.046; 10.1016/j.bbrc.2013.01.046.

Kao, J. *et al.* (2009) 'Molecular Profiling of Breast Cancer Cell Lines Defines Relevant Tumor Models and Provides a Resource for Cancer Gene Discovery', *PLoS ONE*. Edited by M. V. Blagosklonny. Public Library of Science, 4(7), p. e6146. doi: 10.1371/journal.pone.0006146.

Karimian, A. *et al.* (2019) 'Crosstalk between Phosphoinositide 3-kinase/Akt signaling

pathway with DNA damage response and oxidative stress in cancer', *Journal of Cellular Biochemistry*. John Wiley & Sons, Ltd, 120(6), pp. 10248–10272. doi: 10.1002/jcb.28309.

Kasprzycka, M. *et al.* (2006) 'Expression and oncogenic role of Brk (PTK6/Sik) protein tyrosine kinase in lymphocytes', *The American journal of pathology*. Department of Pathology and Laboratory Medicine, University of Pennsylvania, Philadelphia, USA., 168(5), pp. 1631–1641. doi: 10.2353/ajpath.2006.050521.

Kato, I. *et al.* (2009) 'African American-preponderant single nucleotide polymorphisms (SNPs) and risk of breast cancer', *Cancer epidemiology*. Elsevier, 33(1), pp. 24–30.

Keydar, I. *et al.* (1979) 'Establishment and characterization of a cell line of human breast carcinoma origin.', *European journal of cancer*, 15(5), pp. 659–70. Available at: http://www.ncbi.nlm.nih.gov/pubmed/228940 (Accessed: 25 April 2018).

Kim, H. and Muller, W. J. (1999) 'The role of the epidermal growth factor receptor family in mammary tumorigenesis and metastasis', *Experimental cell research*. Institute for Molecular Biology and Biotechnology, McMaster University, Hamilton, Ontario, L8S 4K1, Canada.: Academic Press, 253(1), pp. 78–87. doi: 10.1006/excr.1999.4706.

Klinakis, A. *et al.* (2009) 'Igf1r as a therapeutic target in a mouse model of basal-like breast cancer', *Proceedings of the National Academy of Sciences of the United States of America*. Department of Genetics and Development, Columbia University, 1150 St. Nicholas Avenue, New York, NY 10032, USA., 106(7), pp. 2359–2364. doi: 10.1073/pnas.0810221106; 10.1073/pnas.0810221106.

Koboldt, D. C. *et al.* (2012) 'Comprehensive molecular portraits of human breast tumours', *Nature*, 490(7418), pp. 61–70. doi: 10.1038/nature11412.

Kotepui, M. (2016) 'Diet and risk of breast cancer.', *Contemporary oncology (Poznan, Poland)*. Termedia Publishing, 20(1), pp. 13–9. doi: 10.5114/wo.2014.40560.

Kozera, B. and Rapacz, M. (2013) 'Reference genes in real-time PCR.', *Journal of applied genetics*. Springer, 54(4), pp. 391–406. doi: 10.1007/s13353-013-0173-x.

Kuo, L. J. and Yang, L.-X. (2008) 'Gamma-H2AX - a novel biomarker for DNA double-strand breaks.', *In vivo (Athens, Greece)*, 22(3), pp. 305–9. Available at: http://www.ncbi.nlm.nih.gov/pubmed/18610740 (Accessed: 15 January 2018).

Kyndi, M. *et al.* (2008) 'Estrogen receptor, progesterone receptor, HER-2, and response to

postmastectomy radiotherapy in high-risk breast cancer: the Danish Breast Cancer Cooperative Group.', *Journal of clinical oncology : official journal of the American Society of Clinical Oncology*, 26(9), pp. 1419–26. doi: 10.1200/JCO.2007.14.5565.

Lachapelle, J. and Foulkes, W. D. (2011) 'Triple-negative and basal-like breast cancer: implications for oncologists.', *Current oncology (Toronto, Ont.)*. Multimed Inc., 18(4), pp. 161–4. Available at: http://www.ncbi.nlm.nih.gov/pubmed/21874112 (Accessed: 29 September 2017).

Langbois, A. J. *et al.* (1979) 'Morphological and Biochemical Properties of a New Human Breast Cancer Cell Line1', *CANCER RESEARCH*, 39, pp. 2604–2613. Available at: http://cancerres.aacrjournals.org/content/canres/39/7_Part_1/2604.full.pdf (Accessed: 25 April 2018).

Lange, C. A. and Yee, D. (2008) 'Progesterone and breast cancer.', *Women's health (London, England)*. NIH Public Access, 4(2), pp. 151–62. doi: 10.2217/17455057.4.2.151.

Langlands, F. E. *et al.* (2013) 'Breast cancer subtypes: response to radiotherapy and potential radiosensitisation.', *The British journal of radiology*, 86(1023), p. 20120601. doi: 10.1259/bjr.20120601.

Lasfargues, E. Y., Coutinho, W. G. and Redfield, E. S. (1978) 'Isolation of two human tumor epithelial cell lines from solid breast carcinomas.', *Journal of the National Cancer Institute*, 61(4), pp. 967–78. Available at: http://www.ncbi.nlm.nih.gov/pubmed/212572 (Accessed: 25 April 2018).

Lavin, M. F. and Shiloh, Y. (1997) 'THE GENETIC DEFECT IN ATAXIA-TELANGIECTASIA', *Annual Review of Immunology*, 15(1), pp. 177–202. doi: 10.1146/annurev.immunol.15.1.177.

Lee, M. C. and Newman, L. A. (2007) 'Management of Patients with Locally Advanced Breast Cancer', *Surgical Clinics of North America*, 87(2), pp. 379–398. doi: 10.1016/j.suc.2007.01.012.

Lehmann, B. D. *et al.* (2011) 'Identification of human triple-negative breast cancer subtypes and preclinical models for selection of targeted therapies', *Journal of Clinical Investigation*, 121(7), pp. 2750–2767. doi: 10.1172/JCI45014.

Lenferink, A. E. *et al.* (2001) 'ErbB2/neu kinase modulates cellular p27(Kip1) and cyclin D1

through multiple signaling pathways', *Cancer research*. Department of Medicine, Vanderbilt University School of Medicine, Nashville, Tennessee 37232, USA., 61(17), pp. 6583–6591.

Lewanski, C. R. and Gullick, W. J. (2001) 'Radiotherapy and cellular signalling.', *The Lancet. Oncology*, 2(6), pp. 366–70. doi: 10.1016/S1470-2045(00)00391-0.

Li, J. *et al.* (1997) 'PTEN, a putative protein tyrosine phosphatase gene mutated in human brain, breast, and prostate cancer'. Available at: http://science.sciencemag.org/content/275/5308/1943.short (Accessed: 21 September 2017).

Li, X. *et al.* (2012) 'Brk/PTK6 sustains activated EGFR signaling through inhibiting EGFR degradation and transactivating EGFR', *Oncogene*. Department of Experimental Therapeutics, University of Texas MD Anderson Cancer Center, Houston, TX, USA., 31(40), pp. 4372–4383. doi: 10.1038/onc.2011.608; 10.1038/onc.2011.608.

Liaw, D. *et al.* (1997) 'Germline mutations of the PTEN gene in Cowden disease, an inherited breast and thyroid cancer syndrome.', *Nature genetics*, 16(1), pp. 64–7. doi: 10.1038/ng0597-64.

Lin, H. S. *et al.* (2004) 'Identification of tyrosine kinases overexpressed in head and neck cancer', *Archives of Otolaryngology--Head & Neck Surgery*. Department of Otolaryngology/Head and Neck Surgery, Wayne State University, Detroit, MI 48201, USA. hlin@med.wayne.edu, 130(3), pp. 311–316. doi: 10.1001/archotol.130.3.311 [doi].

Ling, C. C., Yorke, E. and Fuks, Z. (2006) 'From IMRT to IGRT: frontierland or neverland?', *Radiotherapy and oncology : journal of the European Society for Therapeutic Radiology and Oncology*, 78(2), pp. 119–22. doi: 10.1016/j.radonc.2005.12.005.

Liu, F., Zhang, H. and Song, H. (2017) 'Upregulation of MEK5 by Stat3 promotes breast cancer cell invasion and metastasis', *Oncology Reports*, 37(1), pp. 83–90. doi: 10.3892/or.2016.5256.

Liu, L. *et al.* (2006) 'Identification of STAT3 as a specific substrate of breast tumor kinase', *Oncogene*. Department of Microbiology and Molecular Genetics, Stony Brook University, Stony Brook, NY 11794-8691, USA., 25(35), pp. 4904–4912. doi: 10.1038/sj.onc.1209501.

Liu, Q. *et al.* (2014) 'Role of AKT signaling in DNA repair and clinical response to cancer therapy', *Neuro-Oncology*. Narnia, 16(10), pp. 1313–1323. doi: 10.1093/neuonc/nou058.

Livak, K. J. and Schmittgen, T. D. (2001) ‘Analysis of Relative Gene Expression Data Using Real-Time Quantitative PCR and the 2−ΔΔCT Method’, *Methods*, 25(4), pp. 402–408. doi: 10.1006/meth.2001.1262.

Llor, X. *et al.* (1999) ‘BRK/Sik expression in the gastrointestinal tract and in colon tumors’, *Clinical cancer research : an official journal of the American Association for Cancer Research*. Department of Molecular Genetics, University of Illinois College of Medicine, Chicago 60607, USA., 5(7), pp. 1767–1777.

Lofgren, K. A. *et al.* (2011) ‘Mammary gland specific expression of Brk/PTK6 promotes delayed involution and tumor formation associated with activation of p38 MAPK’, *Breast cancer research : BCR*. Department of Medicine (Division of Hematology, Oncology, and Transplantation), University of Minnesota, 420 Delaware St. SE, MMC 806, Minneapolis, MN 55455, USA., 13(5), p. R89. doi: 10.1186/bcr2946; 10.1186/bcr2946.

Longley, D. and Johnston, P. (2005) ‘Molecular mechanisms of drug resistance’, *The Journal of Pathology*. John Wiley & Sons, Ltd., 205(2), pp. 275–292. doi: 10.1002/path.1706.

Lü, L. *et al.* (2012) ‘Exocytosis of MTT formazan could exacerbate cell injury’, *Toxicology in Vitro*, 26(4), pp. 636–644. doi: 10.1016/j.tiv.2012.02.006.

Ludyga, N. *et al.* (2011) ‘Impact of protein tyrosine kinase 6 (PTK6) on human epidermal growth factor receptor (HER) signalling in breast cancer’, *Molecular BioSystems*, 7(5), p. 1603. doi: 10.1039/c0mb00286k.

Ludyga, N. *et al.* (2013) ‘Effects of simultaneous knockdown of HER2 and PTK6 on malignancy and tumor progression in human breast cancer cells’, *Molecular cancer research : MCR*. Institut fur Pathologie, Helmholtz Zentrum Munchen, Ingolstaedter Landstrasse 1, 85764 Neuherberg, Germany.: AACR, 11(4), pp. 381–392. doi: 10.1158/1541-7786.MCR-12-0378; 10.1158/1541-7786.MCR-12-0378.

Lukong, K. E., Huot, M. E. and Richard, S. (2009) ‘BRK phosphorylates PSF promoting its cytoplasmic localization and cell cycle arrest’, *Cellular signalling*. Terry Fox Molecular Oncology Group, Lady Davis Institute for Medical Research, Sir Mortimer B. Davis Jewish General Hospital, Canada., 21(9), pp. 1415–1422. doi: 10.1016/j.cellsig.2009.04.008; 10.1016/j.cellsig.2009.04.008.

Lukong, K. E. and Richard, S. (2008) ‘Breast tumor kinase BRK requires kinesin-2 subunit KAP3A in modulation of cell migration’, *Cellular signalling*. Terry Fox Molecular Oncology Group and the Bloomfield Center for Research on Aging, Lady Davis Institute for Medical Research, Sir Mortimer B. Davis Jewish General Hospital, Montreal Quebec, Canada., 20(2), pp. 432–442. doi: 10.1016/j.cellsig.2007.11.003.

Ly, D. *et al.* (2013) ‘An international comparison of male and female breast cancer incidence rates.’, *International journal of cancer*. NIH Public Access, 132(8), pp. 1918–26. doi: 10.1002/ijc.27841.

Ma, S. *et al.* (2012) ‘Identification of PTK6, via RNA sequencing analysis, as a suppressor of esophageal squamous cell carcinoma’, *Gastroenterology*. Department of Pathology, Li Ka Shing Faculty of Medicine, The University of Hong Kong, Hong Kong, China.: AGA Institute. Published by Elsevier Inc, 143(3), pp. 612–675. doi: 10.1053/j.gastro.2012.06.007; 10.1053/j.gastro.2012.06.007.

Mahmoud, K. A. *et al.* (2014) ‘Discovery of 4-anilino α-carbolines as novel Brk inhibitors’, *Bioorganic & Medicinal Chemistry Letters*. Pergamon, 24(8), pp. 1948–1951. doi: 10.1016/J.BMCL.2014.03.002.

Makki, J. (2015) ‘Diversity of Breast Carcinoma: Histological Subtypes and Clinical Relevance’, *Clinical medicine insights.Pathology*. Senior Pathologist, Pathology Department, Hospital Queen Elizabeth, Kota Kinabalu, Sabah, Malaysia., 8, pp. 23–31.

Mamounas, E. P. *et al.* (2005) ‘Paclitaxel After Doxorubicin Plus Cyclophosphamide As Adjuvant Chemotherapy for Node-Positive Breast Cancer: Results From NSABP B-28’, *Journal of Clinical Oncology*, 23(16), pp. 3686–3696. doi: 10.1200/JCO.2005.10.517.

Mao, Z. *et al.* (2008) ‘DNA repair by nonhomologous end joining and homologous recombination during cell cycle in human cells.’, *Cell cycle (Georgetown, Tex.)*. NIH Public Access, 7(18), pp. 2902–6. doi: 10.4161/cc.7.18.6679.

Mariotti, L. G. *et al.* (2013) ‘Use of the γ-H2AX Assay to Investigate DNA Repair Dynamics Following Multiple Radiation Exposures’, *PLoS ONE*. Edited by C. N. Robson. Public Library of Science, 8(11), p. e79541. doi: 10.1371/journal.pone.0079541.

Marková, E., Schultz, N. and Belyaev, I. Y. (2007) ‘Kinetics and dose-response of residual 53BP1/γ-H2AX foci: Co-localization, relationship with DSB repair and clonogenic survival’,

International Journal of Radiation Biology, 83(5), pp. 319–329. doi: 10.1080/09553000601170469.

Marotta, L. L. C. *et al.* (2011) 'The JAK2/STAT3 signaling pathway is required for growth of CD44+CD24– stem cell–like breast cancer cells in human tumors', *Journal of Clinical Investigation*, 121(7), pp. 2723–2735. doi: 10.1172/JCI44745.

Martin, A.-M. and Weber, B. L. (2000) 'Genetic and Hormonal Risk Factors in Breast Cancer', *Journal of the National Cancer Institute*. Oxford University Press, 92(14), pp. 1126–1135. doi: 10.1093/jnci/92.14.1126.

Mayer, B. J. (2001) 'SH3 domains: complexity in moderation', *Journal of cell science*. Department of Genetics and Developmental Biology, University of Connecticut Health Center, Farmington, CT 06030-3301, USA. bmayer@neuron.uchc.edu, 114(Pt 7), pp. 1253–1263.

Mayor, S. (2017) 'Risk of breast cancer recurrence remains for years after endocrine treatment ends, study finds', *BMJ*. British Medical Journal Publishing Group, 359, p. j5167. doi: 10.1136/BMJ.J5167.

Mazouni, C. *et al.* (2007) 'Residual Ductal Carcinoma In Situ in Patients With Complete Eradication of Invasive Breast Cancer After Neoadjuvant Chemotherapy Does Not Adversely Affect Patient Outcome', *Journal of Clinical Oncology*, 25(19), pp. 2650–2655. doi: 10.1200/JCO.2006.08.2271.

McArdle, L. *et al.* (2001) 'Protein Tyrosine Phosphatase Genes Downregulated in Melanoma', *Journal of Investigative Dermatology*, 117(5), pp. 1255–1260. doi: 10.1046/j.0022-202x.2001.01534.x.

Miah, S. *et al.* (2014) 'BRK targets Dok1 for ubiquitin-mediated proteasomal degradation to promote cell proliferation and migration.', *PloS one*. Public Library of Science, 9(2), p. e87684. doi: 10.1371/journal.pone.0087684.

Miah, S., Martin, A. and Lukong, K. E. (2012) 'Constitutive activation of breast tumor kinase accelerates cell migration and tumor growth in vivo', *Oncogenesis*. Department of Biochemistry, College of Medicine, University of Saskatchewan, Saskatoon, Saskatchewan, Canada., 1, p. e11. doi: 10.1038/oncsis.2012.11; 10.1038/oncsis.2012.11.

Miki, Y. *et al.* (1994) 'A strong candidate for the breast and ovarian cancer susceptibility

gene BRCA1.', *Science (New York, N.Y.)*, 266(5182), pp. 66–71. Available at: http://www.ncbi.nlm.nih.gov/pubmed/7545954 (Accessed: 12 October 2017).

Mitchell, P. J. *et al.* (1994) 'Cloning and characterisation of cDNAs encoding a novel non-receptor tyrosine kinase, brk, expressed in human breast tumours', *Oncogene*. Section of Cell Biology and Experimental Pathology, Institute of Cancer Research, Sutton, Surrey, UK., 9(8), pp. 2383–2390.

Mitchell, P. J. *et al.* (1997) 'Characterisation and chromosome mapping of the human non receptor tyrosine kinase gene, brk', *Oncogene*. Haddow Laboratories, Institute of Cancer Research, Sutton, Surrey, UK., 15(12), pp. 1497–1502. doi: 10.1038/sj.onc.1201292.

Mitchell, P. J., Sara, E. A. and Crompton, M. R. (2000) 'A novel adaptor-like protein which is a substrate for the non-receptor tyrosine kinase, BRK', *Oncogene*. Section of Cell Biology and Experimental Pathology, The Breakthrough Toby Robinson Cancer Research Centre, Institute of Cancer Research, 237 Fulham Road, London SW3 6JB, UK., 19(37), pp. 4273–4282. doi: 10.1038/sj.onc.1203775.

Moasser, M. M. *et al.* (2001) 'The tyrosine kinase inhibitor ZD1839 ("Iressa") inhibits HER2-driven signaling and suppresses the growth of HER2-overexpressing tumor cells', *Cancer research*. Department of Medicine, Memorial Sloan-Kettering Cancer Center, New York, New York 10021, USA. moasserm@mskcc.org, 61(19), pp. 7184–7188.

Montemurro, F. and Scaltriti, M. (2013) 'Biomarkers of Drugs Targeting HER-family Signaling in Cancer', *The Journal of pathology*. Unit of Investigative Clinical Oncology (INCO) and Division of Medical Oncology, Fondazione del Piemonte per l'Oncologia, Institute of Candiolo (IRCCs), Str. Provinciale 142, 10060, Candiolo, Italy. doi: 10.1002/path.4269; 10.1002/path.4269.

Mustacchi, G. and De Laurentiis, M. (2015) 'The role of taxanes in triple-negative breast cancer: literature review', *Drug Design, Development and Therapy*, 9, p. 4303. doi: 10.2147/DDDT.S86105.

NCRAS (2017) 'Chemotherapy, Radiotherapy and Surgical Tumour Resections in England', *National Cancer Registration and Analysis Sevice*. Available at: http://www.ncin.org.uk/cancer_type_and_topic_specific_work/topic_specific_work/main_cancer_treatments (Accessed: 22 July 2018).

Niu, G. and Chen, X. (2010) 'Vascular Endothelial Growth Factor as an Anti-angiogenic Target for Cancer Therapy', *Current Drug Targets*. Imaging Sciences Training Program, Radiology and Imaging Sciences, Clinical Center and National Institute Biomedical Imaging and Bioengineering, NIH, 11(8), pp. 1000–1017.

Notte, A. *et al.* (2013) 'Hypoxia counteracts taxol-induced apoptosis in MDA-MB-231 breast cancer cells: role of autophagy and JNK activation', *Cell Death & Disease*, 4(5), pp. e638–e638. doi: 10.1038/cddis.2013.167.

O'Reilly, E. A. *et al.* (2015) 'The fate of chemoresistance in triple negative breast cancer (TNBC)', *BBA Clinical*. Elsevier, 3, pp. 257–275. doi: 10.1016/J.BBACLI.2015.03.003.

Oelze, M. *et al.* (2015) 'Novel 4-anilino-α-carboline derivatives induce cell death in nonadhesive breast cancer cells through inhibition of Brk activity', *Int. Journal of Clinical Pharmacology and Therapeutics*, 53(12), pp. 1052–1055. doi: 10.5414/CPXCES14EA07.

Ogawa, L. and Lindquist, D. (2018) 'Dual HER2 Suppression with Lapatinib plus Trastuzumab for Metastatic Inflammatory Breast Cancer: A Case Report of Prolonged Stable Disease', *Case Reports in Oncology*, 11(3), pp. 855–860. doi: 10.1159/000494264.

Oldberg, A., Franzen, A. and Heinegard, D. (1986) 'Cloning and sequence analysis of rat bone sialoprotein (osteopontin) cDNA reveals an Arg-Gly-Asp cell-binding sequence', *Proceedings of the National Academy of Sciences of the United States of America*, 83(23), pp. 8819–8823.

Olive, P. L. and Banáth, J. P. (2009) 'Kinetics of H2AX phosphorylation after exposure to cisplatin', *Cytometry Part B: Clinical Cytometry*, 76B(2), pp. 79–90. doi: 10.1002/cyto.b.20450.

Osaki, M., Oshimura, M. and Ito, H. (2004) 'PI3K-Akt pathway: Its functions and alterations in human cancer', *Apoptosis*, 9(6), pp. 667–676. doi: 10.1023/B:APPT.0000045801.15585.dd.

Ostrander, J. H. *et al.* (2007) 'Breast tumor kinase (protein tyrosine kinase 6) regulates heregulin-induced activation of ERK5 and p38 MAP kinases in breast cancer cells', *Cancer research*. Department of Medicine, University of Minnesota Cancer Center, Minneapolis, Minnesota 55455, USA., 67(9), pp. 4199–4209. doi: 10.1158/0008-5472.CAN-06-3409.

Ostrander, J. H. *et al.* (2007) 'Breast tumor kinase (protein tyrosine kinase 6) regulates

heregulin-induced activation of ERK5 and p38 MAP kinases in breast cancer cells.', *Cancer research*. American Association for Cancer Research, 67(9), pp. 4199–209. doi: 10.1158/0008-5472.CAN-06-3409.

Otrock, Z. K. *et al.* (2007) 'Understanding the biology of angiogenesis: review of the most important molecular mechanisms', *Blood cells, molecules & diseases*. Division of Hematology/Oncology, Department of Internal Medicine, American University of Beirut-Medical Center, P.O. Box: 113-6044, Beirut 1107 2802, Lebanon., 39(2), pp. 212–220. doi: 10.1016/j.bcmd.2007.04.001.

Ottenhoff-Kalff, A. E. *et al.* (1992) 'Characterization of protein tyrosine kinases from human breast cancer: involvement of the c-src oncogene product', *Cancer research*. Department of Hematology, University Hospital Utrecht, The Netherlands., 52(17), pp. 4773–4778.

Palka-Hamblin, H. L. *et al.* (2010) 'Identification of beta-catenin as a target of the intracellular tyrosine kinase PTK6', *Journal of cell science*. Department of Biochemistry and Molecular Genetics, University of Illinois at Chicago, Chicago, IL 60607, USA., 123(Pt 2), pp. 236–245. doi: 10.1242/jcs.053264; 10.1242/jcs.053264.

Parisot, J. P. *et al.* (1999) 'Altered expression of the IGF-1 receptor in a tamoxifen-resistant human breast cancer cell line.', *British journal of cancer*. Nature Publishing Group, 79(5–6), pp. 693–700. doi: 10.1038/sj.bjc.6690112.

Park, S. H. *et al.* (2015) 'PTK6 inhibition promotes apoptosis of Lapatinib-resistant Her2+ breast cancer cells by inducing Bim', *Breast Cancer Research*. BioMed Central, 17(1), p. 86. doi: 10.1186/s13058-015-0594-z.

Paronetto, M. P. *et al.* (2007) 'The RNA-binding protein Sam68 modulates the alternative splicing of Bcl-x', *The Journal of Cell Biology*, 176(7), pp. 929–939. doi: 10.1083/jcb.200701005.

Pawlik, T. M. and Keyomarsi, K. (2004) 'Role of cell cycle in mediating sensitivity to radiotherapy', *International Journal of Radiation Oncology*Biology*Physics*, 59(4), pp. 928–942. doi: 10.1016/j.ijrobp.2004.03.005.

Peng, M. *et al.* (2014) 'PTK6/BRK is expressed in the normal mammary gland and activated at the plasma membrane in breast tumors', *Oncotarget*, 5(15), pp. 6038–6048. doi: 10.18632/oncotarget.2153.

Petro, B. J. *et al.* (2004) ‘Differential expression of the non-receptor tyrosine kinase BRK in oral squamous cell carcinoma and normal oral epithelium’, *Oral oncology*. Department of Periodontics, College of Dentistry, M/C 859, University of Illinois at Chicago, 801 S. Paulina Street, Chicago, IL 60612-7212, USA., 40(10), pp. 1040–1047. doi: 10.1016/j.oraloncology.2004.05.010.

Petta, I. *et al.* (2016) ‘Modulation of Protein-Protein Interactions for the Development of Novel Therapeutics.’, *Molecular therapy : the journal of the American Society of Gene Therapy*. Elsevier, 24(4), pp. 707–18. doi: 10.1038/mt.2015.214.

Physical Sciences - Oncology Centers Network *et al.* (2013) ‘A physical sciences network characterization of non-tumorigenic and metastatic cells’, *Scientific Reports*, 3(1), p. 1449. doi: 10.1038/srep01449.

Pires, I. M. *et al.* (2014) ‘HIF-1α-independent hypoxia-induced rapid PTK6 stabilization is associated with increased motility and invasion.’, *Cancer biology & therapy*. Taylor & Francis, 15(10), pp. 1350–7. doi: 10.4161/cbt.29822.

Plataniotis, G. (2010) ‘Hypofractionated radiotherapy in the treatment of early breast cancer.’, *World journal of radiology*. Baishideng Publishing Group Inc, 2(6), pp. 197–202. doi: 10.4329/wjr.v2.i6.197.

Ponzo, M. G. and Park, M. (2010) ‘The Met receptor tyrosine kinase and basal breast cancer’, *Cell cycle (Georgetown, Tex.)*. Rosalind and Morris Goodman Cancer Centre, Department of Experimental Medicine,McGill University, Montreal, QC, CA., 9(6), pp. 1043–1050.

Pópulo, H., Lopes, J. M. and Soares, P. (2012) ‘The mTOR signalling pathway in human cancer.’, *International journal of molecular sciences*, 13(2), pp. 1886–918. doi: 10.3390/ijms13021886.

Prat, A. *et al.* (2014) ‘Molecular features of the basal-like breast cancer subtype based on BRCA1 mutation status’, *Breast Cancer Research and Treatment*, 147(1), pp. 185–191. doi: 10.1007/s10549-014-3056-x.

Prat, A. *et al.* (2015) ‘Clinical implications of the intrinsic molecular subtypes of breast cancer’, *The Breast*, 24, pp. S26–S35. doi: 10.1016/j.breast.2015.07.008.

Pusztai, L. *et al.* (2008) ‘Effect of molecular disease subsets on disease-free survival in

randomized adjuvant chemotherapy trials for estrogen receptor-positive breast cancer', *Journal of clinical oncology : official journal of the American Society of Clinical Oncology*. Department of Breast Medical Oncology, The University of Texas M. D. Anderson Cancer Center, PO Box 301439, Houston, TX 77230-1439, USA. lpusztai@mdanderson.org, 26(28), pp. 4679–4683.

Qiu, H. *et al.* (2005) 'Interaction between Brk kinase and insulin receptor substrate-4', *Oncogene*. Department of Physiology and Biophysics, School of Medicine, State University of New York at Stony Brook, Stony Brook, NY 11794-8661, USA., 24(36), pp. 5656–5664. doi: 10.1038/sj.onc.1208721.

Qiu, H. and Miller, W. T. (2002) 'Regulation of the nonreceptor tyrosine kinase Brk by autophosphorylation and by autoinhibition', *The Journal of biological chemistry*. Department of Physiology and Biophysics, School of Medicine, State University of New York, Stony Brook, NY 11794-8661, USA., 277(37), pp. 34634–34641. doi: 10.1074/jbc.M203877200.

Qiu, H. and Miller, W. T. (2004) 'Role of the Brk SH3 domain in substrate recognition', *Oncogene*. Department of Physiology and Biophysics, Basic Science Tower, T-6, School of Medicine, State University of New York at Stony Brook, Stony Brook, NY 11794-8661, USA., 23(12), pp. 2216–2223. doi: 10.1038/sj.onc.1207339.

Qu, Y. *et al.* (2015) 'Evaluation of MCF10A as a Reliable Model for Normal Human Mammary Epithelial Cells', *PLOS ONE*. Edited by X. Liu. Public Library of Science, 10(7), p. e0131285. doi: 10.1371/journal.pone.0131285.

Ragaz, J. *et al.* (2005) 'Locoregional radiation therapy in patients with high-risk breast cancer receiving adjuvant chemotherapy: 20-year results of the British Columbia randomized trial.', *Journal of the National Cancer Institute*, 97(2), pp. 116–26. doi: 10.1093/jnci/djh297.

Regan Anderson, T. M. *et al.* (2013) 'Breast Tumor Kinase (Brk/PTK6) Is a Mediator of Hypoxia-Associated Breast Cancer Progression', *Cancer research*. Authors' Affiliations: Division of Hematology, Oncology, and Transplantation, Department of Medicine and Pharmacology, Masonic Cancer Center, University of Minnesota, Minneapolis, Minnesota; Center for Cancer Research, Department of Pathology and Laborato, 73(18), pp. 5810–5820. doi: 10.1158/0008-5472.CAN-13-0523; 10.1158/0008-5472.CAN-13-0523.

Regan Anderson, T. M. *et al.* (2016) 'Breast Tumor Kinase (Brk/PTK6) Is Induced by HIF,

Glucocorticoid Receptor, and PELP1-Mediated Stress Signaling in Triple-Negative Breast Cancer.', *Cancer research*. NIH Public Access, 76(6), pp. 1653–63. doi: 10.1158/0008-5472.CAN-15-2510.

Reis-Filho, J. S. and Tutt, A. N. J. (2007) 'Triple negative tumours: a critical review', *Histopathology*, 52(1), pp. 108–118. doi: 10.1111/j.1365-2559.2007.02889.x.

Rikova, K. *et al.* (2007) 'Global survey of phosphotyrosine signaling identifies oncogenic kinases in lung cancer', *Cell*. Cell Signaling Technology, 3 Trask Lane, Danvers, MA 01923, USA., 131(6), pp. 1190–1203. doi: S0092-8674(07)01522-X [pii].

Rocha, A. J. *et al.* (2015) 'Real Time PCR: the Use of Reference Genes and Essential Rules Required to Obtain Normalisation Data Reliable to Quantitative Gene Expression', *Journal of Molecular Biology Research*, 5(1). doi: 10.5539/jmbr.v5n1p45.

Roche, H. and Vahdat, L. T. (2011) 'Treatment of metastatic breast cancer: second line and beyond', *Annals of Oncology*. Oxford University Press, 22(5), pp. 1000–1010. doi: 10.1093/annonc/mdq429.

Rogakou, E. P. *et al.* (1999) 'Megabase chromatin domains involved in DNA double-strand breaks in vivo.', *The Journal of cell biology*, 146(5), pp. 905–16. Available at: http://www.ncbi.nlm.nih.gov/pubmed/10477747 (Accessed: 1 August 2018).

Romain, S. *et al.* (1994) 'Prognostic value of cytosolic tyrosine kinase activity in 249 node-positive breast cancer patients', *British journal of cancer*. Laboratoire d'Oncologie Biologique, APM, Faculte de Medecine Nord, Marseille, France., 70(2), pp. 304–308.

Rothkamm, K. and Lobrich, M. (2003) 'Evidence for a lack of DNA double-strand break repair in human cells exposed to very low x-ray doses', *Proceedings of the National Academy of Sciences*, 100(9), pp. 5057–5062. doi: 10.1073/pnas.0830918100.

Rugo, H. S. *et al.* (2012) 'A phase II study of lapatinib and bevacizumab as treatment for HER2-overexpressing metastatic breast cancer', *Breast cancer research and treatment*, 134(1), pp. 13–20. doi: 10.1007/s10549-011-1918-z.

Sachdev, D. (2008) 'Regulation of breast cancer metastasis by IGF signaling', *Journal of mammary gland biology and neoplasia*. Department of Medicine and Masonic Cancer Center, University of Minnesota, MMC 806, 420 Delaware Street SE, Minneapolis, MN 55455, USA. sachd003@umn.edu, 13(4), pp. 431–441. doi: 10.1007/s10911-008-9105-5;

10.1007/s10911-008-9105-5.

Saitoh, Y. *et al.* (1995) ‘Expression of osteopontin in human glioma. Its correlation with the malignancy’, *Laboratory investigation; a journal of technical methods and pathology*. Department of Neurosurgery, Kumamoto University Medical School, Japan., 72(1), pp. 55–63.

Samanta, D. *et al.* (2014) ‘Hypoxia-inducible factors are required for chemotherapy resistance of breast cancer stem cells.’, *Proceedings of the National Academy of Sciences of the United States of America*. National Academy of Sciences, 111(50), pp. E5429-38. doi: 10.1073/pnas.1421438111.

Sánchez-Jiménez, F. and Sánchez-Margalet, V. (2013) ‘Role of Sam68 in post-transcriptional gene regulation.’, *International journal of molecular sciences*. Multidisciplinary Digital Publishing Institute (MDPI), 14(12), pp. 23402–19. doi: 10.3390/ijms141223402.

Sardar, P. *et al.* (2017) ‘Long-term cardiovascular mortality after radiotherapy for breast cancer: A systematic review and meta-analysis’, *Clinical Cardiology*, 40(2), pp. 73–81. doi: 10.1002/clc.22631.

Schechter, A. L. *et al.* (no date) ‘The neu oncogene: an erb-B-related gene encoding a 185,000-Mr tumour antigen.’, *Nature*, 312(5994), pp. 513–6. Available at: http://www.ncbi.nlm.nih.gov/pubmed/6095109 (Accessed: 13 October 2017).

Schlegel, J. *et al.* (1995) ‘Comparative genomic in situ hybridization of colon carcinomas with replication error’, *Cancer research*. Institut fur Pathologie, Universitat Regensburg, Germany., 55(24), pp. 6002–6005.

Schmandt, R. E. *et al.* (2006) ‘The BRK tyrosine kinase is expressed in high-grade serous carcinoma of the ovary’, *Cancer biology & therapy*. Department of Gynecologic Oncology, The University of Texas MD Anderson Cancer Center, Houston, Texas 77230-1439, USA. rschmand@mdanderson.org, 5(9), pp. 1136–1141.

Semenza, G. L. (2010) ‘Defining the role of hypoxia-inducible factor 1 in cancer biology and therapeutics’, *Oncogene*, 29(5), pp. 625–634. doi: 10.1038/onc.2009.441.

Sharma, A., Singh, K. and Almasan, A. (2012) ‘Histone H2AX Phosphorylation: A Marker for DNA Damage’, in *Methods in molecular biology (Clifton, N.J.)*, pp. 613–626. doi:

10.1007/978-1-61779-998-3_40.

Shen, C. H. *et al.* (2008) 'Breast tumor kinase phosphorylates p190RhoGAP to regulate rho and ras and promote breast carcinoma growth, migration, and invasion', *Cancer research*. Institute of Molecular Medicine, Institute of Toxicology, College of Medicine, National Taiwan University, Taipei, Taiwan., 68(19), pp. 7779–7787. doi: 10.1158/0008-5472.CAN-08-0997; 10.1158/0008-5472.CAN-08-0997.

Shim, H. J., Kim, H. I. and Lee, S.-T. (2017) 'The associated pyrazolopyrimidines PP1 and PP2 inhibit protein tyrosine kinase 6 activity and suppress breast cancer cell proliferation.', *Oncology letters*. Spandidos Publications, 13(3), pp. 1463–1469. doi: 10.3892/ol.2017.5564.

Shin, W.-S. *et al.* (2017) 'PTK6 Localized at the Plasma Membrane Promotes Cell Proliferation and MigratiOn Through Phosphorylation of Eps8', *Journal of Cellular Biochemistry*, 118(9), pp. 2887–2895. doi: 10.1002/jcb.25939.

Sircoulomb, F. *et al.* (2011) '*ZNF703* gene amplification at 8p12 specifies luminal B breast cancer', *EMBO Molecular Medicine*, 3(3), pp. 153–166. doi: 10.1002/emmm.201100121.

van Slooten, H. J. *et al.* (1995) 'Outgrowth of BT-474 human breast cancer cells in immune-deficient mice: a new in vivo model for hormone-dependent breast cancer.', *British journal of cancer*. Nature Publishing Group, 72(1), pp. 22–30. Available at: http://www.ncbi.nlm.nih.gov/pubmed/7599056 (Accessed: 8 March 2018).

Smid, M. *et al.* (2008) 'Subtypes of Breast Cancer Show Preferential Site of Relapse', *Cancer Research*, 68(9), pp. 3108–3114. doi: 10.1158/0008-5472.CAN-07-5644.

Smith-Warner, S. A. *et al.* (1998) 'Alcohol and breast cancer in women: a pooled analysis of cohort studies.', *JAMA*, 279(7), pp. 535–40. Available at: http://www.ncbi.nlm.nih.gov/pubmed/9480365 (Accessed: 12 October 2017).

Smith, E. (2012) 'Tamoxifen - the start of something big'. UK: Science Blog, p. 10.

Smith, S. E. *et al.* (2017) 'Molecular characterization of breast cancer cell lines through multiple omic approaches', *Breast Cancer Research*. BioMed Central, 19(1), p. 65. doi: 10.1186/s13058-017-0855-0.

Soule, H. D. *et al.* (1990) 'Isolation and Characterization of a Spontaneously Immortalized Human Breast Epithelial Cell Line, MCF-101', *CANCER RESEARCH*, 50, pp. 6075–6086.

Available at: http://cancerres.aacrjournals.org/content/canres/50/18/6075.full.pdf (Accessed: 12 March 2018).

Stoss, O. *et al.* (2001) 'The STAR/GSG family protein rSLM-2 regulates the selection of alternative splice sites.', *The Journal of biological chemistry*. American Society for Biochemistry and Molecular Biology, 276(12), pp. 8665–73. doi: 10.1074/jbc.M006851200.

Stoss, O. *et al.* (2004) 'p59fyn-mediated phosphorylation regulates the activity of the tissue-specific splicing factor rSLM-1', *Molecular and Cellular Neuroscience*, 27(1), pp. 8–21. doi: 10.1016/j.mcn.2004.04.011.

Taneja, P. *et al.* (2010) 'Classical and Novel Prognostic Markers for Breast Cancer and their Clinical Significance.', *Clinical Medicine Insights. Oncology*. SAGE Publications, 4, pp. 15–34. Available at: http://www.ncbi.nlm.nih.gov/pubmed/20567632 (Accessed: 14 August 2018).

Taylor, S. J. and Shalloway, D. (1994) 'An RNA-binding protein associated with Src through its SH2 and SH3 domains in mitosis', *Nature*, 368(6474), pp. 867–871. doi: 10.1038/368867a0.

Thakur, M. K. *et al.* (2017) 'Co-crystal structures of PTK6: With Dasatinib at 2.24 Å, with novel imidazo[1,2-a]pyrazin-8-amine derivative inhibitor at 1.70 Å resolution', *Biochemical and Biophysical Research Communications*. Academic Press, 482(4), pp. 1289–1295. doi: 10.1016/J.BBRC.2016.12.030.

Thariat, J. *et al.* (2013) 'Past, present and future of radiotherapy for the benefit of patients', *Nature Reviews Clinical Oncology*, 10(1), pp. 52–60. doi: 10.1038/nrclinonc.2012.203.

Thorn, C. F. *et al.* (2011) 'Doxorubicin pathways: pharmacodynamics and adverse effects.', *Pharmacogenetics and genomics*. NIH Public Access, 21(7), pp. 440–6. doi: 10.1097/FPC.0b013e32833ffb56.

Tomao, F. *et al.* (2015) 'Triple-negative breast cancer: new perspectives for targeted therapies.', *OncoTargets and therapy*. Dove Press, 8, pp. 177–93. doi: 10.2147/OTT.S67673.

Tommasi, S. *et al.* (2007) 'Cytoskeleton and paclitaxel sensitivity in breast cancer: The role of β-tubulins', *International Journal of Cancer*. Wiley Subscription Services, Inc., A Wiley Company, 120(10), pp. 2078–2085. doi: 10.1002/ijc.22557.

Tran, Q. T. *et al.* (2012) ‘EGFR regulation of epidermal barrier function’, *Physiological Genomics*, 44(8), pp. 455–469. doi: 10.1152/physiolgenomics.00176.2011.

Truman, J.-P. *et al.* (2005) ‘Down-regulation of ATM protein sensitizes human prostate cancer cells to radiation-induced apoptosis.’, *The Journal of biological chemistry*. NIH Public Access, 280(24), pp. 23262–72. doi: 10.1074/jbc.M503701200.

Tsukahara, T., Haniu, H. and Matsuda, Y. (2013) ‘PTB-Associated Splicing Factor (PSF) Is a PPARγ-Binding Protein and Growth Regulator of Colon Cancer Cells’, *PLoS ONE*. Edited by K. Roemer, 8(3), p. e58749. doi: 10.1371/journal.pone.0058749.

Tupper, J., Crompton, M. R. and Harvey, A. J. (2011) ‘Breast tumor kinase (Brk/PTK6) plays a role in the differentiation of primary keratinocytes’, *Archives of Dermatological Research*. School of Biological Sciences, Royal Holloway, University of London, Egham, Surrey, UK., 303(4), pp. 293–297. doi: 10.1007/s00403-010-1118-4; 10.1007/s00403-010-1118-4.

Vandesompele, J. *et al.* (2002) ‘Accurate normalization of real-time quantitative RT-PCR data by geometric averaging of multiple internal control genes.’, *Genome biology*, 3(7), p. RESEARCH0034. Available at: http://www.ncbi.nlm.nih.gov/pubmed/12184808 (Accessed: 20 January 2018).

Vasioukhin, V. and Tyner, A. L. (1997) ‘A role for the epithelial-cell-specific tyrosine kinase Sik during keratinocyte differentiation.’, *Proceedings of the National Academy of Sciences of the United States of America*, 94(26), pp. 14477–82. doi: 10.1073/pnas.94.26.14477.

Vazquez, F. *et al.* (2000) ‘Phosphorylation of the PTEN tail regulates protein stability and function.’, *Molecular and cellular biology*. American Society for Microbiology, 20(14), pp. 5010–8. doi: 10.1128/MCB.20.14.5010-5018.2000.

Veronesi, U. *et al.* (1981) ‘Comparing radical mastectomy with quadrantectomy, axillary dissection, and radiotherapy in patients with small cancers of the breast.’, *The New England journal of medicine*, 305(1), pp. 6–11. doi: 10.1056/NEJM198107023050102.

Vignard, J., Mirey, G. and Salles, B. (2013) ‘Ionizing-radiation induced DNA double-strand breaks: A direct and indirect lighting up’, *Radiotherapy and Oncology*, 108(3), pp. 362–369. doi: 10.1016/j.radonc.2013.06.013.

Vinayak, S. and Carlson, R. W. (2013) ‘mTOR inhibitors in the treatment of breast cancer.’,

Oncology (Williston Park, N.Y.), 27(1), p. 38–44, 46, 48 passim. Available at: http://www.ncbi.nlm.nih.gov/pubmed/23461041 (Accessed: 14 January 2018).

Walker, S. R. and Frank, D. A. (2015) 'Targeting BCL6 and STAT3 in triple negative breast cancer: the one-two punch?', *Oncoscience*. Impact Journals, LLC, 2(11), p. 912. doi: 10.18632/oncoscience.270.

Wang, C. *et al.* (2016) 'The Enhancement of Radiation Sensitivity in Nasopharyngeal Carcinoma Cells via Activation of the Rac1/NADPH Signaling Pathway', *Radiation Research*, 185(6), pp. 638–646. doi: 10.1667/RR14331.1.

Wang, C. and Lees-Miller, S. P. (2013) 'Detection and repair of ionizing radiation-induced DNA double strand breaks: new developments in nonhomologous end joining.', *International journal of radiation oncology, biology, physics*. NIH Public Access, 86(3), pp. 440–9. doi: 10.1016/j.ijrobp.2013.01.011.

Wang, T. C. *et al.* (2005) 'Role of breast tumour kinase in the in vitro differentiation of HaCaT cells', *The British journal of dermatology*. Department of Dermatology, College of Medicine, National Taiwan University and National Taiwan University Hospital, Taipei, Taiwan., 153(2), pp. 282–289. doi: 10.1111/j.1365-2133.2005.06604.x.

Wang, Z. *et al.* (2015) 'Clinical implications of β-catenin protein expression in breast cancer', *Int J Clin Exp Pathol*, 8(11), pp. 14989–14994. Available at: www.ijcep.com (Accessed: 11 April 2018).

Wazir, U. *et al.* (2013) 'The clinicopathological significance of lamin A/C, lamin B1 and lamin B receptor mRNA expression in human breast cancer', *Cellular and Molecular Biology Letters*. Springer Vienna, 18(4), pp. 595–611. doi: 10.2478/s11658-013-0109-9.

Weaver, A. M. and Silva, C. M. (2007) 'Signal transducer and activator of transcription 5b: a new target of breast tumor kinase/protein tyrosine kinase 6', *Breast cancer research : BCR*. Department of Microbiology, University of Virginia, Charlottesville, VA 22908, USA., 9(6), p. R79. doi: 10.1186/bcr1794.

Weaver, B. A. (2014) 'How Taxol/paclitaxel kills cancer cells.', *Molecular biology of the cell*. American Society for Cell Biology, 25(18), pp. 2677–81. doi: 10.1091/mbc.E14-04-0916.

Wei, W. and Lewis, M. T. (2015) 'Identifying and targeting tumor-initiating cells in the treatment of breast cancer', *Endocrine Related Cancer*, 22(3), pp. R135–R155. doi:

10.1530/ERC-14-0447.

Weigelt, B., Baehner, F. L. and Reis-Filho, J. S. (2010) 'The contribution of gene expression profiling to breast cancer classification, prognostication and prediction: a retrospective of the last decade', *The Journal of pathology*. Signal Transduction Laboratory, Cancer Research UK, London Research Institute, London, UK., 220(2), pp. 263–280.

Welcsh, P. L. and King, M. C. (2001) 'BRCA1 and BRCA2 and the genetics of breast and ovarian cancer.', *Human molecular genetics*, 10(7), pp. 705–13. Available at: http://www.ncbi.nlm.nih.gov/pubmed/11257103 (Accessed: 14 January 2018).

Wen, X.-F. *et al.* (2006) 'HER2 signaling modulates the equilibrium between pro- and antiangiogenic factors via distinct pathways: implications for HER2-targeted antibody therapy.', *Oncogene*, 25(52), pp. 6986–96. doi: 10.1038/sj.onc.1209685.

Weterings, E. *et al.* (2009) 'The Ku80 Carboxy Terminus Stimulates Joining and Artemis-Mediated Processing of DNA Ends', *Molecular and Cellular Biology*, 29(5), pp. 1134–1142. doi: 10.1128/MCB.00971-08.

Wong-Brown, M. W. *et al.* (2015) 'Prevalence of BRCA1 and BRCA2 germline mutations in patients with triple-negative breast cancer', *Breast Cancer Research and Treatment*, 150(1), pp. 71–80. doi: 10.1007/s10549-015-3293-7.

Wooster, R. *et al.* (1994) 'Localization of a breast cancer susceptibility gene, BRCA2, to chromosome 13q12-13.', *Science (New York, N.Y.)*, 265(5181), pp. 2088–90. Available at: http://www.ncbi.nlm.nih.gov/pubmed/8091231 (Accessed: 12 October 2017).

Wozniak, D. J. *et al.* (2017) 'PTEN is a protein phosphatase that targets active PTK6 and inhibits PTK6 oncogenic signaling in prostate cancer', *Nature Communications*. Nature Publishing Group, 8(1), p. 1508. doi: 10.1038/s41467-017-01574-5.

Wynder, E. L. *et al.* (1997) 'Breast cancer: weighing the evidence for a promoting role of dietary fat.', *Journal of the National Cancer Institute*, 89(11), pp. 766–75. Available at: http://www.ncbi.nlm.nih.gov/pubmed/9182974 (Accessed: 12 October 2017).

Xiang, B. *et al.* (2008) 'Brk is coamplified with ErbB2 to promote proliferation in breast cancer', *Proceedings of the National Academy of Sciences of the United States of America*. Cold Spring Harbor Laboratory, One Bungtown Road, Cold Spring Harbor, NY 11724, USA., 105(34), pp. 12463–12468. doi: 10.1073/pnas.0805009105;

10.1073/pnas.0805009105.

Xie, A., Kwok, A. and Scully, R. (2009) 'Role of mammalian Mre11 in classical and alternative nonhomologous end joining', *Nature Structural & Molecular Biology*, 16(8), pp. 814–818. doi: 10.1038/nsmb.1640.

Xu, J. *et al.* (2015) 'β-Catenin Is Required for the Tumorigenic Behavior of Triple-Negative Breast Cancer Cells', *PLOS ONE*. Edited by B. O. Williams, 10(2), p. e0117097. doi: 10.1371/journal.pone.0117097.

Xu, X. and Stern, D. F. (2003) 'NFBD1/KIAA0170 Is a Chromatin-associated Protein Involved in DNA Damage Signaling Pathways', *Journal of Biological Chemistry*, 278(10), pp. 8795–8803. doi: 10.1074/jbc.M211392200.

Yamamoto, Y. *et al.* (2008) 'Hypoxia-inducible factor 1α is closely linked to an aggressive phenotype in breast cancer', *Breast Cancer Research and Treatment*, 110(3), pp. 465–475. doi: 10.1007/s10549-007-9742-1.

Yamazaki, H. *et al.* (1996) 'Cloning and characterization of KAP3: a novel kinesin superfamily-associated protein of KIF3A/3B', *Proceedings of the National Academy of Sciences of the United States of America*. Department of Anatomy and Cell Biology, Faculty of Medicine, University of Tokyo, Japan., 93(16), pp. 8443–8448.

Yarden, Y. and Sliwkowski, M. X. (2001) 'Untangling the ErbB signalling network.', *Nature reviews. Molecular cell biology*, 2(2), pp. 127–37. doi: 10.1038/35052073.

Yu, S. *et al.* (2017) 'The T47D cell line is an ideal experimental model to elucidate the progesterone-specific effects of a luminal A subtype of breast cancer', *Biochemical and Biophysical Research Communications*, 486(3), pp. 752–758. doi: 10.1016/j.bbrc.2017.03.114.

Yuan, J. and Chen, J. (2010) 'MRE11-RAD50-NBS1 Complex Dictates DNA Repair Independent of H2AX', *Journal of Biological Chemistry*, 285(2), pp. 1097–1104. doi: 10.1074/jbc.M109.078436.

Zeng, H. *et al.* (2011) 'Discovery of novel imidazo[1,2-a]pyrazin-8-amines as Brk/PTK6 inhibitors', *Bioorganic & medicinal chemistry letters*. Department of Chemistry, Merck Research Laboratories, 320 Bent Street, Cambridge, MA 02141, United States. zenghb@hotmail.com: Elsevier Ltd, 21(19), pp. 5870–5875. doi:

10.1016/j.bmcl.2011.07.101; 10.1016/j.bmcl.2011.07.101.

Zeng, X. and Yee, D. (2007) ‘Insulin-like growth factors and breast cancer therapy’, *Advances in Experimental Medicine and Biology*. Department of Pharmacology, University of Minnesota Cancer Center, Minneapolis, MN 55455, USA., 608, pp. 101–112.

Zhang, M. H. *et al.* (2014) ‘Estrogen receptor-positive breast cancer molecular signatures and therapeutic potentials (Review).’, *Biomedical reports*. Spandidos Publications, 2(1), pp. 41–52. doi: 10.3892/br.2013.187.

Zhang, P. *et al.* (2005) ‘Regulated association of protein kinase B/Akt with breast tumor kinase’, *The Journal of biological chemistry*. University of Minnesota Cancer Center and the Department of Medicine, Division of Hematology, Oncology, and Transplantation, and Pharmacology, Minneapolis, Minnesota 55455, USA., 280(3), pp. 1982–1991. doi: 10.1074/jbc.M412038200.

Zhao, C. *et al.* (2003) ‘Elevated expression levels of NCOA3, TOP1, and TFAP2C in breast tumors as predictors of poor prognosis’, *Cancer*. Department of Molecular Cytogenetics, Medical Research Institute, Tokyo Medical and Dental University, Tokyo, Japan.: 2, 98(1), pp. 18–23. doi: 10.1002/cncr.11482.

Zheng, Y. *et al.* (2010) ‘Protein tyrosine kinase 6 directly phosphorylates AKT and promotes AKT activation in response to epidermal growth factor.’, *Molecular and cellular biology*, 30(17), pp. 4280–92. doi: 10.1128/MCB.00024-10.

Zheng, Y. *et al.* (2013) ‘Protein tyrosine kinase 6 protects cells from anoikis by directly phosphorylating focal adhesion kinase and activating AKT’, *Oncogene*. Department of Biochemistry and Molecular Genetics, University of Illinois at Chicago, College of Medicine, Chicago, IL 60607, USA., 32(36), pp. 4304–4312. doi: 10.1038/onc.2012.427; 10.1038/onc.2012.427.

Zheng, Y. and Tyner, A. L. (2013) ‘Context-specific protein tyrosine kinase 6 (PTK6) signalling in prostate cancer’, *European journal of clinical investigation*. Department of Biochemistry and Molecular Genetics, University of Illinois at Chicago, Chicago, IL 60607, USA.: Stichting European Society for Clinical Investigation Journal Foundation, 43(4), pp. 397–404. doi: 10.1111/eci.12050; 10.1111/eci.12050.

Zhong, J. L. *et al.* (2008) ‘Distinct Functions of Natural ADAM-15 Cytoplasmic Domain

Variants in Human Mammary Carcinoma', *Molecular Cancer Research*, 6(3), pp. 383–394. doi: 10.1158/1541-7786.MCR-07-2028.